Investigation of AASHTOWare Pavement ME Design/DARWin-ME Performance Prediction Models for Iowa Pavement Analysis and Design

Final Report
December 2015

IOWA STATE UNIVERSITY
Institute for Transportation

Sponsored by
Iowa Department of Transportation
(InTrans Project 14-496)

About the Institute for Transportation

The mission of the Institute for Transportation (InTrans) at Iowa State University is to develop and implement innovative methods, materials, and technologies for improving transportation efficiency, safety, reliability, and sustainability while improving the learning environment of students, faculty, and staff in transportation-related fields.

About ProSPER

The mission of the Program for Sustainable Pavement Engineering and Research (ProSPER) is to advance research, development, and implementation of next-generation sustainable roadway systems, integrate cutting-edge technologies from various disciplines to tackle real-world highway and airport pavement infrastructure problems, and investigate sustainable paving materials and construction technologies, pavement non-destructive testing and evaluation, performance monitoring, maintenance, repair, and rehabilitation.

Disclaimer Notice

The contents of this report reflect the views of the authors, who are responsible for the facts and the accuracy of the information presented herein. The opinions, findings and conclusions expressed in this publication are those of the authors and not necessarily those of the sponsors.

The sponsors assume no liability for the contents or use of the information contained in this document. This report does not constitute a standard, specification, or regulation.

The sponsors do not endorse products or manufacturers. Trademarks or manufacturers' names appear in this report only because they are considered essential to the objective of the document.

Non-Discrimination Statement

Iowa State University does not discriminate on the basis of race, color, age, ethnicity, religion, national origin, pregnancy, sexual orientation, gender identity, genetic information, sex, marital status, disability, or status as a U.S. veteran. Inquiries regarding non-discrimination policies may be directed to Office of Equal Opportunity, Title IX/ADA Coordinator, and Affirmative Action Officer, 3350 Beardshear Hall, Ames, Iowa 50011, 515-294-7612, email eooffice@iastate.edu.

Iowa Department of Transportation Statements

Federal and state laws prohibit employment and/or public accommodation discrimination on the basis of age, color, creed, disability, gender identity, national origin, pregnancy, race, religion, sex, sexual orientation or veteran's status. If you believe you have been discriminated against, please contact the Iowa Civil Rights Commission at 800-457-4416 or the Iowa Department of Transportation affirmative action officer. If you need accommodations because of a disability to access the Iowa Department of Transportation's services, contact the agency's affirmative action officer at 800-262-0003.

The preparation of this report was financed in part through funds provided by the Iowa Department of Transportation through its "Second Revised Agreement for the Management of Research Conducted by Iowa State University for the Iowa Department of Transportation" and its amendments.

The opinions, findings, and conclusions expressed in this publication are those of the authors and not necessarily those of the Iowa Department of Transportation.

Technical Report Documentation Page

1. Report No.	2. Government Accession No.	3. Recipient's Catalog No.	
InTrans Project 14-496			
4. Title and Subtitle Investigation of AASHTOWare Pavement ME Design/DARWin-ME Performance Prediction Models for Iowa Pavement Analysis and Design		**5. Report Date** December 2015 **6. Performing Organization Code**	
7. Author(s) Halil Ceylan, Sunghwan Kim, Orhan Kaya, and Kasthurirangan Gopalakrishnan		**8. Performing Organization Report No.** InTrans Project 14-496	
9. Performing Organization Name and Address Institute for Transportation Iowa State University 2711 South Loop Drive, Suite 4700 Ames, IA 50010-8664		**10. Work Unit No. (TRAIS)** **11. Contract or Grant No.**	
12. Sponsoring Organization Name and Address Iowa Department of Transportation 800 Lincoln Way Ames, IA 50010		**13. Type of Report and Period Covered** Final Report **14. Sponsoring Agency Code**	
15. Supplementary Notes Visit www.intrans.iastate.edu for color pdfs of this and other research reports.			

16. Abstract

The Mechanistic-Empirical Pavement Design Guide (MEPDG) was developed under National Cooperative Highway Research Program (NCHRP) Project 1-37A as a novel mechanistic-empirical procedure for the analysis and design of pavements. The MEPDG was subsequently supported by AASHTO's DARWin-ME and most recently marketed as AASHTOWare Pavement ME Design software as of February 2013. Although the core design process and computational engine have remained the same over the years, some enhancements to the pavement performance prediction models have been implemented along with other documented changes as the MEPDG transitioned to AASHTOWare Pavement ME Design software.

Preliminary studies were carried out to determine possible differences between AASHTOWare Pavement ME Design, MEPDG (version 1.1), and DARWin-ME (version 1.1) performance predictions for new jointed plain concrete pavement (JPCP), new hot mix asphalt (HMA), and HMA over JPCP systems. Differences were indeed observed between the pavement performance predictions produced by these different software versions. Further investigation was needed to verify these differences and to evaluate whether identified local calibration factors from the latest MEPDG (version 1.1) were acceptable for use with the latest version (version 2.1.24) of AASHTOWare Pavement ME Design at the time this research was conducted.

Therefore, the primary objective of this research was to examine AASHTOWare Pavement ME Design performance predictions using previously identified MEPDG calibration factors (through InTrans Project 11-401) and, if needed, refine the local calibration coefficients of AASHTOWare Pavement ME Design pavement performance predictions for Iowa pavement systems using linear and nonlinear optimization procedures. A total of 130 representative sections across Iowa consisting of JPCP, new HMA, and HMA over JPCP sections were used. The local calibration results of AASHTOWare Pavement ME Design are presented and compared with national and locally calibrated MEPDG models.

17. Key Words	18. Distribution Statement		
hot-mix asphalt—pavement design—performance models—portland cement concrete	No restrictions.		
19. Security Classification (of this report)	**20. Security Classification (of this page)**	**21. No. of Pages**	**22. Price**
Unclassified.	Unclassified.	211	NA

Form DOT F 1700.7 (8-72) **Reproduction of completed page authorized**

INVESTIGATION OF AASHTOWARE PAVEMENT ME DESIGN/DARWIN-ME PERFORMANCE PREDICTION MODELS FOR IOWA PAVEMENT ANALYSIS AND DESIGN

Final Report
December 2015

Principal Investigator
Halil Ceylan, Professor and Director
Program for Sustainable Pavement Engineering and Research (ProSPER)
Institute for Transportation, Iowa State University

Co-Principal Investigators
Kasthurirangan Gopalakrishnan, Research Associate Professor
Iowa State University

Sunghwan Kim, Research Scientist
Iowa State University

Research Assistant
Orhan Kaya

Authors
Halil Ceylan, Sunghwan Kim, Orhan Kaya, and Kasthurirangan Gopalakrishnan

Preparation of this report was financed in part
through funds provided by the Iowa Department of Transportation
through its Research Management Agreement with the
Institute for Transportation
(InTrans Project 14-496)

A report from
Institute for Transportation
Iowa State University
2711 South Loop Drive, Suite 4700
Ames, IA 50010-8664
Phone: 515-294-8103 / Fax: 515-294-0467
www.intrans.iastate.edu

TABLE OF CONTENTS

LIST OF FIGURES

LIST OF TABLES

ACKNOWLEDGMENTS

The authors gratefully acknowledge the Iowa Department of Transportation (DOT) for supporting this study and Chris Brakke, Fereidoon (Ben) Behnami, and Scott Schram with the Iowa DOT for all of the technical assistance provided. Special thanks to Chadwick Becker, Alex Gotlif, and Leslie Titus-Glover with ARA, Inc. for providing valuable comments on the clarification of pavement performance prediction equations and models currently utilized in Pavement ME Design software.

Note: The literature review results have been updated as of 2015 and are included in Appendix A at the end of this report. A previous version of the literature review was published in the following report: Ceylan, H., S. Kim, K. Gopalakrishnan, and D. Ma. 2013. *Iowa Calibration of MEPDG Performance Prediction Models*. Ames, Iowa: Institute for Transportation, Iowa State University.

EXECUTIVE SUMMARY

The national calibration of the Mechanistic-Empirical Pavement Design Guide (MEPDG) was completed under National Cooperative Highway Research Program (NCHRP) Project 1-37A (ARA, Inc. 2004) and NCHRP Project 1-40 (AASHTO 2010). To complement the design guide, pavement analysis and design software (MEPDG version 1.1) was also released along with a project research report (ARA, Inc. 2004). The software has been subsequently improved by adding new pavement prediction models as well as by advancing existing models, so in 2011, the MEPDG software was rebranded as DARWin-ME. The new software, which featured a more intuitive and user-friendly software interface, has recently been marketed as AASHTOWare Pavement ME Design.

Upon completion of the national calibration of the MEPDG pavement prediction models, NCHRP (ARA, Inc. 2004) recommended that state highway agencies conduct local calibration of the models before fully implementing the software. Ceylan et al. (2013) conducted such local calibration of the MEPDG for Iowa pavement systems using MEPDG version 1.1 under InTrans Project 11-401. In this report, locally calibrated pavement performance prediction models acquired through the results of Ceylan et al. (2013) are designated "MEPDG locally calibrated pavement performance prediction models." Preliminary studies were then carried out to determine the differences between MEPDG (version 1.1) and DARWin-ME performance predictions for new jointed plain concrete pavement (JPCP), new hot mix asphalt (HMA), and HMA over JPCP systems. The results reflected quite significant differences between the predictions made by the two software versions, at least in some cases, warranting further investigation to determine whether the local calibration study should be repeated using the DARWin-ME software, now referred to as AASHTOWare Pavement ME Design.

The first objective of this study was to evaluate the accuracy of nationally calibrated and MEPDG locally calibrated pavement performance prediction models. The second objective of the study was to perform a recalibration of these models if their accuracy was found to be insufficient. The recalibration process was implemented using AASHTOWare Pavement ME Design with the assistance of linear and nonlinear optimization techniques to improve model prediction accuracy. AASHTOWare Pavement ME Design version 2.1.24 was utilized as the latest version of software at the time this research was conducted. The pavement sections used by Ceylan et al. (2013) were also used in this study, but with more data points.

The local calibration coefficients identified in this study are presented in Table 31 for JPCP, Table 32 for HMA pavement, and Table 33 for HMA over JPCP systems. The key findings from this study are as follows:

- Mean joint faulting, transverse cracking, and International Roughness Index (IRI) models for Iowa JPCPs were significantly improved as a result of AASHTOWare Pavement ME Design local calibration when compared to the nationally calibrated and MEPDG locally calibrated counterparts.

- The identified AASHTOWare Pavement ME Design local calibration factors significantly increased the accuracy of the rutting model for Iowa HMA pavements compared to the nationally calibrated and MEPDG locally calibrated counterparts.

- The identified AASHTOWare Pavement ME Design local calibration factors increased the accuracy of the IRI model for Iowa HMA pavements when compared to the nationally calibrated and MEPDG locally calibrated models, although nationally calibrated and MEPDG locally calibrated IRI models also provided acceptable predictions.

- A nationally calibrated longitudinal (top-down) cracking model underpredicted this distress while the MEPDG locally calibrated model overpredicted it for Iowa HMA pavements. The accuracy of this model was improved as a result of AASHTOWare Pavement ME Design local calibration.

- All of the nationally calibrated, MEPDG locally calibrated, and AASHTOWare Pavement ME Design locally calibrated alligator (bottom-up) and thermal cracking models provided acceptable predictions for Iowa HMA pavements.

- The identified AASHTOWare Pavement ME Design local calibration factors significantly increased the accuracy of IRI predictions for Iowa HMA over JPCPs.

- The identified AASHTOWare Pavement ME Design local calibration factors increased the accuracy of the rutting model to a quite noticeable extent for Iowa HMA over JPCPs compared to the nationally calibrated and MEPDG locally calibrated models, although nationally calibrated and MEPDG locally calibrated IRI models also provided acceptable predictions for this model.

- All the nationally, MEPDG, and AASHTOWare Pavement ME Design locally calibrated alligator (bottom-up) cracking models provided acceptable predictions for Iowa HMA over JPCPs.

- Nationally calibrated models underpredicted the longitudinal (top-down) cracking model while the MEPDG locally calibrated model exhibited excessive standard error for Iowa HMA over JPCPs. The accuracy of this model was improved as a result of AASHTOWare Pavement ME Design local calibration.

- Nationally calibrated and MEPDG locally calibrated thermal cracking models underpredicted distress. The accuracy of this model was also improved as a result of AASHTOWare Pavement ME Design local calibration.

Recommendations for the use of AASHTOWare Pavement ME Design in Iowa pavement systems are as follows:

- The locally calibrated JPCP performance models (faulting, transverse cracking, and IRI) identified in this study are recommended for use with Iowa JPCPs as alternatives to the nationally calibrated models.

- Because both faulting and transverse cracking predictions were involved in the calculation of IRI, two approaches were utilized in the local calibration of the JPCP IRI model. In Approach 1, the IRI model was locally calibrated using AASHTOWare Pavement ME Design locally calibrated faulting and transverse cracking model predictions, while in Approach 2 nationally calibrated faulting and transverse cracking model predictions were used.

- The use of two approaches in the local calibration of the IRI model was intended to determine whether the IRI model could be locally calibrated with sufficient accuracy without using local calibration procedures for each distress model, thereby requiring additional costs and data resources. Local calibration of the IRI model using Approach 2 would save significant time and funds. The use of Approach 2 in the local calibration of the IRI model would be especially useful for the Iowa DOT, whether the Iowa DOT decides to use nationally calibrated transverse cracking and faulting models and locally calibrates the IRI model, or instead is more interested in attaining locally calibrated IRI predictions rather than locally calibrated transverse cracking and faulting model predictions.

- In this study, it was determined that using Approach 2, a locally calibrated IRI model can predict distress with sufficient accuracy for Iowa JPCP systems.

- The locally calibrated rutting, longitudinal (top-down) cracking, and IRI prediction models identified in this study are recommended for use with Iowa HMA pavements as alternatives to nationally calibrated models.

- The locally calibrated rutting, longitudinal (top-down) cracking, and IRI prediction models identified in this study are recommended for use in HMA over JPCPs as alternatives to nationally calibrated models.

- The nationally calibrated alligator (bottom-up) and transverse (thermal) cracking prediction models are recommended for use with Iowa HMA systems, because even though the accuracy of these models was improved, the improvement was insignificant. Note that Iowa HMA pavements do not experience severe fatigue-related problems. It was also found that the HMA transverse (thermal) cracking model would be unlikely to satisfactorily simulate this distress for Iowa HMA pavements.

- The nationally calibrated alligator (bottom-up) and thermal cracking prediction models are recommended for use with Iowa HMA over JPCP systems because even though the accuracy of these models was improved, the improvement was insignificant.

- In the local calibration of the IRI model for Iowa HMA pavements and HMA over JPCPs, two approaches were followed. In Approach 1, the IRI model was locally calibrated using AASHTOWare Pavement ME Design locally calibrated rutting and top-down (longitudinal) cracking and nationally calibrated alligator (bottom-up) and transverse (thermal) cracking predictions for HMA pavements and HMA over JPCPs, while in Approach 2 all nationally calibrated model predictions were used. Note that in contrast to the HMA IRI model, reflective cracking predictions were added to the IRI model as part of the area of total fatigue

cracking in HMA over JPCPs. In both Approach 1 and Approach 2, nationally calibrated reflection cracking predictions were employed.

- In this study, it was determined that using Approach 2 a locally calibrated IRI model can predict distress with sufficient accuracy for Iowa HMA and HMA over JPCP systems.

- Preliminary studies were carried out to determine whether there are any differences between the latest version of AASHTOWare Pavement ME Design (version 2.2) released in August 2015 and the version used in this study, AASHTOWare Pavement ME Design version 2.1.24. One significant change between these two versions is the prediction of the Freezing Index Factor, a component of the IRI models. The results indicated some differences in IRI model predictions between these two software versions due to different Freezing Index Factor predictions. Note that Freezing Index Factors are predicted by the software using enhanced integrated climatic models (EICM) and automatically incorporated into the calculation of IRI predictions. The Iowa DOT would deal with this issue by (1) running the software input files provided by the researchers of this study and (2) based on the IRI predictions, locally calibrating the IRI model by modifying only the Freezing Index Factor following the steps documented in this report.

INTRODUCTION

The Mechanistic-Empirical Pavement Design Guide (MEPDG) was completed under National Cooperative Highway Research Program (NCHRP) Project 1-37A (ARA, Inc. 2004) and NCHRP Project 1-40 (AASHTO 2010). The MEPDG provides a novel pavement analysis and design tool employing mechanistic structural response models to calculate pavement responses (stresses, strains, and deflection) and nationally calibrated empirical distress transfer functions to predict pavement performance. This new pavement design concept is called mechanistic-empirical (M-E) pavement design.

Following the release of the MEPDG by the NCHRP (ARA, Inc. 2004), to implement the MEPDG, pavement analysis and design software (MEPDG version 1.1) was also released along with the report for research purposes. The software has since been improved by adding new pavement performance prediction models as well as by advancing existing models. The MEPDG software was commercially released in 2011 as DARWin-ME after the software interface was improved to make it more intuitive and user-friendly; the software has recently been rebranded as AASHTOWare Pavement ME Design.

Upon completion of the national calibration of the MEPDG pavement prediction models, the NCHRP (ARA, Inc. 2004) recommended that state highway agencies (SHAs) conduct local calibration of the models before fully implementing the software. The term "local calibration" in the context of the MEPDG implies a mathematical process of reducing the bias and standard error between actual (measured) pavement distress measurements and pavement performance predictions (AASHTO 2010). Local calibration is conducted by optimizing local calibration coefficients that the empirical distress transfer functions use to reduce bias and standard error. Such local calibration studies are needed for states for which the nationally calibrated pavement performance model predictions are insufficiently accurate. It is to be expected that nationally calibrated performance models would not provide similarly accurate pavement performance predictions for each state because the Long-Term Pavement Performance (LTPP) test sections, and very few other experimental test sections, were used in the national calibration of the MEPDG. While some states had many different LTPP test sections used in the national calibration process, some states had very few sections used. This means that the local conditions of some states may not have been well represented in the national calibration process. Also, the American Association of State Highway and Transportation Officials (AASHTO) (2010) documents state that "policies on pavement preservation and maintenance, construction and material specifications, and materials vary across the United States and are not considered directly in the MEDPG," so AASHTO (2010) recommends employing local calibration studies to take these regional differences into account.

Following the release of the MEPDG by the NCHRP (ARA, Inc. 2004), local calibration of the MEPDG was extensively initiated by agencies separate from national-level follow-up research studies. The Iowa Department of Transportation (DOT) is also in the process of implementing the MEPDG. Once the local calibration of the design guide for Iowa is finalized, it is expected that the guide would be used by state highway engineers and their private counterparts. Accurate prediction of distress in a pavement section during its service time is basically dependent on

reliable pavement performance prediction models. It is quite possible that by using locally calibrated pavement prediction models, the Iowa DOT could save a great deal of money because the accurate prediction of such distress during the service life of a pavement section would enable engineers to take necessary and timely precautions as needed and determine the optimum pavement thickness for resisting all types of loading throughout its service life.

The primary goal of local calibration for AASHTOWare Pavement ME Design is to identify optimized calibration coefficients for the performance prediction models taking local conditions into account to reduce the bias and standard error of predictions compared to actual distress measurements (AASHTO 2010). Therefore, optimizing calibration coefficients is a critical step in the local calibration process. However, most local calibration studies described in the literature have not discussed their optimization procedures in detail, instead reporting only local calibration coefficient results. The procedure employed in previous studies (Darter et al. 2014, Wu et al. 2014, Li et al. 2010, and Bustos et al. 2009) is mainly a trial-and-error approach requiring many MEPDG or AASHTOWare Pavement ME Design software runs with ever-changing calibration coefficients. The main reasons that previous studies used such limited approach include (1) a lack of understanding of pavement performance models comprised of numerous equations, (2) neglecting the review of numerous intermediate output files (mostly in text file format) produced along with the final result summary output files (PDF and Excel file formats), and (3) pavement response results that were previously not provided by MEPDG software but that are now provided by AASHTOWare Pavement ME Design software through intermediate output files.

In this study, a step-by-step procedure for local calibration was established and documented in detail. The local calibration results of AASHTOWare Pavement ME Design were obtained and compared with nationally calibrated and MEPDG locally calibrated models.

Objectives

The first objective of this study was to evaluate the accuracy of nationally calibrated and MEPDG locally calibrated pavement performance prediction models obtained through InTrans Project 11-401 (Ceylan et al. 2013). The second objective of this study was to conduct a recalibration of these models if their accuracy was found to be insufficient. This recalibration process was implemented using AASHTOWare Pavement ME Design version 2.1.24, released in August 2014, with the assistance of linear and nonlinear optimization techniques for improving model prediction accuracy.

Summary of Literature Review Results

The national calibration-validation process was successfully completed for the MEPDG and accompanying AASHTOWare Pavement ME Design software (ARA, Inc. 2004, AASHTO 2010). Although these efforts were comprehensive, further calibration and validation studies to suit local conditions are highly recommended by the MEPDG as a prudent step in implementing a new design procedure different from current procedures. Several national-level research studies supported by the NCHRP and Federal Highway Administration (FHWA) have been conducted

following the release of the original research version of the MEPDG software. Parallel to the national-level research projects, many state/local agencies have either conducted or plan to undertake local calibration studies for their own pavement conditions. As part of InTrans Project 11-401, "Iowa Calibration of MEPDG Performance Prediction Models," Ceylan et al. (2013) reported comprehensive literature review results related to local calibration of MEPDG in both national- and state-level research studies prior to 2012. These results have been updated by incorporating newly reported study results at the time of this project (i.e., 2015) as described in Appendix A. Discussions of the literature review results are presented here.

Three NCHRP research projects are closely related to local calibration of the MEPDG and AASHTOWare Pavement ME Design performance predictions:

- NCHRP Project 9-30 (Von Quintus et al. 2003a, Von Quintus et al. 2003b), "Experimental Plan for Calibration and Validation of Hot Mix Asphalt Performance Models for Mix and Structural Design"
- NCHRP Project 1-40B (Von Quintus et al. 2005, Von Quintus et al. 2007, Von Quintus et al. 2009, AASHTO 2010, TRB 2010), "User Manual and Local Calibration Guide for the Mechanistic-Empirical Pavement Design Guide and Software"
- NCHRP Synthesis 457 (Pierce and McGovern 2014), "Implementation of the AASHTO Mechanistic-Empirical Pavement Design Guide and Software"

Note that NCHRP Project 1-40B is a part of NCHRP 01-40 (available at http://onlinepubs.trb.org as of 2014), "Facilitating the Implementation of the Guide for the Design of New and Rehabilitated Pavement Structures," and is intended to ease the implementation and adoption of the MEPDG by SHAs. Note that the AASHTOWare Pavement ME Design software is the final product of the NCHRP 1-40 study.

Under NCHRP Project 9-30 (NCHRP 2003b), pre-implementation studies involving verification and recalibration have been conducted to quantify the bias and residual error of the flexible-pavement distress models included in an initial version of the MEPDG software (Muthadi 2007). Similarly to the national recalibration of flexible pavement models, NCHRP 1-40 recalibrated the national calibration coefficients of rigid pavement performance models by using more rigid pavement sections than NCHRP 1-37A. Nationally recalibrated coefficients (referred to as original national calibrations [ONCs] in this report) for both flexible and rigid pavement performance models were incorporated into MEPDG version 1.0 and AASHTOWare Pavement ME Design software. As a result of adapting new concrete coefficient of thermal expansion (CTE) testing procedures (AASHTO T336-09 2009), another set of national calibration coefficients (called new national calibrations [NNCs]) for rigid pavement models were determined in 2011 using CTE values determined from new test procedures without adjustment. Until the release of latest AASHTOWare Pavement ME Design software (version 2.2), the ONCs were being used as default national calibration coefficients. However, with the latest software version (version 2.2), users now can choose NNC values as default national calibration coefficients.

Based on the findings of the NCHRP 9-30 study, NCHRP Project 1-40B has focused on preparing (1) a user manual for the MEPDG and its software and (2) a detailed, practical guide for highway agencies performing local or regional calibration of the distress models in the MEPDG and its software. Both the manual and the guide have been presented in the form of draft AASHTO recommended practices, including two or more examples or case studies illustrating the step-by-step procedures. It has also been noted that the longitudinal cracking and reflection cracking models have not been extensively considered in local calibration guide development during the NCHRP 1-40B study because of a lack of prediction accuracy (Muthadi 2007, Von Quintus and Moulthrop 2007). The NCHRP 1-40B study was completed in 2009 and published under the title "Guide for the Local Calibration of the Mechanistic-Empirical Pavement Design Guide" through AASHTO (AASHTO 2010).

NCHRP Synthesis 457 (Pierce and McGovern 2014) conducted a survey of 57 highway transportation agencies, with a 92% response rate from 48 US state highway agencies and a 69% response rate from nine Canadian highway transportation agencies, to document strategies and lessons learned from state highway agencies in implementing the MEPDG. Based on the results of these surveys, it was concluded that three agencies have fully implemented the MEPDG in their pavement designs, 46 agencies were in the act of implementing MEPDG, and eight agencies had no plan at survey time to implement the MEPDG (see Figure 1).

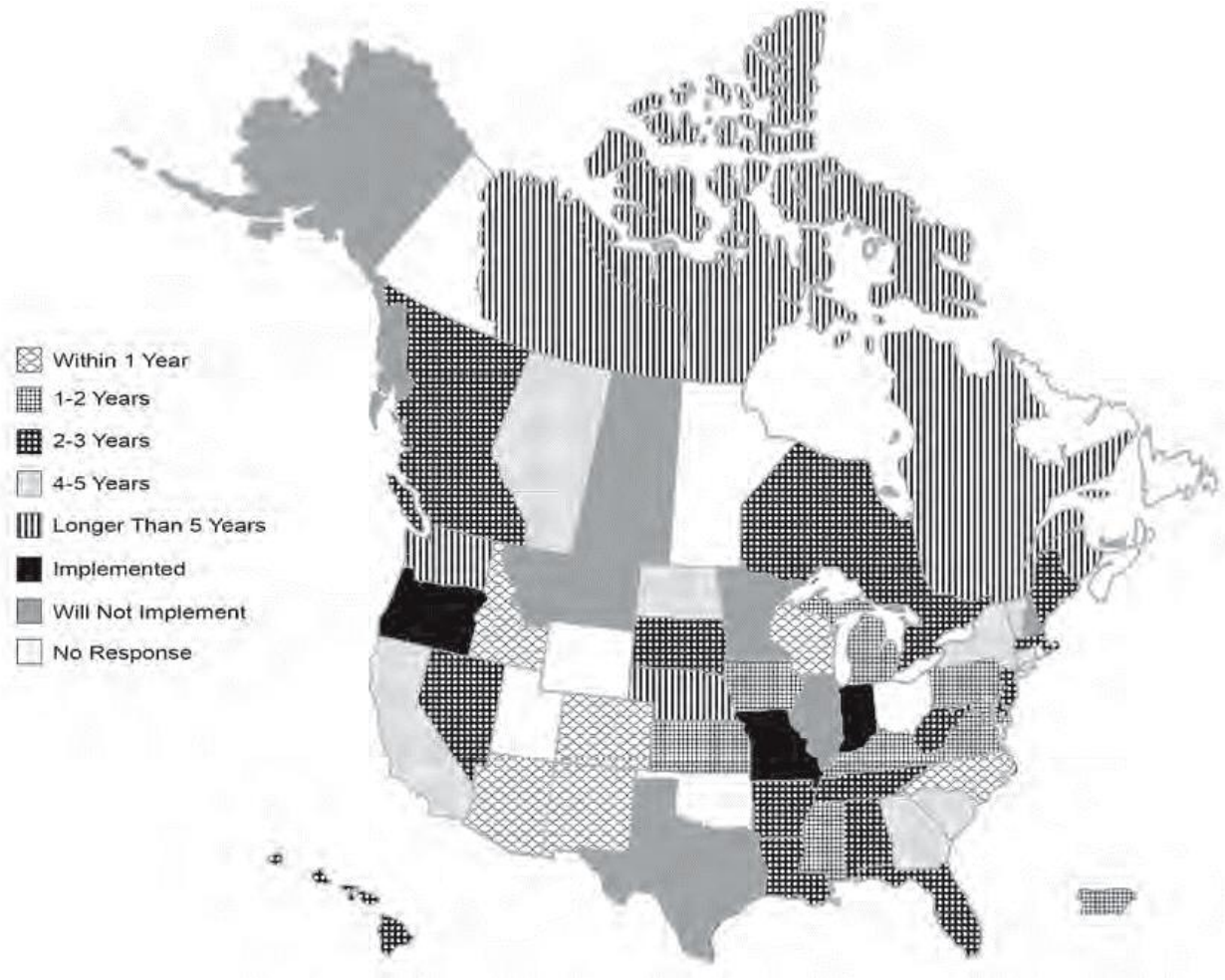

Source: Pierce and McGovern 2014

Figure 1. Summary of agency MEPDG implementation status

Twelve responding agencies also noted that MEPDG pavement performance prediction models were already locally calibrated for their states. Arizona, Colorado, Hawaii, Indiana, Missouri, New Jersey, and Oregon implemented local calibration for hot mix asphalt (HMA) models, and Arizona, Colorado, Florida, Indiana, Missouri, North Dakota, and Oregon implemented local calibration for concrete models. Table 1 and

Table 2 list the states conducting local calibration of HMA and concrete pavement performance prediction models and the models that were locally calibrated.

Table 1. Summary of agency local calibration efforts - asphalt pavement performance models

Agency	IRI	Longitudinal Cracking	Alligator Cracking	Thermal Cracking	Rut Depth		Reflective Cracking
					Asphalt layer	Total	
Arizona	✓	Do not use	✓	*MEPDG*	✓	✓	✓
Colorado	✓	✓	✓	✓	✓	✓	✓
Hawaii	✓	[1]	[1]	[1]	[1]	[1]	[1]
Indiana	✓	Do not use	✓	*MEPDG*	*MEPDG*	Do not use	Do not use
Missouri	✓	*MEPDG*	*MEPDG*	✓	✓	✓	*MEPDG*
New Jersey	✓	[1]	[1]	[1]	[1]	[1]	[1]
Oregon	✓	✓	✓	✓	✓	✓	*MEPDG*

[1]Future plans.
✓Indicates performance prediction models have been locally calibrated.
Source: Pierce and McGovern 2014

Table 2. Agency local calibration - concrete pavement performance models

Agency	JPCP			CRCP	
	IRI	Transverse cracking	Faulting	IRI	Punchouts
Arizona	✓	✓	✓	✓	✓
Colorado	✓	✓	✓	Do not use	Do not use
Florida	✓	✓	✓	Do not use	Do not use
Indiana	✓	*MEPDG*	*MEPDG*	Do not use	Do not use
Missouri	✓	*MEPDG*	*MEPDG*	Do not use	Do not use
North Dakota	✓	*MEPDG*	*MEPDG*	Do not use	Do not use
Oregon	✓	*MEPDG*	*MEPDG*	✓	✓

✓Indicates performance prediction models have been locally calibrated.
Source: Pierce and McGovern 2014

Note in Table 1 that Arizona and Colorado locally calibrate the empirical reflective cracking model originally included in the MEPDG. Major challenges indicated by the surveyed agencies include software complexity, the availability of needed data, the difficulty of defining input levels, and a need for local calibration.

Two research studies supported by the FHWA have been conducted on using pavement management system (PMS) data for local calibration of the MEPDG. The study "Using Pavement Management Data to Calibrate and Validate the New MEPDG, An Eight State Study" (Hudson et al. 2006a, Hudson et al. 2006b) evaluated the potential use of PMS data for MEPDG local calibration. Eight states participated in this study: Florida, Kansas, Minnesota, Mississippi, New Mexico, North Carolina, Pennsylvania, and Washington. The study concluded that all participating states could feasibly use PMS data for MEPDG calibrations and other states not participating in the study could do the same. It was recommended that each SHA should develop a satellite pavement management/pavement design database for each project being designed and constructed using the MEPDG as part of the currently used PMS.

The second follow-up study, FHWA HIF-11-026, "Local Calibration of the MEPDG Using Pavement Management Systems" (APTech, Inc. 2010) was conducted to develop a framework for using existing PMS data to calibrate MEPDG performance models. One state (North Carolina) was selected based on screening criteria to finalize and verify the MEPDG calibration framework based on a set of actual conditions. Using this developed framework, local calibration for the selected state was demonstrated under the assumptions of both MEPDG performance predictions established by NCHRP 1-37A as well as distress measurements from a selected state. Local/state-level research studies have also been conducted in addition to national-level research studies. Studies on rigid pavement performance prediction model calibration, primarily focusing on new jointed plain concrete pavement (JPCP), include studies by Li et al. (2006) in Washington, Schram and Abdelrahman (2006) in Nebraska, Darter et al. (2009) in Utah, Velasquez et al. (2009) in Minnesota, Titus-Glover and Mallela (2009) in Ohio, Mallela et al. (2009) in Missouri, Kim et al. (2010) in Iowa, Bustos et al. (2009) in Argentina, Delgadillo et al. (2011) in Chile, Li et al. (2010) in Washington, Mallela et al. (2013) in Colorado, and Darter et al. (2014) in Arizona.

As a result of these studies, 11 US state highway agencies have approved the use of nationally calibrated coefficients (either ONC or NNC) for new JPCP while eight agencies have adopted locally calibrated coefficients (Mu et al. 2015). The states adopting nationally calibrated coefficients are Utah, Wyoming, Delaware, Indiana, Kansas, New York, North Carolina, Oklahoma, Pennsylvania, South Dakota, and Virginia. The states of Arizona, Colorado, Louisiana, Missouri, Ohio, Washington, and Florida have decided to use at least one of the local calibration coefficients different from the national ones for their JPCP performance prediction models. Table 3 summarizes the calibration coefficients of the state highway agencies for JPCP performance prediction models, along with optimization method, MEPDG version, and the project data source used in the local calibration process.

The following studies have been conducted for new HMA pavement and HMA overlaid pavement systems: Galal and Chehab (2005) in Indiana, Von Quintus and Moulthrop (2007) in Montana, Kang et al. (2007) mainly in Wisconsin, Schram and Abdelrahman (2006) in Nebraska, Muthadi and Kim (2008), Corley-Lay et al. (2010), and Jadoun (2011) in North Carolina, Li et al. (2009) and Li et al. (2010) in Washington, Banerjee et al. (2010) and Banerjee et al. (2011) in Texas, Titus-Glover and Mallela (2009) in Ohio, Darter et al. (2009) in Utah, Souliman et al. (2010) and Mamlouk and Zapata (2010) in Arizona, Kim et al. (2010) in Iowa, Khazanovich et al. (2008), Velasquez et al. (2009), and Hoegh et al. (2010) in Minnesota, Hall et al. (2011) in Arkansas, Tarefder and Rodriquez-Ruiz (2013) in New Mexico, Mallela et al. (2013) in Colorado, Zhou et al. (2013) in Tennessee, and Darter et al. (2014) in Arizona.

Table 3. Local calibration coefficients for JPCP systems

	Calibration coefficients	ONC	NNC	Arizona	Colorado	Lousiana	Missouri	Ohio	Washington	Florida
Cracking	**C1**	2		NNC	NNC	2.6	ONC	ONC	1.93	2.8389
	C2	1.22		NNC	NNC	ONC	ONC	ONC	1.177	0.9647
	C4	1	0.6	0.19	NNC	ONC	ONC	ONC	ONC	0.564
	C5	-1.98	-2.05	-2.067	NNC	ONC	ONC	ONC	ONC	-0.5946
Faulting	**C1**	1.0184	1.2526	0.0355	0.5104	ONC	ONC	ONC	ONC	4.0472
	C2	0.91656	1.1274	0.1147	0.00838	ONC	ONC	ONC	ONC	ONC
	C3	0.00218	0.0027	0.00436	0.00147	ONC	ONC	ONC	ONC	ONC
	C4	0.00088	0.0011	1.10E-07	0.008345	ONC	ONC	ONC	ONC	ONC
	C5	250		20000	5999	ONC	ONC	ONC	ONC	ONC
	C6	0.4		2.0389	0.8404	1.2	ONC	ONC	ONC	0.079
	C7	1.83312	9.1	0.189	5.9293	ONC	ONC	ONC	ONC	ONC
	C8	400		NNC	NNC	ONC	ONC	ONC	ONC	ONC
IRI	**J1**	0.8203		0.6	NNC	ONC	0.82	0.82	ONC	ONC
	J2	0.4417		3.48	NNC	ONC	1.17	3.7	ONC	ONC
	J3	1.4929		1.22	NNC	ONC	1.43	1.711	ONC	2.2555
	J4	25.24		45.2	NNC	ONC	66.8	5.703	ONC	ONC
Optimization techniques used in local calibration		Statistical Analysis		Sensitivity Analysis	Statistical Analysis	Sensitivity Analysis/Trial Error	Statistical Software	Statistical & Non-statistical	Sensitivity Analysis/Trial error	N/A
MEPDG version used in local calibration		N/R		DARWin-ME	DARWin-ME	Pavement ME	N/A	N/A	MEPDG version 1.0	N/A
Project data source		LTPP		LTPP and ADOT PMS	LTPP and CDOT PMS	LA PMS	LTPP and MoDOT	LTPP	WSPMS	N/A

ONC: Original Calibration Coefficients
NNC: New National Calibration
LTPP: Long-Term Pavement Performance Program
CDOT and MoDOT: Colorado Departments of Transportation and Missouri Departments of Transportation
LA PMS and WSPMS: Louisiana and Washington State Pavement Management Systems
N/R: Not Required, N/A: Not Available

Table 4 lists the locally calibrated coefficients of new HMA and HMA overlaid pavement systems for Arizona, Colorado, and Missouri as well as the corresponding optimization method, MEPDG version, and the project data source for each study used in the local calibration process.

Table 4. Local calibration coefficients for flexible and HMA overlaid pavement systems

	Calibration coefficients	National default values	Arizona	Colorado	Missouri
Cracking	**C1 Bottom**	1	National	0.07	National
	C1 Top	7	National	National	National
	C2 Bottom	1	4.5	2.35	National
	C2 Top	3.5	National	National	National
	C3 Bottom	6000	National	National	National
	C3 Top	0	National	National	National
	C4 Top	1000	National	National	National
Fatigue	**BF1**	1	249.00872	130.367	National
	BF2	1	National	National	National
	BF3	1	1.23341	1.2178	National
Thermal Fracture	**Level 1**	1.5	National	7.5	0.625
	Level 2	0.5	National	National	National
	Level 3	1.5	National	National	National
Rutting (asphalt)	**BR1**	1	0.69	1.34	1.07
	BR2	1	National	National	National
	BR3	1	National	National	National
Rutting (subgrade)	**BS1 (fine)**	1	0.37	0.84	0.4375
	BS1 (granular)	1	0.14	0.4	0.01
IRI	**J1 (asphalt)**	40	1.2281	35	17.7
	J2 (asphalt)	0.4	0.1175	0.3	0.975
	J3 (asphalt)	0.008	National	0.02	National
	J4 (asphalt)	0.015	0.028	0.019	0.01
	J1 (over concrete)	40.8	National	National	National
	J2 (over concrete)	0.575	National	National	National
	J3 (over concrete)	0.0014	National	National	National
	J4 (over concrete)	0.00825	National	National	National
Optimization techniques used		Statistical Analysis	Sensitivity Analysis	Statistical Analysis	Statistical and non-statistical
MEPDG version used in local calibration		N/R	DARWin-ME	DARWin-ME	N/A
Project data source		LTPP	LTPP and CDOT PMS	LTPP and CDOT PMS	WIM-IRD and LTPP

N/R: Not Required, N/A: Not Available

Along with local calibration efforts for the new HMA and HMA overlaid pavement performance prediction models in Table 4, some states implemented local calibration for some of the flexible and composite HMA overlaid pavement performance prediction models, as listed below:

- Ohio: HMA rutting, subgrade rutting, and International Roughness Index (IRI) models
- Washington: Fatigue, HMA rutting, subgrade rutting, alligator cracking, and longitudinal cracking models
- Montana: Thermal fracture models
- New Mexico: HMA rutting, subgrade rutting, alligator cracking, and longitudinal cracking models
- North Carolina: HMA rutting and subgrade rutting models
- Texas: HMA rutting and subgrade rutting models

The procedures and findings of all these studies related to both concrete-surfaced and asphalt-surfaced pavements are summarized in Appendix A. Several significant issues relevant to the present study are highlighted below:

- Rutting for asphalt-surfaced pavements: The accuracy of nationally calibrated rutting models was evaluated in Arkansas, Colorado, Missouri, New Mexico, North Carolina, Ohio, Texas, and Washington. Most state-level studies indicate that MEPDG overpredicts total rut depth because significant rutting was predicted in unbound layers and embankment soils. However, rutting predictions could be improved through local calibration.

- Longitudinal (top-down) cracking for asphalt-surfaced pavements: The accuracy of nationally calibrated longitudinal (top-down) cracking models was evaluated in Arkansas, Minnesota, Montana, New Mexico, and Washington. Montana observed significant differences between actual and MEPDG-predicted longitudinal cracking values and did not calibrate this model at the time of its MEPDG implementation. Other states performed local calibration of at least one of the calibration coefficients of this prediction model. However, no consistent trend in the longitudinal (top-down) cracking predictions could be identified that would reduce the bias and standard error and thereby improve the accuracy of this prediction model.

- Alligator (bottom-up) cracking for asphalt-surfaced pavements: The accuracy of nationally calibrated alligator (bottom-up) cracking models was evaluated in Arkansas, Colorado, Minnesota, Missouri, Montana, New Mexico, Ohio, and Washington. A Missouri study found the nationally calibrated alligator model underpredicting in HMA pavements. On the other hand, a Washington study found the nationally calibrated model both underpredicting and overpredicting alligator cracking. Washington, Arkansas, and New Mexico also used a locally calibrated alligator cracking model and, after local calibration, the model accuracy improved to some extent.

- Thermal (transverse) cracking for asphalt-surfaced pavements: The accuracy of nationally calibrated alligator (bottom-up) cracking models was evaluated in Colorado, Missouri, and Montana.

- Reflection cracking for HMA overlaid concrete pavements: Only one state (Arizona) attempted to calibrate the empirical reflection cracking model of HMA overlaid concrete pavements using AASHTOWare Pavement ME Design software. However, the empirical reflection cracking model was replaced by a mechanistic-based reflection cracking model developed in NCHRP Project 1-41 (Lytton et al. 2010) and is provided in the new version of AASHTOWare Pavement ME Design (version 2.2) released in August 2015.

REVIEW OF AASHTOWARE PAVEMENT ME DESIGN SOFTWARE

MEPDG has evolved since its first release in 2004 as a product of NCHRP Project 1-37A (ARA, Inc. 2004). The first version of the software was designated MEPDG version 1.1. New versions of the software have subsequently been released with new features and enhancements added. AASHTO's *MEPDG, Interim Edition: A Manual of Practice* was issued in 2008 to educate users about the design methodology software used (AASHTO 2008). As more features were added to the software, it was rebranded as DARWin-ME in 2011 and AASHTOWare Pavement ME Design in 2014.

After the release of the MEPDG by the NCHRP (ARA, Inc. 2004), the national recalibration of the MEPDG was initiated under NCHRP Project 1-40 using a larger number of pavement sections than was used in NCHRP 1-37A (2004). National calibration coefficients resulting from NCHRP Project 1-40 have been widely used since then, and the previous calibration coefficients have been discarded.

Coefficient of thermal expansion is an important parameter in determining the length change of concrete pavements under different thermal conditions. Crawford et al. (2010) found that the CTE model incorporated in the MEPDG software produced erroneous results due to an error in the test procedure. The test procedure used in the characterization of CTE was initially AASHTO TP 60-00 (2004), and, using this test procedure, CTE values were found to be overpredicted. A new test procedure was accordingly developed (AASHTO T 336-09 2009) and new CTE values specified based on the new test procedure. The related distress models were nationally recalibrated in 2011, and the recalibrated coefficients (i.e., NNC) have recently been incorporated into the latest software version (version 2.2) as default national calibration coefficients. It was suggested to AASHTOWare Pavement ME Design users that they use either ONC in using CTE values determined from the TP 60-00 method (AASHTO TP 60-00 2004) or NNC in using CTE values determined from the newer test procedure (AASHTO T 336-09 2009). The CTE values used in this study were acquired from a previous MEPDG implementation study, Task 6, "Material Thermal Inputs for Iowa Materials" (Wang et al. 2008), which used AASHTO TP 60-00 (2004) in the characterization of CTE values.

In the historical development of MEPDG software, as new features were added and available features expanded and improved, software incorporating the new enhancements has been released along with accompanying release notes to introduce these enhancements. The contents of all release notes issued are summarized below (adapted from http://www.me-design.com/MEDesign/Documents.html):

April 2011 (DARWin-ME Version 1.0)

In this release note, differences between the MEPDG and DARWin-ME are documented. The major new capabilities included in the software were as follows:

- A completely redesigned user interface

- Enterprise database support for sharing and storing projects, materials, traffic, and design considerations across the agency
- Ability to edit and run multiple design analyses simultaneously in batch, sensitivity, thickness optimization, or back calculation modes
- Redesigned and improved output reports in both Excel and Adobe PDF formats
- Climate data editing tools
- Redesigned PDF help documents based on the new software and the Mechanistic-Empirical Pavement Design Guide, Interim Edition: A Manual of Practice
- Significant decreases in analyses run time

December 2011 (DARWin-ME Version 1.1.33)

- Some software issues were resolved.

February 2013 (AASHTOWare Pavement ME Design Version 1.3.28)

- Some software issues were resolved.

July 2013 (AASHTOWare Pavement ME Design Version 1.5.08, Educational Version 1.5.08)

- The educational version of the software could only be used for the design of new asphalt and concrete (JPCP and continuously reinforced concrete pavements [CRCP]), asphalt concrete (AC)/AC overlays, AC/JPCP overlays, or unbonded Portland cement concrete (PCC) overlays for a 30 year limited analysis period.
- Only eight stations representing different climate zones around the country could be used in the educational version. Additionally, batch mode and sensitivity analysis could not be used in this version. Unlike the conventional version, no access was provided to intermediate output files in the educational version.

January 2014 (AASHTOWare Pavement ME Design Version 2.0.19, Educational Version 2.0.19)

- Citrix and Remote Desktop Services were added.
- A layer-by-layer asphalt rutting coefficient could now be used for analysis.
- The US customary bins were converted to rounded International System of Units (SI) metric bins.
- Special axle traffic information could be input by selecting a special traffic checkbox on the main project tab.
- The database was improved to be more stable and provide enhanced selection and insert functionality.
- A file converter was added to convert Version 1.1 files to the new 2.0 format before the software is run.

August 2014 (AASHTOWare Pavement ME Design Version 2.1.24)

- Users could receive back-calculation summary reports, enabling them to use back calculation with thickness optimization on each station project.
- Users could use an automatic updater providing them with an option to automatically check for available system updates.
- A feature for incorporating subgrade moduli in sensitivity analysis for any selected layer was added.

August 2015 (AASHTOWare Pavement ME Design Version 2.2)

- A new reflection cracking model developed from NCHRP Project 1-41 was added.
- Drainage Requirement In Pavements (DRIP) can be used as an accompanying tool to conduct hydraulic design computations for subsurface pavement drainage analysis.
- New calibration coefficients for JPCP cracking, JPCP faulting, and CRCP punch-out models were added.
- LTPP default axle load distributions could be imported.
- A MapME tool providing data from geographical information system data linkages to AASHTOWare Pavement ME Design was added.
- The semi-rigid pavement type replaced the new AC over cement-treated base (CTB) design type.
- Level 1 and Level 2 input data for AC overlays over AC rehabilitated pavements; Level 3 input data for AC overlays over intact JPCP rehabilitated pavements; and new Level 1, Level 2, and Level 3 inputs for PCC overlays over existing AC pavements were provided.

Training Webinar Series

A series of 13 webinars (each about two hours long) was prepared by the FHWA in collaboration with the AASHTO Pavement ME Design Task Force to introduce different aspects of the software. Ten of these webinars were related to the material and design inputs used in the software for the design of different pavement systems, and the remaining three webinars were related to local software calibration. The webinar series can be accessed at http://www.me-design.com. The titles in the webinar series are as follows:

1. Getting Started with ME Design
2. Climatic Inputs
3. Traffic Inputs
4. Material and Design Inputs for New Pavement Design
5. Material and Design Inputs for Pavement Rehabilitation with Asphalt Overlays
6. Material and Design Inputs for Pavement Rehabilitation with Concrete Overlays
7. New Asphalt Pavement Structures
8. Asphalt Overlays of Asphalt Pavements
9. New Concrete Pavement Structures

10. Unbonded Concrete Overlays
11. Introduction to Local Calibration
12. Preparing for Local Calibration
13. Determining the Local Calibration Coefficients

This report presents design examples of new JPCP, new HMA, and HMA over JPCP using AASHTOWare Pavement ME Design (version 2.1.24) (see Appendix B). The design of such pavements was introduced in a step-by-step manner using screenshots from the software.

EVALUATION OF AASHTOWARE PAVEMENT ME DESIGN SOFTWARE: COMPARISON BETWEEN AASHTOWARE PAVEMENT ME DESIGN AND MEPDG PAVEMENT PERFORMANCE PREDICTIONS

To compare pavement performance predictions made by the AASHTOWare Pavement ME Design and MEPDG software, a set of 15 cases used in NCHRP 1-47 (Schwartz et al. 2011) representing different climate and traffic conditions were analyzed. The case name and corresponding description of each case can be seen in Table 5.

Table 5. Fifteen total base cases used in NCHRP Project 1-47

Base Case Name	Description
CDL	Cold-Dry-Low-Traffic
CDM	Cold-Dry-Medium-Traffic
CDH	Cold-Dry-High-Traffic
CWL	Cold-Wet-Low-Traffic
CWM	Cold-Wet-Medium-Traffic
CWH	Cold-Wet-High-Traffic
TL	Temperate-Low-Traffic
TM	Temperate-Medium-Traffic
TH	Temperate-High-Traffic
HDL	Hot-Dry-Low-Traffic
HDM	Hot-Dry-Medium-Traffic
HDH	Hot-Dry-High-Traffic
HWL	Hot-Wet-Low-Traffic
HWM	Hot-Wet-Medium-Traffic
HWH	Hot-Wet-High-Traffic

Source: Schwartz et al. 2011

To represent a variety of different climate conditions in the US, five different locations were selected representing significantly different climates. Climate category, location, weather station, and total available climate data about each station are summarized in Table 6.

Table 6. Climate categories used in NCHRP 1-47

Climate Category	Location	Weather Station	Months of Data
Hot-Wet	Orlando, FL	ORLANDO INTERNATIONALARPT	116
Hot-Dry	Phoenix, AZ	PHOENIX SKY HARBOR INTL AP	116
Cold-Wet	Portland, ME	PORTLAND INTL JETPORT ARPT	11 6
Cold-Dry	International Falls, MN	FALLS INTERNATIONAL ARPT	112
Temperate	Los Angeles, CA	LOS ANGELES INTL AIRPORT	108

Source: Schwartz et al. 2011

To simulate different traffic conditions in the US, three categories of traffic conditions were determined: low, medium, and high. Table 7 shows each traffic category and corresponding annual average daily truck traffic (AADTT) values, AADTT values in the design lane, estimated equivalent single axle loads (ESALs) for both flexible and rigid pavements, and the AADTT range fitting each traffic category.

Table 7. Traffic levels used in NCHRP Project 1-47

Traffic Category	Baseline Inputs			AADTT Range
	AADTT	Est. ESALs (Flexible)	Est. ESALs (Rigid)	
Low	1,000	2M	5M	500-5,000
Medium	7,500	10M	25M	5,000-10,000
High	25,000	30M	75M	20,000-30,000

Source: Schwartz et al. 2011

Using the same input parameters for all cases except for different climate and traffic conditions, simulations in MEPDG v.1.1, AASHTOWare Pavement ME Design v.2.0, and AASHTOWare Pavement ME Design v.2.1.24 were run. Table 8 summarizes the pavement performance predictions for new JPCP cases using MEPDG v.1.1, AASHTOWare Pavement ME Design v.2.0, and AASHTOWare Pavement ME Design v.2.1.24.

As can be seen from Table 8, significant differences in transverse cracking and IRI predictions under cold climate zones between MEPDG v.1.1 and the AASHTOWare Pavement ME Design versions were observed. However, no significant differences between pavement performance predictions using AASHTOWare Pavement ME Design v.2.0 and AASHTOWare Pavement ME Design v.2.1 were observed.

Table 8. Pavement performance prediction comparisons for new JPCP cases

CaseType	CaseType2	Pavement age		Faulting (in) (MEPDG v.1.1)	Faulting (in) (Pavement ME v.2.0)	Faulting (in) (Pavement ME v.2.1.24)	Percent slabs cracked (MEPDG v.1.1)	Percent slabs cracked(Pavement ME v.2.0)	Percent slabs cracked(Pavement ME v.2.1.24)	IRI (in/mile) (MEPDG v.1.1)	IRI (in/mile) (Pavement ME v.2.0)	IRI (in/mile) (Pavement ME v.2.1.24)
Fixed	Fixed											
		mo	yr									
CDL	**New**	300	25	0.01	0.01	0.01	**16.8**	**13.0**	**13.0**	**141.10**	**184.45**	**184.45**
CDM	**New**	300	25	0.05	0.05	0.05	**5.5**	**3.4**	**3.4**	**152.30**	**195.84**	**195.84**
CDH	**New**	300	25	0.13	0.13	0.13	**1.6**	**1.0**	**1.0**	**186.00**	**230.63**	**230.63**
CWL	**New**	300	25	0.02	0.02	0.02	**10.7**	**10.1**	**10.1**	**106.00**	**130.91**	**130.91**
CWM	**New**	300	25	0.09	0.09	0.09	**2.4**	**2.3**	**2.3**	**133.40**	**160.81**	**160.81**
CWH	**New**	300	25	0.17	0.17	0.17	**0.6**	**0.6**	**0.6**	**171.70**	**199.02**	**199.02**
HDL	**New**	300	25	0.01	0.01	0.01	14.7	14.2	14.2	80.80	80.79	80.79
HDM	**New**	300	25	0.05	0.05	0.05	6.6	5.6	5.6	96.30	96.25	96.25
HDH	**New**	300	25	0.16	0.16	0.16	1.9	1.4	1.4	146.40	146.86	146.86
HWL	**New**	300	25	0.01	0.01	0.01	5.1	5.1	5.1	72.80	73.04	73.04
HWM	**New**	300	25	0.05	0.05	0.05	1.9	1.8	1.8	89.30	90.34	90.34
HWH	**New**	300	25	0.13	0.13	0.13	0.4	0.4	0.4	132.20	133.24	133.24
TL	**New**	300	25	0.01	0.01	0.01	1.6	1.6	1.6	68.20	68.43	68.43
TM	**New**	300	25	0.03	0.03	0.03	0.3	0.3	0.3	80.60	81.51	81.51
TH	**New**	300	25	0.10	0.10	0.10	0.1	0.1	0.1	116.70	118.50	118.50

Using the same input parameters for all cases except for different climate and traffic conditions, simulations in MEPDG v.1.1, AASHTOWare Pavement ME Design v.2.0, and AASHTOWare Pavement ME Design v.2.1.24 were run.

Table 9 summarizes pavement performance predictions for new JPCP over stiff foundation cases using MEPDG v.1.1, AASHTOWare Pavement ME Design v.2.0, and AASHTOWare Pavement ME Design v.2.1.24. As can be seen from the table, MEPDG v.1.1 overpredicts transverse cracking and underpredicts IRI for cold climate zones in comparison to the AASHTOWare Pavement ME Design versions. No significant differences between pavement performance predictions using Pavement ME Design v.2.0 and Pavement ME Design v.2.1.24 were observed.

Table 10 summarizes the cracking predictions of MEPDG v.1.1, AASHTOWare Pavement ME Design v.2.0, and AASHTOWare Pavement ME Design v.2.1.24 for new HMA cases. MEPDG v.1.1 underpredicts longitudinal cracking compared to the AASHTOWare Pavement ME Design versions for all climate zones. Some differences in alligator cracking predictions under different climate zones were observed between MEPDG v.1.1 and the AASHTOWare Pavement ME Design versions. Also note that in cold-wet weather conditions, MEPDG v.1.1 overpredicts transverse cracking compared to the AASHTOWare Pavement ME Design versions. No significant differences between pavement performance predictions using AASHTOWare Pavement ME Design v.2.0 and AASHTOWare Pavement ME Design v.2.1.24 were observed.

Table 11 summarizes the rutting and IRI predictions of MEPDG v.1.1, AASHTOWare Pavement ME Design v.2.0, and AASHTOWare Pavement ME Design v.2.1.24 for new HMA cases. Some differences in rutting and IRI predictions under different climate zones can be observed between MEPDG v.1.1 and the AASHTOWare Pavement ME Design versions. No significant differences between pavement performance predictions using AASHTOWare Pavement ME Design v.2.0 and AASHTOWare Pavement ME Design v.2.1.24 were observed.

Table 12 summarizes cracking predictions of MEPDG v.1.1, AASHTOWare Pavement ME Design v.2.0, and AASHTOWare Pavement ME Design v.2.1.24 for HMA over stiff foundation cases. For all climate zones, MEPDG v.1.1 underpredicts longitudinal cracking compared to the AASHTOWare Pavement ME Design versions. Some differences in alligator cracking predictions for different climate zones can be observed between MEPDG v.1.1 and the AASHTOWare Pavement ME Design versions. Also note that in cold-wet weather conditions, MEPDG v.1.1 overpredicts transverse cracking compared to the AASHTOWare Pavement ME Design versions. No significant differences between pavement performance predictions using AASHTOWare Pavement ME Design v.2.0 and AASHTOWare Pavement ME Design v.2.1.24 were observed.

Table 13 summarizes the rutting and IRI predictions of MEPDG v.1.1, AASHTOWare Pavement ME Design v.2.0, and AASHTOWare Pavement ME Design v.2.1.24 for HMA over stiff foundation cases. Some differences in rutting and IRI predictions for different climate zones can be observed between MEPDG v.1.1 and the AASHTOWare Pavement ME Design versions. No significant differences between pavement performance predictions using AASHTOWare Pavement ME Design v.2.0 and AASHTOWare Pavement ME Design v.2.1.24 were observed.

Table 9. Pavement performance prediction comparisons for new JPCP over stiff foundation cases

CaseType	CaseType 2	Pavement age		Faulting (in) (MEPDG v.1.1)	Faulting (in) (Pavement ME v.2.0)	Faulting (in) (Pavement ME v.2.1.24)	Percent slabs cracked (MEPDG v.1.1)	Percent slabs cracked(Pavement ME v.2.0)	Percent slabs cracked(Pavement ME v.2.1.24)	IRI (in/mile) (MEPDG v.1.1)	IRI (in/mile) (Pavement ME v.2.0)	IRI (in/mile) (Pavement ME v.2.1.24)
Fixed	Fixed											
		mo	yr									
CDL	**New**	300	25	0.01	0.01	0.01	**32.5**	**28.8**	**28.8**	**152.10**	**179.13**	**179.13**
CDM	**New**	300	25	0.03	0.04	0.04	**41.0**	**34.6**	**34.6**	**172.00**	**198.46**	**198.46**
CDH	**New**	300	25	0.08	0.08	0.08	**3.8**	**2.3**	**2.3**	**165.20**	**193.71**	**193.71**
CWL	**New**	300	25	0.01	0.01	0.01	**22.6**	**22.0**	**22.0**	**111.60**	**130.32**	**130.32**
CWM	**New**	300	25	0.07	0.07	0.07	**21.8**	**20.8**	**20.8**	**137.30**	**156.06**	**156.06**
CWH	**New**	300	25	0.12	0.12	0.12	**1.1**	**1.0**	**1.0**	**146.70**	**166.49**	**166.49**
HDL	**New**	300	25	0.01	0.01	0.01	23.3	24.2	24.2	86.10	87.25	87.25
HDM	**New**	300	25	0.04	0.04	0.04	30.6	26.6	26.6	108.50	105.50	105.50
HDH	**New**	300	25	0.09	0.09	0.09	5.4	3.3	3.3	117.70	115.06	115.06
HWL	**New**	300	25	0.01	0.01	0.01	7.5	7.9	7.9	73.10	73.66	73.66
HWM	**New**	300	25	0.03	0.03	0.03	7.8	7.6	7.6	86.30	86.25	86.25
HWH	**New**	300	25	0.07	0.07	0.07	0.9	0.8	0.8	100.70	100.48	100.48
TL	**New**	300	25	0.00	0.00	0.00	0.0	2.2	2.2	65.00	67.54	67.54
TM	**New**	300	25	0.02	0.02	0.02	1.6	1.7	1.7	74.60	75.08	75.08
TH	**New**	300	25	0.04	0.04	0.04	0.1	0.1	0.1	87.10	87.38	87.38

Table 10. Pavement performance prediction comparisons for new HMA cases: cracking

CaseType	CaseType2	Pavement age		Longitudinal Cracking (ft/mi) (MEPDG v.1.1)	Longitudinal Cracking (ft/mi) (Pavement ME v.2.0)	Longitudinal Cracking (ft/mi) (Pavement ME v.2.1.24)	Alligator Cracking (%) (MEPDG v.1.1)	Alligator Cracking (%) (Pavement ME v.2.0)	Alligator Cracking (%) (Pavement ME v.2.1.24)	Transverse Cracking (ft/mi) (MEPDG v.1.1)	Transvers Cracking (ft/mi) (Pavement ME v.2.0)	Transverse Cracking (ft/mi) (Pavement ME v.2.1.24)
Fixed	Fixed											
		mo	yr									
CDL	**New**	180	15	**1140**	**3280**	**3280**	**1.97**	**2.89**	**2.89**	0	0	0
CDM	**New**	180	15	**25.3**	**237**	**237**	**1.42**	**2.01**	**2.01**	0	0	0
CDH	**New**	180	15	**0.25**	**13.9**	**13.9**	**1.27**	**1.82**	**1.82**	0	0	0
CWL	**New**	180	15	**3130**	**2420**	**2420**	**3.57**	**2.28**	**2.28**	0.3	0.02	0.02
CWM	**New**	180	15	**168**	**125**	**125**	**2.51**	**1.55**	**1.55**	0.2	0.01	0.01
CWH	**New**	180	15	**1.5**	**3.83**	**3.83**	**2.22**	**1.37**	**1.37**	0.1	0	0
HDL	**New**	180	15	1910	2030	2030	2.59	1.77	1.77	0	0	0
HDM	**New**	180	15	36.1	95.9	95.9	1.94	1.31	1.31	0	0	0
HDH	**New**	180	15	0.33	2.82	2.82	1.78	1.27	1.27	0	0	0
HWL	**New**	180	15	1060	1350	1350	2.55	1.87	1.87	0	0	0
HWM	**New**	180	15	2.5	9.43	9.43	1.88	1.31	1.31	0	0	0
HWH	**New**	180	15	0.07	0.76	0.76	1.8	1.23	1.23	0	0	0
TL	**New**	180	15	598	752	752	1.82	1.29	1.29	0	0	0
TM	**New**	180	15	1.45	4.98	4.98	1.34	0.934	0.934	0	0	0
TH	**New**	180	15	0.03	0.4	0.4	1.3	0.924	0.924	0	0	0

Table 11. Pavement performance prediction comparisons for new HMA cases: rutting and IRI

CaseType	CaseType 2	Pavement age		AC Rutting (in) (MEPDG v.1.1)	AC Rutting (in) (Pavement ME v.2.0)	AC Rutting (in) (Pavement ME v.2.1.24)	Total Rutting (in) (MEPDG v.1.1)	Total Rutting (in) (Pavement ME v.2.0)	Total Rutting (in) (Pavement ME v.2.1.24)	IRI in/mile (MEPDG v.1.1)	IRI in/mile(Pavement ME v.2.0)	IRI in/mile(Pavement ME v.2.1.24)
Fixed	Fixed											
		mo	yr									
CDL	**New**	180	15	**0.17**	**0.20**	**0.20**	**0.50**	**0.58**	**0.58**	**103.9**	**111.9**	**111.9**
CDM	**New**	180	15	**0.38**	**0.44**	**0.44**	**0.70**	**0.80**	**0.80**	**111.5**	**118.4**	**118.4**
CDH	**New**	180	15	**0.51**	**0.57**	**0.57**	**0.81**	**0.92**	**0.92**	**115.8**	**123.2**	**123.2**
CWL	**New**	180	15	**0.23**	**0.19**	**0.19**	**0.59**	**0.52**	**0.52**	**110.5**	**108.4**	**108.4**
CWM	**New**	180	15	**0.51**	**0.41**	**0.41**	**0.86**	**0.73**	**0.73**	**120.5**	**115.3**	**115.3**
CWH	**New**	180	15	**0.68**	**0.54**	**0.54**	**1.01**	**0.85**	**0.85**	**126.2**	**119.7**	**119.7**
HDL	**New**	180	15	0.30	0.29	0.29	0.61	0.58	0.58	102.1	101.8	101.8
HDM	**New**	180	15	0.64	0.64	0.64	0.95	0.92	0.92	115.0	114.2	114.2
HDH	**New**	180	15	0.84	0.82	0.82	1.14	1.10	1.10	122.6	121.1	121.1
HWL	**New**	180	15	0.17	0.20	0.20	0.50	0.50	0.50	101.2	102.0	102.0
HWM	**New**	180	15	0.37	0.44	0.44	0.69	0.74	0.74	108.3	110.4	110.4
HWH	**New**	180	15	0.50	0.57	0.57	0.81	0.86	0.86	113.0	114.9	114.9
TL	**New**	180	15	0.12	0.14	0.14	0.43	0.42	0.42	95.8	95.7	95.7
TM	**New**	180	15	0.26	0.32	0.32	0.56	0.59	0.59	100.7	101.9	101.9
TH	**New**	180	15	0.36	0.40	0.40	0.65	0.68	0.68	104.0	105.2	105.2

Table 12. Pavement performance prediction comparisons for HMA over stiff foundation cases: cracking

CaseType	CaseType 2	Pavement age		Longitudinal Cracking (ft/mi) (MEPDG v.1.1)	Longitudinal Cracking (ft/mi) (Pavement ME v.2.0)	Longitudinal Cracking (ft/mi) (Pavement ME v.2.1.24)	Alligator Cracking (%) (MEPDG v.1.1)	Alligator Cracking (%) (Pavement ME v.2.0)	Alligator Cracking (%) (Pavement ME v.2.1.24)	Transverse Cracking (ft/mi) (MEPDG v.1.1)	Transverse Cracking (ft/mi) (Pavement ME v.2.0)	Transverse Cracking (ft/mi) (Pavement ME v.2.1.24)
Fixed	Fixed											
		mo	yr									
CDL	**New**	180	15	**0**	**0.06**	**0.06**	**0**	**4.48**	**4.48**	**0**	**0.01**	**0.01**
CDM	**New**	180	15	**0.01**	**7.22**	**7.22**	**0**	**4.49**	**4.49**	**0**	**0.01**	**0.01**
CDH	**New**	180	15	**0.34**	**30.8**	**30.8**	**0.032**	**4.70**	**4.70**	**0**	**0**	**0**
CWL	**New**	180	15	**0**	**0.002**	**0.002**	**0**	**4.48**	**4.48**	**0.5**	**0.06**	**0.06**
CWM	**New**	180	15	**0.02**	**0.05**	**0.05**	**0**	**4.49**	**4.49**	**0.4**	**0.04**	**0.04**
CWH	**New**	180	15	**1.73**	**7.71**	**7.71**	**0.0367**	**4.76**	**4.76**	**0.4**	**0.02**	**0.02**
HDL	**New**	180	15	0.01	0.008	0.008	0	4.48	4.48	0	0	0
HDM	**New**	180	15	0.04	0.51	0.51	0.0001	4.49	4.49	0	0	0
HDH	**New**	180	15	0.36	53.8	53.8	0.0422	4.672	4.672	0	0	0
HWL	**New**	180	15	0	0.002	0.002	0	4.48	4.48	0	0	0
HWM	**New**	180	15	0.01	0.04	0.04	0	4.49	4.49	0	0	0
HWH	**New**	180	15	0	2.74	2.74	0.0347	4.67	4.67	0	0	0
TL	**New**	180	15	0	0.002	0.002	0	4.48	4.48	0	0	0
TM	**New**	180	15	0.01	0.03	0.03	0.0001	4.49	4.49	0	0	0
TH	**New**	180	15	0	2.87	2.87	0.0388	4.73	4.73	0	0	0

Table 13. Pavement performance prediction comparisons for HMA over stiff foundation cases: rutting and IRI

CaseType	CaseType2	Pavement age		AC Rutting (in) (MEPDG v.1.1)	AC Rutting (in) (Pavement ME v.2.0)	AC Rutting (in) (Pavement ME v.2.1.24)	Total Rutting (in) (MEPDG v.1.1)	Total Rutting (in) (Pavement ME v.2.0)	Total Rutting (in) (Pavement ME v.2.1.24)	IRI in/mile (MEPDG v.1.1)	IRI in/mile(Pavement ME v.2.0)	IRI in/mile(Pavement ME v.2.1.24)
Fixed	Fixed											
		mo	yr									
CDL	**New**	180	15	**0.10**	**0.12**	**0.12**	**0.36**	**0.39**	**0.39**	**97.1**	**101.0**	**101.0**
CDM	**New**	180	15	**0.47**	**0.55**	**0.55**	**0.75**	**0.85**	**0.85**	**112.7**	**119.1**	**119.1**
CDH	**New**	180	15	**1.03**	**1.21**	**1.21**	**1.30**	**1.49**	**1.49**	**135.0**	**145.1**	**145.1**
CWL	**New**	180	15	**0.13**	**0.11**	**0.11**	**0.41**	**0.37**	**0.37**	**101.0**	**100.0**	**100.0**
CWM	**New**	180	15	**0.63**	**0.52**	**0.52**	**0.92**	**0.80**	**0.80**	**121.6**	**117.0**	**117.0**
CWH	**New**	180	15	**1.38**	**1.12**	**1.12**	**1.67**	**1.39**	**1.39**	**151.7**	**140.9**	**140.9**
HDL	**New**	180	15	0.17	0.19	0.19	0.39	0.39	0.39	91.6	92.2	92.2
HDM	**New**	180	15	0.81	0.82	0.82	1.05	1.04	1.04	117.9	118.0	118.0
HDH	**New**	180	15	1.76	1.70	1.70	1.99	1.92	1.92	156.0	153.4	153.4
HWL	**New**	180	15	0.10	0.13	0.13	0.37	0.38	0.38	94.5	95.5	95.5
HWM	**New**	180	15	0.46	0.55	0.55	0.75	0.82	0.82	109.7	113.0	113.0
HWH	**New**	180	15	1.00	1.14	1.14	1.28	1.41	1.41	131.0	136.4	136.4
TL	**New**	180	15	0.08	0.10	0.10	0.32	0.32	0.32	90.2	90.5	90.5
TM	**New**	180	15	0.35	0.39	0.39	0.61	0.64	0.64	101.7	103.1	103.1
TH	**New**	180	15	0.75	0.81	0.81	1.00	1.05	1.05	117.5	119.9	119.9

LOCAL CALIBRATION METHODOLOGY

Based on the literature review and consultations with Iowa DOT engineers, a set of procedures for local calibration of AASHTOWare Pavement ME Design performance predictions for Iowa pavement systems was developed. The following steps give the details of this procedure:

- **Step 1:** Update and tabulate the Iowa pavement system database for AASHTOWare Pavement ME Design local calibration based on the database developed in InTrans Project 11-401, "Iowa Calibration of MEPDG Performance Prediction Models" (Ceylan et al. 2013).
- **Step 2:** Conduct AASHTOWare Pavement ME Design runs using (1) nationally calibrated and (2) MEPDG locally calibrated coefficients identified in InTrans Project 11-401 (Ceylan et al. 2013).
- **Step 3:** Evaluate the accuracy of both nationally calibrated and MEPDG locally calibrated pavement performance prediction models.
- **Step 4:** If the accuracy of nationally calibrated or MEPDG locally calibrated coefficients for given AASHTOWare Pavement ME Design performance prediction models was found to be adequate, these coefficients were determined to be acceptable for Iowa conditions.
- **Step 5:** If not, the calibration coefficients of AASHTOWare Pavement ME Design were to be refined using various optimization approaches.
- **Step 6:** Evaluate the adequacy of the refined AASHTOWare Pavement ME Design locally calibrated coefficients.
- **Step 7:** Recommend AASHTOWare Pavement ME Design calibration coefficients for Iowa conditions.

Description of Iowa Pavement Sites Selected

A total of 130 representative pavement sites across Iowa, selected from InTrans Project 11-401 (Ceylan et al. 2013), were used for AASHTOWare Pavement ME Design local calibration. The selected pavement sites represent flexible, rigid, and composite pavement systems throughout Iowa at different geographical locations and different traffic levels.

Table 14 lists the number of pavement sections selected for this study.

Table 14. Site selection summary information

Type	Iowa PMIS Code	Number of Sites Selected	Iowa LTPP sections
JPCP	1	35	6
HMA	4	35	1
HMA over JPCP	3 and 3A	60	9

A total of 35 sections for new JPCP (rigid pavements), a total of 35 sections for new HMA pavements (flexible pavements), and a total of 60 sections for HMA over JPCP (composite pavements) were selected. In the selected new JPCP and new HMA roadway segments, 25

sections were used for calibration and 10 sections were used for verification of identified calibration coefficients. In the selected HMA over JPCP roadway segments, 45 sections were used for calibration and 15 sections were used for verification of identified calibration coefficients.

The descriptive information on selected pavement sites, developed in InTrans Project 11-401 (Ceylan et al. 2013), was updated by incorporating information from the new Iowa DOT Pavement Management Information System (PMIS) database. Note that InTrans Project 11-401 (Ceylan et al. 2013) used the Iowa DOT PMIS database for 1998 to 2009 while this study used the one for 1992 to 2013.

Figure 2 presents AADTT distributions for each type of Iowa pavement.

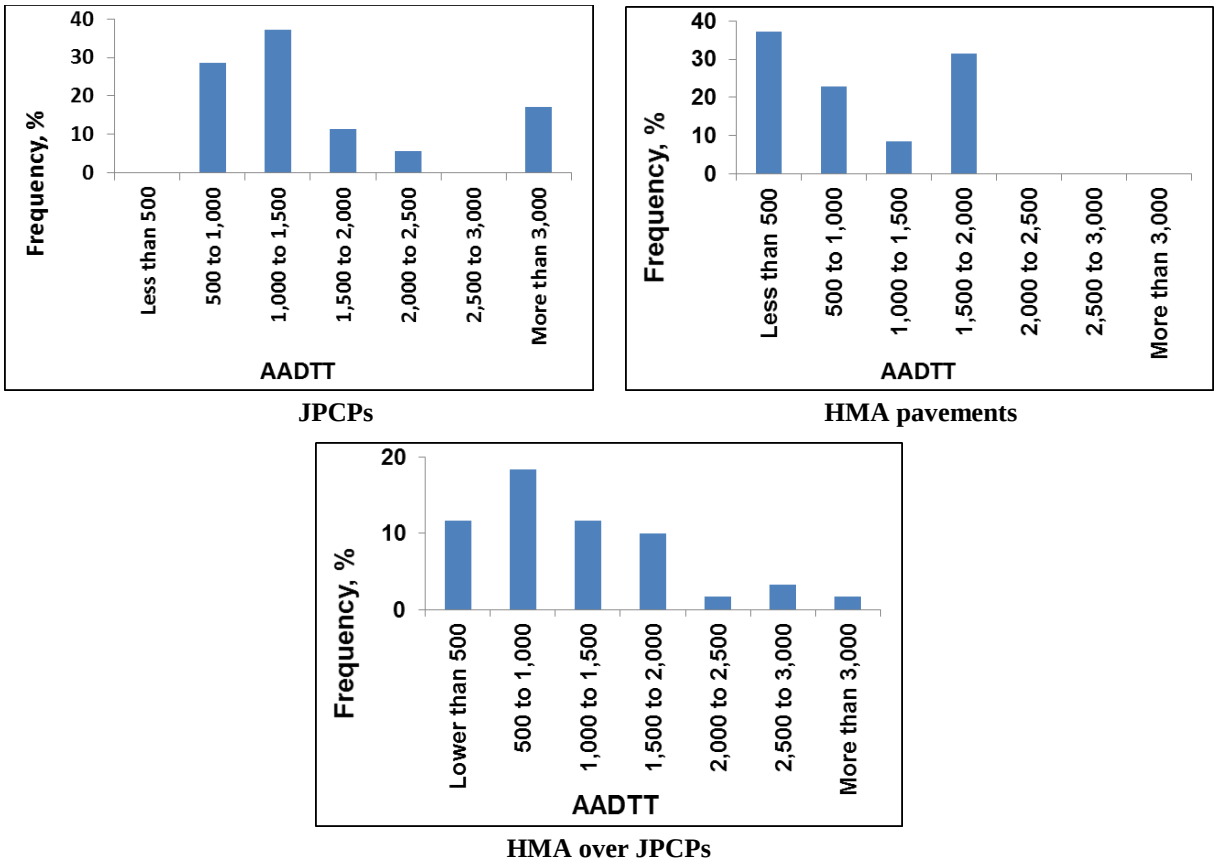

Figure 2. Iowa pavements by AADTT distribution as of 2014

As can be seen in the figure, HMA surface pavements are used more with lower AADTT values and JPCPs are used more with higher AADTT values. To include all Iowa traffic conditions, three categories of traffic levels were used in selecting calibration sites. An AADTT value less than 500 is categorized a low traffic volume, between 500 and 1,000 is categorized as medium traffic volume, and higher than 1,000 is categorized as high traffic volume. The selected sections, shown in Figure 3, also represent a variety of geographical locations across Iowa.

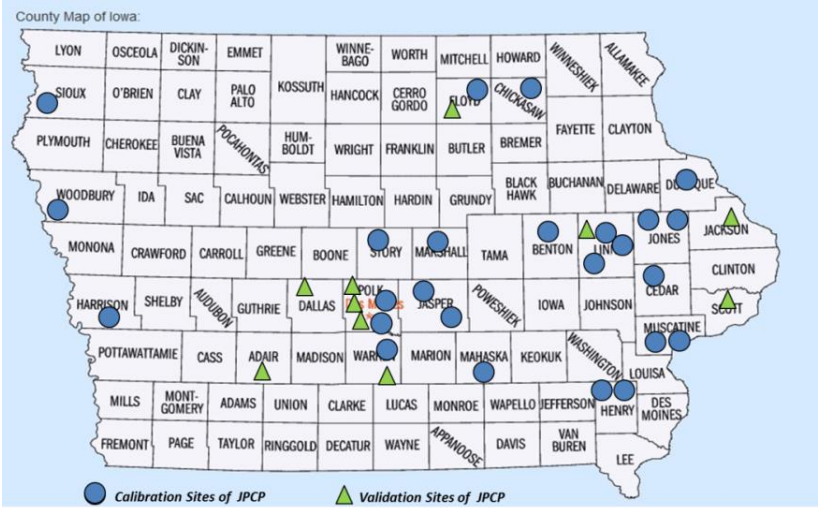

JPCPs

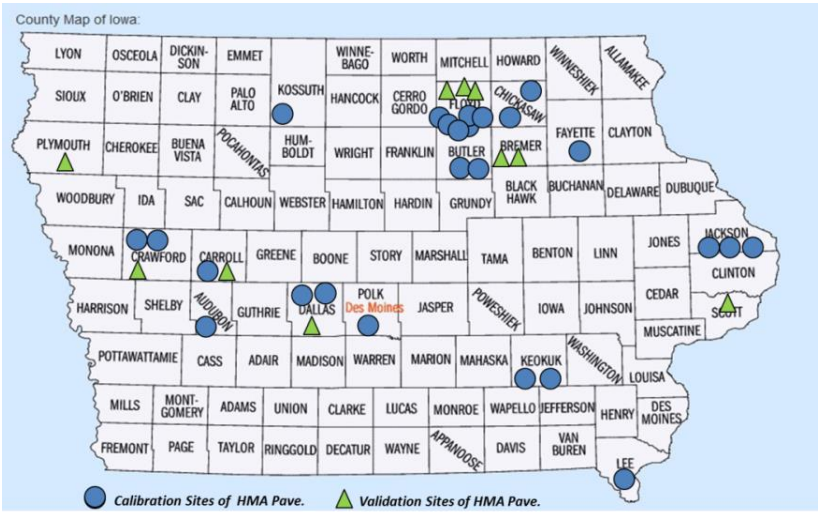

HMA pavements

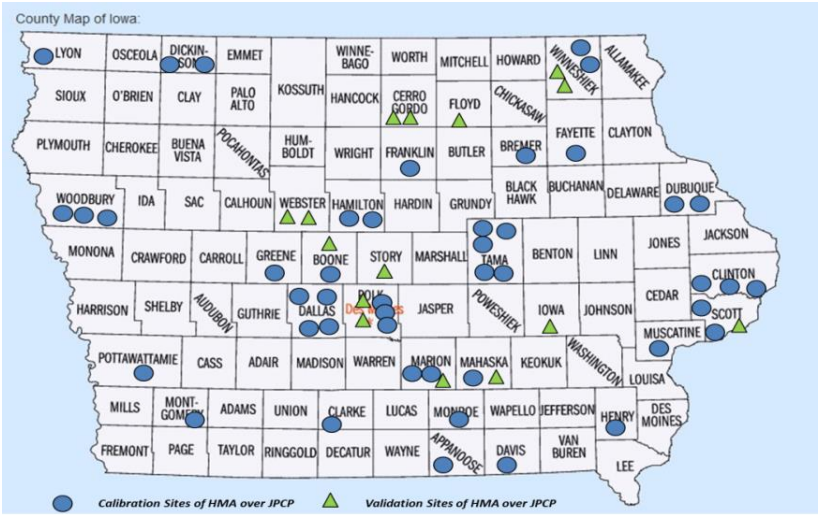

HMA over JPCPs

Figure 3. Geographical locations of selected Iowa pavement sites

The distribution of construction years for each type of pavement is shown in Figure 4. HMA over JPCP sections were categorized based on their JPCP construction and resurfacing years (Figure 4).

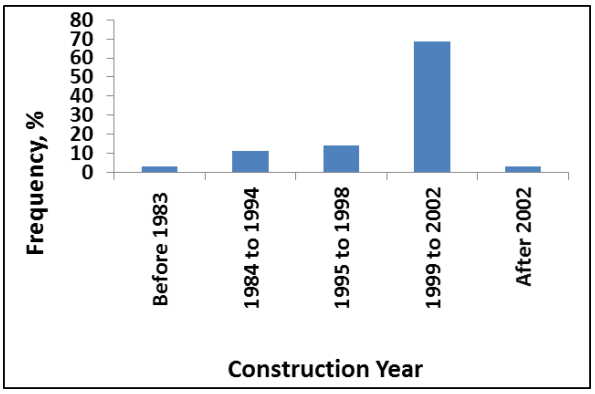

JPCPs

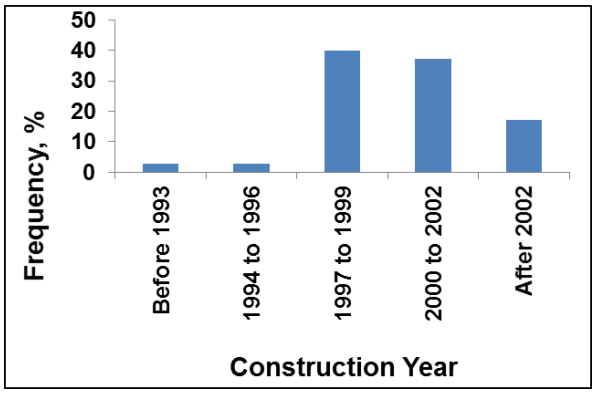

HMA pavements

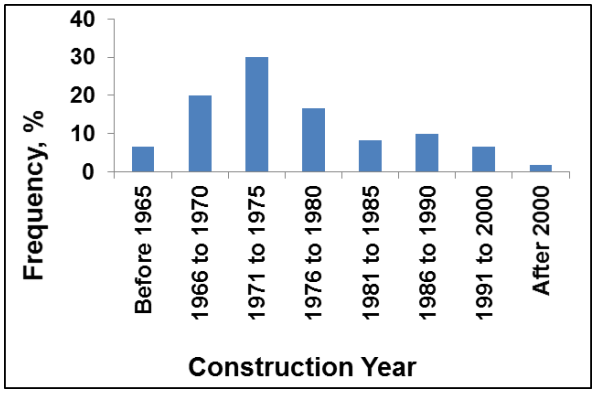

Initial JPCP construction years of HMA over JPCPs

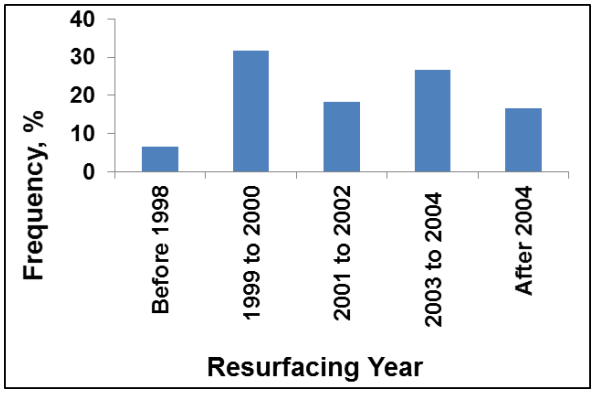

HMA resurfacing years of HMA over JPCPs

Figure 4. Iowa pavements by the distribution of construction years as of 2014

As can be seen from Figure 4, most of the selected Iowa JPCPs were constructed between 1999 and 2002, while most of the selected HMA pavements were constructed after 1997. For the selected Iowa HMA over JPCPs, most of the HMA resurfacings were conducted after 1999.

Figure 5 shows the distribution of PCC surface thicknesses for JPCPs, HMA surface thicknesses for HMA pavements, and HMA overlay and PCC thicknesses for HMA over JPCPs.

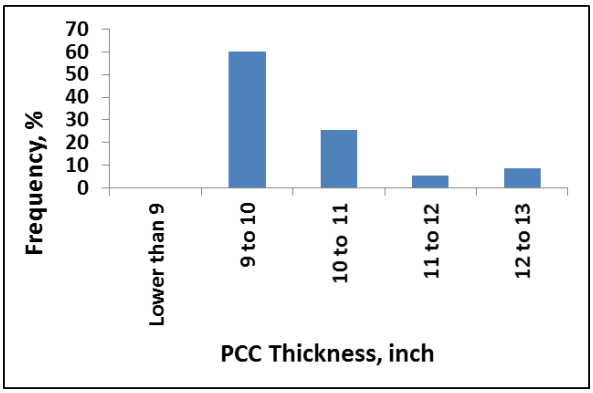

PCC surface thickness for JPCPs

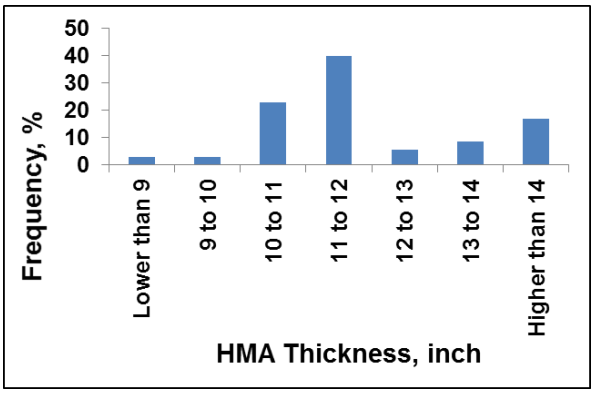

HMA surface thickness for HMA pavements

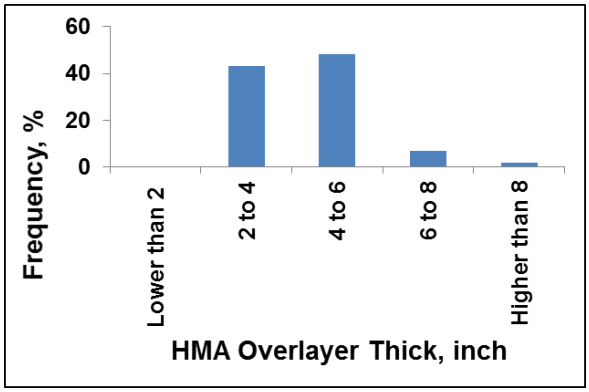

HMA overlay thickness for HMA over JPCPs

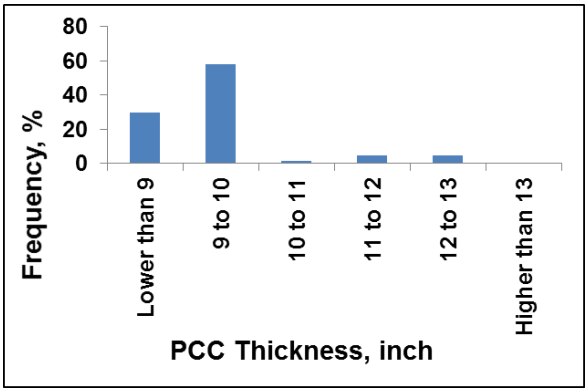

PCC thickness for HMA over JPCPs

Figure 5. Iowa pavements by the distribution of surface thicknesses as of 2014

As can be seen in Figure 5, the PCC thicknesses for about 90% of the selected JPCPs range from 9 to 11 in., while the HMA thicknesses for over 90% of the selected HMA pavements are greater than 10 in. It should be noted that traffic volumes for JPCPs are higher than for HMA pavements (see Figure 2). Also, the HMA overlay thicknesses for over 90% of the HMA over JPCPs range from 2 to 6 in. The distribution of base thicknesses for Iowa JPCP, HMA, and HMA over JPCPs is presented in Figure 6.

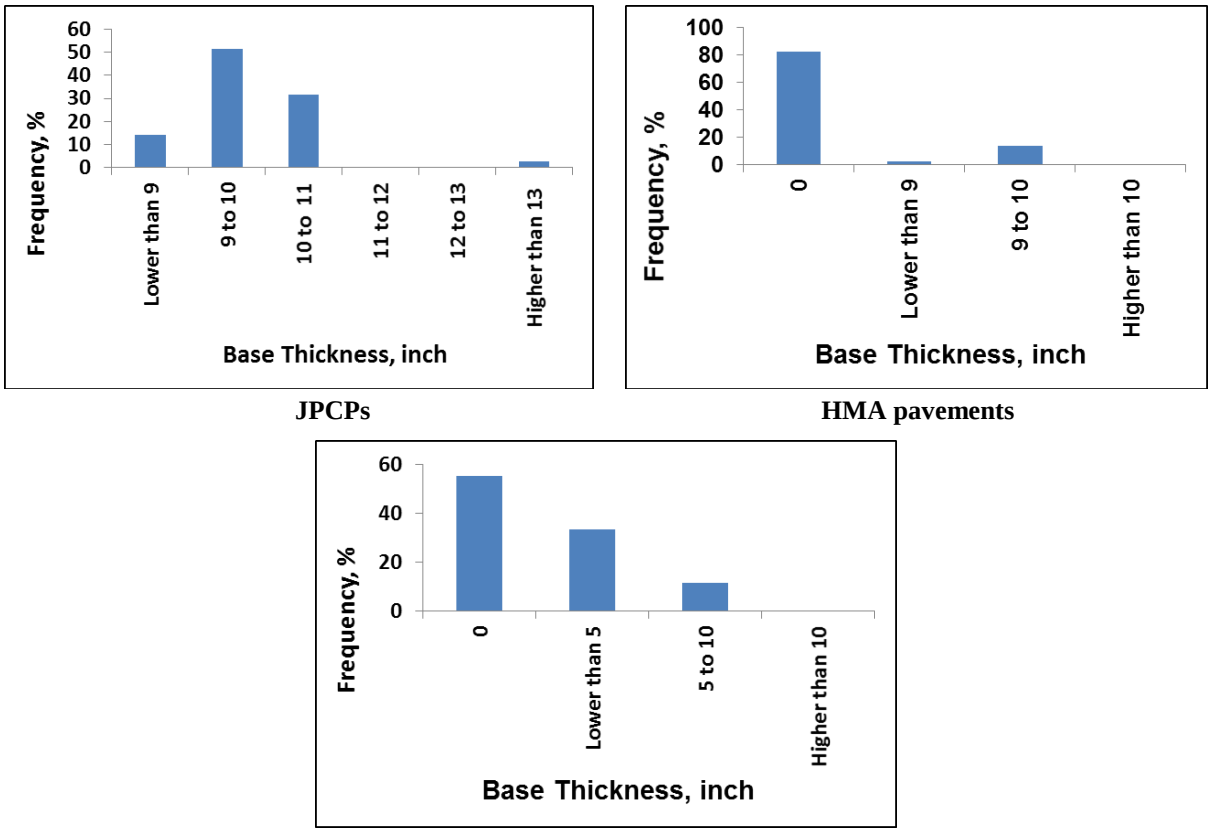

Figure 6. Iowa pavements by the distribution of base thicknesses as of 2014

As can be seen in Figure 6, the most common base thicknesses for about 90% of the JPCPs selected range from 9 to 11 in., while over 80% of the HMA pavements selected have no base layer. It can therefore be concluded that more than 80% of selected HMA pavements are full-depth HMA pavements. On the other hand, the thicknesses for about 90% of the HMA over JPCPs selected range from 0 to 5 in. Also note that there are no base layers thicker than 10 in. for the selected HMA over JPCPs.

Description of the Calibration Database for Iowa Pavement Systems

Input Database

The design input values required for the AASHTOWare Pavement ME Design runs were prepared from the design database developed in InTrans Project 11-401 (Ceylan et al. 2013). The data in the design input database were collected primarily from the Iowa DOT PMIS, material testing records, and previous project reports relevant to MEPDG implementation in Iowa. Detailed descriptions of the input database are provided in the InTrans Project 11-401 report (Ceylan et al. 2013).

Pavement Distress Database

The database of historical performance data for the selected sections developed in InTrans Project 11-401 (Ceylan et al. 2013) was updated by incorporating data from the new Iowa DOT PMIS database. Note that InTrans Project 11-401 (Ceylan et al. 2013) used the Iowa DOT PMIS database from 1998 to 2009 while this study used that from 1992 to 2013. As indicated in InTrans Project 11-401 (Ceylan et al. 2013), some differences between PMIS distress measures and AASHTOWare Pavement ME Design performance predictions were observed. For the calibration of the performance prediction models, the identified differences were resolved by considering the following assumptions:

- AASHTOWare Pavement ME Design provides rutting predictions for individual pavement layers, while the Iowa DOT PMIS provides only the accumulated (total) rutting observed in HMA surfaces. Rutting measurements for individual layers were computed by applying the average percentage of total rutting for different pavement layers and the subgrade, as recommended in NCHRP 1-37A (ARA, Inc. 2004), to the HMA surface rut measurements recorded in the Iowa DOT PMIS.
- AASHTOWare Pavement ME Design transverse cracking predictions for new HMA and HMA overlaid pavements are considered to reflect thermal cracking. The Iowa DOT PMIS transverse cracking measurements for new HMA pavement could be considered as HMA thermal cracking, but those recorded for HMA overlaid pavements could be either reflection cracking or thermal cracking. However, transverse cracking measurements in the Iowa DOT PMIS for HMA overlaid pavements were not differentiated in that way. Considering the empirical nature of the reflection cracking model implemented in AASHTOWare Pavement ME Design (in the latest version available at the time this research), this study considered the Iowa DOT PMIS transverse cracking measurements for HMA overlaid pavements to be HMA thermal cracking to calibrate the HMA thermal cracking model rather than the reflection cracking model.
- The units reported in the Iowa DOT PMIS for transverse cracking of JPCP and alligator and thermal (transverse) cracking of HMA and HMA overlaid pavements are different from those used in AASHTOWare Pavement ME Design. These measured values of distress in the Iowa DOT PMIS were converted into the same units as those of the AASHTOWare Pavement ME Design predictions in accordance with the AASHTO guide for local calibration of the MEPDG (AASHTO 2010).
- Some irregularities in distress measures in the Iowa DOT PMIS were identified. Occasionally, distress magnitudes appeared to decrease with time or show erratic patterns without explanation. In such cases, the distress measure history curves were modified to not to decrease with time.

Figure 7 presents the performance data distribution of selected JPCP sections for the faulting, transverse cracking, and IRI distresses extracted from Iowa DOT PMIS database.

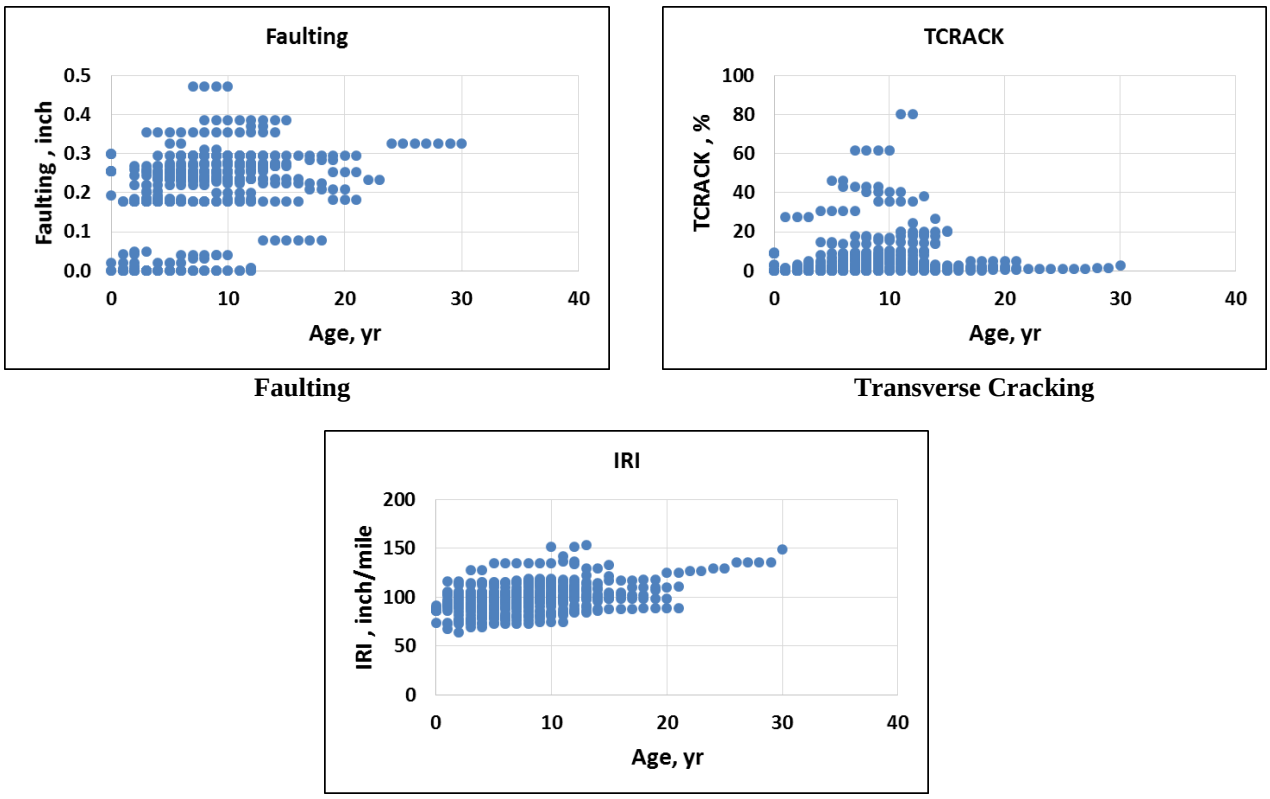

Figure 7. JPCP performance data distribution as of 2014

Some performance measurements, such as faulting measurements greater than 0.45 in. and transverse cracking greater than 80% for a 10 year JPCP service life, are unusual when considering actual Iowa pavement performance experience. Such unusual measurements were considered to be outliers and eliminated in the calibration procedures.

Figure 8 presents the performance data distribution for selected HMA pavement sections for total rutting, HMA rutting, granular-base rutting, subgrade rutting, longitudinal cracking, alligator cracking, transverse cracking, and IRI.

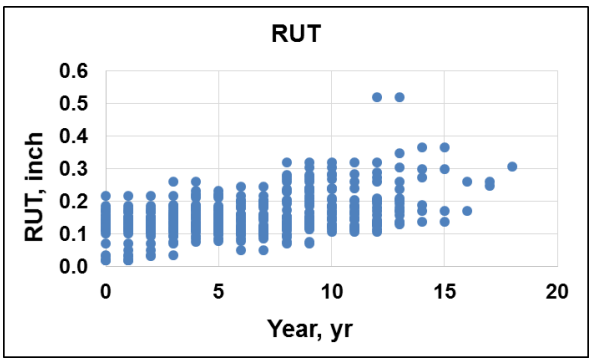

Total rutting

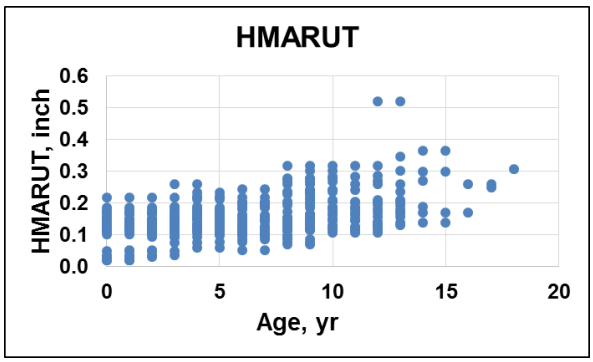

HMA rutting

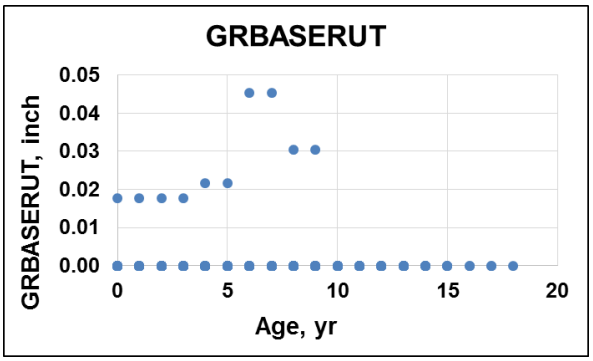

Granular base rutting

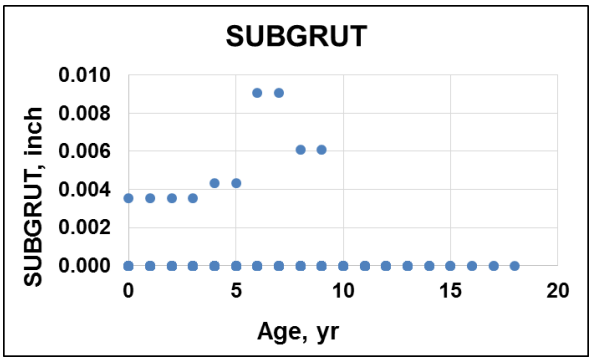

Subgrade rutting

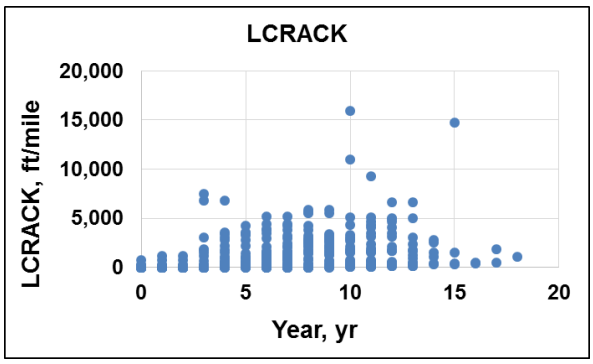

Longitudinal cracking

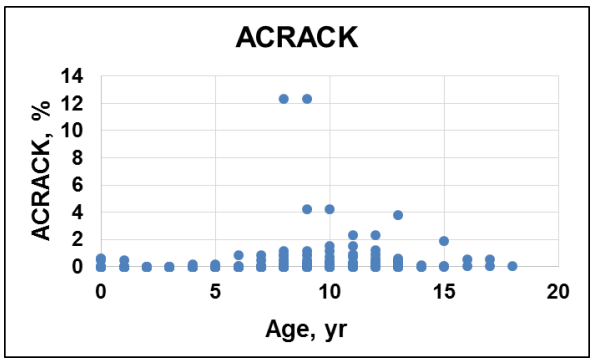

Alligator cracking

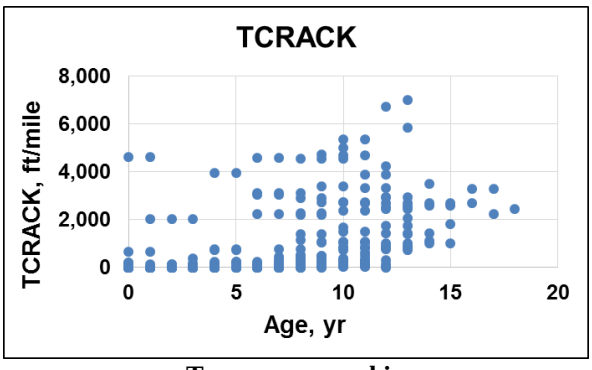

Transverse cracking

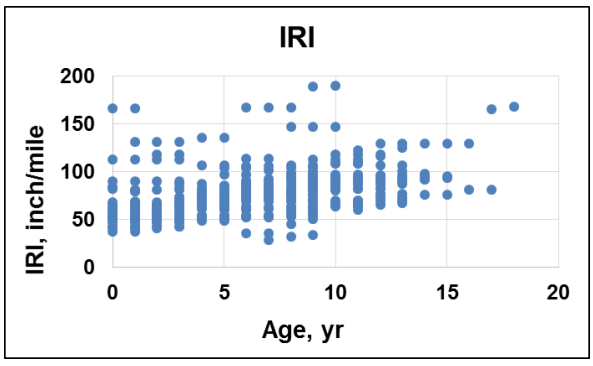

IRI

Figure 8. HMA performance data distribution as of 2014

As can be seen in Figure 8, most total rutting occurs due to HMA rutting; the effect of granular base and subgrade rutting on total rutting is minimal. This is because most flexible pavements in Iowa are full-depth flexible pavements. Some performance measurements, such as longitudinal cracking measurements greater than 15,000 ft/mi and transverse cracking measurements greater than 7,000 ft/mi before the end of a 20 year HMA pavement service life, are unusual when considering actual Iowa pavement performance experience. Such unusual measurements were considered to be outliers and eliminated in the calibration procedures.

Figure 9 presents the performance data distribution for selected HMA over JPCP sections for total rutting, longitudinal cracking, alligator cracking, transverse cracking, and IRI.

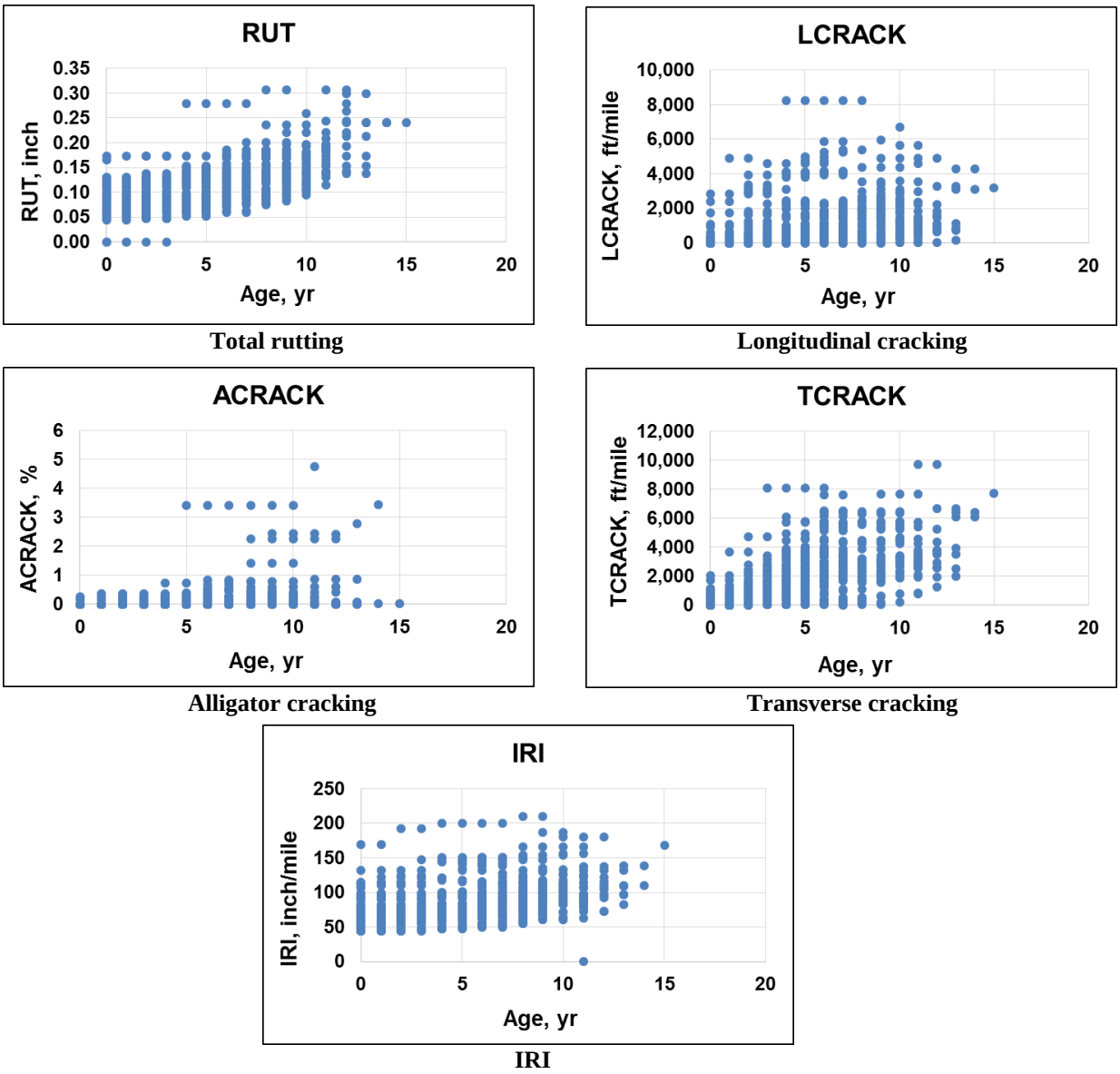

Figure 9. HMA over JPCP performance data distribution as of 2014

Some performance measurements, such as longitudinal cracking measurements greater than 8,000 ft/mi and transverse cracking measurements greater than 10,000 ft/mi for a 10 year HMA over JPCP service life, are unusual when considering actual Iowa pavement performance experience. Such unusual measurements were considered to be outliers and eliminated in calibration procedures.

Description of Optimization Approaches

The purpose of AASHTOWare Pavement ME Design local calibration is to identify a set of empirical transfer function coefficients (calibration coefficients) in pavement performance models to provide adequate accuracy for pavement performance predictions compared to actual pavement performance measurements (observations).

Figure 10 illustrates the flow of optimization procedures used to identify local calibration coefficients having adequate accuracy for Iowa conditions. The local calibration procedure starts with the identification of transfer functions and their components. There are basically two types of transfer functions classified in AASHTOWare Pavement ME Design: (1) functions directly calculating the magnitude of the pavement performance predictions and (2) functions calculating the incremental damage over time and relating such damage to the pavement performance predictions.

As can be seen in Figure 10, there are two approaches to optimizing pavement prediction models depending on whether the components of the transfer functions are known.

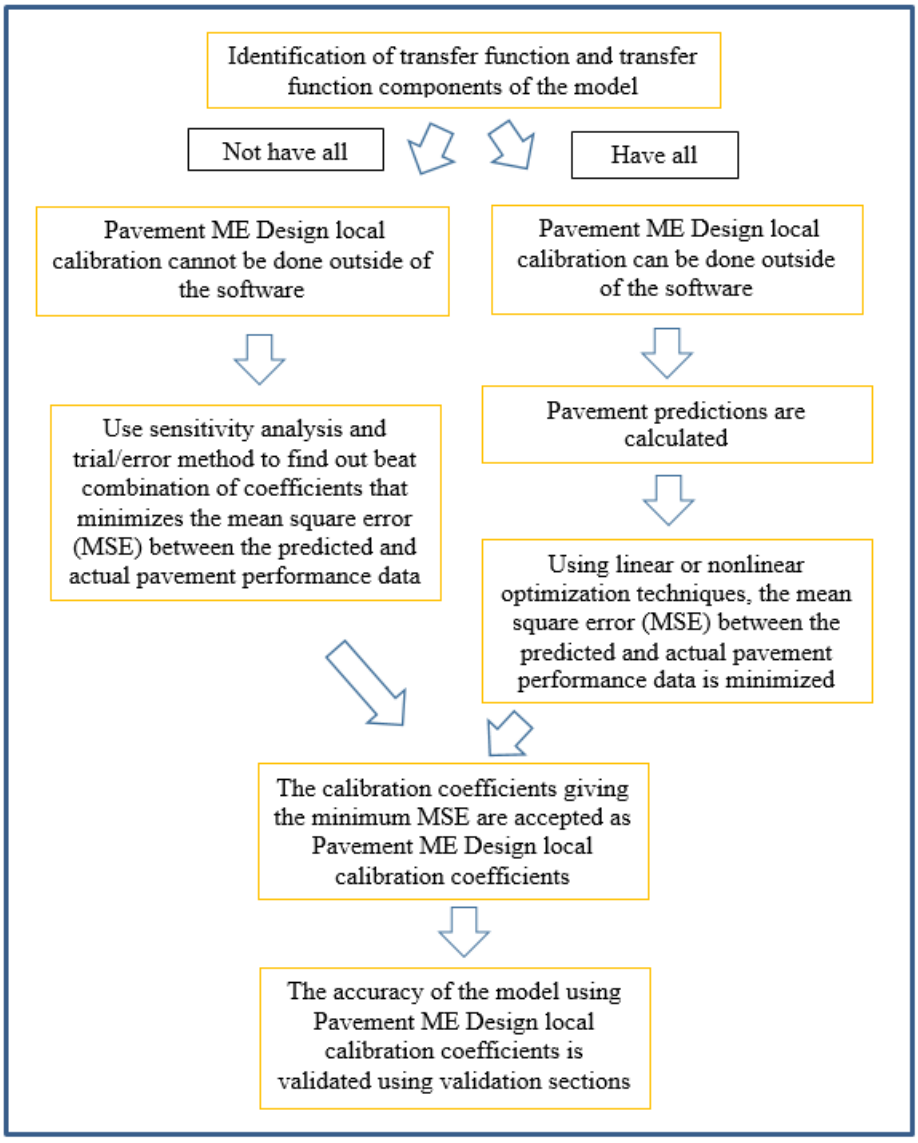

Figure 10. Optimization procedures to identify local calibration coefficients

If all components of the transfer functions are provided by the software in intermediate files known to the designer, model predictions can be calculated outside the software using the transfer functions. In such cases, nonlinear optimization techniques can be applied to calibrate the pavement performance models.

If all the components of the functions are not known, the calibration can be achieved only through trial and error procedures by performing numerous AASHTOWare Pavement ME Design runs to figure out the best combination of calibration coefficients in terms of goodness-of-fit accuracy. To minimize the number of AASHTOWare Pavement ME Design runs, Ceylan et al. (2013) developed a linear optimization approach based on a sensitivity analysis of calibration coefficients.

In AASHTOWare Pavement ME Design version 2.1.24, although some components of the transfer functions are provided in intermediate output files, many are not provided at all. This deficiency of the software was partially remedied in the latest version (version 2.2). For the transfer function developed when not all the components are known, the calibration should be implemented within the software using sensitivity analysis and trial-and-error methods. These methods are extensively described in a previous report (Ceylan et al. 2013).

The optimization procedure is performed by minimizing the mean square error (MSE) between the actual distress measurements and the values predicted by AASHTOWare Pavement ME Design (AASHTO 2010). Once the calibration coefficients are determined, the calibrated models are verified using the validation data set.

Various optimization methods utilized in this study are summarized in Table 15 and discussed in the following section.

Table 15. Optimization techniques used for different pavement distresses

Pavement Type	Distress	Optimization Technique Used
JPCP	Faulting	MS Excel Solver, Brute Force, and Lingo
	Transverse Cracking	MS Excel Solver and Sensitivity Analysis
	IRI	MS Excel Solver, Brute Force, and Lingo
HMA	Rutting	Sensitivity Analysis
	Longitudinal Cracking	Sensitivity Analysis and MS Excel Solver
	Alligator Cracking	Sensitivity Analysis and MS Excel Solver
	Thermal Cracking	Sensitivity Analysis
	IRI	MS Excel Solver, Brute Force, and Lingo
HMA over JPCP	Rutting	Sensitivity Analysis
	Longitudinal Cracking	Sensitivity Analysis and MS Excel Solver
	Alligator Cracking	Sensitivity Analysis and MS Excel Solver
	Thermal Cracking	Sensitivity Analysis
	IRI	MS Excel Solver, Brute Force, and Lingo

Nonlinear Optimization Methods

A nonlinear programming optimization technique provided as a Microsoft (MS) Excel Solver routine has been commonly used to minimize the bias (ε) and the root mean square error (RMSE) between the actual distress measurements and the values predicted by AASHTOWare Pavement ME Design (Velasquez et al. 2009, APTech, Inc. 2010, Jadoun 2011). To use this approach, all input values required by the performance models are needed to satisfy closed-form solution requirements. Based on the linear or nonlinear nature of the equation, MS Excel Solver uses three different methods: generalized reduced gradient (GRG), simplex (Simplex LP), and evolutionary. GRG is used for nonlinear equations, Simplex LP is used for linear equations, and

evolutionary can be used for both nonlinear and linear equations. GRG is a robust and fast tool for determining the best combination of calibration coefficients (Frontline Systems, Inc. 2015).

In addition to GRG in MS Excel Solver, a brute force method (through Microsoft Visual Studio) was implemented by trying all possible combinations of candidate numbers and checking to see whether any combinations satisfied the problem statement. This method is used in this study to ensure that the results produced by MS Excel Solver are correct. Algorithms were composed using the transfer functions, constraints and increments were specified, and the best combinations of calibration coefficients minimizing the MSE between the measured and predicted pavement performance values were determined. The disadvantage of this method is that as defined increments become smaller, the accuracy of the result increases. To make sure that the best combinations of coefficients have been determined, the increments should therefore be minimized.

Along with the other optimization methods, an optimization software tool, Lingo 15.0, was also used in this study. This software solves linear and nonlinear optimization problems with great accuracy. It can determine global solutions to optimization problems for both convex and nonconvex equations (LINDO Systems, Inc. 2015). Note that this software can find global solutions to a problem very quickly. Again, this software was employed to ensure that the results provided by MS Excel Solver are correct.

Linear Optimization Method

A linear optimization approach based on a sensitivity analysis of calibration coefficients was developed (Ceylan et al. 2013) to reduce the computational burden of the trial-and-error procedure in cases where not all the transfer function components are known. In such cases, a sensitivity analysis of each calibration coefficient is conducted and, based on the analysis results, a trial-and-error method is implemented to find the best combination of coefficients providing the minimum MSE between the measured and predicted pavement performance values. The details of this method can be found in Ceylan et al. (2013).

Accuracy Evaluation Criteria

The AASHTOWare Pavement ME Design simulation was executed using nationally calibrated and MEPDG locally calibrated (through Ceylan et al. 2013) model values to predict performance indicators for each selected Iowa DOT PMIS roadway section. Predicted performance measures were then plotted relative to the measured values for the Iowa DOT PMIS roadway sections. Based on the accuracy of the performance predictions made using the nationally calibrated and MEPDG locally calibrated model coefficient values, a determination was made whether it was necessary to modify the nationally calibrated and MEPDG locally calibrated coefficient values for Iowa conditions. If needed, locally calibrated model coefficients were identified to improve the accuracy of model predictions.

The accuracy of performance predictions was evaluated by plotting the measurements against the predictions on a 45 degree line representing equality and by observing the average bias, standard error, coefficient of determination (R^2), and mean absolute percentage error (MAPE) values. The accuracy indicators used in this study are defined as follows:

$$Ave\ Bias = \varepsilon_{ave} = \frac{\sum_{j=1}^{n}(y_j^{measured} - y_j^{predicted})}{n} \quad \textbf{(1)}$$

$$Stand.Error = \sqrt{\frac{\sum_{j=1}^{n}\left(y_j^{measured} - y_j^{predicted}\right)^2}{n}} \quad \textbf{(2)}$$

$$R^2 = \left(\frac{1}{n} \times \sum_{j=1}^{n} \frac{\left[\left(y_j^{measured} - y_{mean}^{measured}\right) \times \left(y_j^{predicted} - y_{mean}^{predicted}\right)\right]}{\sigma_{measured} \times \sigma_{predicted}}\right)^2 \quad \textbf{(3)}$$

$$LOE\ R^2 = 1 - \frac{n-p}{n-1} \times \left(\frac{S_e}{S_y}\right)^2 \quad \textbf{(4)}$$

$$MAPE = \frac{1}{n} \times \sum_{j=1}^{n} \left|\frac{y_j^{measured} - y_j^{predicted}}{y_j^{measured}}\right| \quad \textbf{(5)}$$

where,

- n = Number of data points in each distress comparison
- $y^{measured}$ = Measured distress data points
- $y^{predicted}$ = Measured distress data points
- $\sigma_{measured}$ = Variance of measured distress data points
- $\sigma_{predicted}$ = Variance of predicted distress data points

The average bias basically shows the average of differences between the measured and predicted values, while the standard error of the estimate measures the differences between the predicted and measured values. In this study, two kinds of coefficients of determination were utilized: (1) line of equality (LOE), in which R^2 indicates how well the data fit the LOE, and (2) coefficient of determination, simply R^2, indicating how well the data fit the regression line while minimizing the RMSE between the two data sets (i.e., measurements and predictions). Note that a negative (LOE) R^2 simply means that the data points do not follow the associated model. Lower absolute values of average bias and standard error indicate better accuracy. A positive value for the average bias indicates underestimated predictions. Higher R^2 values show better accuracy. Additionally, for MAPE, the following scale is used to forecast accuracy (Lewis 1982):

- Highly accurate forecast: MAPE < 0.1 (10%)
- Good forecast: 0.1 (10%) < MAPE < 0.2 (20%)

- Reasonable forecast: 0.2 (20%) < MAPE < 0.5 (50%)
- Inaccurate forecast: MAPE > 0.5 (50%)

In addition to the accuracy indicators described, a paired t test was also performed. This test is used to compare the means of two populations to determine whether they differ from one another in a significant way under the assumptions that paired differences are independent and identically normally distributed. In this test, the following null and alternative hypothesis are used:

- H_0: Mean measured distress = mean predicted distress
- H_A: Mean measured distress ≠ mean predicted distress

Equation 6 is used for the calculation of t values used in these tests:

For j=1:n,

$$t = \frac{(y_j^{measured} - y_j^{predicted})_{mean}}{\frac{s_d}{\sqrt{n}}} \quad \textbf{(6)}$$

where,

- n = Number of paired data points
- $y^{measured}$ = Measured distress data points
- $y^{predicted}$ = Measured distress data points
- s_d = Standard deviation of paired data points

This statistic follows a t-distribution with n − 1 degrees of freedom.

The rejection of the null hypothesis (p-value < 0.05) implies that there are grounds for believing that there is a relationship between two phenomena and that the distress prediction is thus unbiased.

LOCAL CALIBRATION RESULTS

The pavement performance models adopted in AASHTOWare Pavement ME Design for JPCP, HMA, and HMA over JPCP are discussed here from a local calibration perspective. The step-by-step procedure for local calibration was documented by considering the availability of transfer function components. The AASHTOWare Pavement ME Design calibration coefficients identified for Iowa pavement systems and the corresponding model accuracies are presented and compared to MEPDG calibration coefficients identified by InTrans Project 11-401 (Ceylan et al. 2013) and national calibration coefficients.

JPCP

The AASHTOWare Pavement ME Design performance predictions for new JPCP include mean joint faulting, transverse slab cracking, and IRI performance models. The identification of transfer functions for these models was noted, and the availability of each component of these functions for local calibration was investigated. Based on the availability of these components, different optimization approaches were utilized. The calibration results from the utilized optimization approaches are presented along with corresponding model accuracies.

Mean Transverse Joint Faulting

An incremental approach method was adopted (AASHTO 2008) for the calculation of mean transverse joint faulting. Based on this method, faulting values for each month were calculated and summed, beginning with the traffic opening date, to determine the faulting value at any time.

Transverse joint faulting predictions can be calculated from the following set of equations:

$$Fault_m = \sum_{i=1}^{m} \Delta Fault_i \quad \textbf{(7)}$$

$$\Delta Fault_i = C_{34} \times (FAULTMAX_{i-1} - Fault_{i-1})^2 \times DE_i \quad \textbf{(8)}$$

$$FAULTMAX_i = FAULTMAX_{i-1} + (C_7/10^6) \sum_{j=1}^{m} DE_j \times \log(1 + C_5 \times 5^{EROD})^{C_6} \quad \textbf{(9)}$$

$$FAULTMAX_0 = C_{12} \times \delta_{curling} \times [\log(1 + C_5 \times 5^{EROD}) \times \log(\frac{P_{200} \times Wet\ Days}{p_s})]^{C_6} \quad \textbf{(10)}$$

where,

- $Fault_m$ = Mean joint faulting at the end of month m, inch
- $\Delta FAULT_i$ = Incremental change (monthly) in mean transverse joint faulting during month i, inches
- $FAULTMAX_i$ = Maximum mean transverse joint faulting for month i, inches
- $FAULTMAX_0$ = Initial maximum mean transverse joint faulting, inches

- *EROD* = Base/subbase erodibility factor
- DE_i = Differential density of energy of subgrade deformation accumulated during month i
- $\delta_{curling}$ = Maximum mean monthly slab corner upward deflection in PCC due to temperature
- curling and moisture warping
- *Ps* = Overburden on subgrade, lbs
- P_{200} = Percent subgrade material passing #200 sieve
- *WetDays* = Average annual number of wet days (greater than 0.1 inch rainfall)
- $C_{1, 2, 3, 4, 5, 6, 7, 12, 34}$ = Calibration coefficients

Calibration coefficients C_{12} and C_{34} are defined by the following equations:

$$C_{12} = C_1 + C_2 \times FR^{0.25} \quad \textbf{(11)}$$

$$C_{34} = C_3 + C_4 \times FR^{0.25} \quad \textbf{(12)}$$

where,

- *FR* = Base freezing index defined as the percentage of time the top base temperature is below freezing (32°F) temperature

Note that Equation 9 is presented in AASHTO Mechanistic-Empirical Pavement Design Guide, Interim Edition: A Manual of Practice (AASHTO 2008) as follows:

$$FAULTMAX_i = FAULTMAX_0 + (C_7) \sum_{j=1}^{m} DE_j \times \log(1 + C_5 \times 5^{EROD})^{C_6} \quad \textbf{(13)}$$

Using Equation 13 from the AASHTO Mechanistic-Empirical Pavement Design Guide, Interim Edition: A Manual of Practice (AASHTO 2008), the same mean transverse joint faulting values reported in the software outputs could not be calculated. Communications with the developers of the AASHTOWare Pavement ME Design software (ARA, Inc., personal communication, August 4, 2014) revealed the following clarifications:

- Division of C_7 *by* 10^6 in Equation 9 is hardcoded into the software, although this division is not shown in the equation (refer to Equation 13).
- $FAULTMAX_{i-1}$ (see Equation 9) should be used instead of $FAULTMAX_0$ (see Equation 15).

The availability of each variable of the equations described above was carefully inspected. All were either extracted from the AASHTOWare Pavement ME Design final and intermediate output files or calculated using the data provided by the AASHTOWare Pavement ME Design output files. The reporting file location or calculation method for each variable is as follows:

- *Erodibility* = Used as input value, known or can be checked from the "Design Properties" tab in final result summary output file

- P_{200} = Used as input value, known or can be checked from the "Layer #" tab in the final result summary output file
- *Wet days* = Can be indirectly found in the intermediate output file of "MonthlyClimateSummary.csv" by summing all the wet days in all months and then multiplying by 12 to obtain annual wet day results
- $FAULTMAX_0$ = Provided in the first column and first row of the "JPCP_faulting.csv" intermediate file for each pavement section
- *DE* = Can be extracted from the "Faulting Data" tab in the final result summary output file
- Curling and warping deflection = Knowing the $FAULTMAX_0$ value from the intermediate file, the curling deflection value can be calculated using the $FAULTMAX_0$ equation (see equation 13)
- *Ps* = Overburden pressure can be determined using the following equation:

$$Ps = 144 \times (Gam_{PCC} \times H_{PCC} + Gam_{base} \times H_{base}) \quad \textbf{(14)}$$

where,
- Gam_{PCC} = Unit weight of concrete (lb/in.^{3})
- Gam_{base} = Unit weight of base (lb/in.^{3})
- H_{PCC} = Concrete thickness (in.)
- H_{base} = base thickness (in.)

The step-by-step faulting calculation made from available variables can be described as follows:

Step 1: Calculate $\delta_{curling}$ using Equation 10.

$$\delta_{curling} = \frac{FAULTMAX_0}{C_{12}} \times [\log(1 + C_5 \times 5^{EROD}) \times \log(\frac{P_{200} \times Wet\ Days}{p_s})]^{C_6} \quad \textbf{(15)}$$

Step 2: Using this $\delta_{curling}$ value, calculate the corrected value of the $FAUTMAX_0$ as follows:

$$FAULTMAX_0^{New} = C_{12}^{New} \times \delta_{curling} \times [\log(1 + C_5^{New} \times 5^{EROD}) \times \log(\frac{P_{200} * Wet\ Days}{p_s})]^{C_6^{New}} \quad \textbf{(16)}$$

Step 3: Using the corrected value of the initial maximum mean transverse joint faulting $FAULTMAX_0^{New}$, calculate the maximum mean transverse joint faulting for each month as follows:

$$FAULTMAX_i^{New} = FAULTMAX_{i-1}^{New} + C_7^{New}/10^6) \sum_{j=1}^{m} DE_j \times \log(1 + C_5^{New} \times 5^{EROD})^{C_6^{New}} \quad \textbf{(17)}$$

Step 4: Calculate the faulting increment as follows:

$$\Delta Fault_i^{New} = C_{34}^{New} \times (FAULTMAX_{i-1}^{New} - Fault_{i-1}^{New})^2 \times DE_i \qquad \text{i=1,2…} \quad \textbf{(18)}$$

Step 5: Calculate the mean joint faulting at the end of month i as follows:

$$Fault_i^{New} = Fault_{i-1}^{New} + \Delta Fault_i^{New} \quad i = 1, 2 \ldots \tag{19}$$

Step 6: The calculated faulting values are compared with the values produced by the software to determine whether the same values were obtained. Figure 11 shows the correlation between the calculated faulting values and the values output by the software.

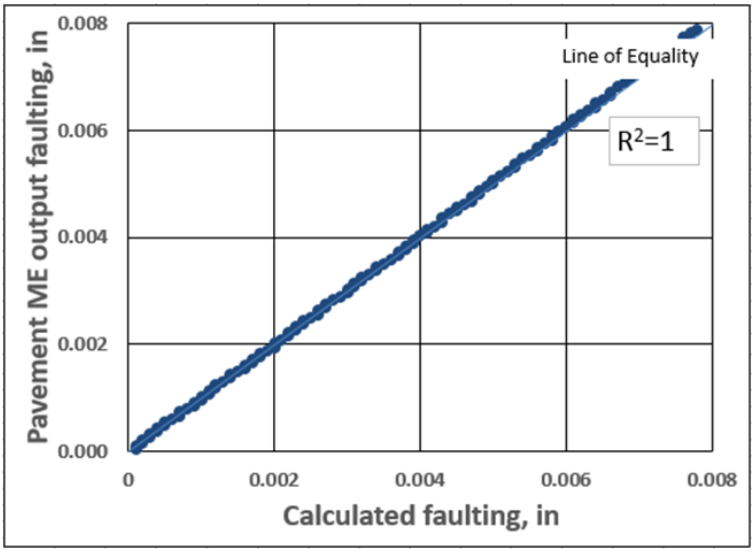

Figure 11. Faulting values comparison between AASHTOWare Pavement ME Design output and calculated values

Calculated mean joint faulting values were compared with the actual Iowa DOT PMIS faulting measurements for each section in the calibration data set. A local calibration coefficients optimization procedure was performed using different nonlinear optimization approaches (MS Excel Solver, Lingo, and brute force) to minimize the MSE between the predicted and actual mean joint faulting values. The set of calibration coefficients determined from the optimization procedure was used as the set of local calibration coefficients. For validation purposes, the local calibration coefficient accuracy was evaluated using an independent validation data set.

Figure 12 and Figure 13 compare the faulting predictions using nationally calibrated, MEPDG locally calibrated, and AASHTOWare Pavement ME Design locally calibrated coefficients for the calibration and validation data sets, respectively.

Calibration Set

National Calibration

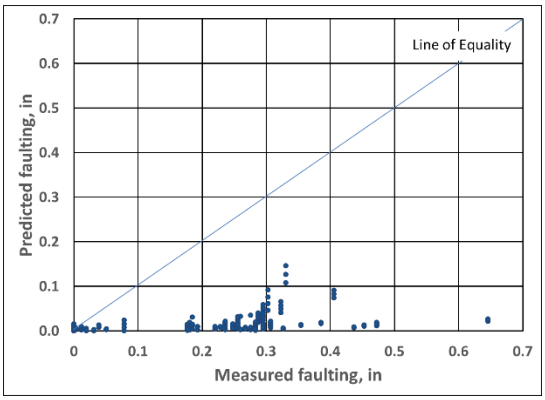

Local Calibration from MEPDG

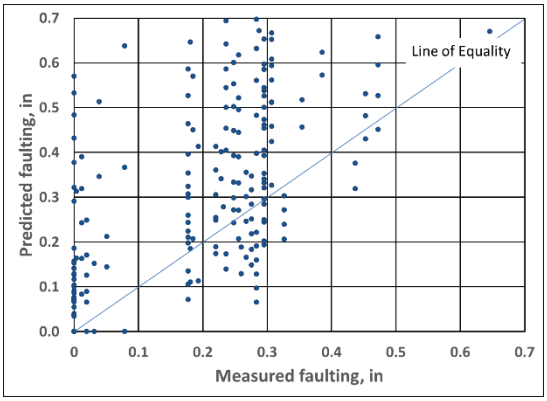

Local Calibration from Pavement ME

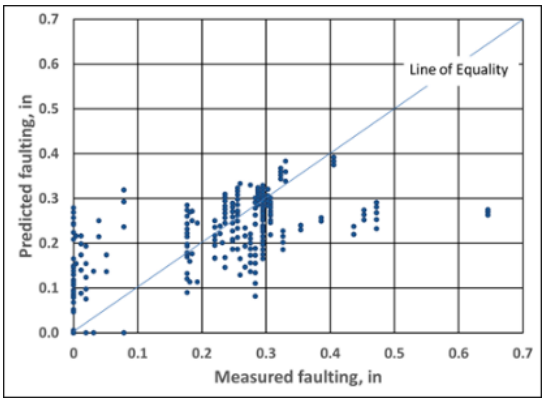

Coefficients	National	Local MEPDG	Local Pavement ME
C1	1.02	2.04	0.85
C2	0.92	1.84	1.39
C3	0.002	0.004	0.002
C4	0.001	0.002	0.274
C5	250.0	250.0	250.8
C6	0.4	0.8	0.4
C7	1.83	1.83	1.45
C8	400	400	400
N	248	248	248
Average Bias, inch	**0.189**	**-0.204**	**0.001**
Stnd Er, inch	**0.23**	**0.34**	**0.11**
LOE R^2	**-1.64**	**-4.66**	**0.47**
R^2	**0.17**	**0.34**	**0.47**

Figure 12. Overall accuracy summary of JPCP faulting model using calibration set

Validation Set

National Calibration

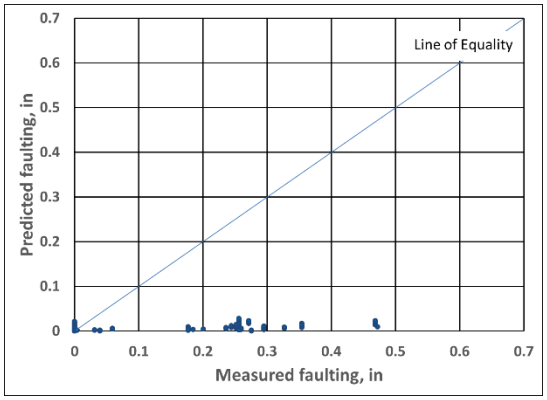

Local Calibration from MEPDG

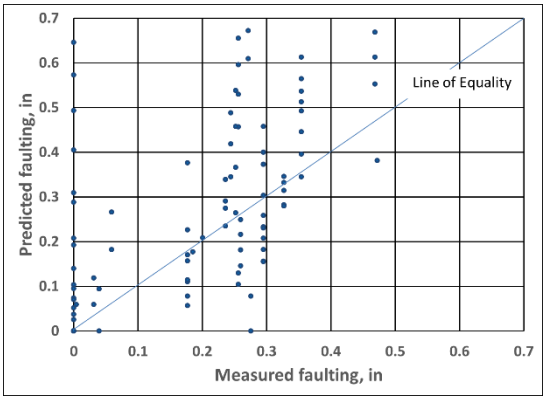

Local Calibration from Pavement ME

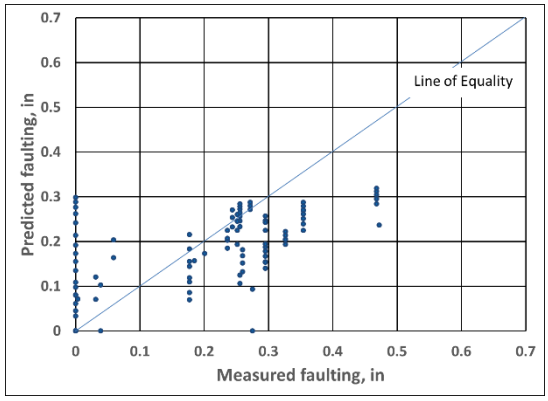

Coefficients	National	Local MEPDG	Local Pavement ME
C1	1.02	2.04	0.85
C2	0.92	1.84	1.39
C3	0.002	0.004	0.002
C4	0.001	0.002	0.274
C5	250	250	251
C6	0.4	0.8	0.4
C7	1.833	1.833	1.452
C8	400	400	400
N	101	101	101
Average Bias, inch	**0.19**	**0.10**	**-0.02**
Stnd Er, inch	**0.24**	**0.22**	**0.12**
LOE R^2	**-1.71**	**-1.26**	**0.36**
R^2	**0.23**	**0.29**	**0.38**

Figure 13. Overall accuracy summary of JPCP faulting model using validation set

Note that AASHTOWare Pavement ME Design software was used for these comparisons by changing each of the three calibration coefficient sets: ONC, local calibration coefficients from a previous study (Ceylan et al. 2013) that were determined from MEPDG runs by using a trial-and-error-based approach, and local calibration coefficients determined from the AASHTOWare Pavement ME Design software runs in this study.

As can be seen in Figures 12 and 13, the nationally calibrated faulting model underpredicted distress for Iowa JPCPs. When using MEPDG locally calibrated coefficients determined through a trial-and-error-based approach from a previous study (Ceylan et al. 2013), significant amount of standard error was still observed, although underprediction was mostly eliminated. As a result of the optimization procedure for the AASHTOWare Pavement ME Design JPCP faulting model, 7 of 8 nationally calibrated coefficients were optimized. Further accuracy improvement in

the AASHTOWare Pavement ME Design JPCP faulting model for Iowa JPCP could be achieved through nonlinear optimization approaches by using fully optimized local calibration coefficients.

Faulting predictions from the locally calibrated AASHTOWare Pavement ME Design model are higher than those from the nationally calibrated model. This finding implies that increases in pavement thickness and dowel diameter are recommended when the locally calibrated AASHTOWare Pavement ME Design faulting model is used instead of the nationally calibrated model, given that faulting is the controlling failure mode. Using the locally calibrated AASHTOWare Pavement ME Design faulting model would make the design more conservative.

Transverse Slab Cracking (Bottom-Up and Top-Down)

Transverse cracking predictions were computed using two models: the fatigue damage model and transverse cracking transfer functions. The fatigue damage model provides a fatigue damage estimate for the given conditions, and the transverse cracking transfer model converts the fatigue damage estimation into transverse cracking predictions equivalent to transverse cracking measurements.

Transverse slab cracking predictions were calculated from a set of equations as follows (AASHTO 2008):

$$\log(N_{allowable}) = C_1\left(\frac{M_R}{\sigma}\right)^{C_2} \quad \textbf{(20)}$$

$$Crack = \frac{100}{1+C_4 \times FD^{C_5}} = \frac{100}{1+C_4 \times (N_{applied}/N_{allowable})^{C_5}} \quad \textbf{(21)}$$

where,

- MR = Modulus of rupture of the concrete
- σ = Critical stress in the slab
- FD = Fatigue damage
- $N_{applied}$ = Applied number of load applications
- $N_{allowable}$ = Allowable number of load applications
- $C_{1, 2, 4, 5}$ = Calibration coefficients

The total slab cracking prediction provided by AASHTOWare Pavement ME Design software is the sum of bottom-up and top-down cracking prediction values because, in JPCP systems, cracks can be initiated either from the bottom of the slab and propagate upwards or vice-versa, but not in both directions. Therefore, providing the combined cracking prediction is more meaningful than providing only bottom-up or top-down values (AASHTO 2008).

The total transverse cracking predictions are calculated as follows:

$$TCrack = \left(Crack_{Bottom-up} + Crack_{Top-down} - Crack_{Bottom-up} \times Crack_{Top-down}\right) \times 100 \textbf{(22)}$$

where,

- *TCrack* = Total transverse cracking (percent, all severities)
- $Crack_{Bottom\text{-}up}$ = Predicted amount of bottom-up transverse cracking (fraction)
- $Crack_{Top\text{-}down}$ = Predicted amount of top-down transverse cracking (fraction)

As can be seen from the equations, for this distress type four calibration coefficients must be calibrated from Equations 20 and 21. These four coefficients can be categorized into two groups: two (C_1 and C_2) are related to the stress ratio (M_R/σ) for fatigue damage estimation, and the other two (C_4 and C_5) are in the transverse cracking transfer model to convert fatigue damage estimations into transverse cracking predictions.

Searching for input variables for Equations 20, 21, and 22 revealed that $N_{applied}$ was not reported in any of the AASHTOWare Pavement ME Design output files. Communications with software developers (ARA, Inc., personal communication, September 24, 2014) regarding this issue confirmed that the latest version of AASHTOWare Pavement ME Design (version 2.1) does not provide this information. It was concluded that it is impossible to calibrate coefficients (C_1, C_2, C_4, and C_5) all together for actual transverse cracking measurements. Rather than using this approach, C_4 and C_5 could be optimized to actual transverse cracking measurements through nonlinear optimization approaches using the *FD* values reported under the "Cracking Data" tab in the final result summary output. However, without actual $N_{allowable}$ measurements, which would require many laboratory fatigue tests, C_1 and C_2 could not be calibrated even through nonlinear optimization approaches. Therefore, alternative approaches, such as trial-and-error, implemented using a linear optimization approach as a screening procedure (Ceylan et al. 2013, Kim et al. 2014), were used to calibrate the coefficients of C_1 and C_2. The step-by-step procedure for locally calibrating the JPCP transverse cracking model is as follows:

Step 1: A sensitivity analysis of all transverse cracking model calibration coefficients was performed; the results are shown in Table 16.

Table 16. Sensitivity analysis results of transverse cracking calibration coefficients

Calibration factors	Coefficient Sensitivity Index	Rank
$\mathbf{C_1}$	-2.58	1
$\mathbf{C_2}$	-2.52	2
$\mathbf{C_4}$	-0.11	3
$\mathbf{C_5}$	0.24	4

Detailed descriptions of this sensitivity analysis are provided in Appendix C. Based on the sensitivity analysis results, the C_1 and C_2 coefficients in the fatigue damage model were found to be more sensitive to transverse slab cracking predictions than the C_4 and C_5 coefficients in the transverse cracking transfer function. Taking this information into account, a set of C_1 and C_2 coefficients was selected via a linear optimization approach using the sensitivity index as a screening procedure to reduce the computational burden of the trial-and-error procedure. Among the many sets of C_1 and C_2 coefficients selected, the C_1 and C_2 coefficients resulting in the minimum MSE between transverse cracking predictions and measurements were determined through a trial-and-error procedure using AASHTOWare Pavement ME Design.

Step 2: The determined C_1 and C_2 coefficients were input into AASHTOWare Pavement ME Design to execute its runs for each section to produce a calibration data set. Both bottom-up and top-down fatigue damage estimations from the AASHTOWare Pavement ME Design runs were extracted under the "Cracking Data" tab in the final result summary output files.

Step 3: Using these fatigue damage predictions, C_4 and C_5 calibration coefficients were calibrated with the help of various nonlinear optimization approaches (MS Excel Solver, Lingo, and brute force) applied to Equations 21 and 22.

Figure 14 and Figure 15 compare the transverse cracking predictions using nationally calibrated, MEPDG locally calibrated, and AASHTOWare Pavement ME Design locally calibrated coefficients for the calibration and validation sets, respectively.

Calibration Set

National Calibration

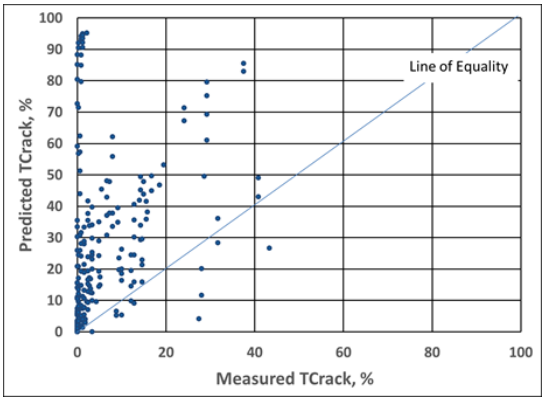

Local Calibration from MEPDG

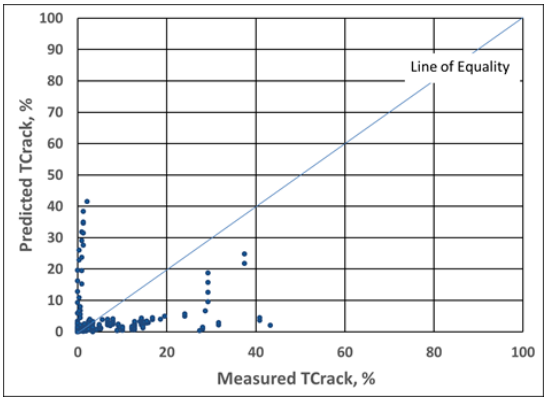

Local Calibration from Pavement ME

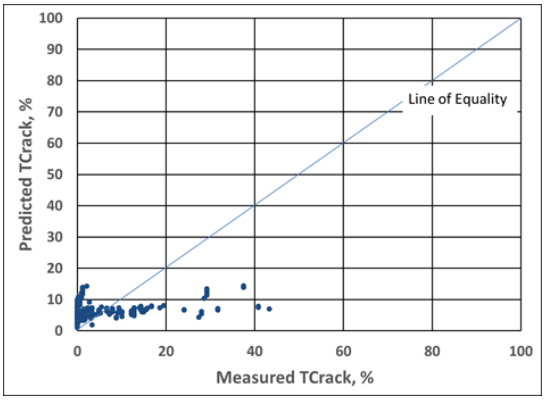

Coefficients	National	Local MEPDG	Local Pavement ME
C1	2	2.17	2.25
C2	1.22	1.32	1.4
C4	1	1.08	4.06
C5	-1.98	-1.81	-0.44
N	240	240	240
Average Bias, %	19.67	-1.90	0.36
Stnd er, %	31.38	10.86	8.18
LOE R^2	-11.58	-0.51	0.14
R^2	0.11	0.02	0.15

Figure 14. Overall accuracy summary of JPCP transverse cracking model using calibration set

Validation Set

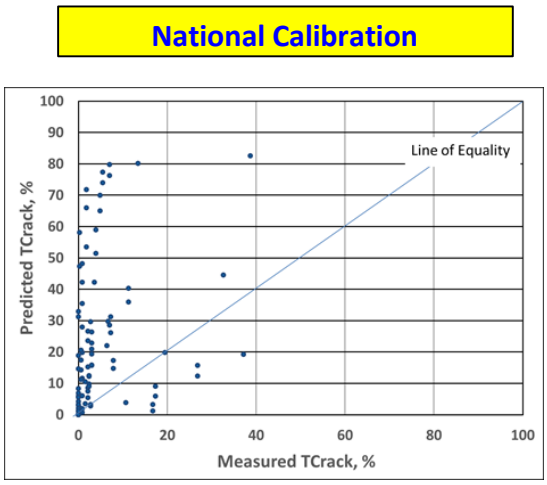

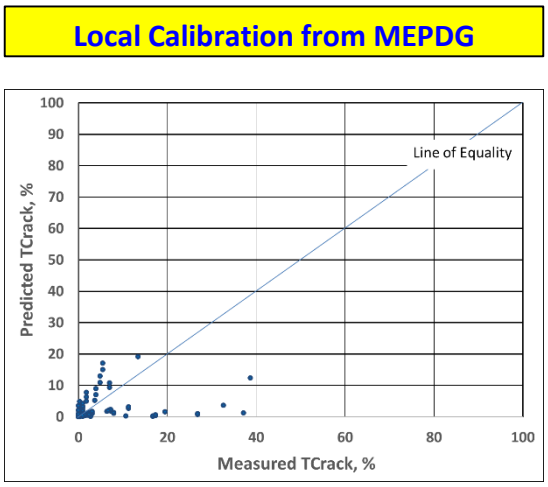

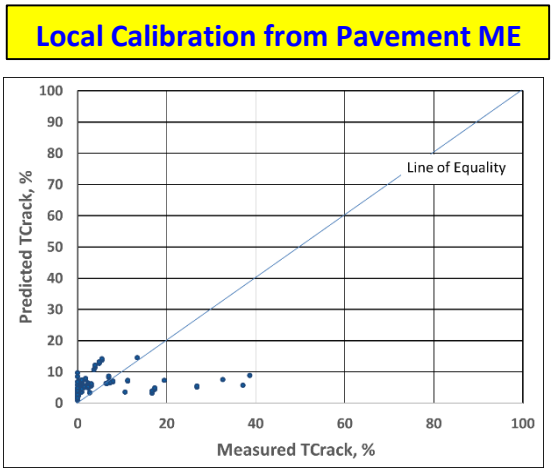

Coefficients	National	Local MEPDG	Local Pavement ME
C1	2	2.17	2.25
C2	1.22	1.32	1.4
C4	1	1.08	4.06
C5	-1.98	-1.81	-0.44
N	101	101	101
Average Bias, %	16.59	-2.29	0.99
Stnd er, %	28.02	8.23	7.75
LOE R^2	-11.70	-0.10	0.03
R^2	0.07	0.06	0.06

Figure 15. Overall accuracy summary of JPCP transverse cracking model using validation set

As can be seen in Figures 14 and 15, the transverse cracking model using the nationally calibrated coefficients could not accurately predict transverse cracking distress in Iowa JPCP. This might be explained by the fact that typical Iowa JPCP has a joint spacing of 20 ft while JPCP in most other states has less than 20 ft of joint spacing, which is reflected in the LTPP data used for national calibration. Using MEPDG locally calibrated coefficients, the accuracy of model predictions was improved compared to using nationally calibrated coefficients. Further accuracy improvement was attempted for AASHTOWare Pavement ME Design by minimizing standard error. Significant accuracy enhancements can be accomplished using locally calibrated AASHTOWare Pavement ME Design transverse cracking predictions (see Figure 14 and Figure 15).

Figure 16 presents fatigue damage predictions using nationally calibrated, MEPDG locally calibrated, and AASHTOWare Pavement ME Design locally calibrated fatigue damage calibration coefficients (i.e., C_1 and C_2 coefficients).

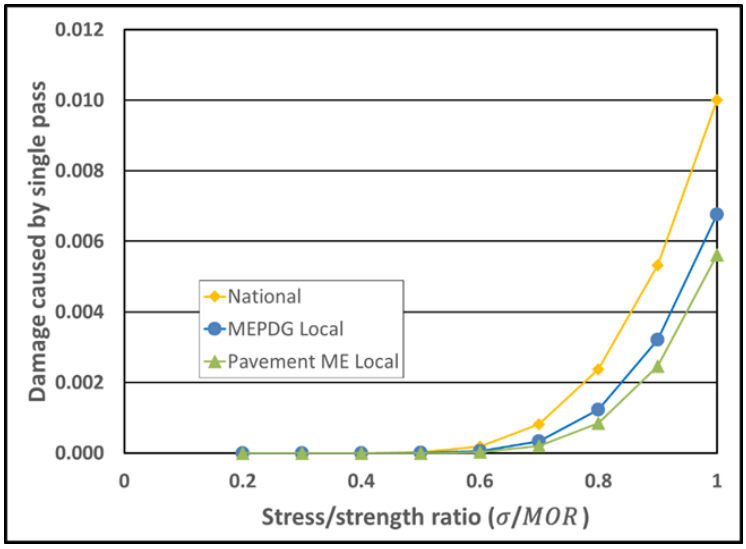

Figure 16. Fatigue damage prediction comparisons

For the given stress/strain ratios (σ/MOR), using AASHTOWare Pavement ME Design locally calibrated fatigue damage calibration coefficients can provide fewer damage predictions in comparison to using nationally calibrated and MEPDG locally calibrated fatigue damage calibration coefficients. This implies that using AASHTOWare Pavement ME Design locally calibrated fatigue damage calibration coefficients will lead to thinner pavement thickness and wider joint spacing in Iowa JPCP design than when using nationally calibrated and MEPDG locally calibrated fatigue damage calibration coefficients, given that the other coefficients (i.e., C_4 and C_5 coefficients) remain the same and that transverse cracking is the controlling distress mode in JPCP design.

Smoothness (IRI)

IRI is the smoothness performance index employed in AASHTOWare Pavement ME Design. The AASHTOWare Pavement ME Design IRI prediction model for JPCP consists of the transverse cracking prediction, the joint faulting prediction, the spalling prediction, and a site factor, along with the calibration coefficients. The AASHTO Mechanistic-Empirical Pavement Design Guide, Interim Edition: A Manual of Practice (AASHTO 2008) presents the JPCP IRI prediction equation employed in MEPDG as follows:

$$IRI = IRIini + C1 \times CRK + C2 \times SPALL + C3 \times TFAULT + C4 \times SF \quad \textbf{(23)}$$

where,

- *IRI* = Predicted IRI, in./mi
- *IRIini* = Initial smoothness measured as IRI, in./mi
- *CRK* = Percent slabs with transverse cracks (all severities)
- *SPALL* = Percentage of joints with spalling (medium and high severities)
- *TFAULT* = Total joint faulting cumulated, in.
- *SF* = Site factor
- $C_{1,2,3,4}$ = Calibration coefficients

The site factor of Equation 20 can be calculated as follows:

$$SF = AGE(1 + 0.5556 \times FI)(1 + P_{200}) \times 10^{-6} \quad \textbf{(24)}$$

where,

- *AGE* = Pavement age, yr
- *FI* = Freezing index, °F-days
- P_{200} = Percent subgrade material passing No. 200 sieve

However, the JPCP IRI values reported in the AASHTOWare Pavement ME Design software outputs could not be obtained using Equation 23. Communications with the AASHTOWare Pavement ME design software developers (ARA, Inc., personal communication, July 7, 2015) resulted in the following corrected JPCP IRI equation used in AASHTOWare Pavement ME Design:

$$IRI = IRIini + C1 \times CRK + C2 \times SPALL + C3 \times TFAULT \times 5280/JSP + C4 \times SF \quad \textbf{(25)}$$

where,

- *JSP* = Joint spacing, ft

Because the percentage of both transverse cracking and faulting are involved in the calculation of IRI, either nationally calibrated or locally calibrated transverse cracking and faulting models can be used for local calibration of the IRI model. Two approaches for local calibration of the coefficients of the IRI model were investigated as follows:

- **Approach 1**: Calibrate using either locally calibrated or nationally calibrated distress prediction models. Note that nationally calibrated distress prediction models can be used when they provide good accuracy in distress measurements.
- **Approach 2**: Calibrate only using nationally calibrated distress prediction models without considering the accuracy of distress model predictions with respect to distress measurements.

The purpose of using two approaches in the local calibration of the IRI model is to determine whether the IRI model can be locally calibrated with good accuracy without using the local

calibration procedure for each of the distress models, which expends financial and data resources.

The availability of each variable required for IRI calculation was carefully inspected. It was found that all the variables could either be extracted from general or intermediate output files or calculated using data provided by the output files. The location or calculation method of each variable can be described as follows:

- *IRIini* is input in the software as an initial IRI value. It can also be obtained from the final result summary output file.
- *CRK and TFAULT* can be obtained from the "Distress Data" tab in the final result summary output file.
- *SPALL* can be obtained from the "Spalling.txt" intermediate output file.
- *SF* can be calculated using Equation 24.
- *FI for SF calculation* can be obtained from the "Climate Inputs" tab in the final result summary output file.
- P_{200} is a used input value or can be taken from the "Layer #" tab in the final result summary output file.
- Note that AASHTOWare Pavement ME Design uses an intermediate file "JPCPIRIInput.txt" in calculating IRI predictions.

Figure 17 demonstrates that the JPCP IRI values calculated using Equation 25 are the same as those obtained from AASHTOWare Pavement ME Design software output files.

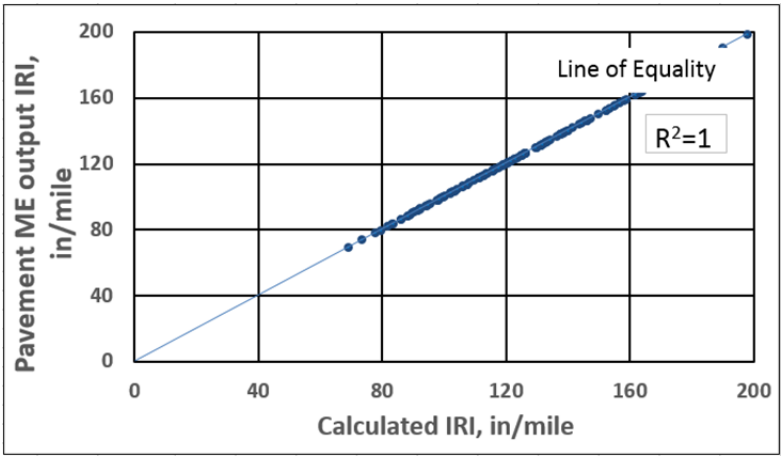

Figure 17. Comparison of calculated IRI values and values output from AASHTOWare Pavement ME Design

As can be seen in Equation 25, both transverse cracking and faulting predictions are involved in the calculation of IRI. In this study, both locally and nationally calibrated transverse cracking and faulting predictions were used for local calibration of the JPCP IRI model. The step-by-step procedure for local calibration of the JPCP IRI model is as follows:

Step 1: Site factor values for each year of each pavement section in the calibration data set were calculated using Equation 25. Using these values along with the other input variables required by Equation 25, IRI predictions for each year and each pavement section were calculated. Note that locally calibrated transverse cracking and faulting model predictions are used as inputs in the IRI equation in Approach 1, while nationally calibrated transverse cracking and faulting model predictions are used as inputs in the IRI equation in Approach 2. Initially, nationally calibrated C_1, C_2, C_3, and C_4 coefficients were used in the calculation of IRI, and these coefficients were also used as inputs in the AASHTOWare Pavement ME Design software runs to ensure that the calculated and AASHTOWare Pavement ME Design output IRI values were the same (using Approach 1) (Figure 17).

Step 2: The differences between the IRI predictions and measurements of each pavement section in the calibration data set were calculated and summed to produce MSE.

Step 3: The optimization procedure for local calibration coefficients was performed using various nonlinear optimization approaches (MS Excel Solver, Lingo, and brute force) to minimize the MSE between the predicted and actual IRI values. The set of calibration coefficients providing the minimum MSE was in turn taken as the AASHTOWare Pavement ME Design local calibration coefficient set for the IRI model.

Approach 1

Figure 18 and Figure 19 compare the IRI predictions using nationally calibrated, MEPDG locally calibrated, and AASHTOWare Pavement ME Design locally calibrated coefficients for the calibration and validation sets, respectively.

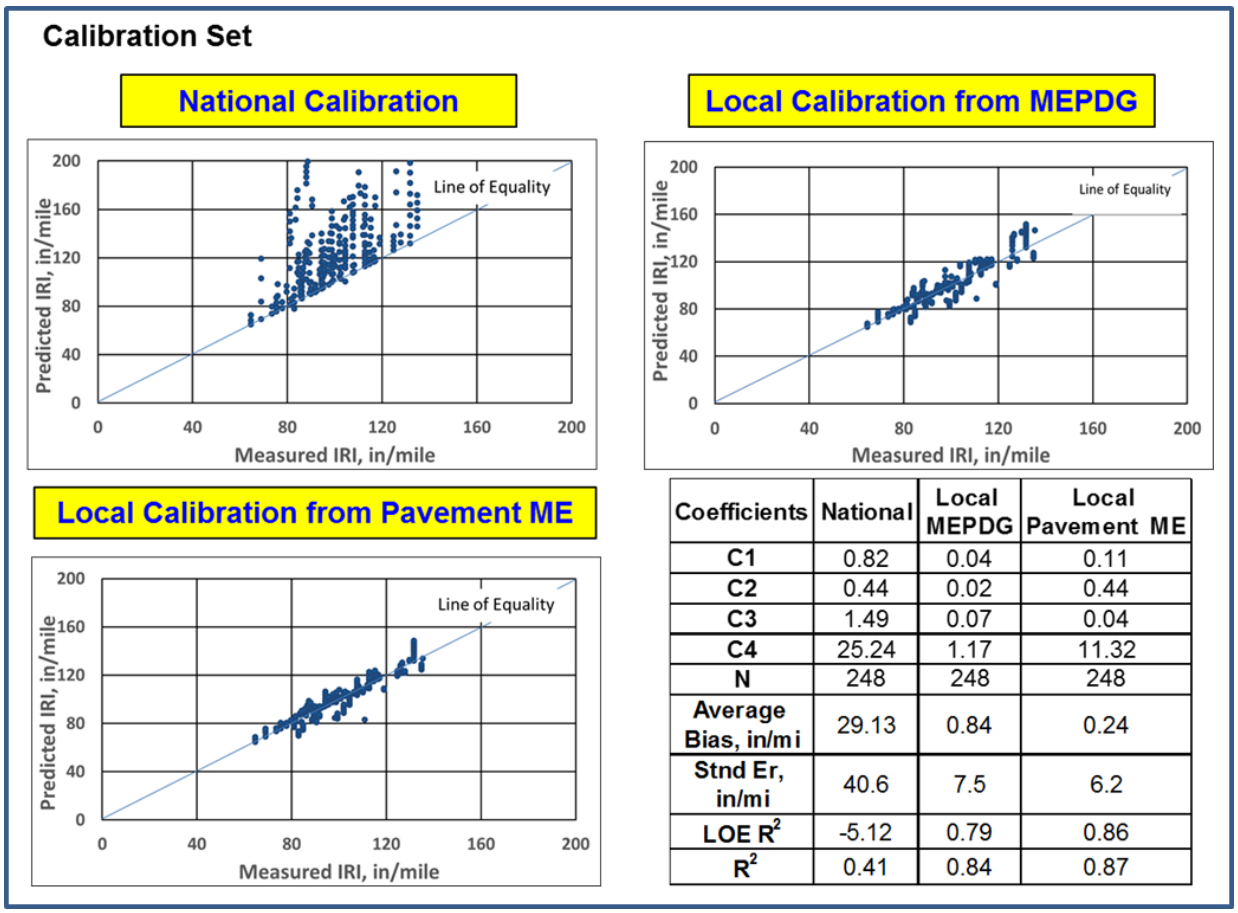

Coefficients	National	Local MEPDG	Local Pavement ME
C1	0.82	0.04	0.11
C2	0.44	0.02	0.44
C3	1.49	0.07	0.04
C4	25.24	1.17	11.32
N	248	248	248
Average Bias, in/mi	29.13	0.84	0.24
Stnd Er, in/mi	40.6	7.5	6.2
LOE R^2	-5.12	0.79	0.86
R^2	0.41	0.84	0.87

Figure 18. Overall accuracy summary of the JPCP IRI model using calibration set (Approach 1)

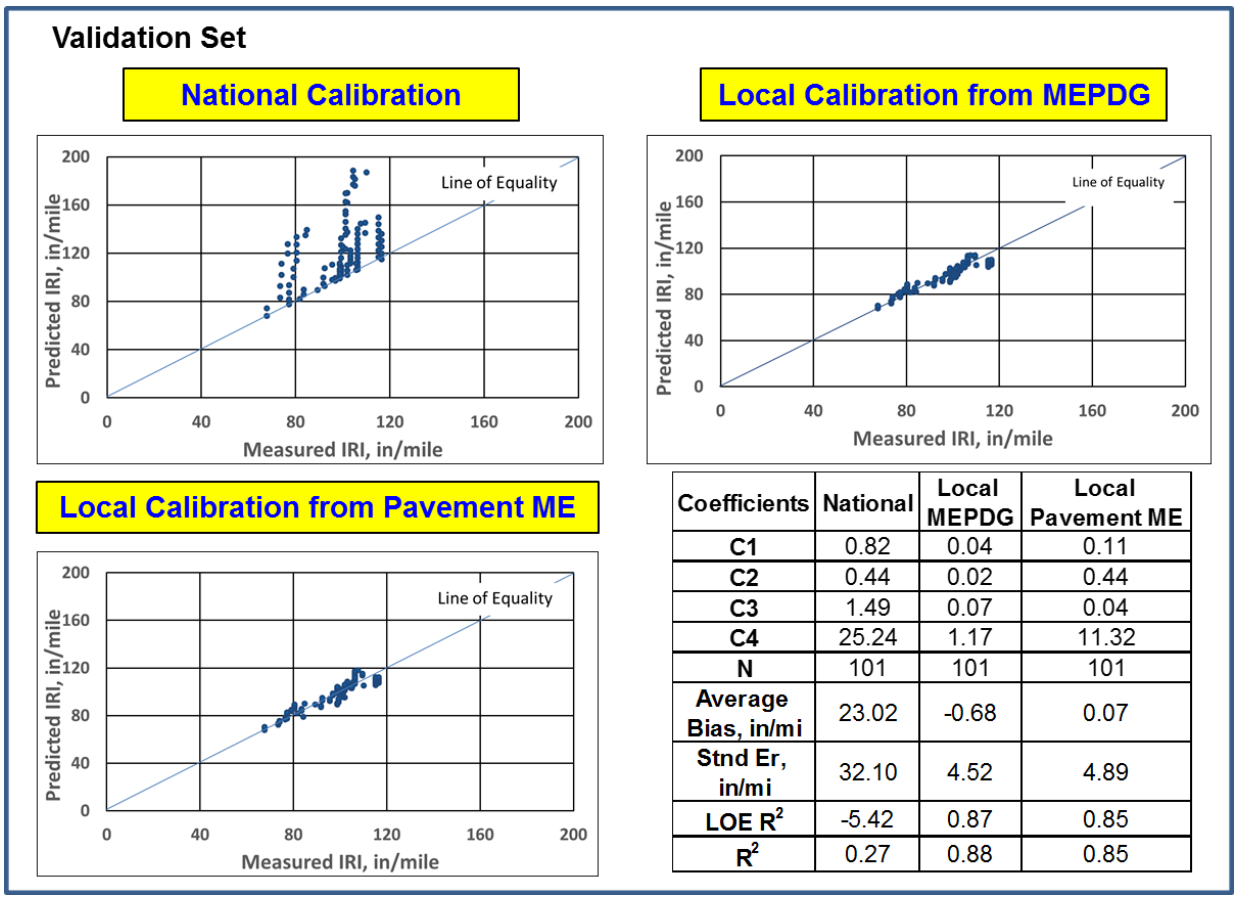

Coefficients	National	Local MEPDG	Local Pavement ME
C1	0.82	0.04	0.11
C2	0.44	0.02	0.44
C3	1.49	0.07	0.04
C4	25.24	1.17	11.32
N	101	101	101
Average Bias, in/mi	23.02	-0.68	0.07
Stnd Er, in/mi	32.10	4.52	4.89
LOE R^2	-5.42	0.87	0.85
R^2	0.27	0.88	0.85

Figure 19. Overall accuracy summary of the JPCP IRI model using validation set (Approach 1)

Approach 1 was used for local calibrations for both MEPDG and AASHTOWare Pavement ME Design. As can be seen in Figures 18 and 19, both the MEPDG and AASHTOWare Pavement ME Design locally calibrated models produce more accurate predictions than the nationally calibrated model. Additionally, the locally calibrated AASHTOWare Pavement ME Design model is more accurate than the MEPDG locally calibrated model.

Approach 2

An alternative approach (Approach 2) was also used to locally calibrate the IRI model using AASHTOWare Pavement ME Design. In this approach, nationally calibrated transverse cracking and faulting model predictions were used as inputs in the IRI equation. As seen in Figure 20 and Figure 21, Approach 2 can also significantly improve IRI predictions.

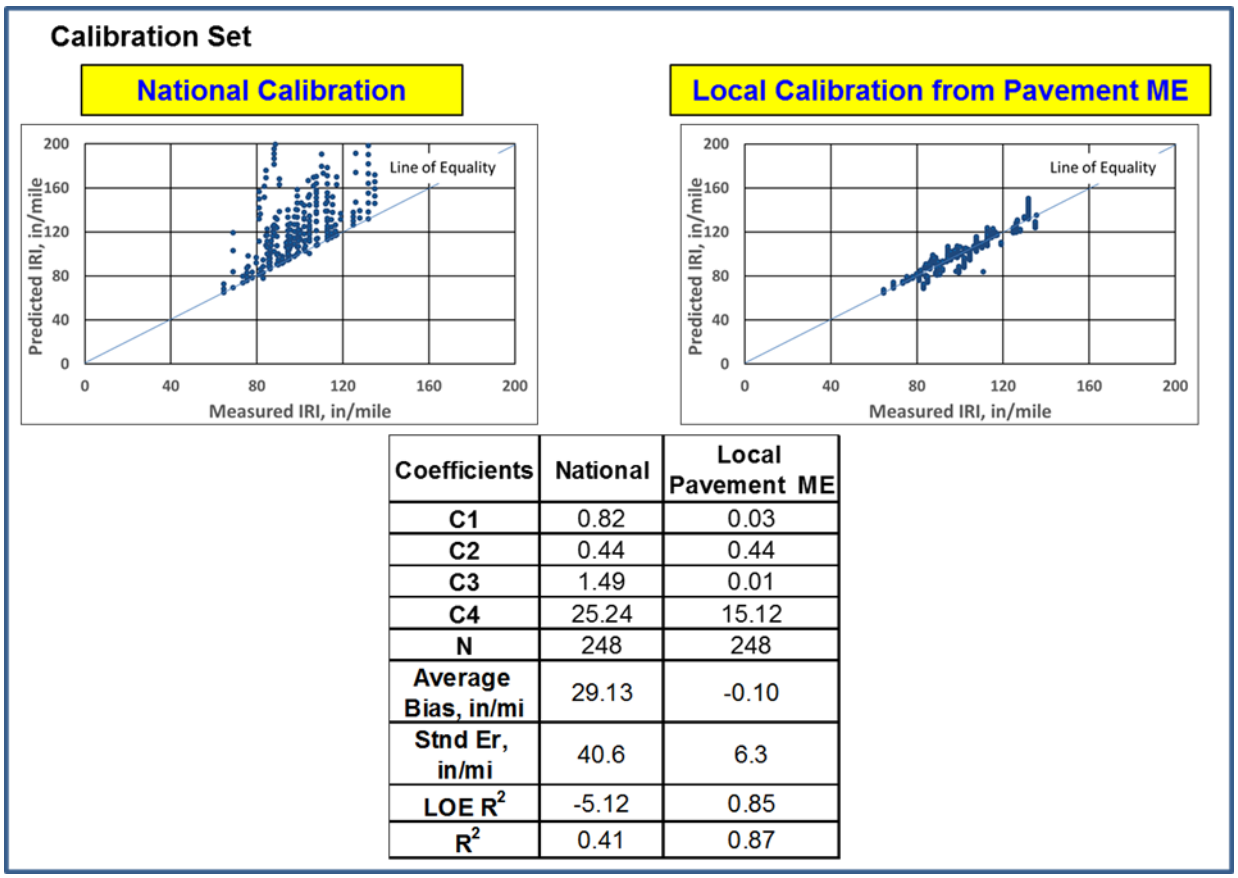

Coefficients	National	Local Pavement ME
C1	0.82	0.03
C2	0.44	0.44
C3	1.49	0.01
C4	25.24	15.12
N	248	248
Average Bias, in/mi	29.13	-0.10
Stnd Er, in/mi	40.6	6.3
LOE R^2	-5.12	0.85
R^2	0.41	0.87

Figure 20. Overall accuracy summary of JPCP IRI model using calibration set (Approach 2)

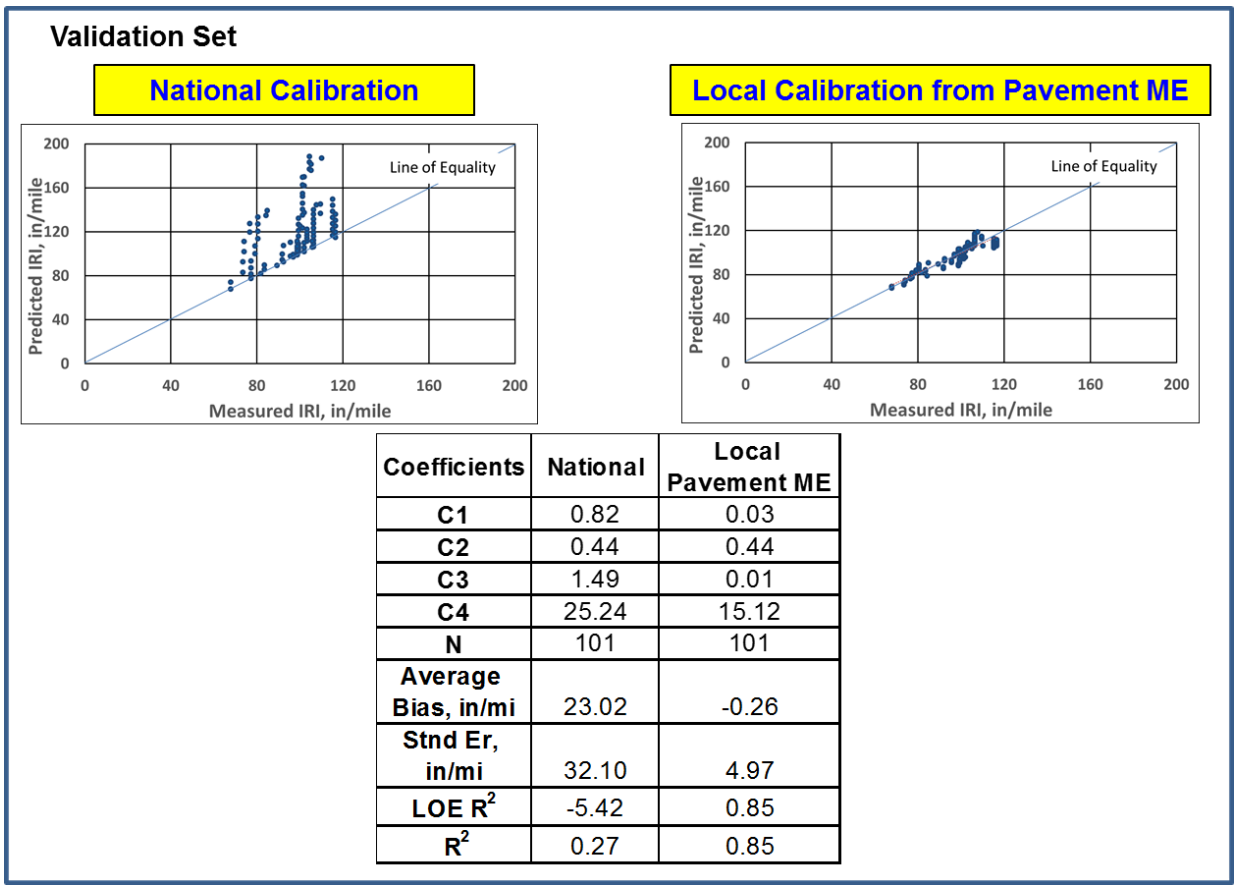

Coefficients	National	Local Pavement ME
C1	0.82	0.03
C2	0.44	0.44
C3	1.49	0.01
C4	25.24	15.12
N	101	101
Average Bias, in/mi	23.02	-0.26
Stnd Er, in/mi	32.10	4.97
LOE R^2	-5.42	0.85
R^2	0.27	0.85

Figure 21. Overall accuracy summary of JPCP IRI model using validation set (Approach 2)

The purpose of using two approaches in the local calibration of the IRI model was to determine whether the IRI model can be locally calibrated with sufficient accuracy without using the local calibration procedure for each distress model, thereby conserving financial and data resources. A locally calibrated IRI model using Approach 2 would save significant amounts of time and funds. Using Approach 2 to locally calibrate the IRI model would be especially useful for those SHAs that are more interested in obtaining locally calibrated IRI predictions than locally calibrated transverse cracking and faulting predictions. In this study, it was determined that Approach 2 with a locally calibrated IRI model can predict this distress with sufficient accuracy for Iowa JPCP systems.

HMA

The AASHTOWare Pavement ME Design performance prediction models for new HMA pavement include rutting, longitudinal (top-down) cracking, alligator (bottom-up) cracking, thermal (transverse) cracking, and IRI. Rutting predictions consist of HMA layer rutting, granular base rutting, subgrade rutting, and total surface rutting. Similar to those for JPCP, the HMA fatigue models use a damage estimate model along with fatigue distress transfer function models to provide longitudinal cracking and alligator cracking predictions equivalent to actual cracking measurements.

Rut Depth

AASHTOWare Pavement ME Design outputs rutting depth values in each sublayer, including an HMA-surfaced layer, an unbound aggregate base layer, and a subgrade, as well as total rutting in the HMA pavement. The total rut depth in AASHTOWare Pavement ME Design is calculated as the summation of rutting depths at each sublayer. The accumulated permanent or plastic deformation in the HMA layer/sublayer is calculated using the following equations (AASHTO 2008):

$$\Delta_{p(HMA)} = \varepsilon_{p(HMA)} \times h_{HMA} = \beta_{1r} \times k_z \times \varepsilon_{r(HMA)} \times 10^{k_{1r}} \times n^{k_{2r}\beta_{2r}} \times T^{k_{3r}\beta_{3r}} \quad \textbf{(26)}$$

where,

- $\Delta_{p(HMA)}$ = Accumulated permanent or plastic vertical deformation in the HMA layer/sublayer, in.
- $\varepsilon_{p(HMA)}$ = Accumulated permanent or plastic axial strain in the HMA layer/sublayer, in./in.
- $\varepsilon_{r(HMA)}$ = Resilient or elastic strain calculated by the structural response model at the mid-depth of each HMA sublayer, in./in.
- h_{HMA} = Thickness of the HMA layer/sublayer, in.
- n = Number of axle load repetitions
- T = Mix or pavement temperature, °F
- k_z = Depth confinement factor
- $k_{1r,2r,3r}$ = Global field calibration parameters (from the NCHRP 1-40D recalibration; k_{1r} = -3.35412, k_{2r} = 0.4791, k_{3r} = 1.5606)
- $\beta_{1r,2r,3r}$ = Local or mixture field calibration constants; for the global calibration, these constants were all set to 1.0

$$k_z = (C_1 + C_2 \times D) \times 0.328196^D \quad \textbf{(27)}$$

$$C_1 = -0.1039 \times H_{HMA}^2 + 2.4868 \times H_{HMA} - 17.342 \quad \textbf{(28)}$$

$$C_2 = 0.0172 \times H_{HMA}^2 - 1.7331 \times H_{HMA} + 27.428 \quad \textbf{(29)}$$

where,

- D = Depth below the surface, in.
- H_{HMA} = Total HMA thickness, in.

The accumulated permanent or plastic deformation in the base/subgrade is calculated using the following equations (AASHTO 2008):

$$\Delta_{p(soil)} = \beta_{s1} \times k_{s1} \times \varepsilon_v \times h_{soil} \times \frac{\varepsilon_0}{\varepsilon_r} \times e^{-(\frac{\rho}{n})^{\beta}} \quad \textbf{(30)}$$

where,

- $\Delta_{p(soil)}$ = Permanent or plastic deformation for the layer/sublayer, in.
- n = Number of axle load applications
- ε_0 = Intercept determined from laboratory repeated load permanent deformation tests, in./in.
- ε_r = Resilient strain imposed in laboratory tests to obtain material properties ε_0, ε, and ρ, in./in.
- ε_v = Average vertical resilient or elastic strain in the layer/sublayer and calculated by the structural response model, in./in.
- h_{soil} = Thickness of the unbound layer/sublayer, in.
- k_{s1} = Global calibration coefficients; k_{sl}= 1.673 for granular materials and 1.35 for fine-grained materials
- β_{s1} = A local calibration constant for rutting in the unbound layers; set to 1.0 for the global calibration procedure

$$Log\beta = -0.61119 - 0.017638 \times (W_c) \quad \textbf{(31)}$$

$$\rho = 10^9 \times (\frac{C_0}{1-(10^9)^{\beta}})^{\frac{1}{\beta}} \quad \textbf{(32)}$$

$$C_0 = Ln\left(\frac{a_1 M_r^{b_1}}{a_9 M_r^{b_9}}\right) = 0.0075 \quad \textbf{(33)}$$

where,

- W_c = Water content, %
- M_r = Resilient modulus of the unbound layer or sublayer, psi
- $a_{1,9}$ = Regression constants; a_1= 0.15 and a_9= 20.0
- $b_{1,9}$ = Regression constants; b_1= 0.0 and b_9= 0.0

Searching the equations in the AASHTOWare Pavement ME Design outputs revealed that not all of the required variables can be determined from the software output or from the intermediate output files to conduct local calibration outside the software.

The availability and location of each available variable for the HMA rutting model can be described as follows:

- $\varepsilon_{r(HMA)}$ is not provided by the software.
- h_{HMA} is an input value. It is known or can be checked from the "Grand Summary" tab in the final result summary output file.

- n is not provided by the software.
- T is not provided by the software.
- k_z can be calculated using Equations 27, 28, and 29.

The availability and location of each available variable for the subgrade rutting model can be described as follows:

- n is not provided by the software.
- ε_0 is not provided by the software.
- ε_r is not provided by the software.
- ε_v is not provided by the software.
- h_{soil} is an input value. It is known or can be checked from the "Grand Summary" tab in the final result summary output file.
- W_c is an input value. It is known or can be checked from the "Layer #" tab in the final result summary output file.
- M_r is an input value. It is known or can be checked from the "Layer #" tab in the final result summary output file.

Although AASHTOWare Pavement ME Design provides a vertical strain output file, "VertStrain.txt", which reports different vertical strain values for different subseasons, axle numbers, AC moduli, and load locations for each month, it is not known whether this reported vertical strain value is used in the equation during software execution. Leslie Titus-Glover of ARA, Inc. (Titus-Glover, ARA, Inc., 2015) provided a procedure for conducting local calibration by inputting different combinations of calibration coefficients into the software and choosing the combination that provides the most accurate prediction; a sensitivity analysis of the HMA rutting model calibration coefficients was conducted for that purpose, with detailed descriptions provided in Appendix C. Table 17 shows the sensitivity analysis results.

Table 17. Sensitivity analysis results of HMA rutting calibration coefficients

Calibration factors	Coefficient Sensitivity Index	Rank
BR2	9.65	1
BR3	8.94	2
BR1	1.00	3

Based on the sensitivity analysis results, an experimental matrix including different sets of calibration coefficients was prepared as shown in Table 18. After trying different sets of calibration coefficients, the set consisting of 1.1 and 1 for BR2 and BR3, respectively, resulted in the most accurate predictions (Table 18).

Table 18. Experimental matrix for local calibration of the HMA rutting model

BR2	BR3	R^2
1.15	1	0.12
1.1	1.05	0.26
1.1	1	0.55
1.05	1.05	0.53

Rutting measurement estimations from Iowa DOT PMIS data indicated that almost all total rutting is a result of HMA layer rutting, which is related to the fact that most selected HMA pavements are full-depth asphalt pavements, a reflection of present-day HMA pavement design and construction practices in Iowa. As a result, the local calibration coefficient for $\beta s1$ related to subgrade rutting was chosen as 0.001 to minimize subgrade rutting predictions.

Figure 22 and Figure 23 show the total rutting predictions using nationally calibrated, MEPDG locally calibrated, and AASHTOWare Pavement ME Design locally calibrated coefficients for the calibration and validation sets, respectively.

Calibration Set

National Calibration

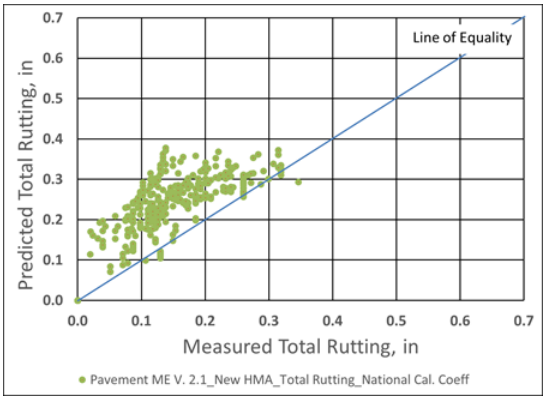

Local Calibration from MEPDG

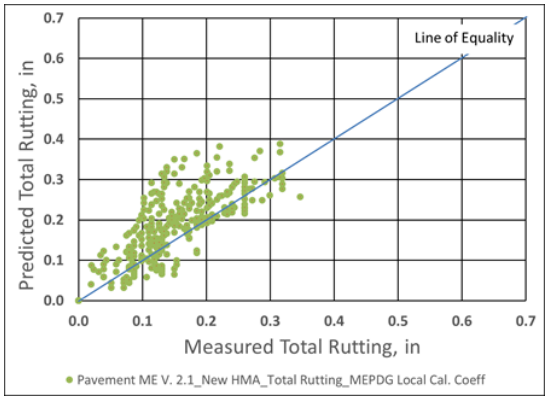

Local Calibration from Pavement ME

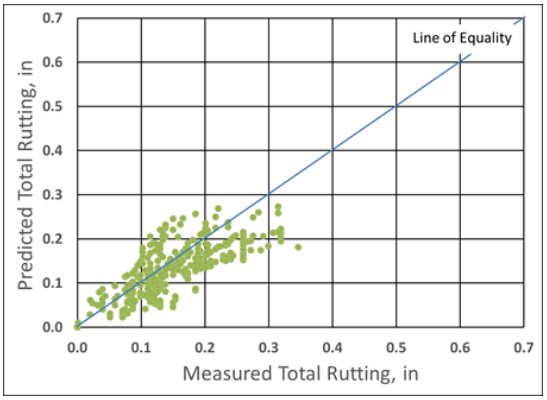

Coefficients	National	Local MEPDG	Local Pavement ME
B1	1	1	1
B2	1	1.15	1.1
B3	1	1	1
Bs1	1	0.001	0.001
N	299	299	299
Mean Bias, in	0.09	0.04	-0.02
Stnd Er, in	0.05	0.07	0.05
LOE R^2	-0.89	0.21	0.57
R^2	0.60	0.63	0.63
MAPE	0.80	0.40	0.30

Figure 22. Overall accuracy summary of HMA rutting model using calibration set

Validation Set

National Calibration

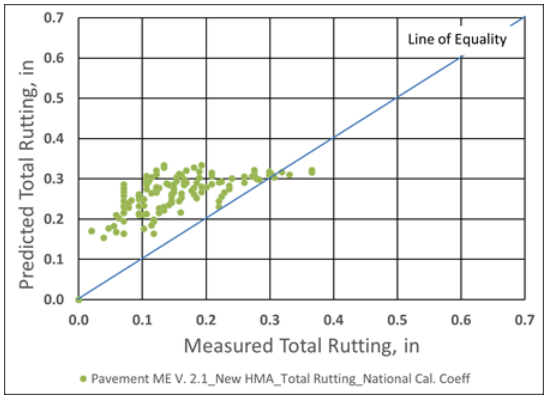

Local Calibration from MEPDG

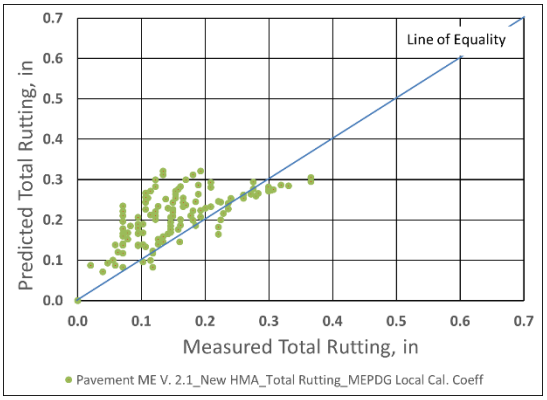

Local Calibration from Pavement ME

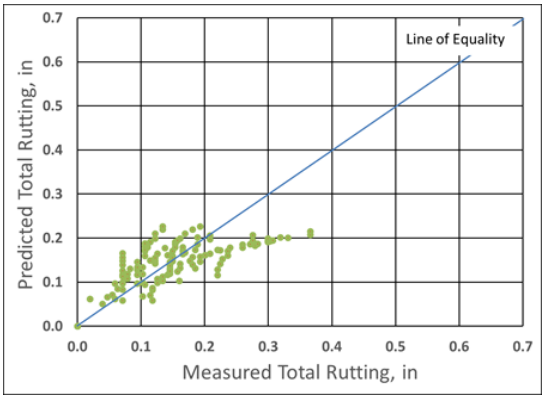

Coefficients	National	Local MEPDG	Local Pavement ME
B1	1	1	1
B2	1	1.15	1.1
B3	1	1	1
Bs1	1	0,001	0,001
N	133	133	133
Mean Bias, in	0.10	0.05	-0.01
Stnd Er, in	0.12	0.08	0.06
LOE R^2	-1.06	0.12	0.55
R^2	0.51	0.56	0.56
MAPE	1.02	0.57	0.32

Figure 23. Overall accuracy summary of HMA rutting model using validation set

As can be seen in Figures 22 and 23, although the MEPDG locally calibrated rutting model gives more accurate predictions than the nationally calibrated model, the accuracy is further improved when using the AASHTOWare Pavement ME Design locally calibrated rutting model identified in this study (Figure 22 and Figure 23).

Load-Related Cracking

AASHTOWare Pavement ME Design predicts two types of load-related cracking for flexible pavement systems: alligator cracking (bottom-up) and longitudinal cracking (top-down). The allowable number of axle load applications required for evaluating fatigue failure of the HMA layer can be calculated as follows (AASHTO 2008):

$$N_{f-HMA} = k_{f1} \times C \times C_H \times \beta_{f1} \times {\varepsilon_t}^{k_{f2}\beta_{f2}} \times {E_{HMA}}^{k_{f3}\beta_{f3}} \quad \textbf{(34)}$$

where,

- N_{f-HMA} = Allowable number of axle load applications for a flexible pavement and HMA overlays
- ε_t = = Tensile strain at critical locations calculated by the structural response model, in./in.
- E_{HMA} = Dynamic modulus of the HMA measured in compression, psi
- $k_{f1,f2,f3}$= Global field calibration parameters (from the NCHRP 1-40D recalibration; k_{f1} = 0.007566, k_{f2} = -3.9492, and k_{f3} = -1.281)
- $\beta_{f1,f2,f3}$ = Local or mixture-specific field calibration constants; for the global calibration effort, these constants were set to 1.0

$$C = 10^M \quad \textbf{(35)}$$

$$M = 4.84 \times \left(\frac{V_{be}}{V_a+V_b} - 0.69\right) \quad \textbf{(36)}$$

where,

- V_{be} = Effective asphalt content by volume, %
- V_a = Percent air voids in the HMA mixture
- C_H = Thickness correction term, dependent on type of cracking

For bottom-up or alligator cracking:

$$C_H = \frac{1}{0.000398+\frac{0.003602}{1+e^{(11.02-3.49\times H_{HMA})}}} \quad \textbf{(37)}$$

For top-down or longitudinal cracking:

$$C_H = \frac{1}{0.01+\frac{12.00}{1+e^{(15.676-2.8186\times H_{HMA})}}} \quad \textbf{(38)}$$

where,

- H_{HMA} = Total HMA thickness, in.

The cumulative damage index (DI) at critical locations is required for load-related cracking predictions and can be calculated by summing the incremental damages over time (Miner's hypothesis), as shown in the following equation:

$$DI = \sum(\Delta DI)_{j,m,l,p,T} = \sum(\frac{n}{N_{f-HMA}})_{j,m,l,p,T} \quad \textbf{(39)}$$

where,

- n = Actual number of axle load applications within a specific time period
- j = Axle load interval
- m = Axle load type (single, tandem, tridem, quad, or special axle configuration
- l = Truck type, identified using the truck classification groups included in the MEPDG
- p = Month
- T = Median temperature for the five temperature intervals or quintiles used to subdivide each month, °F

Alligator cracking and longitudinal cracking predictions, in term of area and length, respectively, can be calculated using the cumulative damage index along with the calibration coefficients of the transfer function equations, as shown in the following equations (AASHTO 2008):

$$FC_{Bottom} = \frac{1}{60} \times \frac{C_4}{1+e^{(C_1 \times C_1^* + C_2 \times C_2^* \times Log(DI_{Bottom} \times 100))}} \quad \textbf{(40)}$$

where,

- FC_{Bottom} = Area of alligator cracking that initiates at the bottom of the HMA layers, % of total lane area
- DI_{Bottom} = Cumulative damage index at the bottom of the HMA layers
- $C_{1,2,4}$ = Transfer function regression constants
- C_1^* and C_2^* = See equations 41 and 42

$$C_1^* = -2 \times C_2^* \quad \textbf{(41)}$$

$$C_2^* = -2.40874 - 39.748(1 + H_{HMA})^{-2.856} \quad \textbf{(42)}$$

where,

- H_{HMA} = Total HMA thickness, in.

$$FC_{Top} = 10.56 \times \frac{C_4}{1+e^{(C_1 - C_2 Log(DI_{Top}))}} \quad \textbf{(43)}$$

where,

- FC_{Top} = Length of longitudinal cracks that initiate at the top of the HMA layer, ft/mi

- DI_{Top} = Cumulative damage index near the top of the HMA surface
- $C_{1,2,4}$ = Transfer function regression constants

The availability of each variable of the equations above was carefully inspected. For this distress type, not all of the variables required could have been determined from the software output or intermediate output files to conduct local calibration outside the software.

The availability and location of each available variable for the fatigue model can be described as follows:

- ε_t is not provided by the software.
- E_{HMA} is not provided by the software.
- V_{be} is an input value. It is known or can be obtained from the "Layer #" tab in the final result summary output file
- V_a is an input value. It is known can be obtained from the "Layer #" tab in the final result summary output file.
- H_{HMA} is an input value. It is known can be obtained from the "Layer #" tab in the final result summary output file.
- *n* is not provided by the software.

The availability and location of each available variable for the alligator and longitudinal cracking transfer functions can be described as follows:

- DI_{Bottom} is provided in the "Fatigue Data" tab of the final result summary output file.
- DI_{Top} is provided in the "Fatigue Data" tab of the final result summary output file.

In both alligator and longitudinal cracking prediction models, there are two sets of coefficients: one set comes from the fatigue model, the other comes from the top-down or bottom-up cracking transfer functions. Sensitivity analysis of HMA fatigue and determination of alligator and longitudinal cracking model calibration coefficients were conducted to obtain an idea of the sensitivity of the related calibration coefficients, with results given in Appendix C. Table 19, Table 20, and Table 21 summarize the sensitivity analysis results of the HMA fatigue, alligator (bottom-up) cracking, and longitudinal (top-down) cracking models, respectively.

Table 19. Sensitivity analysis results of HMA fatigue model calibration coefficients

Calibration factors	Coefficient Sensitivity Index	Rank
BF2	-5153.72	1
BF3	77.67	2
BF1	-1.04	3

Table 20. Sensitivity analysis results of HMA alligator (bottom-up) cracking model calibration coefficients

Calibration factors	Coefficient Sensitivity Index	Rank
C1_bottom	-5.65	1
C2_bottom	-1.24	2
C4_bottom	1.00	3

Table 21. Sensitivity analysis results of HMA longitudinal (top-down) cracking model calibration coefficients

Calibration factors	Coefficient Sensitivity Index	Rank
C1_Top	-9.54	1
C2_Top	-5.64	2
C4_Top	1.00	3

By considering the availability of each equation variable and using the results of the sensitivity analysis, this study focused on the recalibration of the top-down and bottom-up transfer function coefficients rather than the fatigue model coefficients. Note that fatigue model calibration would require laboratory testing to yield accurate results. Nonlinear optimization techniques were used to calibrate both top-down and bottom-up transfer function coefficients.

Figure 24 and Figure 25 compare HMA alligator (bottom-up) cracking predictions using nationally calibrated, MEPDG locally calibrated, and AASHTOWare Pavement ME Design locally calibrated coefficients for the calibration and validation sets, respectively.

Calibration Set

National Calibration

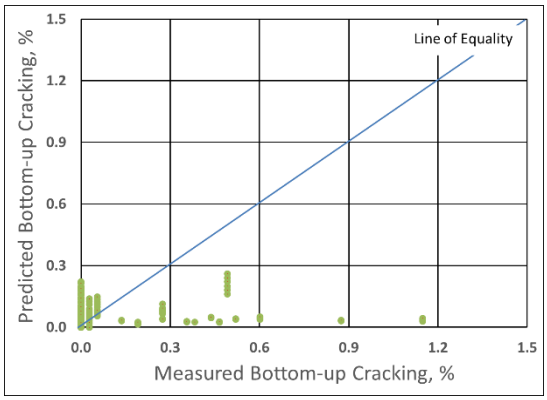

Local Calibration from MEPDG

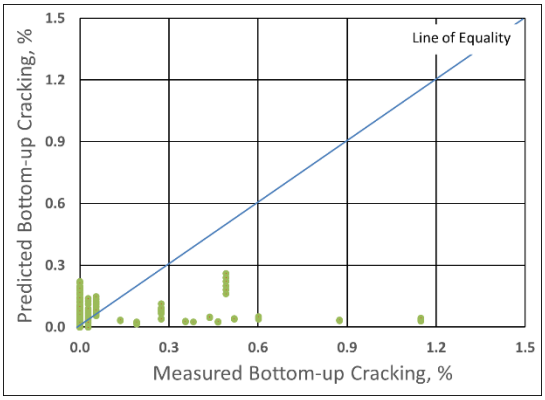

Local Calibration from Pavement ME

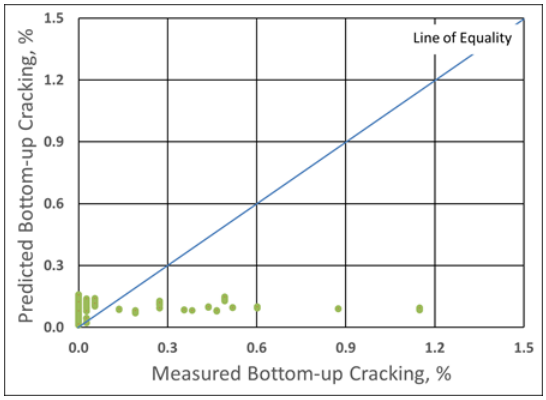

Coefficients	National	Local MEPDG	Local Pavement ME
C1_Bottom	1.00	1.00	1.25
C2_Bottom	1.00	1.00	0.30
C3 _Bottom	6,000	6,000	6,000
N	299	299	299
Mean Bias, %	-0.05	-0.05	-0.01
Stnd Er, %	0.33	0.33	0.33
LOE R^2	-0.04	-0.04	0.003
R^2	0.001	0.001	0.006

Figure 24. Overall accuracy summary of HMA alligator (bottom-up) cracking model using calibration set

Validation Set

National Calibration

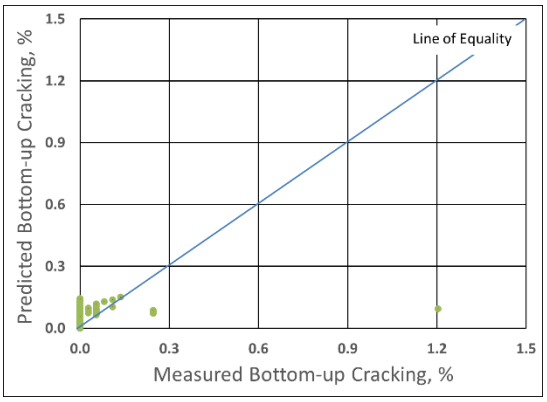

Local Calibration from MEPDG

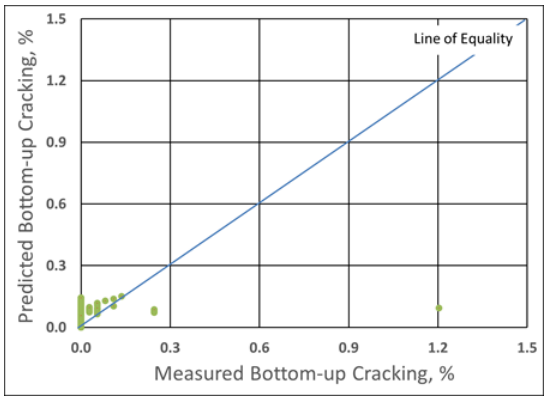

Local Calibration from Pavement ME

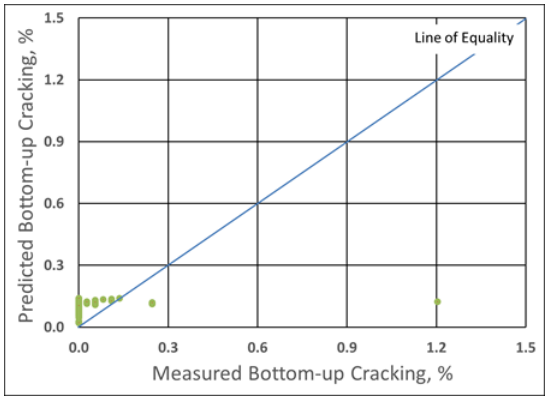

Coefficients	National	Local MEPDG	Local Pavement ME
C1_Bottom	1.00	1.00	1.25
C2_Bottom	1.00	1.00	0.30
C3_Bottom	6,000	6,000	6,000
N	133	133	133
Mean Bias, %	-0.01	-0.01	0.03
Stnd Er, %	0.37	0.37	0.38
LOE R^2	0.03	0.03	0.01
R^2	0.04	0.04	0.03

Figure 25. Overall accuracy summary of HMA alligator (bottom-up) cracking model using validation set

As can be seen in Figures 24 and 25, although the AASHTOWare Pavement ME Design locally calibrated model improves the alligator (bottom-up) cracking predictions compared to the nationally calibrated and MEPDG locally calibrated models, the improvement is insignificant. Neither the nationally calibrated nor the AASHTOWare Pavement ME Design locally calibrated alligator (bottom up) cracking models could provide high accuracy for this model. It can be concluded that the alligator (bottom-up) cracking model in itself is not able to simulate the field behavior of Iowa HMA pavements very well. Additionally, it should be noted that most of the tested pavement sections have 0% alligator cracking measurements, while very few sections have as much as 1.1% alligator cracking. These 0% cracking data points lower the accuracy of the model. It should also be noted that the measured alligator (bottom up) cracking values for Iowa HMA pavements are not high; therefore, it can be observed that Iowa HMA pavements do not generally have severe alligator (bottom-up) cracking problems (see Figure 24 and Figure 25).

Figure 26 and Figure 27 compare HMA longitudinal (top-down) cracking predictions using nationally calibrated, MEPDG locally calibrated, and AASHTOWare Pavement ME Design locally calibrated coefficients for the calibration and validation sets, respectively.

Calibration Set

National Calibration

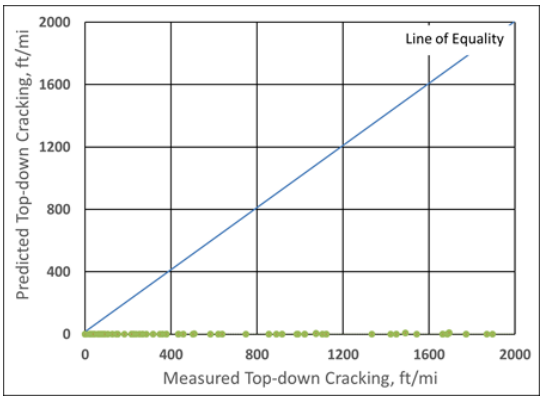

Local Calibration from MEPDG

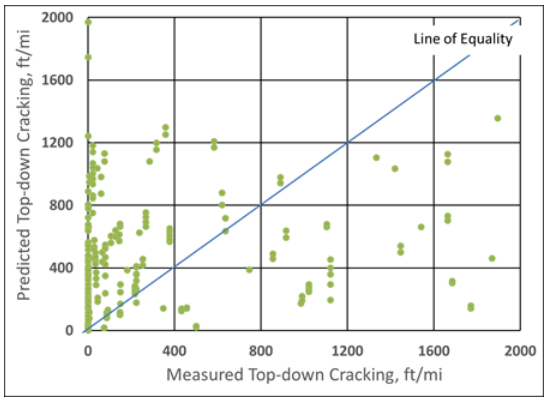

Local Calibration from Pavement ME

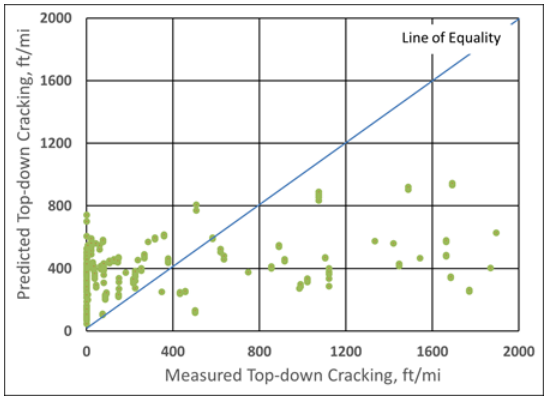

Coefficients	National	Local MEPDG	Local Pavement ME
C1_Top	7	0.82	2.32
C2_Top	3.5	1.18	0.47
C4_Top	1,000	1,000	1,000
N	228	228	228
Mean Bias, ft/mile	-394	164	-9
Stnd Er, ft/mile	813	829	692
LOE R^2	-0.31	-0.36	0.05
R^2	0.07	0.06	0.05

Figure 26. Overall accuracy summary of HMA longitudinal (top-down) cracking model using calibration set

Validation Set

National Calibration

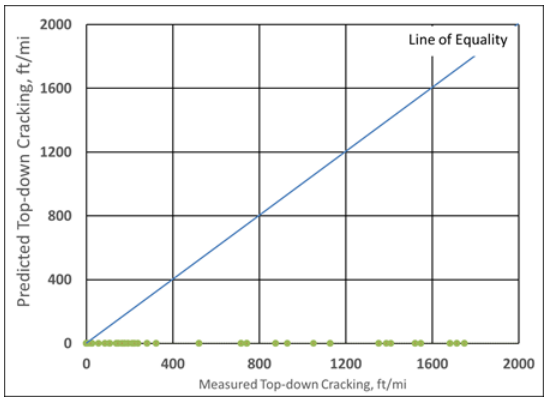

Local Calibration from MEPDG

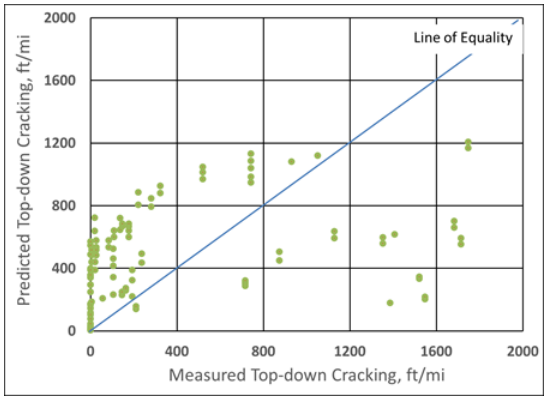

Local Calibration from Pavement ME

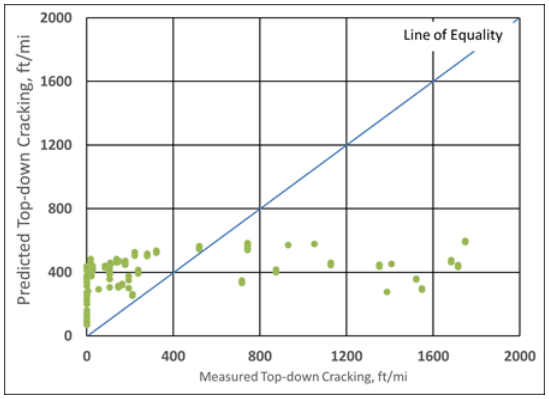

Coefficients	National	Local MEPDG	Local Pavement ME
C1_Top	7	0.82	2.32
C2_Top	3.5	1.18	0.47
C4_Top	1,000	1,000	1,000
N	111	111	111
Mean Bias, ft/mile	-418	67	-32
Stnd Er, ft/mile	717	546	547
LOE R^2	-0.53	0.11	0.11
R^2	0.13	0.14	0.14

Figure 27. Overall accuracy summary of HMA longitudinal (top-down) cracking model using validation set

As can be seen in Figures 26 and 27, compared to the nationally calibrated model, the MEPDG locally calibrated model reduces the bias, although even the MEPDG locally calibrated model has a significant amount of standard error. The model was further improved with AASHTOWare Pavement ME Design local calibration (see Figure 26 and Figure 27).

Transverse (Thermal) Cracking

According to AASHTO (2008), the logarithmic ratio between crack depth and HMA layer thickness plays the most important role in predicting the degree of transverse (thermal) cracking:

$$TC = \beta_{t1} \times N \times [\frac{1}{\sigma_d} \times Log\left(\frac{C_d}{H_{HMA}}\right)] \quad \textbf{(44)}$$

where,

- TC = Observed amount of thermal cracking, ft/mi
- β_{t1} = Regression coefficient determined through global calibration (400)
- $N[z]$ = Standard normal distribution evaluated at [z]
- σ_d = Standard deviation of the log of the depth of cracks in the pavement
- C_d = Crack depth, in.
- H_{HMA} = Thickness of HMA layers, in.

$$\Delta C = (k \times \beta_t)^{n+1} \times A \times \Delta K^n \quad \textbf{(45)}$$

$$A = 10^{(4.389 - 2.52 \times \log(E \times \sigma_m \times n))} \quad \textbf{(46)}$$

where,

- k = Regression coefficient determined through field calibration
- β_t = Calibration parameter
- A, n = Fracture parameters for the asphalt mixture
- ΔK = Change in the stress intensity factor due to a cooling cycle
- E = Mixture stiffness
- σ_m = Undamaged mixture tensile strength

The availability of each variable of the above equations was carefully inspected. For this distress type, not all of the required variables could be obtained from either the software output or the intermediate output files to conduct local calibration outside the software. The availability and location of each available variable can be described as follows:

- $N[z]$ is not provided by the software.
- σ_d is a fixed number, 0.769 in.
- C_d is available in the "Distress data" tab of the final result summary output file.
- H_{HMA} is an input value. It is known or can be checked from "Grand Summary" tab in the final result summary output file.
- *A, n* is not provided by the software.
- ΔK is not provided by the software.
- $\sigma_m$is not provided by the software.
- E is an input value. It is known or can be checked from "HMAInput.xlxs" intermediate output file for different temperature conditions.

Local calibration of the transverse (thermal) cracking model within the software was conducted using different calibration coefficients and choosing the best method (trial-and-error). To do this, a sensitivity analysis of the thermal cracking Level 3 coefficient was initially performed. Table 22 shows this coefficient's sensitivity analysis result for this model.

Table 22. Sensitivity analysis results of HMA and thermal cracking calibration coefficients

Calibration factors	Coefficient Sensitivity Index	Rank
K_Level 3	3.17	1

It could also be seen that the model with the nationally calibrated coefficients underpredicts thermal cracking for Iowa HMA pavements. Therefore, based on these sensitivity analysis results, a set of trial calibration coefficients was determined for use in local calibration; Table 23 shows these trial calibration coefficients.

Table 23. Trial calibration coefficients

Coefficient	Trial value	R^2
K_Level 3	2	0.16
K_Level 3	2.5	0.07
K_Level 3	3	0.03

Running the software using these coefficients for 35 HMA sections, the calibration coefficient providing the minimum MSE between the field-measured thermal cracking values and the software predictions for selected Iowa HMA pavements was determined. Using the validation set, the accuracy of the transverse cracking model using this coefficient was verified. As a result of these analyses, the final local coefficient was determined to be 2 (Table 23).

Figure 28 and Figure 29 compare HMA transverse (thermal) cracking predictions using nationally calibrated, MEPDG locally calibrated, and AASHTOWare Pavement ME Design locally calibrated coefficients for the calibration and validation sets, respectively.

Calibration Set

National Calibration

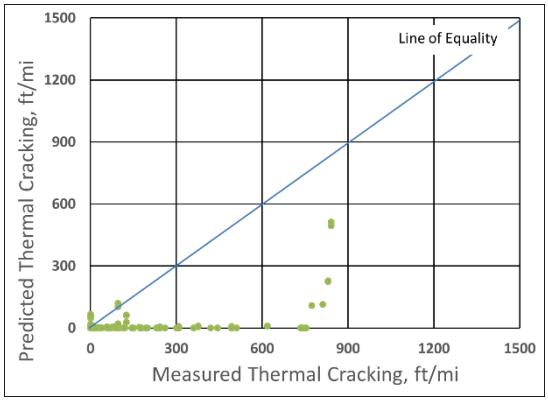

Local Calibration from MEPDG

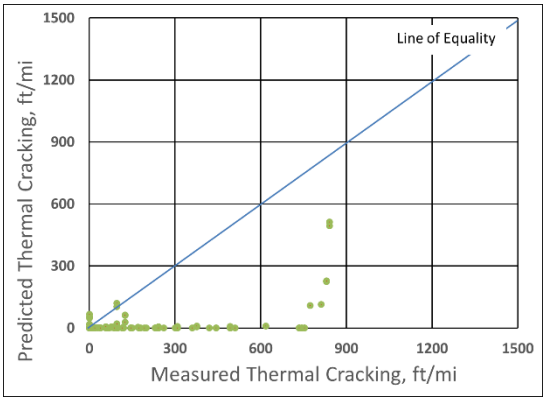

Local Calibration from Pavement ME

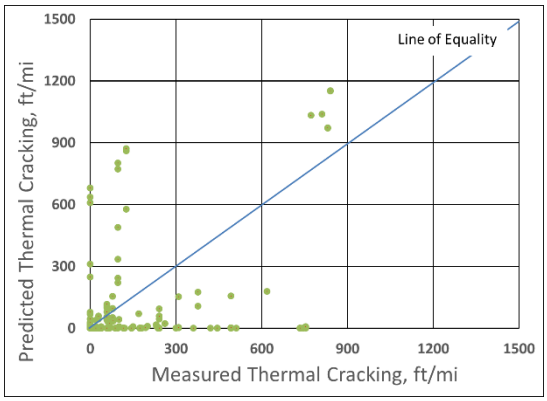

Coefficients	National	Local MEPDG	Local Pavement ME
K_Level 3	1.5	1.5	2
N	232	232	232
Mean Bias, ft/mile	-120	-120	-57
Stnd Er, ft/mile	223	223	238
LOE R^2	-0.18	-0.18	-0.34
R^2	0.21	0.21	0.16

Figure 28. Overall accuracy summary of HMA transverse cracking model using calibration set

Validation Set

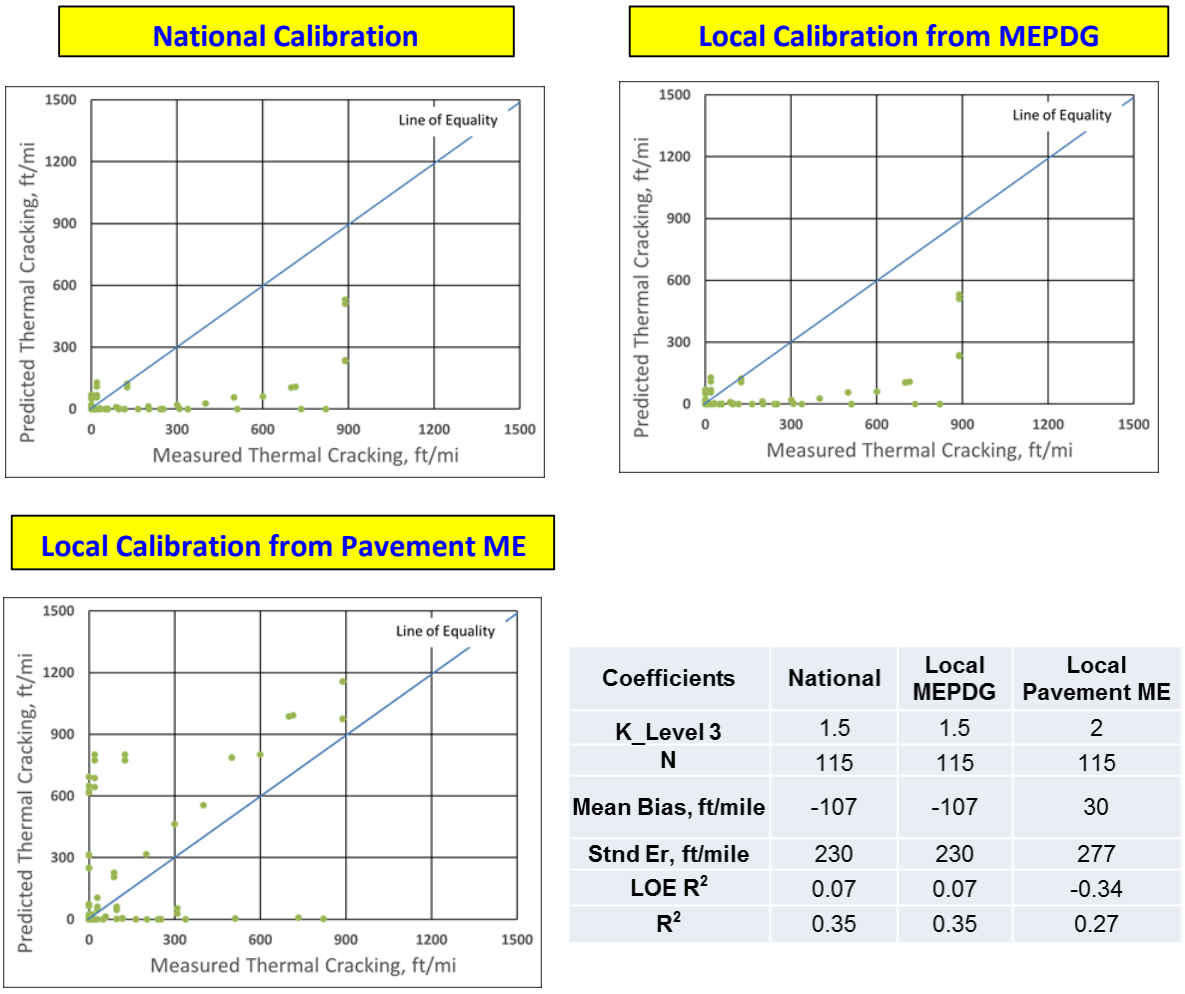

Coefficients	National	Local MEPDG	Local Pavement ME
K_Level 3	1.5	1.5	2
N	115	115	115
Mean Bias, ft/mile	-107	-107	30
Stnd Er, ft/mile	230	230	277
LOE R^2	0.07	0.07	-0.34
R^2	0.35	0.35	0.27

Figure 29. Overall accuracy summary of HMA transverse cracking model using validation set

As can be seen in Figures 28 and 29, the nationally calibrated and MEPDG locally calibrated model predictions are the same because they both have the same calibration coefficient. Both the nationally calibrated and AASHTOWare Pavement ME Design locally calibrated HMA transverse (thermal) cracking models could not provide high accuracy for this distress. It can be concluded that the HMA transverse (thermal) cracking model itself is not very capable of simulating the field behavior of Iowa HMA pavements. Additionally, we should realize that most of the pavement sections have less than 300 ft/mi of thermal cracking, and very few sections range as high as 600–900 ft/mi of thermal cracking. Data points in the range of 600–900 ft/mi of thermal cracking would lower the accuracy of the model (see Figure 28 and Figure 29).

Smoothness (IRI)

All surface-related distresses are involved when dealing with the prediction of smoothness in HMA pavements.

The equation for the IRI transfer function for new HMA pavements is as follows:

$$IRI = IRI_0 + C_4 \times (SF) + C_2 \times (FC_{Total}) + C_3 \times (TC) + C_1 \times (RD) \quad \textbf{(47)}$$

where,

- IRI_0 = Initial IRI after construction, in./mi
- SF = Site factor (refer to Equation 35)
- FC_{Total} = Area of fatigue cracking (combined alligator, longitudinal, and reflection cracking in the wheel path), percent of total lane area. All load-related cracks are combined on an area. The basis-length of cracks is multiplied by 1 ft to convert length into an area basis.
- TC = Length of transverse cracking (including the reflection of transverse cracks in existing HMA pavements), ft/mi
- RD = Average rut depth, in.
- $C_{1,2,3,4}$ = Calibration coefficients; 40, 0.4, 0.008, and 0.015 are national calibration coefficients, respectively

The site factor is calculated as follows:

$$SF = Age[0.02003(PI + 1) + 0.007947(Precip + 1) + 0.000636(FI + 1)] \quad \textbf{(48)}$$

where,

- Age = Pavement age, year
- PI = Percent plasticity index of the soil
- FI = Average annual freezing index, °F days
- $Precip$ = Average annual precipitation or rainfall, in.

The availability of each variable of the IRI transfer function was carefully inspected. All variables were either extracted from general or intermediate output files or calculated using the data provided by the output files. The location or calculation method used for each variable can be described as follows:

- IRI_0 is input into the software as an initial IRI value and is either known or capable of being found in the "Grand Summary" tab in the final result summary output file.
- SF can be calculated using Equation 48.

- FC_{Total}, or the top-down and bottom-up cracking, can be obtained from the "Distress" tab in the final result summary output file.
- *TC* can be obtained from the "Distress" tab in the final result summary output file.
- *FI for SF calculation* can be obtained from the climate output file titled "Climate Inputs".
- P_{200} can be obtained from the "Layer #" tab in the final result summary output file.

The predicted IRI values were compared with the actual Iowa DOT PMIS IRI data for each section in each year. The local calibration procedure was performed until a combination of calibration coefficients producing the minimum MSE between the predicted and actual IRI values was found. This combination of calibration coefficients was announced as a set of local calibration coefficients. These announced local calibration coefficients were validated using validation pavement sections. Similarly to new JPCP IRI calibrations, two approaches were used for new HMA IRI calibrations:

- **Approach 1**: Calibrate using either locally calibrated or nationally calibrated distress prediction models. Note that nationally calibrated distress prediction models can be used when they provide good accuracy in distress measurements.
- **Approach 2**: Calibrate using only nationally calibrated distress prediction models without considering the accuracy of the distress model predictions.

Approach 1

If the AASHTOWare Pavement ME Design locally calibrated distress prediction models cannot produce accurate predictions in the calculation of IRI, nationally calibrated models should be used. Note that in the calculation of the JPCP IRI model using Approach 1, all AASHTOWare Pavement ME Design locally calibrated faulting and cracking predictions were used because of their high accuracy. However, because HMA transverse (thermal) and bottom-up cracking predictions could not have provided accurate predictions, nationally calibrated models for these types of distress were utilized in the calculation of the HMA IRI model using Approach 1.

Figures 30 and 31 compare the IRI predictions using nationally calibrated, MEPDG locally calibrated, and AASHTOWare Pavement ME Design locally calibrated coefficients for the calibration and validation sets, respectively.

Calibration Set

National Calibration

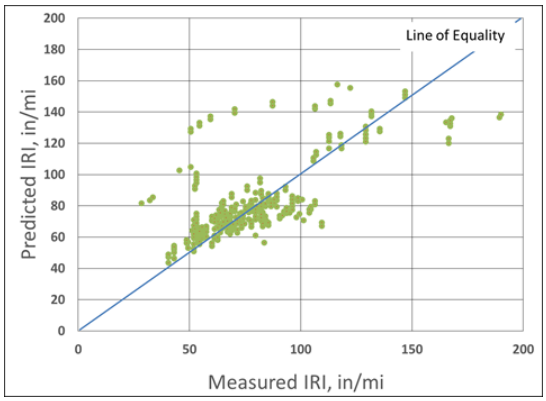

Local Calibration from MEPDG

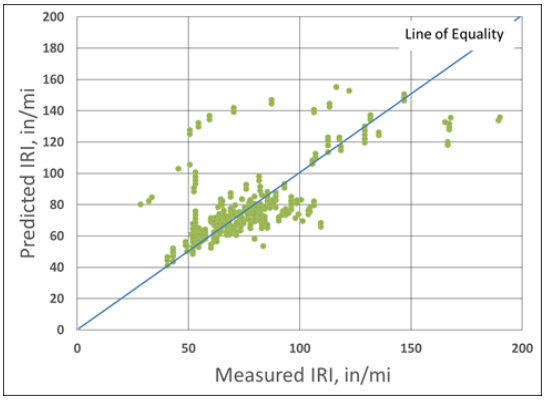

Local Calibration from Pavement ME

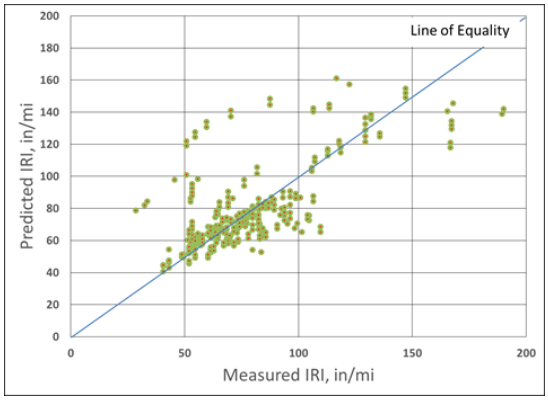

Coefficients	National	Local MEPDG	Local Pavement ME
C1	40	40	5
C2	0.4	0.4	0.4
C3	0.008	0.008	0.008
C4	0.015	0.015	0.026
N	299	299	299
Mean Bias, in/mi	3.58	1.90	0.98
Stnd Er, in/mi	21.00	20.97	20.53
LOE R^2	0.43	0.43	0.45
R^2	0.49	0.48	0.51
MAPE	0.19	0.19	0.18

Figure 30. Overall accuracy summary of HMA IRI model using calibration set (Approach 1)

Validation Set

National Calibration

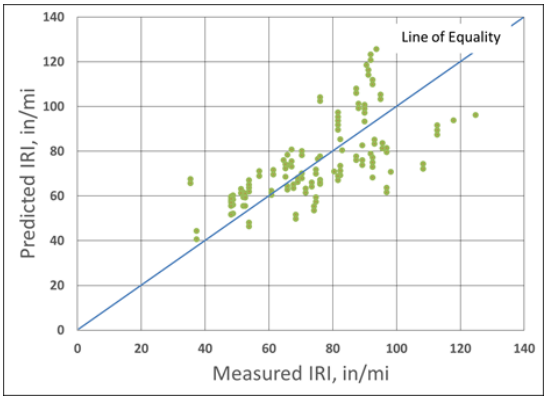

Local Calibration from MEPDG

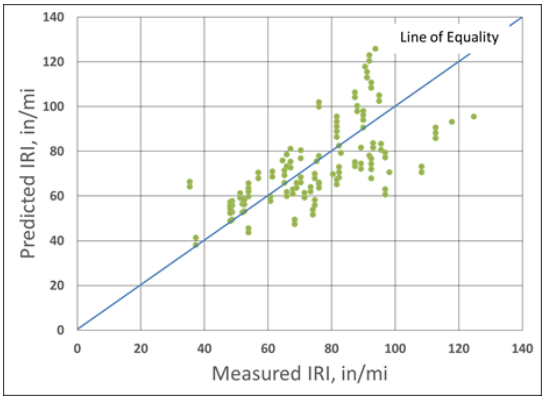

Local Calibration from Pavement ME

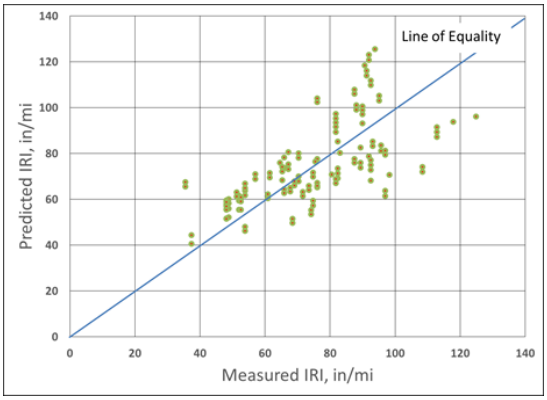

Coefficients	National	Local MEPDG	Local Pavement ME
C1	40	40	5
C2	0.4	0.4	0.4
C3	0.008	0.008	0.08
C4	0.015	0.015	0.026
N	133	133	133
Mean Bias, in/mi	0.50	-1.20	-2.32
Stnd Er, in/mi	15.21	15.17	15.17
LOE R^2	0.37	0.37	0.37
R^2	0.45	0.46	0.45
MAPE	0.17	0.16	0.15

Figure 31. Overall accuracy summary of HMA IRI model using validation set (Approach 1)

The AASHTOWare Pavement ME Design locally calibrated IRI model shown in Figures 30 and 31 was calibrated using Approach 1; in the calculation of IRI predictions, AASHTOWare Pavement ME Design used locally calibrated rutting and top-down (longitudinal) cracking predictions. As can be seen from the figures, the MEPDG locally calibrated IRI model improved accuracy compared to the nationally calibrated model. The model accuracy was further improved using the AASHTOWare Pavement ME Design locally calibrated IRI model, as can be seen from the figures.

Implementing a paired t test using measured IRI values and AASHTOWare Pavement ME Design locally calibrated predictions for selected pavement sections, a p value was calculated as P(T <= t) two-tail = 0.88 > 0.05. This result implies that, with 95% certainty, there is no significant difference between the actual and AASHTOWare Pavement ME Design predicted IRI values (Table 24).

Table 24. Pair t test results for HMA IRI model (Approach 1)

	Actual IRI	Predicted IRI
Mean	77.21715	77.08087
Variance	646.307	602.1901
Observations	432	432
Pearson Correlation	0.71164	
Hypothesized Mean Difference	0	
df	431	
t Stat	0.149166	
P(T<=t) one-tail	0.440746	
t Critical one-tail	1.648397	
P(T<=t) two-tail	0.881493	
t Critical two-tail	1.965483	

Approach 2

An alternative approach (Approach 2) was used to locally calibrate the IRI model using AASHTOWare Pavement ME Design software. In this approach, with respect to the local calibration of the IRI model, nationally calibrated rutting, transverse (thermal), and fatigue cracking model predictions were used. Figure 32 and Figure 33 compare the local calibration results using nationally calibrated and AASHTOWare Pavement ME Design locally calibrated models in Approach 2.

Calibration Set

National Calibration

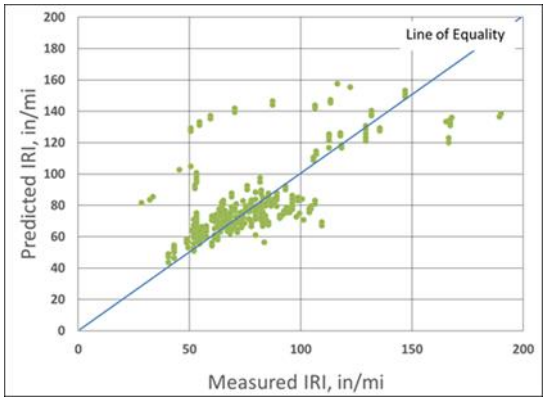

Local Calibration from Pavement ME

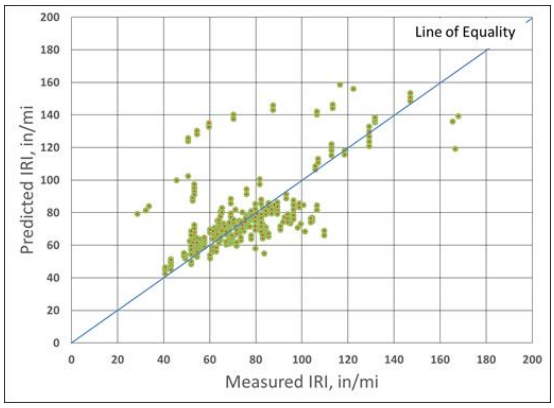

Coefficients	National	Local Pavement ME
C1	40	25
C2	0.4	0.4
C3	0.008	0.008
C4	0.015	0.019
N	299	299
Mean Bias, in/mi	3.58	2.03
Stnd Er, in/mi	21.00	20.48
LOE R^2	0.43	0.46
R^2	0.49	0.44
MAPE	0.19	0.18

Figure 32. Overall accuracy summary of HMA IRI model using calibration set (Approach 2)

Validation Set

National Calibration

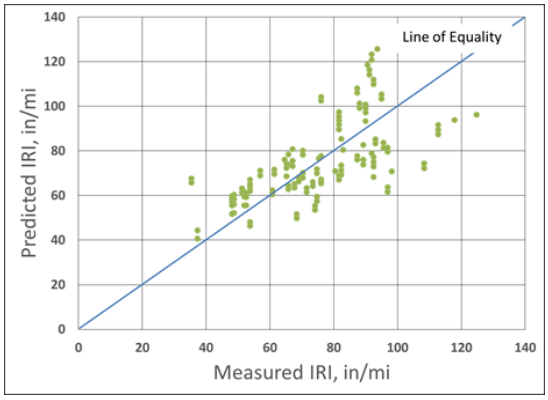

Local Calibration from Pavement ME

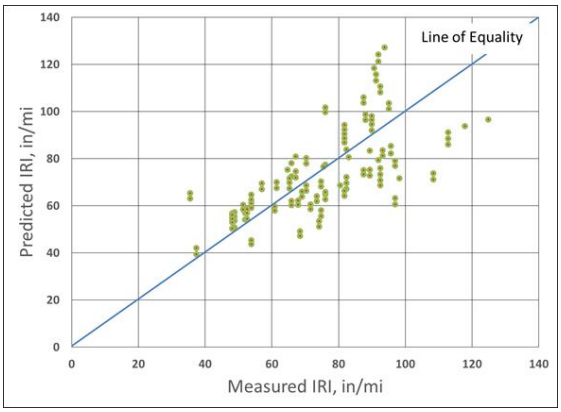

Coefficients	National	Local Pavement ME
C1	40	25
C2	0.4	0.4
C3	0.008	0.008
C4	0.015	0.019
N	133	133
Mean Bias, in/mi	0.50	-1.15
Stnd Er, in/mi	15.21	15.09
LOE R^2	0.37	0.38
R^2	0.45	0.47
MAPE	0.17	0.16

Figure 33. Overall accuracy summary of HMA IRI model using validation set (Approach 2)

It is important to highlight that although the rutting model was further improved using AASHTOWare Pavement ME Design local calibration coefficients, this improvement was not significant (Figure 32 and Figure 33). The purpose of using two approaches in the local calibration of the IRI model was to determine whether the IRI model could be locally calibrated with sufficient accuracy without the need for the local calibration procedure of each of the distress models, which would require significant additional financial and data resources. A locally calibrated IRI model using Approach 2 would save significant sources in terms of both time and funds. Using Approach 2 in the local calibration of the IRI model would be especially useful for those SHAs that are only interested in attaining locally calibrated IRI predictions rather than locally calibrated rutting, fatigue, and thermal cracking predictions. In this study, it was determined that using Approach 2, a locally calibrated IRI model can predict this distress with sufficient accuracy for Iowa HMA pavement systems.

Also, a paired t test was performed for this approach, and the p value was found to be P(T <= t) two-tail = 0.25 > 0.05. This result implies that, with 95% certainty, there is no significant difference between the national field-measured and AASHTOWare Pavement ME Design–predicted IRI values using Approach 2 (Table 25).

Table 25. Pair t test results for HMA IRI model (Approach 2)

	Actual IRI	IRI Av
Mean	77.21715	78.27098
Variance	646.307	567.1067
Observations	432	432
Pearson Correlation	0.70723	
Hypothesized Mean Difference	0	
df	431	
t Stat	-1.15913	
P(T<=t) one-tail	0.123523	
t Critical one-tail	1.648397	
P(T<=t) two-tail	0.247047	
t Critical two-tail	1.965483	

HMA over JPCP

AASHTOWare Pavement ME Design HMA over JPCP include rutting, longitudinal (top-down) cracking, alligator (bottom-up) cracking, thermal (transverse) cracking, reflective cracking, and IRI.

Rut Depth

The total rut depth in AASHTOWare Pavement ME Design is calculated as the sum of the vertical deformations in each sublayer. Rutting predictions are divided into HMA layer rutting, granular base layer rutting, subgrade layer rutting, and total pavement rutting. However, most of the total rutting predictions come from the HMA layer because the existing JPCP can provide a strong foundation to the HMA surface overlay and thus prevent granular base and subgrade layer rutting. The same HMA layer rutting equation (Equation 26) as that used for HMA pavements is used for HMA overlays. Also, the sensitivity analysis of calibration coefficients used for HMA layer rutting in HMA pavements is the same as that used for HMA over JPCP (Table 17).

Based on the sensitivity analysis results, an experimental matrix including different sets of calibration coefficients was prepared and is shown in Table 26.

Table 26. Experimental matrix for local calibration of HMA layer rutting model of HMA over JPCP

BR2	BR3	Mean Bias (in.)
1.01	1	0.002
1.01	0.99	-0.004
0.99	1.01	-0.006

Trying different sets of calibration coefficients, the set with values of 1.01 and 1 for BR2 and BR3, respectively, produced the most accurate predictions.

Figure 34 and Figure 35 compare the total rutting predictions using nationally calibrated, MEPDG locally calibrated, and AASHTOWare Pavement ME Design locally calibrated coefficients for the calibration and validation sets, respectively.

Calibration Set

National Calibration

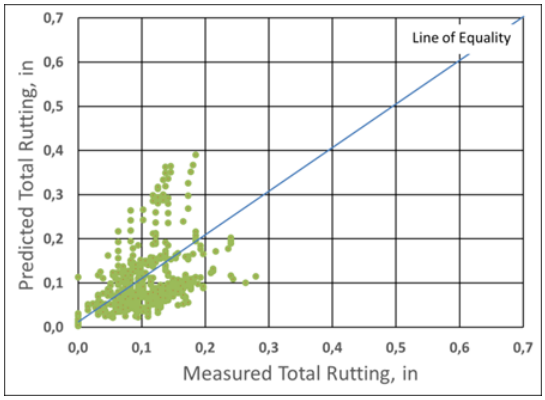

Local Calibration from MEPDG

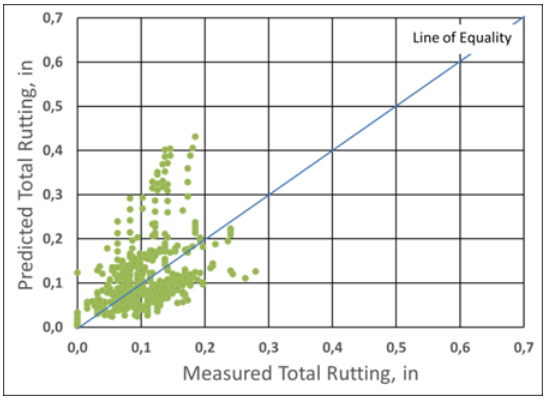

Local Calibration from Pavement ME

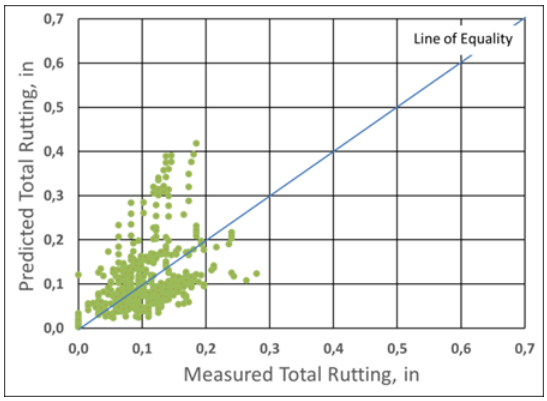

Coefficients	National	Local MEPDG	Local Pavement ME
B1	1	1	1
B2	1	1.15	1.01
B3	1	1	1
Bs1	1	0.0001	0.0001
N	489	489	489
Mean Bias, in	-0.005	0.005	0.002
Stnd Er, in	0.07	0.07	0.07
LOE R^2	-0.76	-1.08	-0.96
R^2	0.19	0.19	0.19

Figure 34. Overall accuracy summary of HMA layer rutting model of HMA over JPCP using calibration set

Validation Set

National Calibration

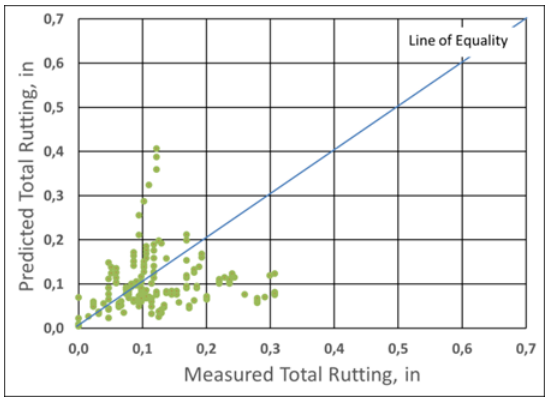

Local Calibration from MEPDG

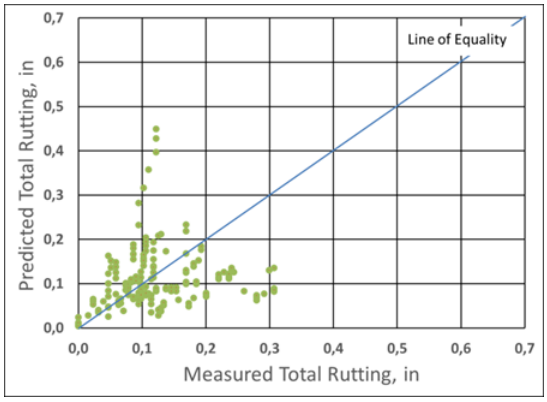

Local Calibration from Pavement ME

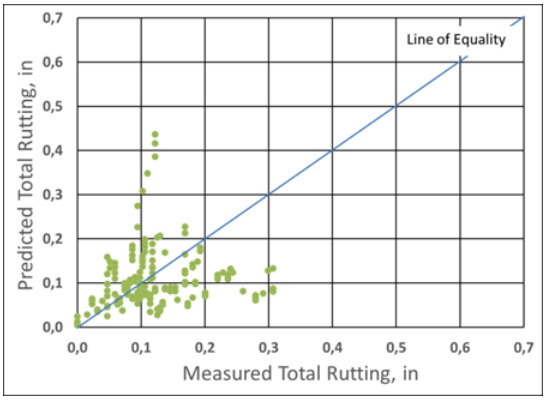

Coefficients	National	Local MEPDG	Local Pavement ME
B1	1	1	1
B2	1	1.15	1.01
B3	1	1	1
Bs1	1	0.0001	0.0001
N	168	168	168
Mean Bias, in	-0.02	-0.01	-0.01
Stnd Er, in	0.09	0.09	0.09
LOE R^2	-0.55	-0.62	-0.59
R^2	0.03	0.04	0.04

Figure 35. Overall accuracy summary of HMA layer rutting model of HMA over JPCP using calibration set

As can be seen in Figures 34 and 35, while the MEPDG locally calibrated rutting model gives more accurate predictions than the nationally calibrated model, the accuracy was further improved using the AASHTOWare Pavement ME Design locally calibrated rutting model (Figure 34 and Figure 35).

Load-Related Cracking

Because load-related cracking is a distress type related to the HMA surface course, the same load-related cracking equations used for new HMA pavements are also used for HMA overlaid pavements. Fatigue models were used to estimate fatigue damage and were input into the transfer functions for longitudinal cracking and alligator cracking predictions to obtain equivalent cracking measurements. Similarly to HMA pavements, the fatigue model was not modified for

HMA over JPCP systems. Extracting fatigue damage predictions from the fatigue model, alligator (bottom-up) and longitudinal (top-down) cracking predictions were calculated using the related transfer functions (Equations 40 and 43). These transfer functions were locally calibrated using a nonlinear optimization technique (MS Excel Solver).

Figure 36 and Figure 37 compare HMA alligator (bottom-up) cracking predictions for selected HMA over JPCP sections using nationally calibrated, MEPDG locally calibrated, and AASHTOWare Pavement ME Design locally calibrated coefficients for the calibration and validation sets, respectively.

Calibration Set

National Calibration

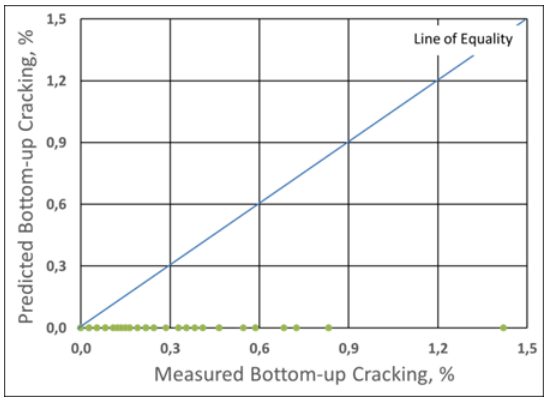

Local Calibration from MEPDG

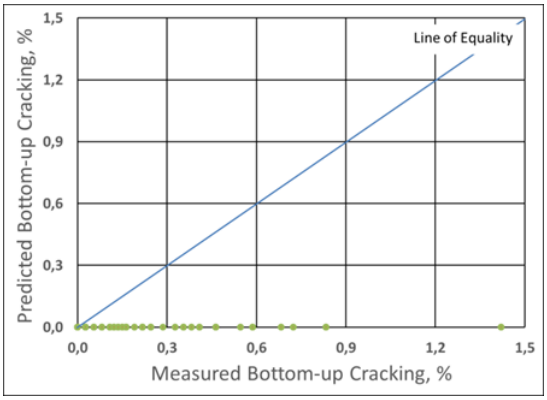

Local Calibration from Pavement ME

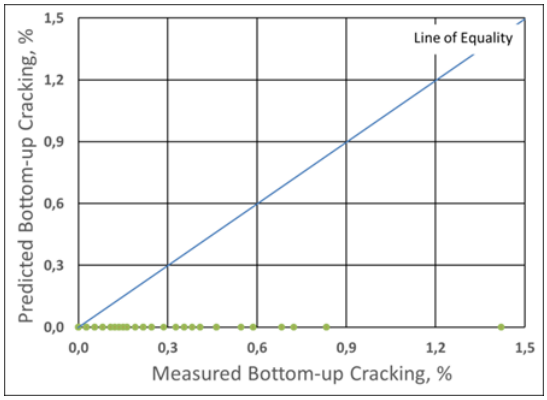

Coefficients	National	Local MEPDG	Local Pavement ME
C1_Bottom	1	1	2.44
C2_Bottom	1	1	0,18
C3_Bottom	6,000	6,000	6,000
N	489	489	489
Mean Bias, %	-0.16	-0.16	-0.16
Stnd Er, %	0.54	0.54	0.54
LOE R^2	-0.09	-0.09	-0.09
R^2	0.003	0.003	0.005

Figure 36. Overall accuracy summary of HMA alligator (bottom-up) cracking model of HMA over JPCP using calibration set

Validation Set

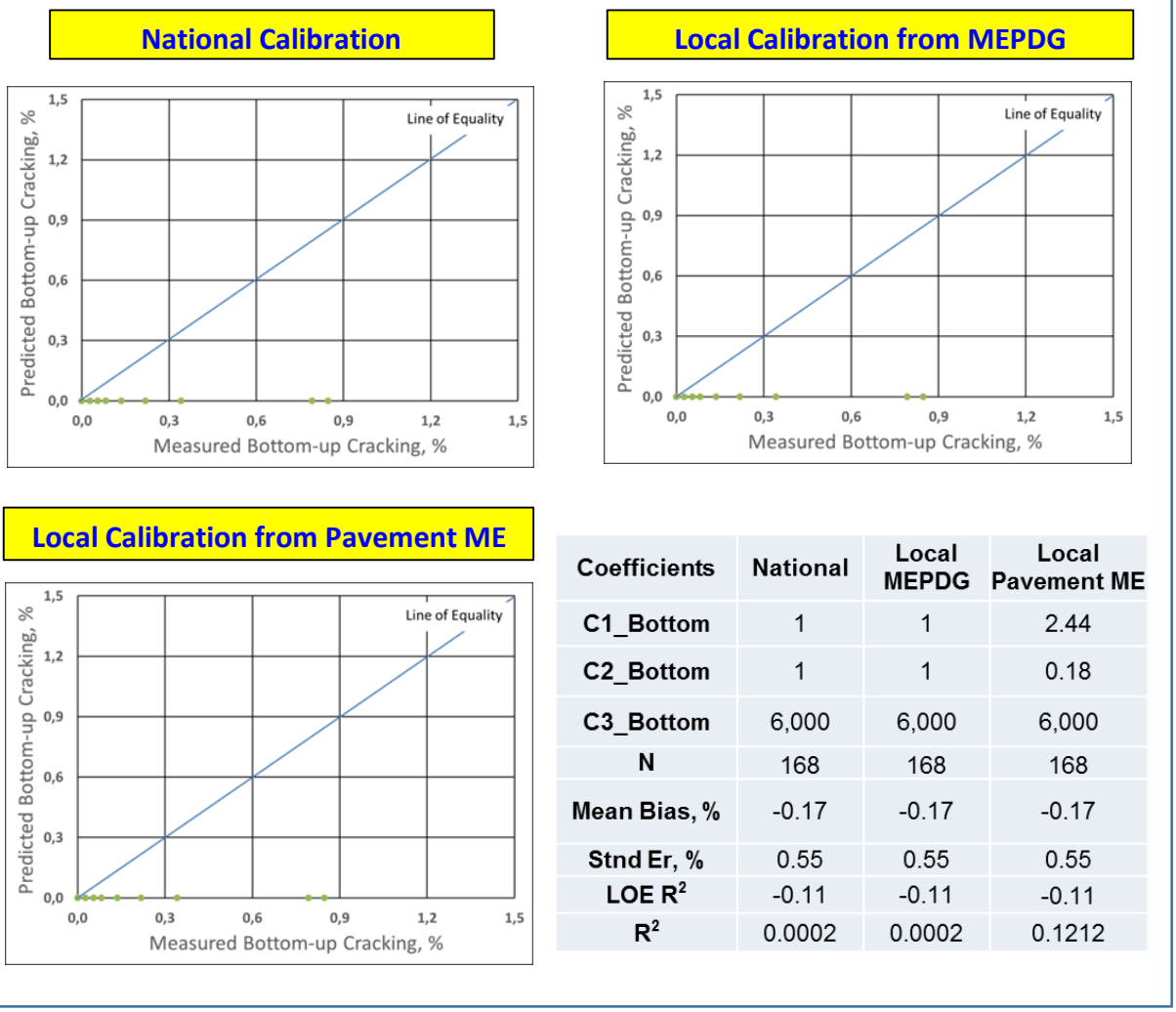

Coefficients	National	Local MEPDG	Local Pavement ME
C1_Bottom	1	1	2.44
C2_Bottom	1	1	0.18
C3_Bottom	6,000	6,000	6,000
N	168	168	168
Mean Bias, %	-0.17	-0.17	-0.17
Stnd Er, %	0.55	0.55	0.55
LOE R^2	-0.11	-0.11	-0.11
R^2	0.0002	0.0002	0.1212

Figure 37. Overall accuracy summary of HMA alligator (bottom-up) cracking model of HMA over JPCP using validation set

As can be seen in Figures 36 and 37, although the AASHTOWare Pavement ME Design locally calibrated model improved the alligator (bottom-up) cracking predictions, the improvement was insignificant. Neither the nationally calibrated nor the AASHTOWare Pavement ME Design locally calibrated alligator (bottom up) cracking models could provide high accuracy for this model. It can be concluded that the alligator (bottom-up) cracking model itself would not be able to simulate the field behavior of Iowa HMA over JPCP very well. Additionally, it should be noted that most pavement sections have fewer than 0.3% measured alligator cracks, and very few sections exhibit a range of 0.6–1.4% measured alligator cracking. Also note that the measured alligator (bottom-up) cracking values for Iowa HMA over JPCP is not high; it can therefore be concluded that Iowa HMA over JPCP sections do not have a severe alligator (bottom-up) cracking problem.

Figure 38 and Figure 39 compare HMA longitudinal (top-down) cracking predictions for selected HMA over JPCP sections using nationally calibrated, MEPDG locally calibrated, and AASHTOWare Pavement ME Design locally calibrated coefficients for the calibration and validation sets, respectively.

Calibration Set

National Calibration

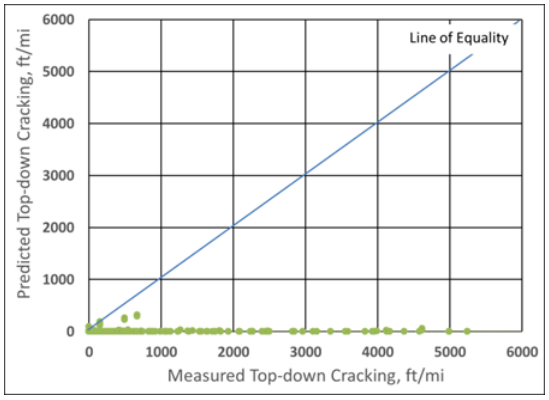

Local Calibration from MEPDG

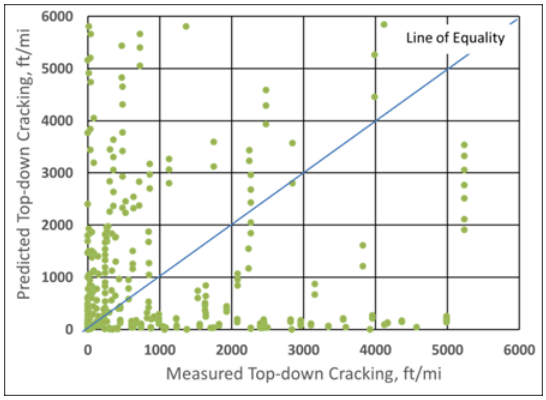

Local Calibration from Pavement ME

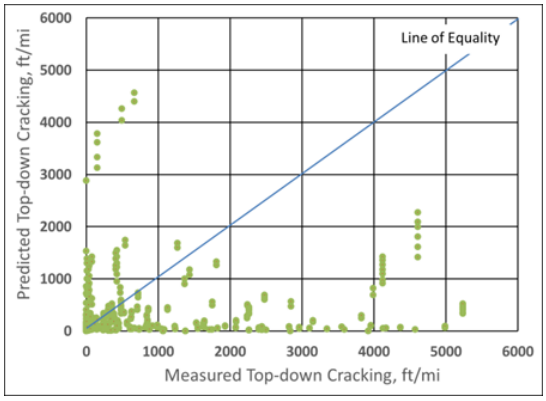

Coefficients	National	Local MEPDG	Local Pavement ME
C1_Top	7	7	2.3
C2_Top	3.5	3.5	2
C4_Top	1,000	1,000	1,000
N	489	489	489
Mean Bias, ft/mile	-1,204	603	-853
Stnd Er, ft/mile	2,015	3,118	1,928
LOE R^2	-0.56	-2.74	-0.43
R^2	0.0015	0.0000	0.0002

Figure 38. Overall accuracy summary of HMA longitudinal (top-down) cracking model of HMA over JPCP using calibration set

Validation Set

National Calibration

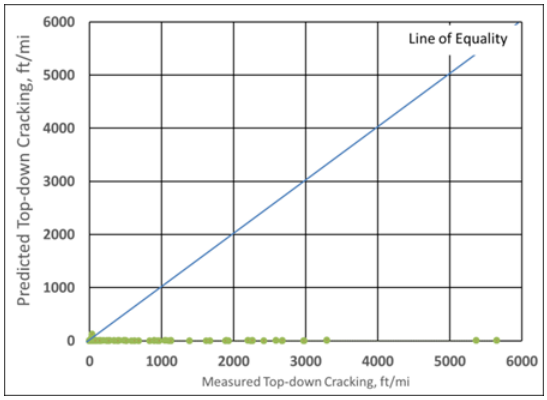

Local Calibration from MEPDG

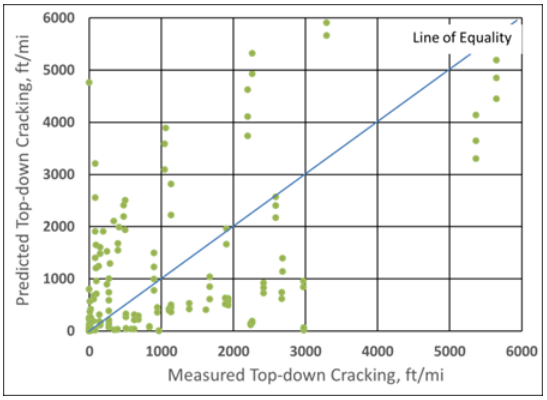

Local Calibration from Pavement ME

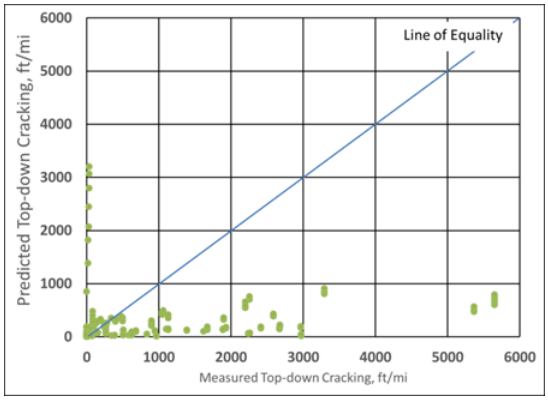

Coefficients	National	Local MEPDG	Local Pavement ME
C1_Top	7	7	2.3
C2_Top	3.5	3.5	2
C4_Top	1000	1000	1000
N	168	168	168
Mean Bias, ft/mile	-1,124	341	-833
Stnd Er, ft/mile	1,812	2,304	1,691
LOE R^2	-0.64	-1.65	-0.43
R^2	0.0075	0.0690	0.0049

Figure 39. Overall accuracy summary of HMA longitudinal (top-down) cracking model of HMA over JPCP using validation set

As can be seen in Figures 38 and 39, compared to the nationally calibrated model, the MEPDG locally calibrated model reduces the bias, although even the MEPDG locally calibrated model exhibits a significant amount of standard error. The model was further improved with AASHTOWare Pavement ME Design local calibration.

Transverse (Thermal) Cracking

Local calibration of the transverse (thermal) cracking model was performed for selected HMA over JPCP sections within AASHTOWare Pavement ME Design by submitting various combinations of calibration coefficients to the software and choosing the combination providing the most accurate predictions (nonlinear optimization). A set of calibration coefficients was used to determine the optimal set (Table 27). This analysis produced a final coefficient value of 2.7.

Table 27. Trial calibration coefficients

Coefficient	Trial value	R^2	Mean bias, in.
K_Level 3	1.8	0.018	-1,683
K_Level 3	2.1	0.025	-1,512
K_Level 3	2.4	0.027	-1,331
K_Level 3	2.7	0.027	-1,141

Figure 40 and Figure 41 compare HMA over JPCP transverse (thermal) cracking predictions for selected HMA over JPCP sections using nationally calibrated, MEPDG locally calibrated, and AASHTOWare Pavement ME Design locally calibrated coefficients for the calibration and validation sets, respectively.

Calibration Set

National Calibration

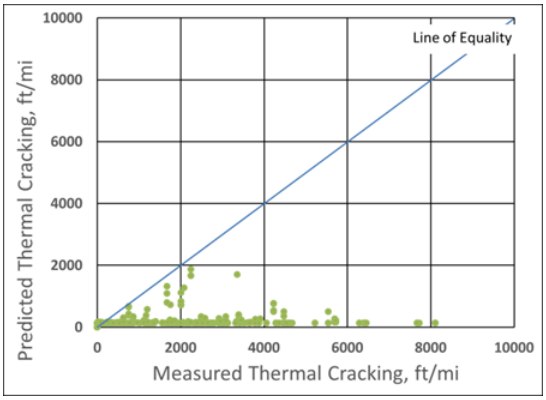

Local Calibration from MEPDG

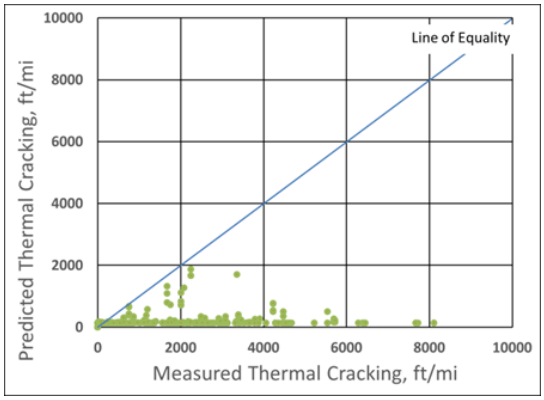

Local Calibration from Pavement ME

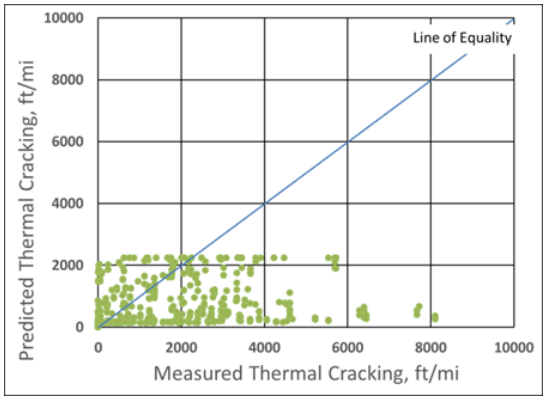

Coefficients	National	Local MEPDG	Local Pavement ME
K_Level 3	1.5	1.5	2.7
N	489	489	489
Mean Bias, ft/mile	-1,785	-1,785	-1,141
Stnd Er, ft/mile	2,495	2,495	2,124
LOE R^2	-1.04	-1.04	-0.48
R^2	0.01	0.01	0.03

Figure 40. Overall accuracy summary of HMA transverse cracking model of HMA over JPCP using validation set

Validation Set

National Calibration

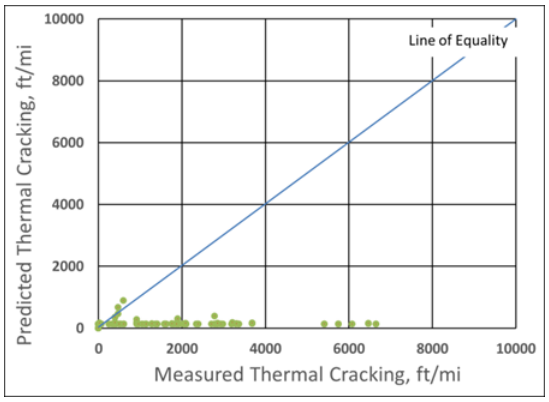

Local Calibration from MEPDG

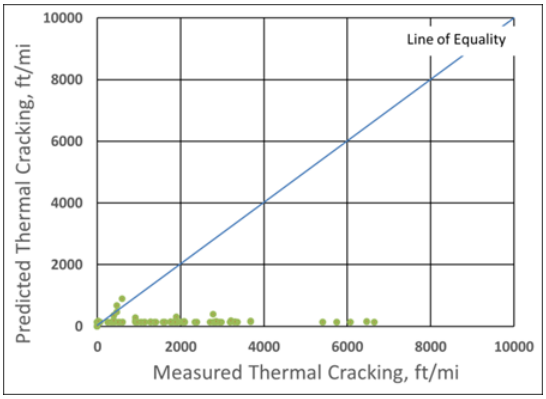

Local Calibration from Pavement ME

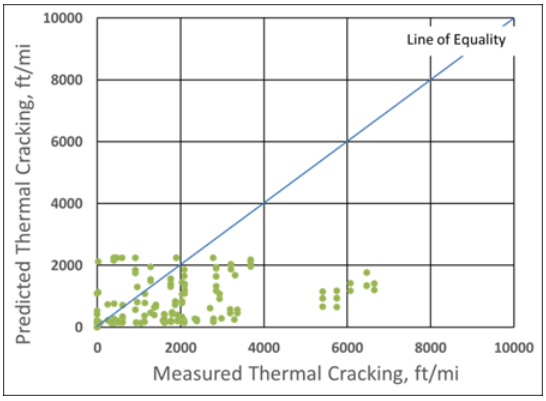

Coefficients	National	Local MEPDG	Local Pavement ME
K_Level 3	1.5	1.5	2.7
N	168	168	168
Mean Bias, ft/mile	-1,714	-1,714	-1,085
Stnd Er, ft/mile	2,397	2,397	1,912
LOE R^2	-1.08	-1.08	-0.32
R^2	0.0001	0.0001	0.1170

Figure 41. Overall accuracy summary of HMA transverse cracking model of HMA over JPCP using validation set

As can be seen in Figures 40 and 41, the nationally calibrated and MEPDG locally calibrated model predictions are the same because they both use the same calibration coefficient. Both nationally calibrated and AASHTOWare Pavement ME Design locally calibrated HMA over JPCP transverse (thermal) cracking models could not provide high accuracy for this model. It can be concluded that the HMA over JPCP transverse (thermal) cracking model itself is unable to simulate the field behavior of Iowa HMA over JPCP sections very well. Additionally, most of the pavement sections have fewer than 4,000 ft/mi of thermal cracking, while very few sections have thermal cracking measurements in the range of 6,000–8,000 ft/mi. The data points in the range of 6,000–8,000 ft/mi of thermal cracking would therefore lower the accuracy of the model (see Figure 40 and Figure 41).

Smoothness (IRI)

In the IRI calculation, the equation used for HMA pavements is also used for HMA over JPCP sections because the surface course in both pavement types is HMA. The only difference in the HMA over JPCP IRI model compared to the HMA IRI model is that reflective cracking predictions from the empirical model are included in the IRI equations as part of total transverse cracking predictions. Similar to new HMA IRI calibrations, two approaches were used for HMA over JPCP IRI calibrations:

- **Approach 1**: In the calculation of IRI predictions, AASHTOWare Pavement ME Design locally calibrated rutting and longitudinal (top-down) cracking predictions and nationally calibrated transverse (thermal), alligator (bottom-up), and reflective cracking predictions were used. Note that in contrast to the HMA IRI model, reflective cracking predictions were added to the model as a part of the area of total fatigue cracking (see Equation 47).

- **Approach 2**: In the calculation of IRI predictions, all nationally calibrated rutting, longitudinal (top-down), alligator (bottom-up), transverse (thermal), and reflective cracking predictions were utilized. Note that unlike the HMA IRI model, reflective cracking predictions were added to the model as a part of the area of total fatigue cracking (see Equation 47).

Approach 1

The IRI model was locally calibrated using the MS Excel Solver optimization tool. Figure 42 and Figure 43 compare the IRI predictions using nationally calibrated, MEPDG locally calibrated, and AASHTOWare Pavement ME Design locally calibrated coefficients for the calibration and validation sets, respectively.

Calibration Set

National Calibration

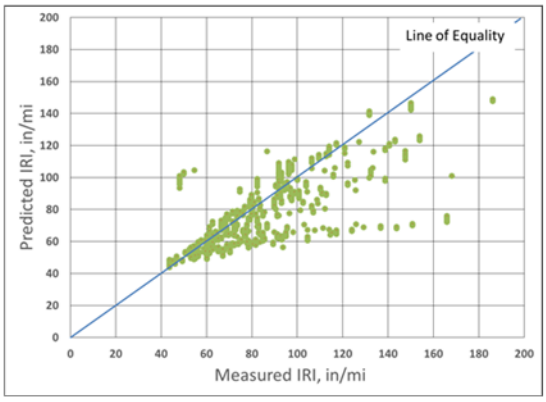

Local Calibration from MEPDG

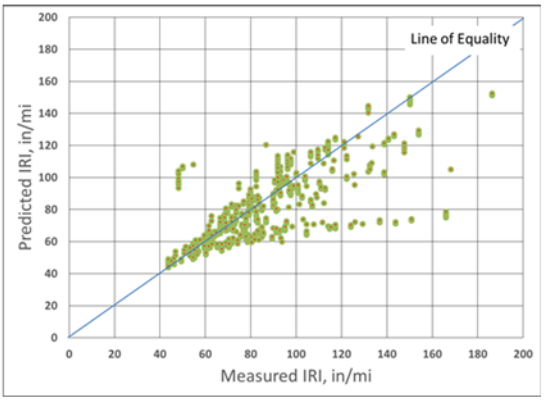

Local Calibration from Pavement ME

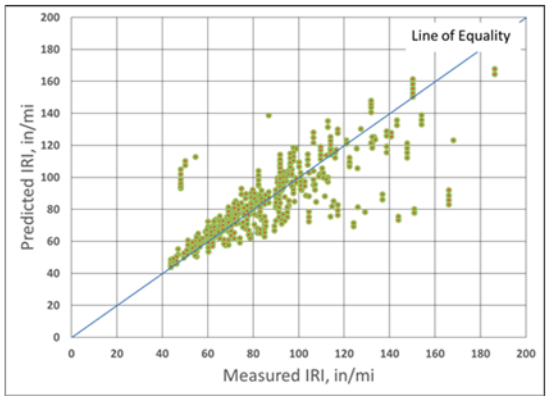

Coefficients	National	Local MEPDG	Local Pavement ME
C1	40.8	40.8	10.13
C2	0.575	0.575	0.575
C3	0.0014	0.0014	0.0014
C4	0.00825	0.00825	0.02432
N	489	489	489
Average Bias, in/mi	-8.24	-5.52	-1.31
Stnd Er, in/mi	21.05	19.83	16.98
LOE R^2	0.41	0.47	0.61
R^2	0.51	0.52	0.62
MAPE	0.15	0.13	0.11

Figure 42. Overall accuracy summary of HMA over JPCPs IRI model for calibration set (Approach 1)

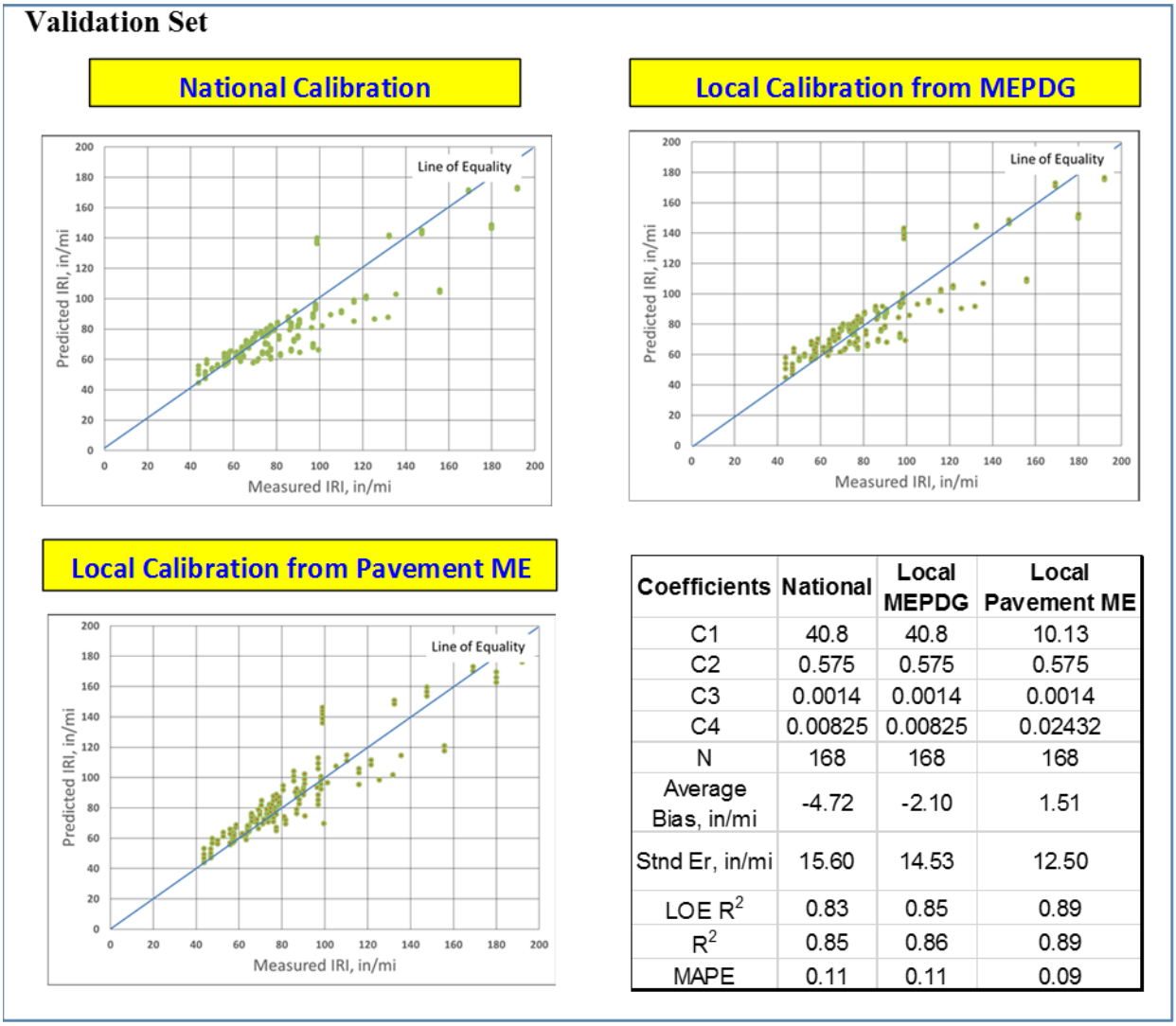

Coefficients	National	Local MEPDG	Local Pavement ME
C1	40.8	40.8	10.13
C2	0.575	0.575	0.575
C3	0.0014	0.0014	0.0014
C4	0.00825	0.00825	0.02432
N	168	168	168
Average Bias, in/mi	-4.72	-2.10	1.51
Stnd Er, in/mi	15.60	14.53	12.50
LOE R^2	0.83	0.85	0.89
R^2	0.85	0.86	0.89
MAPE	0.11	0.11	0.09

Figure 43. Overall accuracy summary of HMA over JPCPs IRI model for validation set (Approach 1)

The AASHTOWare Pavement ME Design locally calibrated IRI model shown in Figures 42 and 43 was calibrated using Approach 1: in the calculation of IRI predictions, AASHTOWare Pavement ME Design locally calibrated rutting and top-down (longitudinal) cracking predictions were used. As can be seen in the figures, the MEPDG locally calibrated IRI model improved the accuracy compared to the nationally calibrated model. The model accuracy was further improved using the AASHTOWare Pavement ME Design locally calibrated IRI model, as can be seen from the figures.

Implementing a paired t test using measured IRI values and AASHTOWare Pavement ME Design locally calibrated predictions for selected pavement sections, a p value was calculated as P(T <= t) two-tail = 0.34 > 0.05. This result implies that, with 95% certainty, there are no significant differences between the actual and AASHTOWare Pavement ME Design–predicted IRI values (Table 28).

Table 28. Paired t test results for HMA IRI model for selected HMA over JPCP sections (Approach 1)

	Actual IRI	IRI Av
Mean	86.64803	86.05753
Variance	914.4023	710.8831
Observations	657	657
Pearson Correlation	0.85092	
Hypothesized Mean Difference	0	
df	656	
t Stat	0.951236	
P(T<=t) one-tail	0.170918	
t Critical one-tail	1.64718	
P(T<=t) two-tail	0.341835	
t Critical two-tail	1.963587	

Approach 2

Approach 2 was also used to locally calibrate the HMA over JPCP IRI model using AASHTOWare Pavement ME Design. In this approach, nationally calibrated rutting and fatigue cracking model predictions were used in the local calibration of the IRI model.

Calibrating the IRI model in this way, similar model accuracies to those of Approach 1 were obtained. It was found that the calibration coefficients established using Approach 1 also produced accurate predictions in this approach. This is because the most sensitive coefficient in the IRI transfer function is C_4, related to the site factor, and the site factor values are the same in both approaches; using nationally calibrated rutting and top-down (longitudinal) cracking models rather than AASHTOWare Pavement ME Design locally calibrated models do not significantly change the IRI predictions. Also note that the second most sensitive calibration coefficient for the IRI model is C_1, related to rutting. It is important to highlight that although the rutting model was further improved using AASHTOWare Pavement ME Design local calibration coefficients, the difference between the nationally calibrated and AASHTOWare Pavement ME Design locally calibrated rutting model predictions was not significant, so the effect of using the nationally calibrated rutting model rather than the AASHTOWare Pavement ME Design locally calibrated model was not significant. That would also mean that the local calibration of the IRI model for Iowa HMA over JPCP sections could be performed with sufficient accuracy by the nationally calibrated rutting and top-down (longitudinal) cracking models. As can be seen in Figure 44 and Figure 45, the AASHTOWare Pavement ME Design locally calibrated IRI model improved model accuracy significantly compared to the nationally calibrated model.

Calibration Set

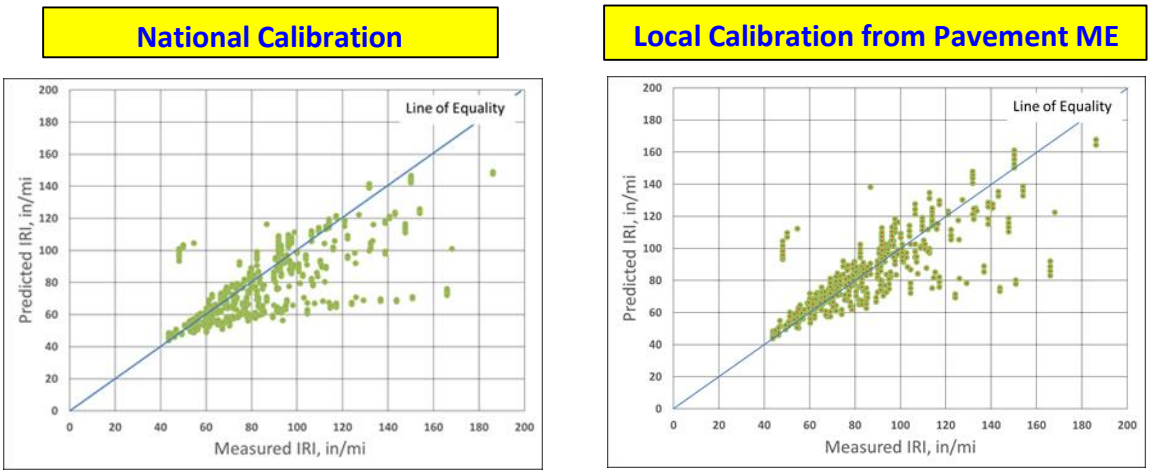

Coefficients	National	Local Pavement ME
C1	40.8	10.13
C2	0.575	0.575
C3	0.0014	0.0014
C4	0.00825	0.02432
N	489	489
Average Bias, in/mi	-8.24	-1.73
Stnd Er, in/mi	21.05	16.98
LOE R^2	0.41	0.61
R^2	0.51	0.62
MAPE	0.15	0.11

Figure 44. Overall accuracy summary of HMA over JPCPs IRI model for calibration set (Approach 2)

Validation Set

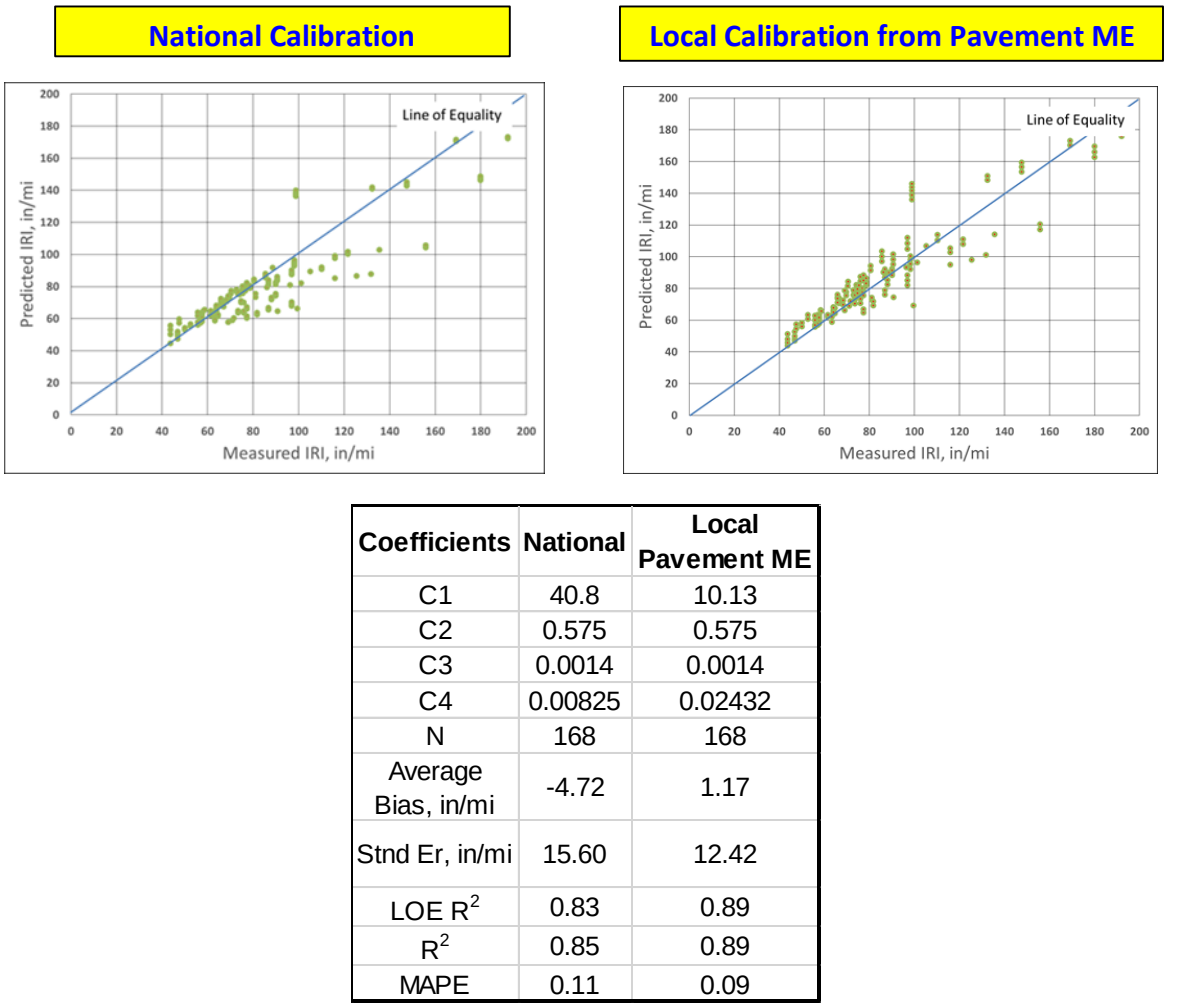

Coefficients	National	Local Pavement ME
C1	40.8	10.13
C2	0.575	0.575
C3	0.0014	0.0014
C4	0.00825	0.02432
N	168	168
Average Bias, in/mi	-4.72	1.17
Stnd Er, in/mi	15.60	12.42
LOE R^2	0.83	0.89
R^2	0.85	0.89
MAPE	0.11	0.09

Figure 45. Overall accuracy summary of HMA over JPCPs IRI model for validation set (Approach 2)

Local calibration of the IRI model using Approach 2 would save significant resources, both time and funds. Use of Approach 2 in the local calibration of IRI model would be especially useful for those SHAs that are mainly interested in only attaining locally calibrated IRI predictions rather than locally calibrated rutting, fatigue, and thermal cracking predictions. In this study, it was determined that using Approach 2, the locally calibrated IRI model can predict this distress with sufficient accuracy for Iowa HMA over JPCP systems.

A paired t test was also applied to this approach, and the calculated p value was P(T <= t) two-tail = 0.11 > 0.05. This result implies that, with 95% certainty, there is no significant difference between national field-measured and AASHTOWare Pavement ME Design–predicted IRI values using Approach 2 (Table 29).

Table 29. Pair t test results for HMA IRI model for selected HMA over JPCP sections (Approach 2)

	Actual IRI	IRI Av
Mean	86.64803	85.66045
Variance	914.4023	710.7439
Observations	657	657
Pearson Correlation	0.851534	
Hypothesized Mean Difference	0	
df	656	
t Stat	1.594009	
P(T<=t) one-tail	0.055708	
t Critical one-tail	1.64718	
P(T<=t) two-tail	0.111416	
t Critical two-tail	1.963587	

DISCUSSION OF FUTURE ENHANCEMENTS OF AASHTOWARE PAVEMENT ME DESIGN

AASHTO has a taskforce on AASHTOWare Pavement ME Design to maintain system performance, keep up with technology, implement new models, develop enhancements, and maintain communication and input from users (AASHTO 2014). Under the support of the AASHTO taskforce on AASHTOWare Pavement ME Design, AASHTOWare Pavement ME Design continues to be upgraded. One of the enhancement items in the current work plan is the development of Application Programming Interfaces (APIs). APIs can provide AASHTOWare Pavement ME Design users with the capability of interacting with the program and creating their own derivative applications, either to directly enhance AASHTOWare Pavement ME Design or for some other purpose. As discussed previously, full optimization of the local calibration coefficients requires the availability of all input variables of the various equations comprising each of the pavement performance models. For example, local calibration of the fatigue model for HMA surface pavements requires the values of ε_t (tensile strain in critical locations) to fully optimize the coefficients (β_{f1}, β_{f2}, β_{f3}). However, this study has revealed that the version of AASHTOWare Pavement ME Design (version 2.1.24) used in this study does not provide these values. Incorporating APIs in AASHTOWare Pavement ME Design would allow AASHTOWare Pavement ME Design users to directly obtain such input values from API outputs and implement them to achieve "true" local calibration. API tools are provided to AASHTOWare Pavement ME Design users in the latest version of the software (version 2.2), released in August 2015.

Along with the APIs, there have been some other enhancements in the newly released AASHTOWare Pavement ME Design software (version 2.2) , including a DRIP tool for drainage assessment, LTPP high-quality traffic data, an improved reflection cracking model, an enhanced climate data set, MapME, and Level 1 and Level 2 AC rehabilitation inputs for concrete overlays. Details of these enhancements are as follows (AASHTO 2015):

- A new reflection cracking model was incorporated into AASHTOWare Pavement ME Design version 2.2. This model was documented in the NCHRP 1-41 study (Lytton et al. 2010). Table 30 gives pavement and distress types related to the new reflection cracking effects.

Table 30. Pavement and distress types the new reflection cracking effects

Pavement Type	Distress Type
AC OL over Existing AC (no interlayer, AC interlayer, seal coat)	Alligator Cracking
	Transverse Cracking
AC OL over Existing Intact JPCP	Transverse Cracking
AC OL over Existing Fractured JPCP or Intact CRCP	Transverse Cracking
Semi-Rigid (New AC over CTB)	Alligator Cracking
	Transverse Cracking

Source: AASHTO 2015

- The new calibration coefficients for JPCP cracking, JPCP faulting, and CRCP punch-out models using the CTE values acquired using the new test specification (AASHTO T 336-09 2009) were added to the latest version of the software. Users with CTE values acquired using the AASHTO T 339-09 test method can use these new calibration coefficients for the aforementioned models. Also note that these new calibration coefficients are documented in the NCHRP 20-07/327 study (Mallela et al. 2011).

- DRIP is a Windows-based microcomputer program used to conduct hydraulic design computations for subsurface drainage analysis of pavements. DRIP has many features, such as roadway geometry calculations, sieve analysis calculations, inflow calculations, permeable base design, separator layer design, and edge drain design. DRIP can be applied to decision making for drainage design by using its grain-size distribution graphs and sensitivity analysis plots. DRIP can be downloaded from the AASHTOWare Pavement ME Design website (www.me-design.com).

- LTPP default axle load distributions can be imported and used in the new software version (version 2.2). The LTPP default axle load distributions are categorized into four groups in AASHTOWare Pavement ME Design version 2.2: Global, Heavy, Typical, and Light. Also note that the right-click choices "Single", "Tandem", Tridem", or "Quad" axle load distribution are disabled in AASHTOWare Pavement ME Design version 2.2.

- In AASHTOWare Pavement ME Design version 2.2, an option for users to define the climate data range was added.

- MapME provides data from geographical information system data linkages to AASHTOWare Pavement ME Design.

- The semi-rigid pavement type replaced the new AC over CTB design type in AASHTOWare Pavement ME Design version 2.2.

- Level 1 and Level 2 input data for AC overlays over AC rehabilitated pavements; Level 3 input data for AC overlays over intact JPCP rehabilitated pavements; and new Level 1, Level 2, and Level 3 inputs for PCC overlays over existing AC pavements are provided in AASHTOWare Pavement ME Design version 2.2.

CONCLUSIONS AND RECOMMENDATIONS

The AASHTOWare Pavement ME Design local calibration for Iowa pavement systems was conducted by (1) evaluating the accuracy of the nationally calibrated AASHTOWare Pavement ME Design performance models and the locally calibrated MEPDG performance models, identified through InTrans Project 11-401 (Ceylan et al. 2013), and (2) recalibrating these models when the accuracies of the models were found to be insufficient. The recalibration of these models was performed using AASHTOWare Pavement ME Design version 2.1.24 with the help of linear and nonlinear optimization techniques to improve the accuracy of model predictions. A step-by-step local calibration procedure was established for each pavement performance prediction model in this study by extensively reviewing the transfer functions used in these models. The required components of the transfer functions needed to implement local calibration were documented as well as well as their locations in intermediate and general output files and how to calculate them. More pavement performance measurements were used in this study than in InTrans Project 11-401 (Ceylan et al. 2013). Specific conclusions were drawn for each pavement type, and corresponding performance prediction models and recommendations for the use of identified local calibration coefficients as well as future research were provided.

Conclusions: JPCP

- The mean joint faulting, transverse cracking, and IRI models for Iowa JPCPs were significantly improved as a result of AASHTOWare Pavement ME Design local calibration compared to the nationally calibrated and MEPDG locally calibrated counterparts.

Conclusions: HMA Pavements

- The identified AASHTOWare Pavement ME Design local calibration factors significantly increased the accuracy of the rutting models for Iowa HMA pavements compared to the nationally calibrated and MEPDG locally calibrated counterparts.

- The identified AASHTOWare Pavement ME Design local calibration factors increased the accuracy of the IRI model for Iowa HMA pavements compared to the nationally calibrated and MEPDG locally calibrated models, although the nationally calibrated and MEPDG locally calibrated IRI models also provided acceptable predictions.

- The nationally calibrated longitudinal (top-down) cracking model underpredicted distress measurements while the MEPDG locally calibrated model overpredicted distress measurements for Iowa HMA pavements. The accuracy of this model was improved as a result of AASHTOWare Pavement ME Design local calibration.

- All the nationally calibrated, MEPDG locally calibrated, and AASHTOWare Pavement ME Design locally calibrated alligator (bottom-up) and thermal cracking models provide acceptable predictions for Iowa HMA pavements.

Conclusions: HMA over JPCP

- The identified AASHTOWare Pavement ME Design local calibration factors increased the accuracy of the rutting model for Iowa HMA over JPCP compared to the nationally calibrated and MEPDG locally calibrated models, although the nationally calibrated and MEPDG locally calibrated IRI models also provided acceptable predictions for this model.

- The identified local calibration factors significantly increased the accuracy of IRI predictions for Iowa HMA over JPCP.

- The nationally calibrated model underpredicted longitudinal (top-down) cracking while the MEPDG locally calibrated model had excessive standard error for Iowa HMA over JPCPs. The accuracy of this model was improved as a result of AASHTOWare Pavement ME Design local calibration.

- All of the nationally calibrated, MEPDG locally calibrated, and AASHTOWare Pavement ME Design locally calibrated alligator (bottom-up) cracking models and thermal cracking models provided acceptable predictions for Iowa HMA over JPCPs.

Recommendations: Use of the Identified Local Calibration Coefficients

- The local calibration coefficients recommended for the Iowa DOT to be used in design practice as alternatives to the nationally calibrated counterparts are summarized in Table 31 for Iowa JPCP, Table 32 for Iowa HMA, and Table 33 for Iowa HMA over JPCP. Note that the recommended local calibration coefficients in red in Tables 31 through 33 show that these numbers are different from their counterparts in the nationally calibrated models.

Table 31. Nationally calibrated and AASHTOWare Pavement ME Design locally calibrated coefficients for Iowa JPCP systems

Distress	Factors	National	Local
Faulting	C1	1.0184	0.85
	C2	0.91656	1.39
	C3	0.0021848	0.002
	C4	0.0008837	0.274
	C5	250	250.8
	C6	0.4	0.4
	C7	1.83312	1.45
	C8	400	400
Cracking	C1 (fatigue)	2	2.25
	C2 (fatigue)	1.22	1.4
	C4 (crack)	1	4.06
	C5 (crack)	-1.98	-0.44
IRI: Approach 1	C1	0.8203	0.11
	C2	0.4417	0.44
	C3	1.4929	0.04
	C4	25.24	11.32
IRI: Approach 2	C1	0.8203	0.03
	C2	0.4417	0.44
	C3	1.4929	0.01
	C4	25.24	15.12

Note: The recommended local calibration coefficients are in red.

Table 32. Nationally calibrated and AASHTOWare Pavement ME Design locally calibrated coefficients for Iowa HMA pavement systems

Distress	Factors	National	Local
HMA Rut	B1	1	1
	B2	1	1.1
	B3	1	1
GB Rut	B1_Granular	1	0.001
SG Rut	B1_Fine-grain	1	0.001
Fatigue for ACrack and LCrack	B1	1	1
	B2	1	1
	B3	1	1
LCrack	C1_Top	7	2.32
	C2_Top	3.5	0.47
	C4_Top	1000	1000
ACrack	C1_Bottom	1	1
	C2_Bottom	1	1
	C4_Bottom	6000	6000
TCrack	K_Level 3	1.5	1.5
IRI: Approach 1	C1	40	5
	C2	0.4	0.4
	C3	0.008	0.008
	C4	0.015	0.026
IRI: Approach 2	C1	40	25
	C2	0.4	0.4
	C3	0.008	0.008
	C4	0.015	0.019

Note: The recommended local calibration coefficients are in red.

Table 33. Nationally calibrated and AASHTOWare Pavement ME Design locally calibrated coefficients for Iowa HMA over JPCP systems

Distress	Factors	National	Local
HMA Rut	B1	1	1
	B2	1	1.01
	B3	1	1
GB Rut	B1_Granular	1	0.001
SG Rut	B1_Fine-grain	1	0.001
Fatigue for ACrack and LCrack	B1	1	1
	B2	1	1
	B3	1	1
LCrack	C1_Top	7	2.3
	C2_Top	3.5	2
	C4_Top	1000	1000
ACrack	C1_Bottom	1	1
	C2_Bottom	1	1
	C4_Bottom	6000	6000
TCrack	K_Level 3	1.5	1.5
IRI: Approach 1	C1	40.8	10.13
	C2	0.575	0.575
	C3	0.0014	0.0014
	C4	0.00825	0.02432
IRI: Approach 2	C1	40.8	10.13
	C2	0.575	0.575
	C3	0.0014	0.0014
	C4	0.00825	0.02432

Note: The recommended local calibration coefficients are in red.

- The locally calibrated JPCP performance models (faulting, transverse cracking, and IRI) identified in this study are recommended for use with Iowa JPCPs as alternatives to the nationally calibrated models.

- Because in the calculation of IRI both faulting and transverse cracking predictions are involved, two approaches were utilized in the local calibration of the JPCP IRI model. In Approach 1, the IRI model was locally calibrated using AASHTOWare Pavement ME Design locally calibrated faulting and transverse cracking model predictions, while in Approach 2 nationally calibrated faulting and transverse cracking model predictions were used.

- The use of two approaches in the local calibration of the IRI model was intended to

determine whether the IRI model could be locally calibrated with sufficient accuracy without using local calibration procedures for each distress model, which would require additional financial and data resources. Local calibration of the IRI model using Approach 2 would save significant time and funds. Using Approach 2 in the local calibration of the IRI model would be especially useful for the Iowa DOT, whether it decides to use nationally calibrated transverse cracking and faulting models and locally calibrate the IRI model or is more interested in attaining locally calibrated IRI predictions rather than locally calibrated transverse cracking and faulting model predictions.

- In this study, it was determined that using Approach 2, a locally calibrated IRI model can predict distress with sufficient accuracy for Iowa JPCP systems.

- The locally calibrated rutting, longitudinal (top-down) cracking, and IRI prediction models identified in this study are recommended as alternatives to the nationally calibrated models for use in predicting the performance of Iowa HMA pavements.

- The locally calibrated rutting, longitudinal (top-down) cracking, and IRI prediction models identified in this study are recommended as alternatives to the nationally calibrated models for use in predicting the performance of HMA over JPCPs.

- The nationally calibrated alligator (bottom-up) and transverse (thermal) cracking prediction models are recommended for use in predicting the performance of Iowa HMA systems, because even though the accuracy of these models was improved by local calibration, the improvement was insignificant. Note that Iowa HMA pavements do not experience severe fatigue-related problems. It was also found that the HMA transverse (thermal) cracking model would be unlikely to satisfactorily simulate this distress for Iowa HMA pavements.

- The nationally calibrated alligator (bottom-up) and thermal cracking prediction models are recommended for use with Iowa HMA over JPCP systems, because even though the accuracy of these models was improved by local calibration, the improvement was insignificant.

- In locally calibrating the IRI model for Iowa HMA pavements and HMA over JPCPs, two approaches were followed. In Approach 1, the IRI model was locally calibrated using the AASHTOWare Pavement ME Design locally calibrated rutting and top-down (longitudinal) cracking predictions and the nationally calibrated alligator (bottom-up) and transverse (thermal) cracking predictions for HMA pavements and HMA over JPCPs. In Approach 2, all nationally calibrated model predictions were used. Note that in contrast to the HMA IRI model, reflective cracking predictions were added to the IRI model as part of the area of total fatigue cracking in HMA over JPCPs. In both Approach 1 and Approach 2, nationally calibrated reflection cracking predictions were employed.

- In this study, it was determined that using Approach 2 a locally calibrated IRI model can predict distress with sufficient accuracy for Iowa HMA and HMA over JPCP systems.

- Preliminary studies were carried out to determine whether there are any differences between the latest version of AASHTOWare Pavement ME Design (version 2.2) released in August 2015 and the version used in this study, AASHTOWare Pavement ME Design version 2.1.24. One significant change between these two versions is the prediction of Freezing Index Factor, a component of the IRI models. The results indicated some differences in IRI model predictions between these two software versions due to the different Freezing Index Factor predictions. Note that Freezing Index Factors are predicted by the software using enhanced integrated climatic models (EICM) and automatically incorporated into the calculation of IRI predictions. The Iowa DOT would deal with this issue by (1) running the software input files provided by the researchers of this study and (2) based on the IRI predictions, locally calibrating the IRI model by modifying only the Freezing Index Factor following the steps documented in this report.

Recommendations: Future Research

Under the support of the AASHTO taskforce on AASHTOWare Pavement ME Design, the AASHTOWare Pavement ME Design software is continually upgraded to implement new models and enhancements and to maintain communication and seek continued feedback from users (AASHTO 2014). It is rational to use the advancing pavement design and analysis tools for achieving cost-effective pavement asset management. Considering the future updates that the AASHTOWare Pavement ME Design software is likely to undergo at the national level, future research topics related to its use for Iowa pavement systems are as follows:

- Reflective cracking is one of the most common types of distresses that occur in Iowa composite pavements (HMA/JPCP), which constitute over 50% of the entire Iowa highway system. Recently, the reflective cracking model developed through NCHRP 1-41 (Lytton et al. 2010, Ceylan et al. 2011) has been successfully integrated into the new version of AASHTOWare Pavement ME Design (version 2.2, released on August 12, 2015). Because the Iowa DOT is one of the few SHAs at the forefront of implementing AASHTOWare Pavement ME Design and has a significant percentage of composite pavements (more than 50%) in its highway network, it is expected to significantly benefit from the local calibration of the recently integrated reflective cracking prediction model in AASHTOWare Pavement ME Design.

- Material properties are important design inputs affecting AASHTOWare Pavement ME Design predictions, but the characterization of these properties requires time and considerable resources. Considering such difficulties, AASHTOWare Pavement ME Design allows the designer to select the estimated design inputs with low accuracy in the Level 3 option under a hierarchical approach. The primary reason for the low accuracy of the design inputs estimation is related to the predictive equation based on the conventional multivariate regression analysis (e.g., Witczak equation for HMA dynamic modulus predictions). Ceylan et al. (2008, 2009a, 2009b) developed a novel approach for predicting the HMA dynamic modulus using an artificial neural network (ANN) methodology. The developed ANN-based dynamic modulus models exhibit significantly better overall prediction accuracy, better local accuracy at high and low temperature extremes, less prediction bias, and better balance

between temperature and mixture influences than do their regression-based counterparts. Such model developments for Iowa materials will be greatly beneficial to the Iowa DOT, not only in the use of AASHTOWare Pavement ME Design with high accuracy results, but also in the quality control and quality assurance of paving materials.

- The AASHTOWare Pavement ME Design performance criteria for different classes of Iowa roads are recommended for future investigation. As part of this recommended investigation, the highly accurate models to predict Iowa distress history would be developed by using various conventional regression methods and computational intelligence tools. Such a model would lead to improved decision making in designing pavement geometry and structure for different classes of Iowa roads.

- It is recommended that the Iowa DOT develop a satellite pavement management/pavement design database for each project being designed and constructed using AASHTOWare Pavement ME Design as part of the current PMIS. This database should be in a comparable format to that of AASHTOWare Pavement ME Design inputs and outputs. The database could be utilized to identify the causes of specific pavement failures in each project and recalibrate AASHTOWare Pavement ME Design performance prediction models for nontraditional paving materials such as recycled materials, warm mix asphalt (WMA), etc.

- As of 2015, new pavement performance prediction models (e.g., the top-down cracking model) are under development to be incorporated into the AASHTOWare Pavement ME Design software in future releases. Similarly to these models, the recently developed bonded concrete overlay of asphalt pavement mechanistic-empirical (BCOA-ME) model is considered to be implemented in the AASHTOWare Pavement ME Design software in the future. As such new pavement performance models are added to the software or as the existing models are refined/modified, the verification and calibration of such new models for Iowa pavement systems are recommended to increase the versatility of the use of AASHTOWare Pavement ME Design and incorporate advanced pavement design methodologies.

REFERENCES

AASHTO. 2008. *Mechanistic-Empirical Pavement Design Guide, Interim Edition: A Manual of Practice*. Washington, DC.

AASHTO. 2010. *Guide for the Local Calibration of the Mechanistic-Empirical Pavement Design Guide*. Washington, DC.

AASHTO. 2014. *AASHTOWare Newsletter, October 2014*. www.aashtoware.org/Pavement/Pages/Newsletter.aspx. Accessed July 15, 2015.

AASHTO. 2015. *AASHTOWare Pavement ME Design Release Notes, August 2015*. me-design.com/MEDesign/Documents.html. Accessed September 15, 2015.

AASHTO T 336-09.2009. *Standard Method of Test for Coefficient of Thermal Expansion of Hydraulic Cement Concrete*. Standard Specifications for Transportation Materials and Methods of Sampling and Testing, American Association of State Highway and Transportation Officials. Washington, DC.

AASHTO TP 60-00. 2004. *Standard Method of Test for Coefficient of Thermal Expansion of Hydraulic Cement Concrete*. Standard Specifications for Transportation Materials and Methods of Sampling and Testing, American Association of State Highway and Transportation Officials. Washington, DC.

APTech, Inc. 2010. *Local Calibration of the MEPDG Using Pavement Management*, FHWA-HIF-11-026, Washington, DC: Federal Highway Administration.

ARA, Inc., ERES Consultants Division. 2004. *Guide for Mechanistic-Empirical Design of New and Rehabilitated Pavement Structures*. www.trb.org/mepdg. National Cooperative Highway Research Program 1-37A. Washington, DC: Transportation Research Board.

Banerjee, A., Aguiar-Moya, J. P., and Prozzi, J. A. 2009. Calibration of mechanistic-empirical pavement design guide permanent deformation models: Texas experience with long-term pavement performance. *Transportation Research Record: Journal of the Transportation Research Board.* 2094: 12-20. Washington DC: Transportation Research Board.

Banerjee, A., J. A. Prozzi, and J. P. Aguiar-Moya. 2010. Calibrating the MEPDG permanent deformation performance model for different maintenance and rehabilitation strategies. Presented at the 89th annual meeting of the Transportation Research Board. Washington, DC: Transportation Research Board.

Banerjee, A., J. A. Prozzi, and A. Freiman. 2011. Regional Calibration of Permanent Deformation Performance Models for Rehabilitated Flexible Pavements. Presented at the Annual 90th annual meeting of the Transportation Research Board. Washington, DC: Transportation Research Board.

Bustos, M. G., Cordo, C., Girardi, P., and Pereyra, M. S. 2009. Developing a Methodology to Calibrate Mechanistic-Empirical Pavement Design Guide Procedures for Rigid Pavement Design in Argentina. Presented at the 88th annual meeting of the Transportation Research Board. Washington, DC: Transportation Research Board.

Brown, S. F., M. I. Darter, G. Larson, M. Witczak, and M. El-Basyouny. 2006. Independent Review of the *Mechanistic-Empirical Pavement Design Guide* and Software. *National Cooperative Highway Research Program Research Results Digest.* No. 307. Key findings from NCHRP Project 1-40A. Washington, DC: Transportation Research Board.

Ceylan, H., Gopalakrishnan, K., and Kim, S. 2008. Advanced approaches to hot mix asphalt dynamic modulus prediction. *Canadian Journal of Civil Engineering.* 35(7):699-707.

Ceylan, H., Gopalakrishnan, K., and Kim, S. 2009a. Looking to the future: the next generation hot mix asphalt dynamic modulus prediction models. *International Journal of Pavement Engineering*. 10(5):341-352.

Ceylan, H., Schwartz, C. W., Kim, S., and Gopalakrishnan, K. 2009b. Accuracy of predictive models for dynamic modulus of hot mix asphalt. *Journal of Materials in Civil Engineering*. 21(6):286-293.

Ceylan, H., Gopalakrishnan, K., and Lytton, R. 2011. Neural networks modeling of stress growth in asphalt overlays due to load and thermal effects during reflection cracking. *Journal of Materials in Civil Engineering*. 23(3):221-229.

Ceylan, H., S. Kim, K. Gopalakrishnan, and D. Ma. 2013. *Iowa Calibration of MEPDG Performance Prediction Models*. Ames, Iowa: Institute for Transportation, Iowa State University.

Corley-Lay, J. B., F. Jadoun, J. Mastin, and R. Kim. 2010. Comparison of NCDOT and LTPP monitored flexible pavement distresses. *Transportation Research Record: Journal of the Transportation Research Board.* 2153:91-96. Washington DC: Transportation Research Board.

Crawford, G., J. Gudimettla, and J. Tanesi. 2010. Inter–laboratory study on measuring coefficient of thermal expansion of concrete. Presented at the annual meeting of the Transportation Research Board. Washington, DC: Transportation Research Board.

Darter, M. I., J. Mallela, L. Titus-Glover, C. Rao, G. Larson, A. Gotlif, H. L. Von Quintus, L. Khazanovich, M. Witczak, M. El-Basyouny, S. El-Badawy, A. Zborowski, and C. Zapata. 2006. Changes to the *Mechanistic-Empirical Pavement Design Guide* Software through Version 0.900. *National Cooperative Highway Research Program Research Results Digest.* No. 308. Key findings from NCHRP Project 1-40D. Washington, DC: Transportation Research Board.

Darter, M. I., L. T. Glover, and H. L. Von Quintus. 2009. *Implementation of the Mechanistic-Empirical Pavement Design Guide in Utah: Validation, Calibration, and Development of the UDOT MEPDG User's Guide*. Report no. UT-09.11, Champaign, Illinois: ARA, Inc.

Darter, M. I., L. T. Glover, H. L. Von Quintus, B. Bhattacharya, and J. Mallela. 2014. *Calibration and Implementation of the AASHTO Mechanistic-Empirical Pavement Design Guide in Arizona.* Champaign, Illinois: ARA, Inc.

Delgadillo, R., C. Wahr, and J. P. Alarcón. 2011. Towards the implementation of the MEPDG in Latin America, preliminary work carried out in Chile. Presented at the 90th Annual Meeting of the Transportation. Washington, DC: Transportation Research Board.

Frontline Systems, Inc. www.solver.com. Accessed July 15, 2015.

Galal, K. A., and G. R. Chehab. 2005. Implementing the mechanistic-empirical design guide procedure for a Hot-Mix Asphalt-rehabilitated pavement in Indiana. *Transportation Research Record: Journal of the Transportation Research Board.* 1919:121-133. Washington DC: Transportation Research Board.

Hall, K. D., D. X. Xiao, and K. C. P. Wang. 2011. Calibration of the MEPDG for flexible pavement design in Arkansas. *Transportation Research Record: Journal of the Transportation Research Board.* 2226:135-141. Washington DC: Transportation Research Board.

Hoegh, K., L. Khazanovich, M. R. Jensen. 2010. Local calibration of MEPDG rutting model for MnROAD test section. *Transportation Research Record: Journal of the Transportation Research Board.* 2180:130-141. Washington DC: Transportation Research Board.

Hudson, W. R., P. Visser, C. Monismith, and C. Dougan. 2006a. *Using Pavement Management Data to Calibrate and Validate the New MEPDG, An Eight State Study Volume I.* Washington, DC: Federal Highway Administration.

Hudson, W. R., P. Visser, C. Monismith, and C. Dougan. 2006b. *Using Pavement Management Data to Calibrate and Validate the New MEPDG, An Eight State Study Volume II.* Washington, DC: Federal Highway Administration.

Jadoun, F. M. 2011. Calibration of the flexible pavement distress prediction models in the Mechanistic-Empirical Pavement Design Guide (MEPDG) for North Carolina. PhD dissertation, North Carolina State University.

Kang, M., T. M. Adams, and H. Bahia. 2007. *Development of a Regional Pavement Performance Database of the AASHTO Mechanistic-Empirical Pavement Design Guide: Part 2: Validations and Local Calibration*. Madison, Wisconsin: Midwest Regional University Transportation Center, University of Wisconsin-Madison.

Khazanovich, L., L. Yut, S. Husein, C. Turgeon, and T. Burnham. 2008. Adaptation of Mechanistic–Empirical Pavement Design Guide for design of Minnesota low-volume Portland Cement Concrete Pavements. *Transportation Research Record: Journal of the Transportation Research Board.* 2087:57-67. Washington DC: Transportation Research Board.

Kim, S., H. Ceylan, K. Gopalakrishnan, and O. Smadi. 2010. Use of pavement management information system for verification of Mechanistic-Empirical Pavement Design Guide performance predictions. *Transportation Research Record: Journal of the Transportation Research Board.* 2153:30-39. Washington DC: Transportation Research Board.

Lewis, C. D. 1982. *Industrial and Business Forecasting Methods*. London: Butterworths.

Li, J, S. T. Muench, J. P. Mahoney, N. Sivaneswaran, and L. M. Pierce. 2006. Calibration of NCHRP 1-37A software for the Washington State Department of Transportation: rigid pavement portion. *Transportation Research Record: Journal of the Transportation Research Board.* 1949:43-53. Washington DC: Transportation Research Board.

Li, J., L. M. Pierce, and J. S. Uhlmeyer. 2009. Calibration of flexible pavement in mechanistic-empirical pavement design guide for Washington State. *Transportation Research Record: Journal of the Transportation Research Board.* 2095:73-83. Washington DC: Transportation Research Board.

Li, J., D. R. Luhr, and J. S. Uhlmeyer. 2010. Pavement performance modeling using piecewise approximation. *Transportation Research Record: Journal of the Transportation Research Board.* 2153:24-29. Washington DC: Transportation Research Board.

LINDO Systems, Inc. *Lingo 15.0*. www.lindo.com. Accessed July 15, 2015.

Lytton, R. L., F. L. Tsai, S. Lee, R. Luo, S. Hu, and F. Zhou. 2010. *NCHRP Report 669: Models for Predicting Reflection Cracking of Hot-Mix Asphalt Overlays*. National Cooperative Highway Research Program Project 1-41. Washington, DC: Transportation Research Board.

Mallela. J., L. Titus-Glover, H. Von Quintus, M. I. Darter, M. Stanley, C. Rao, and S. Sadasivam. 2009. *Implementing the AASHTO Mechanistic-Empirical Pavement Design Guide in Missouri. Volume I: Study Findings, Conclusions, and Recommendations.* Applied Research Associates, Inc.

Mallela, J., M. I. Darter, L. Titus-Glover, C. Rao, and B. Bhattacharya. 2011. *Recalibration of AASHTO-ME Rigid Pavement National Models Based on Corrected CTE Values*. NCHRP 20-07/Task 288, Transportation Research Board of the National Academies. Washington, DC.

Mallela, J. L. Titus-Glover, S. Sadasivam, B. B. Bhattacharya, M. I. Darter and H. Von Quintus. 2013. *Implementation of the AASHTO Mechanistic-Empirical Pavement Design Guide for Colorado*. Applied Research Associates, Inc.

Mallela, J., L. Titus-Glover, B. B. Bhattacharya, A. Gotlif, and M. I. Darter. Recalibration of the JPCP cracking and faulting models in the AASHTO ME Design. *Transportation Research Record: Journal of the Transportation Research Board.* No. 5222. Washington DC: Transportation Research Board.

Mamlouk, M. S., and C. E. Zapata. 2010. Necessary assessment of use of state pavement management system data in mechanistic-empirical pavement design guide calibration process. *Transportation Research Record: Journal of the Transportation Research Board.* 2153:58-66. Washington DC: Transportation Research Board.

Miller, J. S. and W. Y. Bellinger. 2003. *Distress Identification Manual for the Long-Term Pavement Performance (LTPP) Project*. FHWA-RD-03-031 (4th edition). Federal Highway Administration.

Mu F., J. W. Mack, and R. A. Rodden. 2015. Review of national and state-level calibrations of the AASHTOWare Pavement ME Design for new jointed plain concrete pavement. *Proceedings of ASCE Airfield and Highway Pavements*. pp. 708-719.

Muthadi, N. R. 2007. Local calibration of the MEPDG for flexible pavement design. MS thesis, North Carolina State University.

Muthadi, N. R., and R. Kim. 2008. Local calibration of mechanistic-empirical pavement design guide for flexible pavement design. *Transportation Research Record: Journal of the Transportation Research Board.* 2087:131-141. Washington DC: Transportation Research Board.

Pierce, L. M., and G. McGovern. 2014. *NCHRP Synthesis 457 Implementation of the AASHTO Mechanistic-Empirical Pavement Design Guide and Software: A Synthesis of Highway Practice.* Washington, DC: Transportation Research Board.

Schram, S., and M. Abdelrahman. 2006. Improving prediction accuracy in mechanistic-empirical pavement design guide. *Transportation Research Record: Journal of the Transportation Research Board.* 1947:59-68. Washington DC: Transportation Research Board.

Schwartz, C. W., R. Li, S. H. Kim, H. Ceylan, and K. Gopalakrishnan. 2011. *Sensitivity Evaluation of MEPDG Performance Prediction*. National Cooperative Highway Research Program Project 1- 47. Washington, DC: Transportation Research Board.

Souliman, M. I., M. S. Mamlouk, M. M. El-Basyouny, and C. E. Zapata. 2010. Calibration of the AASHTO MEPDG for flexible pavement for Arizona conditions. Presented at the 89th Annual Meeting of the Transportation Research Board. Washington, DC: Transportation Research Board.

Tarefder, R. and J. I. Rodriguez-Ruiz. 2013. Local calibration of MEPDG for flexible pavements in New Mexico. *Journal of Transportation Engineering* 139:10.

Titus-Glover, L. and J. Mallela. 2009. *Guidelines for Implementing NCHRP 1-37A M-E Design Procedures in Ohio: Volume 4 - MEPDG Models Validation & Recalibration.* Applied Research Associates, Inc.

TRB. 2009. *NCHRP Projects*, www.trb.org/CRP/NCHRP/NCHRPProjects.asp. Accessed February 2009.

Velasquez, R., K. Hoegh, l. Yut, N. Funk, G. Cochran, M. Marasteanu, and L. Khazanovich. 2009. *Implementation of the MEPDG for New and Rehabilitated Pavement Structures for Design of Concrete and Asphalt Pavements in Minnesota*. MN/RC 2009-06, Minneapolis, Minnesota: University of Minnesota.

Von Quintus, H. L., C. Schwartz, R. H. McCuen, and D. Andrei. 2003a. Jackknife Testing—An Experimental Approach to Refine Model Calibration and Validation. *National Cooperative Highway Research Program Research Results Digest.* No. 283. Key findings from NCHRP Project 9-30. Washington, DC: Transportation Research Board.

Von Quintus, H. L., C. Schwartz, R. H. McCuen, and D. Andrei. 2003b. Refining the Calibration and Validation of Hot Mix Asphalt Performance Models: An Experimental Plan and Database. *National Cooperative Highway Research Program Research Results Digest.* No. 284. Key findings from NCHRP Project 9-30. Washington, DC: Transportation Research Board.

Von Quintus, H. L., M. I. Darter, and J. Mallela. 2005. *Phase I – Local Calibration Adjustments for the HMA Distress Prediction Models in the M-E Pavement Design Guide Software*. Interim Report. National Cooperative Highway Research Program 1-40 B. Washington, DC: Transportation Research Board.

Von Quintus, H. L., and J. S. Moulthrop. 2007. *Mechanistic-Empirical Pavement Design Guide Flexible Pavement Performance Prediction Models: Volume I- Executive Research Summar*y. FHWA/MT-07-008/8158-1. Texas: Fugro Consultants, Inc.

Von Quintus, H. L., M. I. Darter, and J. Mallela. 2007. *Recommended Practice for Local Calibration of the ME Pavement Design Guide*. National Cooperative Highway Research Program Project 1-40B Draft. Round Rock, Texas: ARA, Inc.

Von Quintus, H. L. 2008a. MEPDG overview & national perspective. Presented at North-Central MEPDG User Group, Ames, IA: February 19, 2008.

Von Quintus, H. L. 2008b. Local calibration of MEPDG—An overview of selected studies. Presented at 2008 AAPT Symposium Session: Implementation of the New MEPDG, Philadelphia, Pennsylvania: April 29, 2008.

Von Quintus, H. L., M. I. Darter, and J. Mallela. 2009. *Examples Using the Recommended Practice for Local Calibration of the MEPDG Software*. National Cooperative Highway Research Program Project 1- 40B Manual of Practice. Washington, DC: Transportation Research Board.

Wu Z., D. W. Xiao, Z. Zhang, and W. H. Temple. 2014. Evaluation of AASHTO Mechanistic-Empirical Pavement Design Guide for Designing Rigid Pavements in Louisiana. *International Journal of Pavement Research and Technology.* 7(6):405-416.

Zapata, C. E. 2010. *A National Database of Subgrade Soil-Water Characteristic Curves and Selected Soil Properties for Use with the MEPDG*. National Cooperative Highway Research Program Project 9-23A (NCHRP Web Only Document 153). Washington, DC: Transportation Research Board.

Zhou C., B. Huang, X. Shu, and Q. Dong. 2013. Validating MEPDG with Tennessee Pavement Performance Data. *Journal of Transportation Engineering* 139(3).

Wang, K., J. Hu, and Z. Ge. 2008. *Task 6: Material Thermal Input for Iowa*. Ames, Iowa: Center for Transportation Research and Education, Iowa State University.

APPENDIX A: LITERATURE REVIEW RESULTS

The national calibration-validation process was successfully completed for the *Mechanistic-Empirical Pavement Design Guide (MEPDG)* (ARA, Inc. 2004). Although this effort was comprehensive, a further validation study is highly recommended for the MEPDG or AASHTOWare Pavement ME Design as a prudent step in implementing a new design procedure that greatly differs from the current procedures. The objective of this task was to review all of available existing literature with regard to implementing the MEPDG and local calibration at national and local research levels. A comprehensive literature review was undertaken specifically to identify the following information:

- Identify local calibration steps detailed in national level research studies (NCHRP and FHWA research projects) for local calibration.
- Examine how state agencies apply the national level research projects' local calibration procedures in their pavement systems.
- Summarize the MEPDG or AASHTOWare Pavement ME Design pavement performance models' local calibration coefficients reported in the literature.

Summary of National-Level Projects for MEPDG Local Calibration

AASHTO Guide for the Local Calibration of the MEPDG Developed from NCHRP Projects

At the request of the AASHTO Joint Task Force on Pavements (JTFP), the NCHRP initiated project 1-40, "Facilitating the Implementation of the Guide for the Design of New and Rehabilitated Pavement Structures," following NCHRP 1- 37A (ARA, Inc. 2004) for implementation and adoption of the recommended MEPDG (TRB 2009). A key component of NCHRP 1-40 is an independent, third-party review to test the design guide's underlying assumptions, evaluate its engineering reasonableness and design reliability, and to identify opportunities for its implementation in day-to-day design production work. Beyond this immediate requirement, NCHRP 1-40 includes a coordinated effort to acquaint state department of transportation (DOT) pavement designers with the principles and concepts employed in the recommended guide, assist them with the interpretation and use of the guide and its software and technical documentation, develop step-by-step procedures to help state DOT engineers calibrate distress models on the basis of local and regional conditions for use in the recommended guide, and perform other activities to facilitate its acceptance and adoption.

There are two NCHRP research projects that are closely related to the local calibration of MEPDG performance predictions. They are (1) NCHRP 9-30 (Von Quintus et al. 2003a, Von Quintus et al. 2003b), "Experimental Plan for Calibration and Validation of Hot Mix Asphalt Performance Models for Mix and Structural Design," and (2) NCHRP 1-40B (Von Quintus et al. 2005, Von Quintus et al. 2007, Von Quintus et al. 2009, AASHTO 2010, TRB 2010), "User Manual and Local Calibration Guide for the Mechanistic-Empirical Pavement Design Guide and Software." Under the NCHRP 9-30 project, pre-implementation studies involving verification and recalibration were conducted in order to quantify the bias and residual error of the flexible

pavement distress models included in the MEPDG (Muthadi 2007). Based on the findings from the NCHRP 9-30 study, the NCHRP 1-40B project focused on preparing (1) a user manual for the MEPDG and software and (2) a detailed, practical guide for highway agencies for local or regional calibration of the distress models in the MEPDG and software. The manual and guide have been presented in the form of draft AASHTO recommended practices; the guide shall contain two or more examples or case studies illustrating the step-by-step procedures. It was also recommended that the longitudinal cracking model be dropped from the local calibration guide development under NCHRP 1-40B due to a lack of accuracy in the predictions (Muthadi 2007, Von Quintus and Moulthrop 2007). NCHRP 1-40B was completed in 2009 and has been published as *Guide for the Local Calibration of the Mechanistic-Empirical Pavement Design Guide* by AASHTO.

NCHRP 1-40B (Von Quintus et al. 2007) initially provided the three primary steps for calibrating the MEPDG to local conditions and materials as follows:

Step 1. Verification of MEPDG performance models with national calibration factors: Run the current version of the MEPDG software for new field sections using the best available materials and performance data. The accuracy of the prediction models was evaluated using the bias (defined as average overprediction or underprediction) and the residual error (defined as the predicted minus observed distress), as illustrated in Figure A.1. If there is a significant bias and residual error, it is recommended to calibrate the models to local conditions, leading to the second step.

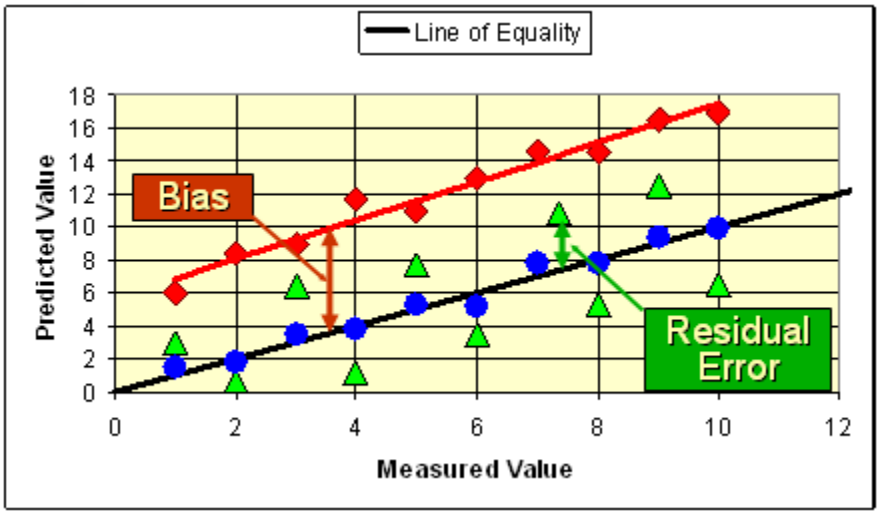

Source: Von Quintus 2008a

Figure A.1. Bias and the residual error

Step 2. Calibration of the model coefficients: Eliminate the bias and minimize the standard error between the predicted and measured distresses.

Step 3. Validation of MEPDG performance models with local calibration factors: Once the bias is eliminated and the standard error is within the agency's acceptable level after calibration,

validation is performed on the models to check for the reasonableness of the performance predictions.

NCHRP 1-40B (Von Quintus et al. 2009) has also detailed these steps more into 11 steps for local calibration of the MEPDG. These 11 steps are depicted in Figure A.2 and Figure A.3, and each of the 11 steps is summarized in the following subsections.

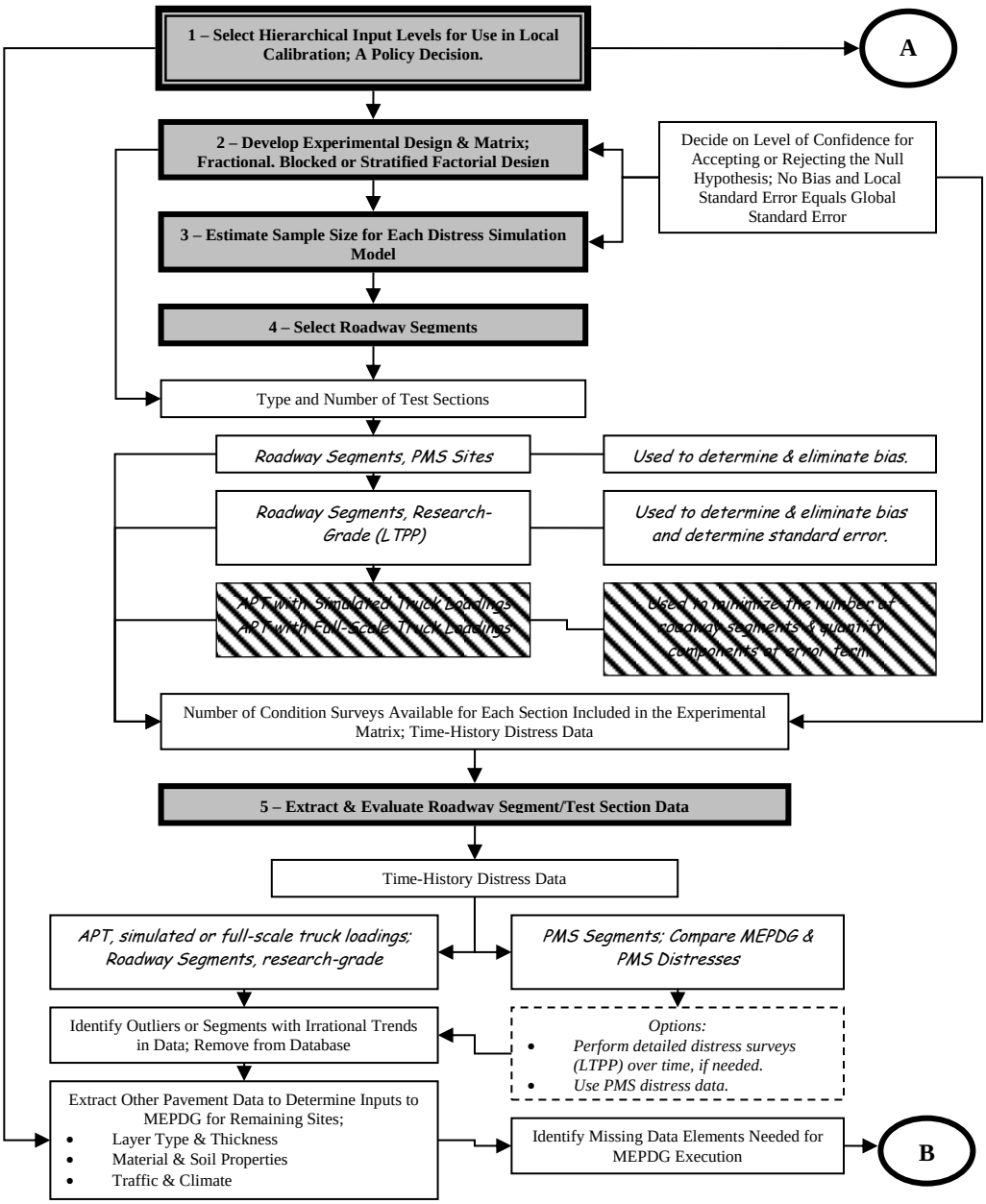

Source: Von Quintus et al. 2009

Figure A.2. Flowchart for the procedure and steps suggested for local calibration: Steps 1 through 5

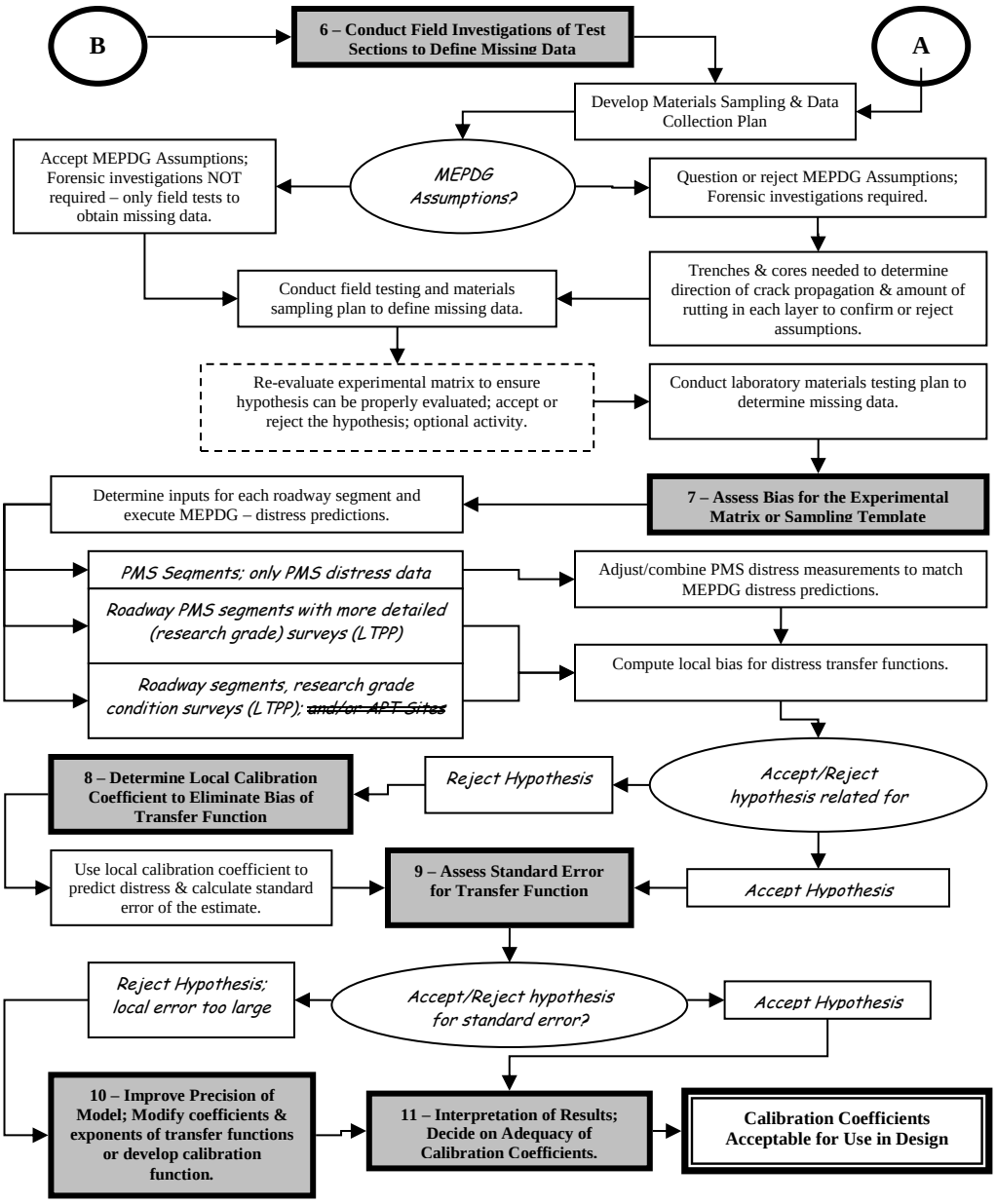

Source: Von Quintus et al. 2009

Figure A.3. Flowchart for the procedure and steps suggested for local calibration: Steps 6 through 11

Step 1: Select Hierarchical Input Level

The hierarchical input level to be used in the local validation-calibration process should be consistent with the way the agency intends to determine the inputs for day-to-day use. Some of input Level 3 data may be available in the state DOT pavement management system (PMS). It is also important to point out that the calibration using Level 1 and 2 input data is dependent upon material and mixture characteristics. Further linkage of material and mixture characteristics to

pavement performance is critical to the Level 1 and 2 calibrations. The general information from which the inputs were determined for each input category is discussed in Step 5.

Step 2: Experimental Factorial and Matrix or Sampling Template

A detailed sampling template should be created considering traffic, climate, pavement structure, and materials representing local conditions. The number of roadway segments selected for the sampling template should result in a balanced factorial with the same number of replicates within each category.

Step 3: Estimate Sample Size for Each Performance Indicator Prediction Model

The sample size (total number of roadway segments or projects) can be estimated with a statistical confidence level of significance. The selection of higher confidence levels can provide more reliable data but increase the number of segments needed. The number of distress observations per segment is dependent on the measurement error or within segment data variability over time (i.e., the higher the within-project data dispersion or variability, the larger the number of observations needed for each distress). The number of distress measurements made within a roadway segment is also dependent on the within-project variability of the design features and site conditions. The NCHRP 1-40B project report (AASHTO 2010) provides the following equation for the determination of the number of distress observations:

$$N = \left(\frac{z_\alpha \left(s_y \right)}{e_t} \right)^2 \quad \textbf{(A.1)}$$

where, z_α = 1.282 for a 90% confidence interval, s_y = standard deviation of the maximum true or observed values, and e_t = tolerable bias. The tolerable bias will be estimated from the levels that are expected to trigger some major rehabilitation activity, which are agency dependent. The s_e/s_y value (ratio of the standard error and standard deviation of the measured values) will also be agency dependent.

Step 4: Select Roadway Segments

Roadway segments should be selected to cover a range of distress values that are of similar ages within the sampling template. Roadway segments exhibiting premature or accelerated distress levels, as well as those exhibiting superior performance (low levels of distress over long periods of time), can be used, but with caution. The roadway segments selected for the sampling template when using hierarchal input Level 3 should represent average performance conditions. It is important that the same number of performance observations per age per each roadway segment be available in selecting roadway segments for the sampling template. It would not be good practice to have some segments with ten observations over ten years and other segments having only two or three observations over ten years. The segments with one observation per

year would have a greater influence on the validation-calibration process than the segments with less than one observation per year.

Step 5: Extract and Evaluate Roadway Segment/Test Section Data

This step is grouped into four activities: (1) extracting and reviewing the performance data, (2) comparing the performance indicator magnitudes to the trigger values, (3) evaluating the distress data to identify anomalies and outliers, and (4) determining the inputs to the MEPDG. First, measured time-history distress data should be made from accelerated pavement testing (APT) or extracted from the agency PMS. The extraction of data from the agency PMS should require a prior step of reviewing PMS database to determine whether the measured values are consistent with the values predicted by the MEPDG. The NCHRP 1-40B project report (AASHTO 2010) demonstrates the conversion procedures of pavement distress measurement units between the PMS and the MEPDG for the flexible pavements PMS database of the Kansas Department of Transportation (KSDOT) and the rigid pavements PMS database of the Missouri Department of Transportation (MODOT). These examples from the NCHRP 1-40B project report (AASHTO 2010) are reproduced below.

For the flexible pavement performance data in KSDOT, the measured cracking values are different, while the rutting and International Roughness Index (IRI) values are similar and assumed to be the same. The cracking values and how they were used in the local calibration process are defined below.

- *Fatigue Cracking.* KSDOT measures fatigue cracking using the number of wheel path feet per 100 foot sample by crack severity but does not distinguish between alligator cracking and longitudinal cracking in the wheel path. In addition, reflection cracks are not distinguished separately from the other cracking distresses. The PMS data were converted to a percentage value similar to what is reported in the highway performance monitoring system (HPMS) from Kansas. In summary, the following equation was used to convert KSDOT cracking measurements to a percentage value that is predicted by the MEPDG:

$$FC = \left(\frac{FCR_1(0.5) + FCR_2(1.0) + FCR_3(1.5) + FCR_4(2.0)}{8.0} \right) \quad \textbf{(A.2)}$$

  All load-related cracks are included in one value. Thus, the MEPDG predictions for load-related cracking were combined into one value by simply adding the length of longitudinal cracks and reflection cracks for hot mix asphalt (HMA) overlays, multiplying by 1.0 ft, dividing that product by the area of the lane, and adding that value to the percentage of alligator cracking predicted by the MEPDG.

- *Transverse Cracking.* Another difference is that KSDOT records thermal or transverse cracks as the number of cracks by severity level. The following equation has been used by KSDOT to convert its measured values to the MEPDG-predicted value of ft/mi:

$$TC = \left(\frac{TCR_o + TCR_1 + TCR_2 + TCR_3}{(10)(12)(52.8)} \right) \quad \textbf{(A.3)}$$

- The value of 10 in the above equation is needed because the data are stored with an implied decimal. The value of 12 ft is the typical lane width, and the value of 52.8 coverts from a 100 foot sample to a per mile basis. Prior to 1999, KSDOT did not record the number or amount of sealed transverse cracking (TCR0). As a result, the amount of transverse cracks sometimes goes to 0.

  For the rigid pavement performance data from MODOT, the measured transverse cracking values are different from the MEPDG values, while the transverse joint faulting and IRI values are similar and assumed to be the same. The transverse cracking values and how they were used in the local calibration process are defined below.

- *Transverse Cracking*. The MEPDG requires the percentage of all portland cement concrete (PCC) slabs with mid-panel fatigue transverse cracking. Both MODOT and the Long-Term Pavement Performance (LTPP) project describe transverse cracking as cracks that are predominantly perpendicular to the pavement slab centerline. Measured cracking is reported in 3 severity levels (low, medium, and high) and is provided in distress maps showing the exact location of all transverse cracking identified during visual distress surveys. Thus, the databases contain, for a given number of slabs within a 500 ft pavement segment, the total number of low, medium, and high severity transverse cracking areas. Because LTPP does not provide details on whether a given slab has multiple cracks, as shown in Figure A.4, a simple computation of the percentage of slabs with this kind of data can be misleading.

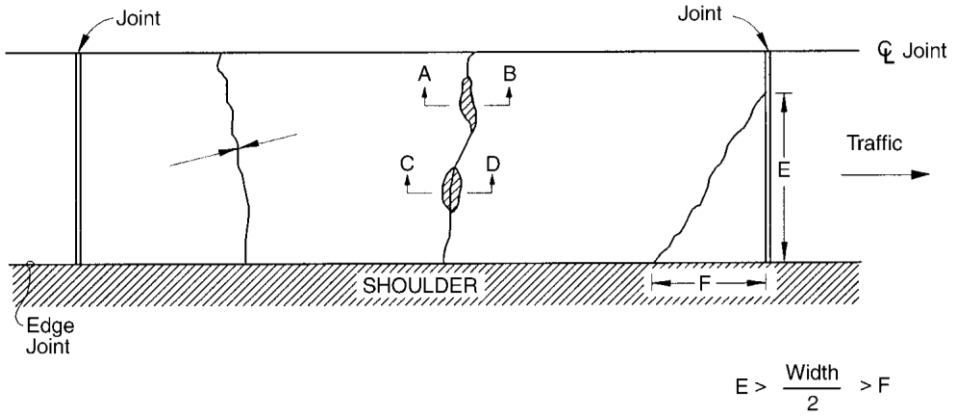

Source: Miller and Bellinger 2003

Figure A.4. LTPP transverse cracking

Therefore, in order to produce an accurate estimate of percent slab cracked, distress maps or videos prepared as part of the distress data collection were reviewed to determine the actual number of slabs with transverse "fatigue" cracking for the 500 ft pavement segments. The total number of slabs was also counted. Percent slabs cracked was defined as follows:

$$Percent\ Slabs\ Cracked = \left(\frac{Number\ of\ cracked\ slabs}{Total\ number\ of\ slabs} \right) \times 100 \quad \textbf{(A.4)}$$

- *Transverse Joint Faulting*. This value is measured and reported by MODOT and LTPP as the difference in elevation to the nearest 1 mm between the pavement surfaces on either side of a transverse joint. The mean joint faulting for all joints within a 500 ft pavement section is reported. This is comparable to the MEPDG predicted faulting value.

- *IRI*. The values included in the MODOT PMS database are comparable to the MEPDG-predicted IRI.

The second activity of Step 5 is to compare the distress magnitudes to the trigger values for each distress. In other words, answer the question, "Does the sampling template include values close to the design criteria or trigger value?" This comparison is important to provide an answer as to whether the collected pavement distress data can be properly utilized to validate and accurately determine the local calibration values. For example, low values of fatigue cracking measurements compared to agency criteria are difficult to validate, and it is difficult to accurately determine the local calibration values or adjustments for predicting the increase in cracking over time.

The distress data for each roadway segment included in the sampling template should be evaluated to ensure that the distress data are reasonable time-history plots. Any zeros that represent non-entry values should be removed from the local validation-calibration database. Distress data that return to zero values within the measurement period may indicate some type of maintenance or rehabilitation activity. Measurements should be taken after structural rehabilitation is removed from the database, or the observation period should end prior to the rehabilitation activity. Distress values that are zero as a result of some maintenance or pavement preservation activity that is a part of the agency's management policy should be removed, but future distress observation values after that activity should be used. If the outliers or anomalies in the data can be explained and are a result of some nontypical condition, they should be removed. If the outlier or anomaly cannot be explained, it should remain in the database.

The MEPDG pavement input database related to each selected roadway segment should be prepared to execute MEPDG software. The existing resources for these input data for Level 3 analyses are agency PMS, traffic database, as-built plans, construction database files, etc. If adequate data for Level 3 are unavailable, the mean value from the specifications is used or the average value determined for the specific input from other projects with similar conditions. The default values of the MEPDG could also be utilized in this case.

Step 6: Conduct Field and Forensic Investigations

Field and forensic investigations could be conducted to check the assumptions and conditions included in the MEPDG for the global (national) calibration effort. These field and forensic investigations include measuring the rutting in the individual layers, determining where the

cracks initiated or the direction of crack propagation, and determining permanent curl/warp, effective temperature, etc. The field and forensic investigations are not necessary if the agency accepts the assumptions and conditions included in the MEPDG.

Step 7: Assess Local Bias from Global Calibration Factors

The MEPDG software is executed using the global calibration values to predict the performance indicators for each roadway segment selected. The null hypothesis is first checked for the entire sampling matrix. The null hypothesis in the equation below is that the average residual error ($e_r = y_{Measured} - x_{predicted}$) or bias is zero for a specified confidence level or level of significance.

$$H_O : \sum_{i=1}^{n} \left(y_{Measured} - x_{Predicted} \right)_i = 0 \qquad \textbf{(A.5)}$$

It is helpful for assessment to make plots of a comparison between the predicted ($x_{predicted}$) and the measured values ($y_{Measured}$) and a comparison between the residual errors (e_r) and the predicted values ($x_{predicted}$) for each performance indicator (see Figure A.5).

Two other model parameters can be also used to evaluate model bias—the intercept (b_o) and slope (m) estimators using the following fitted linear regression model between the measured ($y_{Measured}$) and predicted ($x_{predicted}$) values:

$$\hat{y}_i = b_o + m(x_i) \qquad \textbf{(A.6)}$$

The intercept (b_o) and slope (m) estimators can provide not only the accuracy quantity of each prediction but also the identification of dependent factors such as pavement structure (new construction versus rehabilitation) and HMA mixture type (conventional HMA versus Superpave mixtures) for each prediction. As an illustration, Figure A.5 and Figure A.6 present comparisons of the intercept and slope estimators to the line of equality for the predicted and measured rut depths using the global calibration values.

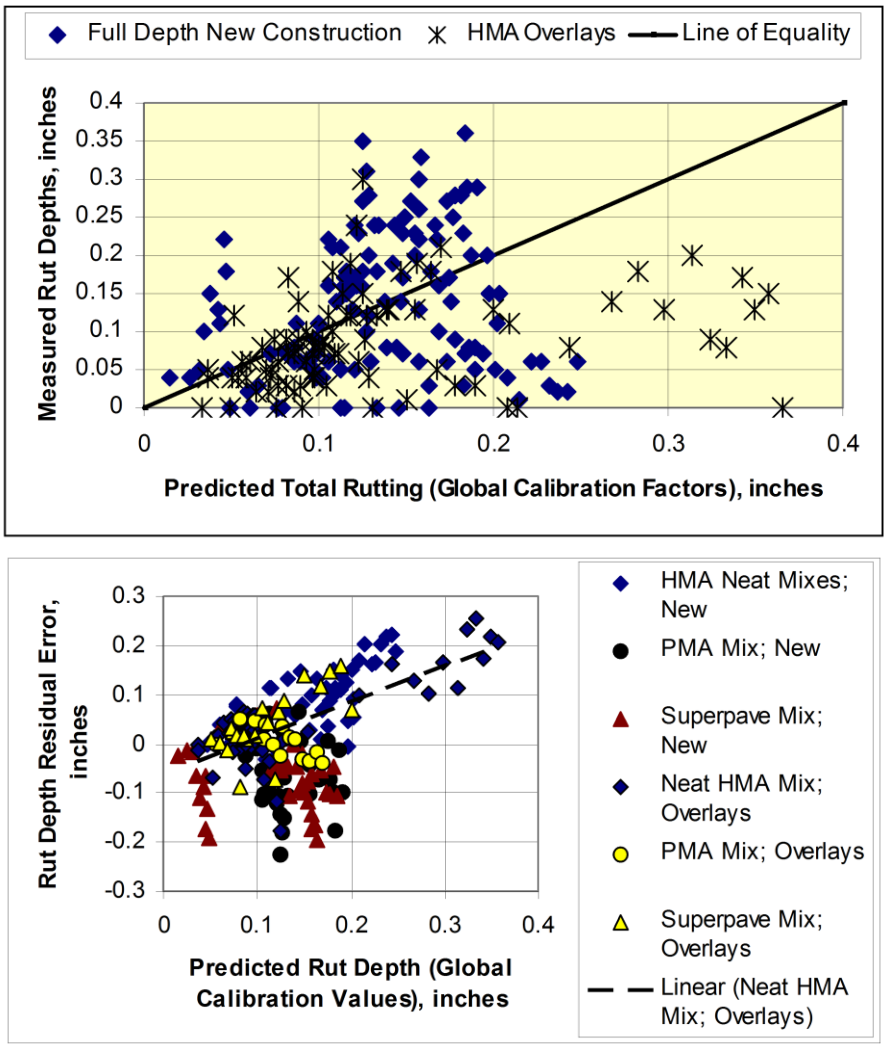

Source: Von Quintus et al. 2009

Figure A.5. Comparison of predicted and measured rut depths using the global calibration values in the KSDOT study

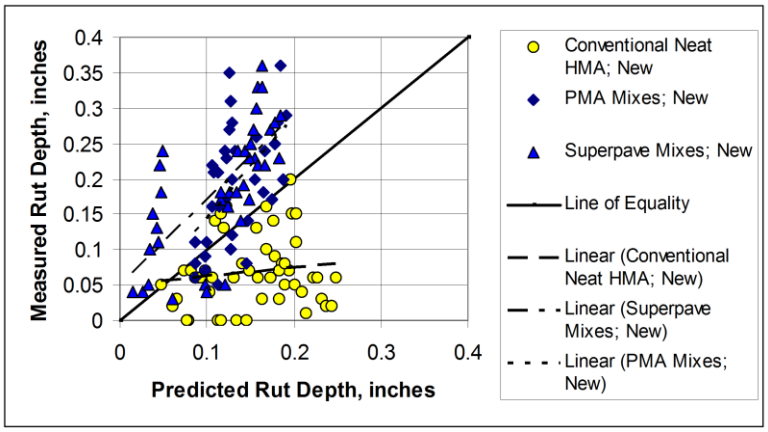

a. Intercept and slope estimators that are dependent on mixture type for the new construction PMS segments.

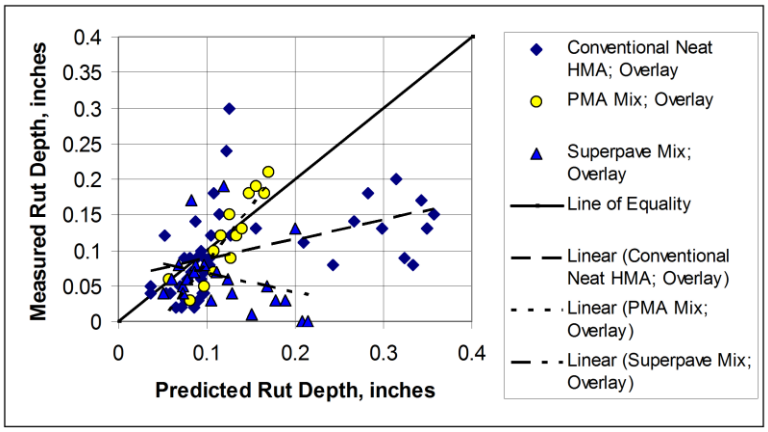

b. Intercept and slope estimators that are dependent on mixture type for the rehabilitation PMS segments.

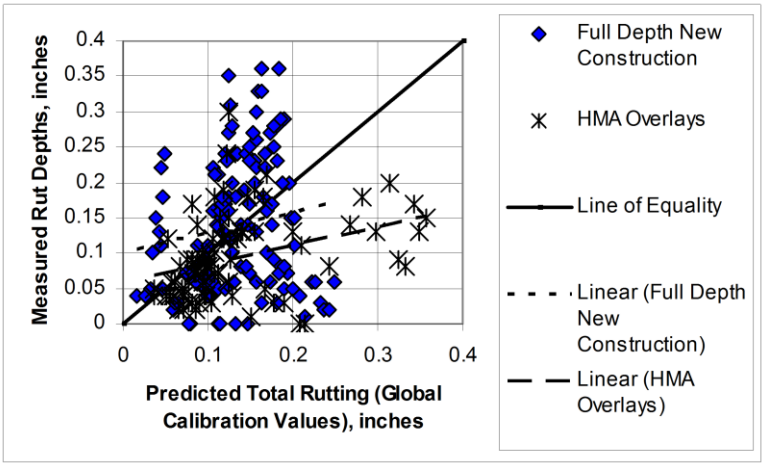

c. Intercept and slope estimators that are structure dependent for the PMS segments.

Source: Von Quintus et al. 2009

Figure A.6. Comparison of the intercept and slope estimators to the line of equality for the predicted and measured rut depths using the global calibration values in the KSDOT study

Step 8: Eliminate Local Bias of Distress Prediction Models

The MEPDG software includes two sets of parameters for the local calibration of most performance indicator transfer functions. One set is defined as agency-specific values, and the other set as local calibration values. Figure A.7 shows a screen shot of the Tools section, where these values can be entered into the software for each performance indicator on a project basis.

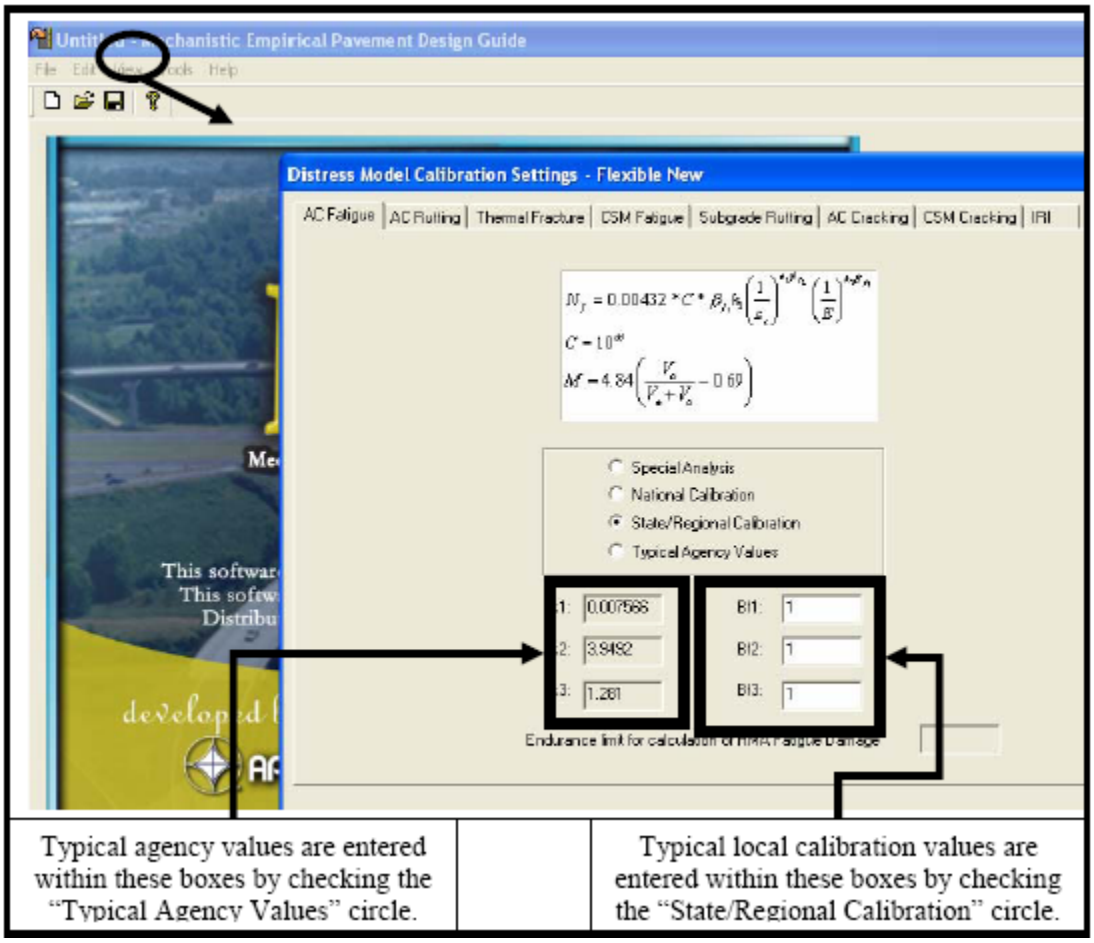

Source: Von Quintus 2008b

Figure A.7. Screen shot of the MEPDG software for local calibration and agency-specific values

The default values of the MEPDG performance indicator transfer functions are global calibration values for agency-specific values (k_1, k_2, and k_3 in Figure A.7) and are given a value of one for local calibration values (β_1, β_2, and β_3 in Figure A.7). These parameters are used to make adjustments to the predicted values so that the difference between the measured and predicted values, defined as the residual error, is minimized. Either one can be used with success. Appendix A presents screen shots of the MEPDG software (Version 1.1) Tools section for all of the performance indicators of rehabilitated HMA pavement and new PCC pavement.

The NCHRP 1-40B project report (AASHTO 2010) lists the coefficients of the MEPDG transfer functions or distress and IRI prediction models that should be considered for revising the predictions to eliminate model bias for flexible pavements and HMA overlays. Table A.1 from the NCHRP 1-40B project report (AASHTO 2010) was prepared to provide guidance in eliminating any local model bias in the predictions. The distress-specific parameters can be dependent on site factors, layer parameters, or the policies of the agency.

Table A.1. Calibration parameters to be adjusted for eliminating bias and reducing the standard error of the flexible pavement transfer functions

(a) HMA pavements

Distress	Eliminate Bias	Reduce Standard Error
Rutting	k_{r1}, β_{s1} or β_{r1}	k_{r2}, k_{r3}, and β_{r2}, β_{r3}
Alligator cracking	C_2 or k_{f1}	k_{f2}, k_{f3}, and C_1
Longitudinal cracking	C_2 or k_{f1}	k_{f2}, k_{f3}, and C_1
Load related cracking – semi-rigid pavements	C_2 or β_{c1}	C_1, C_2, and C_4
Thermal cracking	β_{t3}	β_{t3}
IRI	C_4	C_1, C_2, and C_3

(b) PCC pavements

Distress	Eliminate Bias	Reduce Standard Error
Faulting	C_1	$C_2 - C_8$
JPCP transverse cracking	C_1 or C_4	C_2 and C_5
CRCP fatigue cracking	C_1	C_2
CRCP punchouts	C_3	C_4 and C_5
CRCP crack widths	C_6	C_6
JPCP IRI	C_4	C_1
CRCP IRI	C_4	C_1 and C_2

Source: Von Quintus et al. 2009

The process to eliminate the bias is applied to the globally calibrated pavement performance transfer functions that were found to result in bias in Step 7. The process used to eliminate the bias depends on the cause of that bias and the accuracy desired by the agency. The NCHRP 1-40B project report (AASHTO 2010) addresses three possible sources of bias and the bias elimination procedures corresponding to each possibility and is reproduced below.

1. The residual errors are, for the most part, always positive or negative with a low standard error of the estimate in comparison to the trigger value, and the slope of the residual errors versus predicted values is relatively constant and close to zero. In other words, the precision of the prediction model is reasonable, but the accuracy is poor. In this case, the local calibration coefficient is used to reduce the bias. This condition generally requires the least level of effort and the fewest number of runs or iterations of the MEPDG while varying the local calibration values to reduce the bias. The statistical assessment described in Step 7 should be conducted on the locally calibrated pavement performance to check the obtaining agency's acceptable bias.

2. The bias is low and relatively constant with time or with the number of loading cycles, but the residual errors have a wide dispersion varying from positive to negative values. In other words, the accuracy of the prediction model is reasonable, but the precision is poor. In this case, the coefficient of the prediction equation is used to reduce the bias, but the value of the local calibration coefficient is probably dependent on some site feature, material property, and/or design feature included in the sampling template. This condition generally requires more runs and a higher level of effort to reduce dispersion of the residual errors. The statistical assessment described in Step 7 should be conducted on the locally calibrated pavement performance to check the obtaining agency's acceptable bias.

3. The residual errors versus the predicted values exhibit a significant and variable slope that is dependent on the predicted value. In other words, the precision of the prediction model is poor, and the accuracy is dependent on time or the number of loading cycles—there is poor correlation between the predicted and measured values. This condition is the most difficult to evaluate because the exponent of the number of loading cycles needs to be considered. This condition also requires the highest level of effort and many more MEPDG runs while varying the local calibration values to reduce bias and dispersion. The statistical assessment described in Step 7 should be conducted on the local calibrated pavement performance to check the obtaining agency's acceptable bias.

Step 9: Assess Standard Error of the Estimate

After the bias has been reduced or eliminated for each of the transfer functions, the standard error of the estimate (SEE) from the local calibration is evaluated in comparison to the SEE from the global calibration. The SEE for each globally calibrated transfer function is included under the Tools section of the MEPDG software. Figure A.8 illustrates the comparison of the SEE for the globally calibrated transfer functions and the SEE for the locally calibrated transfer functions.

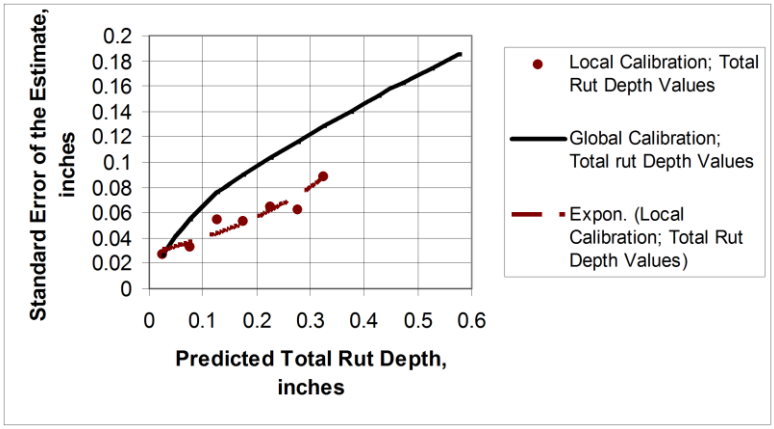

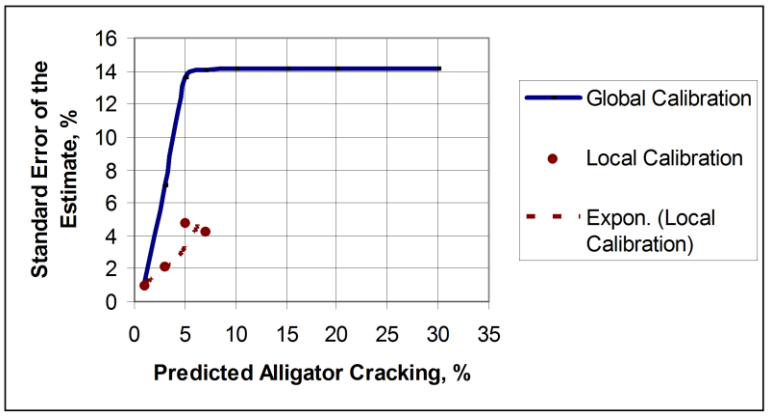

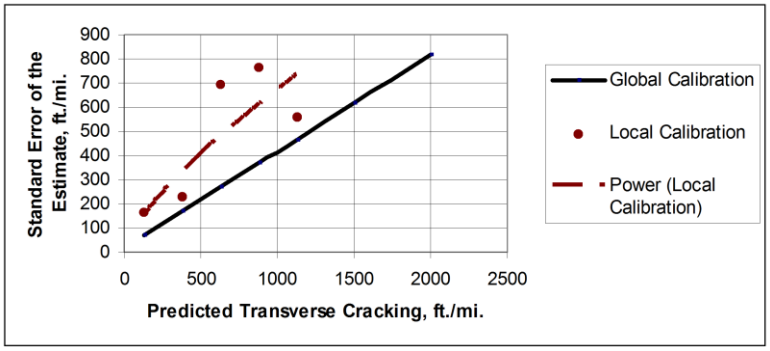

Source: Von Quintus et al. 2009

Figure A.8. Comparison of the standard error of the estimate for the globally calibrated and locally calibrated transfer function in the KSDOT study

Step 10: Reduce Standard Error of the Estimate

If the SEE from the local calibration is found in Step 9 to be statistically different in comparison to the SEE included in the MEPDG for each performance indicator, a statistical analysis of variance (ANOVA) can be conducted to determine if the residual error or bias is dependent on some other parameter or material/layer property for the selected roadway segments. If no correlation can be identified, the local calibration factors determined from Step 8 and the SEE

values obtained from Step 9 can be considered as the final products for the selected roadway segments. If some correlation to some parameters (for example, HMA mixture volumetric properties) can be identified, the local calibration values should be determined for each type of correlated parameter, or a new calibration function should be developed. NCHRP Project 1-40B and Von Quintus (2008b) documents HMA mixture–specific factors used to modify or adjust the MEPDG global calibration factors for the rut depth and the bottom-up cracking transfer functions where sufficient data are available.

Step 11: Interpretation of Results and Deciding on Adequacy of Calibration Factors

The purpose of this step is to decide whether to adopt the local calibration values or continue to use the global values that were based on the data included in the LTPP program from around the US. To make that decision, an agency should identify major differences between the LTPP projects and the standard practice of the agency in specifying, constructing, and maintaining its roadway network. More importantly, the agency should determine whether the local calibration values can explain those differences. The agency should evaluate any change from unity for the local calibration parameters to ensure that the change provides engineering reasonableness.

NCHRP Synthesis 457 was issued in 2014 (Pierce and McGovern 2014) to document strategies for facilitating the implementation of the MEPDG (and accompanying AASHTOWare Pavement ME Design software) and the reasons why some state highway agencies (SHAs) had not yet implemented the MEPDG. This document is a product of surveys and follow-up questions with highway transportation agencies (US SHAs, Puerto Rico, the District of Columbia, and Canadian provincial and territorial governments). In total, 57 agencies (48 U.S. [92%] and 9 Canadian [69%]) provided responses to the agency survey. Among the 57 responding agencies, full implementation of the MEPDG was conducted by 3 agencies, 46 indicated that they are in the process of implementation, and the remaining 8 indicated that they have no plans at this time for implementing the MEPDG. The agencies were also requested to provide information about the pavement types they use.

New construction pavement types used by the responding agencies included thick asphalt pavement (46 agencies), jointed plain concrete pavement (JPCP) (44 agencies), thin asphalt pavement (41 agencies), and semi-rigid pavement (29 agencies). Agencies also indicated designing full-depth asphalt pavements (21 agencies) and composite pavements (18 agencies), while 9 agencies reported designing continuously reinforced concrete pavement (CRCP).

Responding agencies were also asked to provide information about the pavement design methods they use. Table A.2 lists agencies' pavement design methods.

Table A.2. Agency use of pavement design methods

Method	New Construction		Rehabilitation		Number of Agencies
	Asphalt	Concrete	Asphalt	Concrete	
AASHTO 1972	7	2	5	1	7
AASHTO 1986	1	0	2	0	2
AASHTO 1993	35	23	31	19	39
AASHTO 1998 Supplement	4	11	4	8	13
AASHTO *MEPDG*[1]	12	10	10	7	13
Agency Empirical Procedure	7	1	9	3	13
WINPAS (ACPA 2012)	0	5	0	4	7
MS-1 (AI 1999)	1	0	3	0	3
ME-based Design Table or Catalog	1	3	0	2	3
Other ME Procedure	8	3	6	2	11
Other	5	7	7	8	14

[1]A number of agencies indicated that the *MEPDG* is currently being used or under evaluation; however, only three agencies indicated that the *MEPDG* has been implemented.

Source: Pierce and McGovern 2014

Table A.3 presents a summary of agency responses about MEPDG use or planned use by pavement type.

Table A.3. Summary of MEPDG use or planned use by pavement type

Pavement Type	Number of Responses
New asphalt pavement	45
New JPCP	39
Asphalt overlay of existing asphalt pavement	38
Asphalt overlay of existing JPCP	34
Asphalt overlay of existing fractured JPCP	27
Unbonded JPCP overlay of existing JPCP	22
JPCP overlay of existing asphalt pavement	21
Asphalt overlay of existing CRCP	15
Bonded overlay of existing JPCP	13
New CRCP	12
Asphalt overlay of existing fractured CRCP	11
Unbonded JPCP overlay of existing CRCP	11
CRCP overlay of existing flexible pavement	7
Unbonded CRCP overlay of existing JPCP	7
Bonded concrete overlay of existing CRCP	6
Unbonded CRCP overlay of existing CRCP	6

Source: Pierce and McGovern 2014

The agencies were also asked about their local calibration efforts. Table A.4 and Table A.5 list local calibration coefficients for agencies that conducted local calibration for concrete and asphalt pavements at the time of the survey.

Table A.4. Agency local calibration coefficients - concrete

Feature	*MEPDG*	Arizona	Colorado	Florida	Missouri
Cracking					
C1	2.0	2.0	2.0	2.8389	2.0
C2	1.22	1.22	1.22	0.9647	1.22
C4	1.0	0.19	0.6	0.5640	1.0
C5	–1.98	–2.067	–2.05	–0.5946	–1.98
Std. Dev.	[1]	[4]	[7]	[1]	[1]
Faulting					
C1	1.0184	0.0355	0.5104	4.0472	1.0184
C2	0.91656	0.1147	0.00838	0.91656	0.91656
C3	0.002848	0.00436	0.00147	0.002848	0.002848
C4	0.000883739	1.1E-07	0.008345	0.000883739	0.000883739
C5	250	20000	5999	250	250
C6	0.4	2.309	0.8404	0.0790	0.4
C7	1.8331	0.189	5.9293	1.8331	1.8331
C8	400	400	[8]	400	400
Std. Dev.	[2]	[5]		[2]	[2]
Punchout					
C1	2.0	2.0			2.0
C2	1.22	1.22			1.22
C3	216.8421	85	Not applicable	Not applicable	216.8421
C4	33.15789	1.4149			33.15789
C5	–0.58947	–0.8061			–0.58947
Crack	[1]	[1]			[1]
Std. Dev.	[3]	[6]			[3]
IRI (CRCP)					
C1	3.15	3.15	Not applicable	Not applicable	3.15
C2	28.35	28.35			28.35
Std. Dev.	5.4	5.4			5.4
IRI (JPCP)					
J1	0.8203	0.6	0.8203	0.8203	0.82
J2	0.4417	3.48	0.4417	0.4417	1.17
J3	1.4929	1.22	1.4929	2.2555	1.43
J4	25.24	45.2	25.24	25.24	66.8
Std. Dev.	5.4	5.4	5.4	5.4	5.4

[1] Pow(5.3116 x CRACK,0.3903) + 2.99
[2] Pow(0.0097 x FAULT,0.05178) + 0.014
[3] 2 + 2.2593 x Pow(0.4882 x PO)
[4] Pow(9.87x CRACK,0.4012) + 0.5
[5] Pow(0.037 x FAULT,0.6532) + 0.001
[6] 1.5 + 2.9622 x Pow(PO,0.4356)
[7] Pow(57.08 x CRACK, 0.33) + 1.5
[8] 0.0831 x Pow(FAULT,0.3426) + 0.00521
[9] 0.1 for A-7-6 soils
[10] 0.001 for A-7-6 soils
[11] 3 for A-7-6 soils

Source: Pierce and McGovern 2014

Table A.5. Agency local calibration coefficients - asphalt

Feature	*MEPDG*	Arizona	Colorado	Missouri	Oregon
Cracking					
C1 Bottom	1.0	1.0	0.07	1.0	0.56
C1 Top	7.0	7.0	7.0	7.0	1.453
C2 Bottom	1.0	4.5	2.35	1.0	0.225
C2 Top	3.5	3.5	3.5	3.5	0.097
C3 Bottom	6000	6000	6000	6000	6000
C3 Top	0	0	0	0	0
C4 Top	1000	1000	1000	1000	1000
Std. Dev. Top	[1]	[1]	[1]	[1]	[1]
Std. Dev. Bottom	[2]	[2]	[12]	[2]	[2]
Fatigue					
BF1	1	249.00872	130.3674	1	1
BF2	1	1	1	1	1
BF3	1	1.23341	1.2178	1	1
Thermal Fracture					
Level 1	1.5	1.5	7.5	0.625	1.5
Level 2	0.5	0.5	0.5	0.5	0.5
Level 3	1.5	1.5	1.5	1.5	1.5
Std. Dev. (Level 1)	[3]	[3]	[3]	[3]	[3]
Std. Dev. (Level 2)	[4]	[4]	[4]	[4]	[4]
Std. Dev. (Level 3)	[5]	[5]	[5]	[5]	[5]
Rutting (asphalt)					
BR1	1.0	0.69	1.34[13]		1.48
BR2	1.0	1.0	1.0		1.0
BR3	1.0	1.0	1.0		0.9
Std. Dev.	[6]	[9]	[14]	[6]	[6]
Rutting (subgrade)					
BS1 (fine)	1.0	0.37	0.84	0.4375	1.0
Std. Dev. (fine)	[7]	[10]	[15]	[7]	[7]
BS1 (granular)	1.0	0.14	0.4	0.01	1.0
Std. Dev. (granular)	[8]	[11]	[16]	[8]	[8]
IRI					
C1 (asphalt)	40	1.2281	35	17.7	40
C2 (asphalt)	0.4	0.1175	0.3	0.975	0.4
C3 (asphalt)	0.008	0.008	0.02	0.008	0.008
C4 (asphalt)	0.015	0.028	0.019	0.01	0.015
C1 (over concrete)	40.8	40.8	40.8	40.8	40.8
C2 (over concrete)	0.575	0.575	0.575	0.575	0.575
C3 (over concrete)	0.0014	0.0014	0.0014	0.0014	0.0014
C4 (over concrete)	0.00825	0.00825	0.00825	0.00825	0.00825

[1] $200 + 2300/(1 + \exp(1.072 - 2.1654 \times LOG_{10}(TOP + 0.0001)))$
[2] $1.13 + 13/(1 = \exp(7.57 - 15.5 \times LOG_{10}(BOTTOM + 0.0001)))$
[3] 0.1468 x THERMAL + 65.027
[4] 0.2841 x THERMAL + 55.462
[5] 0.3972 x THERMAL + 20.422
[6] 0.24 x Pow(RUT, 0.8026) + 0.001
[7] 0.1235 x Pow(SUBRUT, 0.5012) + 0.001
[8] 0.1447 x Pow(BASERUT, 0.6711) + 0.001
[9] 0.0999 x Pow(RUT, 0.174)+0.001
[10] 0.05 x Pow(SUBRUT, 0.085) + 0.001
[11] 0.05 x Pow(BASERUT, 0.115) + 0.00110
[12] $1 + 15(1 + \exp(-1.6673 - 2.4656*LOG10(BOTTOM+0.0001)))$
[13] Under review
[14] 0.2052 x Pow(RUT,0.4) + 0.001
[15] 0.1822 x Pow(SUBRUT, 0.5) +0.001
[16] 0.2472 x Pow(BASERUT, 0.67) + 0.001
[17] 0.01 for A-7-6 soil

Source: Pierce and McGovern 2014

FHWA Projects

Two research studies supported by the FHWA have been conducted to use PMIS data for local calibration of the MEPDG. One is "Using Pavement Management Data to Calibrate and Validate the New MEPDG, An Eight State Study" (Hudson et al. 2006a, Hudson et al. 2006b). This study evaluated the potential use of PMIS on MEPDG calibrations from eight participating states: Florida, Kansas, Minnesota, Mississippi, New Mexico, North Carolina, Pennsylvania, and Washington. The study concluded that all the participating states could feasibly use PMIS data for MEPDG calibrations and that other states not participating in this study could also do so. It is recommended by the study that each SHA should develop a satellite pavement management/pavement design database for each project being designed and constructed using the MEPDG as part of the current PMIS used.

Following the previous study, "Local calibration of the MEPDG Using Pavement Management Systems" (APTech, Inc. 2010) was conducted to develop a framework for using existing PMIS data to calibrate the MEPDG performance model. One state (North Carolina) was selected based on screening criteria to finalize and verify the MEPDG calibration framework based on the set of actual conditions. In developing the framework, local calibration of the selected state was demonstrated under the assumptions of both the MEPDG performance predictions established in NCHRP 1-37 A and the distress measurements from the selected state. Note that the North Carolina DOT used subjective distress severity ratings in accordance with the state DOT manual rather than the LTPP manual. Table A.6 listed the assumptions used for MEPDG local calibration in this study.

Table A.6. List of assumptions in the local calibration of the MEPDG for North Carolina under FHWA HIF-11-026

Type	Performance Predictions[1]	Assumptions
HMA	Rutting	• Rutting measurement was assumed to progress from zero to the assumed numeric value over the life of the pavement in order to convert NCDOT subjective rut rating into an estimated measured value. ✓ Low severity – 0.5 in. (12.7 mm) ✓ Moderate severity – 1.0 in. ✓ High severity – Not applicable • Rut depth progression was based on the number of NCDOT rut depth ratings and distributed over the measurement period to best reflect the slope of the MEPDG predicted rut depth over time. • For HMA overlay, the rut condition prior to the applied overlay was selected.
	Alligator Cracking	• A sigmoid function form of MEPDG alligator cracking is the best representation of the relationship between cracking and damage. The relationship must be "bounded" by 0 ft^2 cracking as a minimum and 6,000 ft^2 cracking as a maximum[2]. • Alligator cracking is to 50 percent cracking of the total area of the lane (6000 ft^2) at a damage percentage of 100 percent[2]. • Since alligator cracking is related to loading and asphalt layer thickness, alligator crack prediction is similar for a wide range of temperatures[2]. • All load-related cracking was considered to initiate from the bottom up (alligator cracking). • The alligator cracking measurement was estimated from tensile strains at the bottom of the asphalt layer calculated from a layer elastic analysis program by inputting MEPDG asphalt dynamic modulus corresponding to the NCDOT measured alligator distress rating. • The estimated alligator cracking measurement was distributed over the age of the pavement section.
	Thermal Cracking	• The model will not predict thermal cracking on more than 50 percent of the total section length[2]. • The maximum length of thermal cracking is 4224 ft/mi (400 ft/500 ft × 5280 ft/mi) [2]. • Cracks were assumed to be full-lane width (i.e., 12 ft) for all severity levels. • For each pavement section, the section length was divided by the reported NCDOT cracking frequency and multiplied by the crack length (assumed to be 12 ft) to obtain the total estimated crack length per pavement section. • As with rutting and alligator cracking, the distress severity from the last NCDOT survey was used to calculate the thermal cracking numeric value.
JPCP	Transverse Cracking	• JPCP in NCDOT was assumed to be designed on average perform to the selected design criteria (15 percent slab cracking) at the specified reliability (90 percent). • The layer properties for these design runs were selected primarily as default values, as were most of the traffic characteristics.
	Faulting	• The layer properties for these design runs were selected primarily as default values, as were most of the traffic characteristics.

[1]Longitudinal cracking, reflection cracking, and smoothness were not considered in the calibration due to a lack of data and the deficiency of the model.
[2] These assumptions are made from MEPDG performance models in NCHRP 1-37A.
Source: APTech, Inc. 2010

MEPDG/AASHTOWare Pavement ME Design Local Calibration Studies at the State Level

In addition to national-level projects, multiple state-level research efforts have been conducted to locally calibrate the MEPDG using each step described in NCHRP 1-40B. However, few research studies regarding MEPDG validation for local pavement sections have been finalized

because the MEPDG has constantly been updated through NCHRP projects (Brown et al. 2006, Darter et al. 2006) after the release of the initial MEPDG software (Version 0.7). This section summarizes up-to-date MEPDG local calibration research efforts at the state level.

Flexible Pavements

A study by Galal and Chehab (2005) in Indiana compared the distress measures of existing HMA overlays over rubblized PCC slab sections obtained using the AASHTO 1993 design guide with the MEPDG (Version 0.7) performance prediction results using the same design inputs. The results indicated that the MEPDG provides a good estimation of the distress measures, except for top-down cracking. The authors emphasized the importance of locally calibrating the performance prediction models.

The Montana DOT conducted a local calibration study of the MEPDG for flexible pavements (Von Quintus and Moulthrop 2007). In this study, the results from the NCHRP 1-40B (Von Quintus et al. 2005) verification runs were used to determine any bias and standard error, and the results were compared to the standard error reported from the original calibration process that was completed under NCHRP Project 1-37A (ARA, Inc. 2004). Bias was found for most of the distress transfer functions. National calibration coefficients included in version 0.9 of the MEPDG were used initially to predict the distresses and smoothness of the Montana calibration refinement test sections to determine any prediction model bias. These runs were considered a part of the validation process, similar to the process used under NCHRP Projects 9-30 and 1-40B.The findings from this study are summarized for each performance model below:

- Rutting prediction model: The MEPDG overpredicted total rut depth because significant rutting was predicted in unbound layers and embankment soils.
- Alligator cracking prediction model: The MEPDG fatigue cracking model was found to be reasonable.
- Longitudinal cracking prediction model: No consistent trend in the predictions could be identified to reduce the bias and standard error and improve the accuracy of this prediction model. It is believed that there is a significant lack-of-fit modeling error for the occurrence of longitudinal cracks.
- Thermal cracking prediction model: The MEPDG prediction model with the local calibration factor was found to be acceptable for predicting transverse cracks in HMA pavements and overlays in Montana.
- Smoothness prediction model: The MEPDG prediction equations are recommended for use in Montana because there are too few test sections with higher levels of distress in Montana and adjacent states to accurately revise this regression equation.

Von Quintus (2008b) summarized the flexible pavement local calibration results for the MEPDG from NCHRP Projects 9-30 and 1-40 B and the Montana DOT studies listed in Table A. These results, originally from Von Quintus (2008b), are presented in Table A.7 to Table A.10 for the rut depth, fatigue cracking, and thermal cracking transfer functions. These could be useful reference for states with similar conditions at the studied sites. Detailed information about the studied sites is described in Von Quintus (2008b).

Table A.7. Listing of local validation-calibration projects

Project Identification	Transfer Functions Included in the Local Validation and/or Calibration Efforts for Each Project				
	Rut Depths	Area Cracking	Longitudinal Cracking	Thermal Cracking	Smoothness or IRI
NCHRP Projects 9-30 & 1-40B; *Local Calibration Adjustments for HMA Distress Prediction Models in MEPDG Software*, (Von Quintus, et al., 2005a & b)	√	√	√		
Montana DOT, *MEPDG Flexible Pavement Performance Prediction Models for Montana*, (Von Quintus & Moulthrop, 2007a & b)	√	√	√	√	√
NCHRP Project 1-40B, *Examples Using Recommended Practice for Local Calibration of MEPDG Software*, Kansas Pavement Management Data, (Von Quintus, et al., 2008b)	√	√		√	√
NCHRP Project 1-40B, *Examples Using Recommended Practice for Local Calibration of MEPDG Software*, LTPP SPS-1 and SPS-5 Projects, (Von Quintus, et al., 2008b)	√	√		√	√

Source: Von Quintus 2008b

Table A.8. Summary of local calibration values for the rut depth transfer function

Project Identification		Unbound Materials/Soils, β_{s1}		HMA Calibration Values		
		Fine-Grained	Coarse-Grained	β_{r1}	β_{r3}	β_{r2}
NCHRP Projects 9-30 & 1-40B; Verification Studies, Version 0.900 of the MEPDG.		0.30	0.30	Values dependent on volumetric properties of HMA; the values below represent the overall range.		
		Insufficient information to determine effect of varying soil types.		6.9 to 10.8	0.65 to 0.90	0.90 to 1.10
Montana DOT; Based on version 0.900 of the MEPDG		0.30	0.30	Values dependent on the volumetric properties of HMA; the values below represent overall averages.		
				7.0	0.70	1.13
Kansas DOT; PM Segments; HMA Overlay Projects; All Mixtures (Version 1.0)		0.50	0.50	1.5	0.95	1.00
Kansas PM Segments; New Construction	Convent.	0.50	0.50	1.5	0.90	1.00
	Superpave			1.5	1.20	1.00
	PMA			2.5	1.15	1.00
LTPP SPS-1 & SPS-5 Projects built in accordance with specification; conventional HMA mixtures (Version 1.0).		0.50	0.50	Value dependent on the air void & asphalt content		1.00
				1.25 to 1.60	0.90 to 1.15	1.00
LTPP SPS-1 Projects with anomalies or construction difficulties, unbound layers.		Values dependent on density and moisture content; values below represent the range found.		---	---	---
		0.50 to 1.25	0.50 to 3.0			

Source: Von Quintus 2008b

Table A.9. Summary of local calibration values for the area fatigue cracking transfer function

Project Identification		β_{f1}	β_{f2}	β_{f3}	C_2
NCHRP Projects 9-30 & 1-40B; Verification Studies, Version 0.900 of the MEPDG		Values dependent on the volumetric properties.			
		0.75 to 10.0	1.00	0.70 to 1.35	1.0 to 3.0
Montana DOT; Based on version 0.900 of the MEPDG, with pavement preservation treatments		Values dependent on the volumetric properties.			
		13.21	1.00	1.25	1.00
Northwest Sites; Located in States Adjacent to Montana, without pavement preservation treatments		Values dependent on the volumetric properties.			
		1.0 to 5.0	1.00	1.00	1.0 to 3.0
Kansas DOT; PM Segments; HMA Overlay Projects; All HMA Mixtures		0.05	1.00	1.00	1.00
Kansas DOT; PM Segments; New Construction	Conventional HMA Mixes	0.05	1.00	1.00	1.00
	PMA	0.005	1.00	1.00	1.00
	Superpave	0.0005	1.00	1.00	1.00
Mid-West Sites	LTPP SPS-1 Projects built in accordance with specifications	0.005	1.00	1.00	1.00
	LTPP SPS-1 Projects with anomalies or production difficulties	1.00	1.00	1.00	1.0 to 4.0
	LTPP SPS-5 Projects; Debonding between HMA Overlay and Existing Surface	0.005	1.00	1.00	1.0 to 4.0

Source: Von Quintus 2008b

Table A.10. Summary of the local calibration values for the thermal cracking transfer function

Project Identification		β_{t1}	β_{t2}	β_{t3}
Montana DOT; application of pavement preservation treatments.		---	---	0.25
Northwest Sites, located in states adjacent to Montana, but without pavement preservation treatments; appears to be agency dependent.		---	---	1.0 to 5.0
Kansas PM Segments; Full-Depth Projects	PMA	---	---	2.0
	Conventional	---	---	2.0
	Superpave	---	---	3.5
Kansas PMS Segments; HMA Overlay Projects	PMA	---	---	2.0
	Conventional	---	---	7.5
	Superpave	---	---	7.5
LTPP Projects; HMA produced in accordance with specifications	Conventional	---	---	Dependent on Asphalt Content & Air Voids
LTPP Projects; Severely aged asphalt	Conventional	---	---	7.5 to 20.0

Source: Von Quintus 2008b

Kang et al. (2007) prepared a regional pavement performance database for a Midwest implementation of the MEPDG. The authors collected input data required by the MEPDG as well as measured fatigue cracking data for flexible and rigid pavements from state transportation agencies in Michigan, Ohio, Iowa, and Wisconsin. They reported that gathering the data was labor-intensive because the data resided in various and incongruent data sets. Furthermore, some pavement performance observations included temporary effects of maintenance, and those observations needed to be removed through a tedious data cleaning process. Due to the lack of reliability in the collected pavement data, the calibration factors were evaluated based on Wisconsin data, and the distresses predicted by the national calibration factors were compared to the field-collected distresses for each state except Iowa. This study concluded that the default national calibration values do not predict the distresses observed in the Midwest. The collection of more reliable pavement data is recommended for a future study.

Schram and Abdelrahman (2006) attempted to calibrate two MEPDG IRI models for JPCP and HMA overlays of rigid pavements at the local project level using Nebraska Department of Roads (NDOR) pavement management data. The focused dataset was categorized by annual daily truck traffic (ADTT) and surface layer thickness. Three categories of ADTT were considered: low (0–200 trucks/day), medium (201–500 trucks/day), and high (over 500 trucks/day). The surface layer thicknesses that were considered ranged from 6 to 14 inches for JPCP and 0 to 8 inches for HMA layers. The results showed that project-level calibrations reduced the default model prediction error by nearly twice that of network-level calibrations. Table A.11 and Table A.12, as reported in this study, contain coefficients for the smoothness model of HMA overlays of rigid pavements and JPCP.

Table A.11. IRI calibration coefficients of HMA overlaid rigid pavements for surface layer thickness within ADTT

ADTT	Thickness	*C*1	*C*2	*C*3	*N*	R^2	SEE (m/km)
Low	2″–3″	0.1318	0.0018	0.3971	3	0.994	0.02
	4″–5″	0.0704	−0.0048	−2.8771	16	0.813	0.11
	5″–6″	−0.0038	0.2409	−4.6360	5	0.039	1.15
Medium	2″–3″	0.0639	0.1337	−0.7896	21	0.612	0.5
	3″–4″	0.0733	0.0282	1.4725	65	0.532	0.36
	4″–5″	0.0781	−0.0032	1.1116	82	0.546	0.31
	5″–6″	0.0649	0.0169	3.5543	84	0.535	0.31
	6″–7″	0.0794	−0.0312	4.3652	31	0.888	0.17
	7″–8″	0.0674	−0.0164	1.7122	19	0.674	0.13
	8″–9″	0.0683	0.0192	−3.6231	13	0.936	0.1
High	0″–1″	0.2019	0.1158	−10.0646	27	0.392	0.45
	2″–3″	0.1866	0.0498	−16.7082	19	0.565	0.6
	3″–4″	0.1835	−0.0579	8.1863	32	0.010	0.9
	4″–5″	0.1170	−0.0100	1.4057	101	0.299	0.51
	5″–6″	0.2422	0.0371	−23.4448	62	0.713	0.85
	6″–7″	0.0756	0.0127	0.9250	64	0.597	0.22
	7″–8″	0.0604	0.0574	−2.4936	7	0.624	0.2
	8″–9″	0.0578	0.0706	−10.9179	28	0.103	0.25
	9″–10″	0.1005	−0.0001	−0.5216	8	0.845	0.13

Source: Schram and Abdelrahman 2006

Table A.12. IRI calibration coefficients of JPCP for surface layer thickness within ADTT

ADTT	Thickness	*C*1	*C*2	*C*3	*C*4	*N*	R^2	SEE (in./mi)
Low	6″–7″	0.0000	0.0000	1.0621	74.8461	33	0.434	26.885
	7″–8″	0.0000	0.0000	1.9923	46.9256	37	0.961	8.235
	8″–9″	0.8274	0.0000	0.0000	86.9721	39	0.904	14.465
	9″–10″	0.3458	0.0000	1.5983	64.3453	110	0.537	26.230
	10″–11″	0.0300	0.0000	3.4462	10.7893	37	0.893	17.280
	11″–12″	—	—	—	—	—	—	—
	12″–13″	—	—	—	—	—	—	—
	13″–14″	—	—	—	—	—	—	—
	14″–15″	—	—	—	—	—	—	—
Medium	6″–7″	0.0000	0.0000	4.1422	0.0000	3	0.966	5.094
	7″–8″	0.0000	1.5628	0.0000	71.9009	22	0.968	9.952
	8″–9″	0.0000	0.0000	1.7162	53.0179	122	0.291	40.537
	9″–10″	0.1910	0.0000	0.9644	89.3990	609	0.686	24.945
	10″–11″	0.0000	0.0000	2.0945	73.1246	314	0.812	18.535
	11″–12″	0.0000	0.0090	1.3617	100.0000	27	0.792	10.166
	12″–13″	—	—	—	—	—	—	—
	13″–14″	0.0000	0.0100	2.2226	24.9354	4	0.924	3.948
	14″–15″	—	—	—	—	—	—	—
High	6″–7″	—	—	—	—	—	—	—
	7″–8″	—	—	—	—	—	—	—
	8″–9″	0.0000	0.1376	0.4352	79.5526	46	0.151	48.576
	9″–10″	0.1561	0.0000	1.1024	62.9556	81	0.333	31.255
	10″–11″	0.0000	0.0000	1.6344	100.0000	228	0.653	22.295
	11″–12″	0.1125	1.8207	1.1678	100.0000	29	0.739	13.366
	12″–13″	0.0000	0.0000	1.5331	100.0000	151	0.719	17.724
	13″–14″	0.0100	0.0100	0.5184	0.0000	4	0.623	1.728
	14″–15″	0.1904	0.0000	2.1387	51.4053	146	0.838	9.018

Source: Schram and Abdelrahman 2006

Muthadi and Kim (2008) calibrated the MEPDG for flexible pavements located in North Carolina using version 1.0 of the MEPDG software. Two distress models, rutting and alligator cracking, were used for this effort. A total of 53 pavement sections were selected from the LTPP program and the North Carolina (NCDOT) databases for the calibration and validation process. Based on the calibration procedures suggested by NCHRP 1-40B, a flowchart was made for this study. The verification results of the MEPDG performance models with national calibration factors showed bias (systematic difference) between the measured and predicted distress values. The Microsoft Excel Solver program was used to minimize the sum of the squared errors (SSE) of the measured and the predicted rutting or cracking by varying the coefficient parameters of the transfer function. Table A.13 lists local calibration factors for the rutting and alligator cracking transfer functions obtained in this study. This study concluded that the standard error for the rutting model and the alligator cracking model is significantly lower after the calibration.

Table A.13. North Carolina local calibration factors for the rutting and alligator cracking transfer functions

Recalibration	Calibration Coefficient	National Calibration	National Recalibration	Local Calibration
Rutting				
AC	k_1	−3.4488	−3.35412	−3.41273
	k_2	1.5606	1.5606	1.5606
	k_3	0.479244	0.479244	0.479244
GB	β_{GB}	1.673	2.03	1.5803
SG	β_{SG}	1.35	1.67	1.10491
Fatigue				
AC	k_1	0.00432	0.007566	0.007566
	k_2	3.9492	3.9492	3.9492
	k_3	1.281	1.281	1.281
	C_1	1	1	0.437199
	C_2	1	1	0.150494

Source: Muthadi and Kim 2008

The Washington State DOT (Li et al. 2009) developed procedures to calibrate the MEPDG (version 1.0) flexible pavement performance models using data obtained from the Washington State Pavement Management System (WSPMS). Calibration efforts were concentrated on the asphalt mixture fatigue damage, longitudinal cracking, alligator cracking, and rutting models. Thirteen calibration factors were to be considered in the four related models. An elasticity analysis was conducted to describe the effects of these calibration factors on the pavement distress models (i.e., the higher the absolute value of elasticity, the greater impact the factor has on the model). The calibration results of typical Washington State flexible pavement systems determined from this study is presented in Table A.14. This study also reported that a software bug in MEPDG version 1.0 does not allow calibration of the roughness model.

Table A.14. Locally calibrated coefficient results of typical Washington State flexible pavement systems

Calibration Factor	Default	Calibrated
AC[a] fatigue		
B_{f1}	1	0.96
B_{f2}	1	0.97
B_{f3}	1	1.03
Longitudinal cracking		
C_1	7	6.42
C_2	3.5	3.596
C_3	0	0
C_4	1,000	1,000
Alligator cracking		
C_1	1	1.071
C_2	1	1
C_3	6,000	6,000
AC rutting		
B_{r1}	1	1.05
B_{r2}	1	1.109
B_{r3}	1	1.1
Subgrade rutting		
B_{s1}	1	0
IRI		
C_1	40	N/A
C_2	0.4	N/A
C_3	0.008	N/A
C_4	0.015	N/A

Source: Li et al. 2009

Similar to the study conducted in North Carolina (Muthadi and Kim 2008), Banerjee et al. (2009) minimized the SSE between the observed and the predicted surface permanent deformation to determine the coefficient parameters (β_{r1} and β_{r3}) of the HMA permanent deformation performance model using values based on expert knowledge assumed for the subgrade permanent deformation calibration factors (β_{s1}) and the HMA mixture temperature dependency calibration factors (β_{r2}). Pavement data from the Texas SPS-1 and SPS-3 experiments in the LTPP database were used to run the MEPDG and calibrate the guide to Texas conditions. The set of state-default calibration coefficients for Texas was determined based on joint minimization of the SSE for all sections after the determination of the Level 2 input calibration coefficients for each section. The resulting calibration factors obtained from this study are given in Figure A.9. Banerjee et al. (2011) also determined the coefficient parameters (β_{r1} *and* β_{r3}) of rutting for rehabilitated flexible pavements under six of the regional areas in the US.

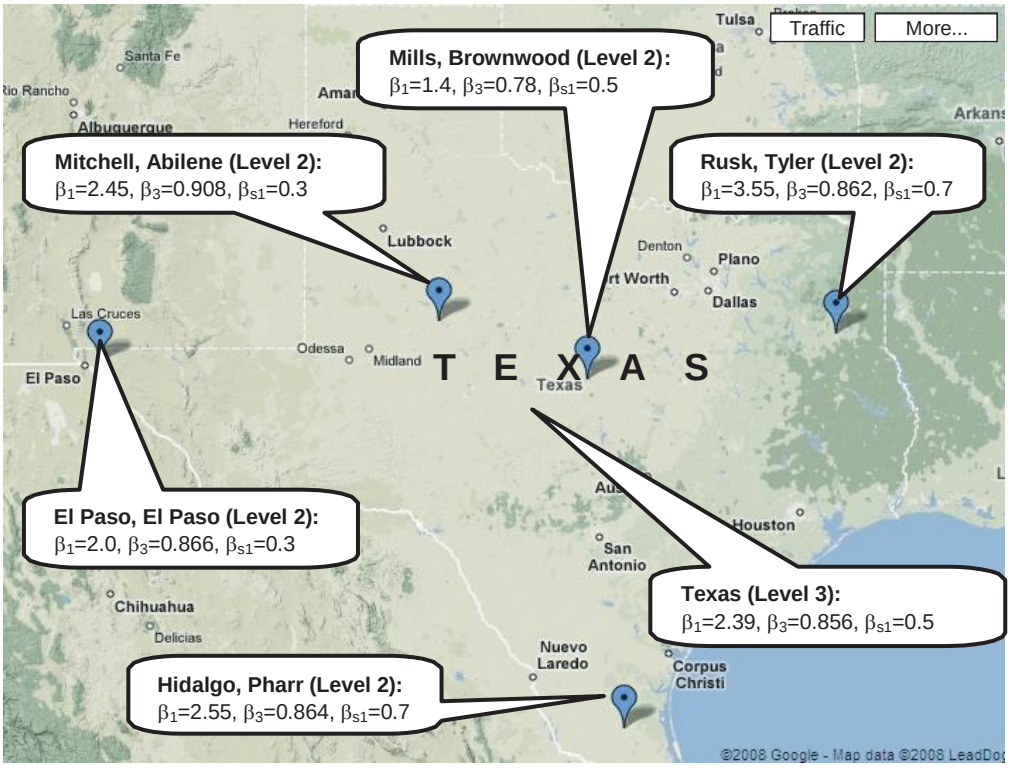

Source: Banerjee et al. 2009, Map ©2008 Google – Map data ©2008 LeadDo…

Figure A.9. Regional and state-level calibration coefficients of the HMA rutting depth transfer function for Texas

Velasquez et al. (2009) evaluated the sensitivity of input parameters for pavement performance prediction models in Minnesota. Longitudinal cracking prediction of the nationally calibrated MEPDG was found to be poor.

Titus-Glover and Mallela (2009) investigated the implementation of the NCHRP 1-37A mechanistic-empirical (ME) design procedure in Ohio. The rutting and IRI models for flexible pavement were locally calibrated.

Souliman et al. (2010) presented the calibration of the MEPDG (version 1.0) predictive models for flexible pavement design in Arizona conditions. This calibration was performed using 39 Arizona pavement sections included in the LTPP database. The calibration factors obtained from this study are given in Table A.15.

Table A.15. Calibration coefficients of the MEPDG flexible pavement distress models in Arizona conditions

MEPDG Model	Coefficients before Calibration	Coefficients after Calibration	Net Effect of Calibration
Alligator Fatigue Transfer Function	β_{f1} =1	β_{f1} = 0.729	Increased prediction
	β_{f2} =1	β_{f2} = 0.8	
	β_{f3} =1	β_{f3} = 0.8	
	C_1=1.0	C_1= 0.732	
	C_2=1.0	C_2= 0.732	
Longitudinal Fatigue Transfer Function	β_{f1} =1	β_{f1} =0.729	Decreased prediction
	β_{f2} =1	β_{f2} =0.8	
	β_{f3} =1	β_{f3} =0.8	
	C_1=7.5	C_1=1.607	
	C_2=3.5	C_2= 0.803	
AC Rutting Model	β_{r1} =1	β_{r1} = 3.63	Increased prediction
	β_{r2} =1	β_{r2} = 1.1	
	β_{r3} =1	β_{r3} = 0.7	
Granular Base Rutting Model	β_{gb} =1	β_{gb} = 0.111	Decreased prediction
Subgrade Rutting Model	β_{sg} =1	β_{sg} = 1.38	Increased prediction
Roughness Model	C_1= 40	C_1= 5.455	Decreased prediction
	C_2= 0.4	C_2= 0.354	
	C_3= 0.008	C_3= 0.008	
	C_4= 0.015	C_4= 0.015	

Source: Souliman et al. 2010

Hoegh et al. (2010) utilized time-history rutting performance data for pavement sections at the Minnesota Department of Transportation (MnDOT) full-scale pavement research facility (MnROAD) for the evaluation and local calibration of the MEPDG rutting model. Instead of an adjustment of the calibration parameters in the current MEPDG rutting model, a modified rutting model was suggested to account for the forensic and predictive evaluations of the local conditions. This study demonstrated that current MEPDG subgrade and base rutting models grossly overestimate rutting for the MnROAD test sections. Instead of calibrating the fatigue cracking performance model, Velasquez et al. (2009) calibrated the MEPDG fatigue damage model against MnPAVE, which is mechanistic-empirical design–based software calibrated in Minnesota. The alligator cracking predicted by the MEPDG was approximately five times greater than that predicted by MnPAVE. This difference was minimized by setting 0.1903 for the fatigue damage model coefficient B_{f1}.

Glover and Mallela (2009) calibrated the MEPDG rutting and IRI models by using LTPP data from Ohio roads. Due to a lack of data (no distress observations or records), the other distress predictions were not calibrated. Similar to the Ohio study, Darter et al. (2009) were able to calibrate only the MEPDG rutting model due to a lack of data. However, the authors found that the nationally calibrated IRI model for flexible pavement produced a goodness of fit between the measured and predicted IRI and SEE values approximately the same as that reported in NCHRP 1-37A.

Some type of maintenance or rehabilitation activity can make actual distress measurements decrease in distress time-history plots (Kim et al. 2010). Banerjee et al. (2010) found that the calculation factors of the MEPDG permanent deformation performance models are influenced by maintenance strategies. Liu et al. (2010) suggested that the historical pavement performance model should account for rehabilitation or maintenance activity using piecewise approximation. The whole pavement serviceable life was divided into three zones: Zone 1 for early-age pavement distress, Zone 2 for the rehabilitation stage, and Zone 3 for over-distressed situations. The historical pavement performance data were regressed independently in each time zone. This approach is able to accurately predict the pavement distress progression trends in each individual zone by eliminating the possible impacts of the biased data in the other zones. It is also possible to compare the pavement distress progression trends in each individual zone with the MEPDG incremental damage approach predictions.

Mamlouk and Zapata (2010) discussed the differences between the Arizona Department of Transportation (ADOT) PMS data and the LTPP database used in the original development and national calibration of the MEPDG distress models. Differences were found between the rutting, asphalt cracking, and IRI data and all layer back-calculated moduli from nondestructive tests performed by ADOT and the data from the LTPP. Differences in distress data included the types of data measured, types of measuring equipment, data processing methods, units of measurements, sampling methods, unit length of the pavement sections, number of runs of the measuring devices, and the survey manuals used. Similar findings were reported for the NCDOT PMS by Corley-Lay et al. (2010).

Hall et al. (2011) also discussed differences in defining transverse cracking between the MEPDG and the LTPP distress survey manual. Transverse cracking in the MEPDG is related to thermal cracking caused by thermal stress in the pavement, while in the LTPP distress survey manual transverse cracking encompasses the cracks predominately perpendicular to the pavement centerline due to various causes. Because the pavement sections selected in this study were generally in good condition in terms of transverse cracking and rutting, local calibration coefficients were optimized for the alligator cracking and longitudinal cracking models. In the local calibration of the smoothness model, some concerns arose because this model depends on other predicted distress. Therefore, the local calibration of this model was not carried out. Table A.16 compares the national default and locally calibrated coefficients for different pavement prediction models.

Table A.16. Summary of calibration factors

Calibration Factor	Default	Calibrated
Alligator cracking		
C1	1	0.688
C2	1	0.294
C3	6000	6000
Longitudinal cracking		
C1	7	3.016
C2	3.5	0.216
C3	0	0
C4	1000	1000
AC rutting		
βr1	1	1.20
βr2	1	1
βr3	1	0.80
Base rutting		
Bs1	1	1
Subgrade rutting		
Bs1	1	0.50

Source: Hall et al. 2011

The alligator cracking and rutting models in the MEPDG for flexible pavement systems in North Carolina were locally calibrated (Jadoun 2011). The scope of this paper was determining rutting and fatigue model coefficients (k values) using the 12 most commonly used HMA mixtures in North Carolina and evaluating the effectiveness of two recalibration methods used in attaining rutting and fatigue cracking model coefficients. The two calibration methods used in the recalibration procedure are Approach 1, the generalized reduced gradient (GRG) method, and Approach 2, the genetic algorithm (GA) method. Using these two approaches, the local calibration coefficients for rutting and alligator cracking shown in Table A.17 were obtained.

Table A.17. Comparison between local calibration coefficients from Approaches 1 and 2

Distress Type	Parameter	Approach I-R	Approach II-R
Rutting	β_{r1}	13.1000	0.94750
	β_{r2}	0.40000	0.86217
	β_{r3}	1.40000	1.35392
	β_{gb}	0.30300	0.53767
	β_{sg}	1.10200	1.50000
Distress Type	Parameter	Approach I-F	Approach II-F
Alligator Cracking	β_{f1}	3.87800	3.50000
	β_{f2}	0.80000	0.72364
	β_{f3}	0.80000	0.60000
	C_1	0.24500	0.24377
	C_2	0.24500	0.24377

Source: Jadoun 2011

Local calibration of the MEPDG for flexible pavement systems in New Mexico was performed using a total of 24 New Mexico pavement sections (Tarefder and Rodriguez-Ruiz 2013). As a result of this local calibration, the rutting, alligator cracking, longitudinal cracking, and roughness models were locally calibrated, and the model coefficients that minimized the difference between predicted and measured distresses were determined. The following coefficients were obtained as a result of this local calibration process:

- Total rutting: β_{r1}=1.1, β_{r2}=1.1, β_{r3}=0.8, B_{GB}=0.8, and B_{SG}=1.2
- Alligator cracking: C_1=0.625, C_2=0.25, and C_3=6,000
- Longitudinal cracking: C_1=3, C_2=0.3, and C_3=1,000
- IRI: Site factor=0.015

The following conclusions were documented in Tarefder and Rodriguez-Ruiz (2013):

- Using national coefficients, it was realized that the rutting verification results had a significant bias that required initiating local calibration for this model. Only total rutting data were provided by NMDOT, so only this parameter could be calibrated. As a result of local calibration, the standard error was mitigated and bias was eliminated.
- A significant bias was also found in the verification results for alligator cracking, so the model coefficients of C_1, C_2, and C_3 were calibrated and the sum-of-squares errors were decreased.
- The local calibration of longitudinal cracking was problematic because most of the measured longitudinal cracking values were almost zero, making the model difficult to calibrate. Although the error was reduced for the model, the improvement in the model accuracy was not as significant as for the rutting and alligator cracking models.
- As a result of IRI verification runs, it was realized that the models already produced accurate predictions, so it was determined that local calibration for this model did not significantly reduce the error.

Mallela et al. (2013) employed the local calibration procedure to calibrate DARWin-ME for Colorado conditions. Based on the verification of the new and rehabilitated flexible pavement performance prediction models, the alligator cracking, rutting, transverse cracking, and smoothness (IRI) models were recalibrated for Colorado conditions. As a result of local calibration, the accuracy of the pavement prediction models was significantly improved.

Zhou et al. (2013) compared the pavement performance predictions from MEPDG version 1.100 for selected highways in Tennessee to the distress values extracted from the Tennessee DOT PMS database for these highway sections. In this analysis, a new pavement design procedure was used rather than an overlay design procedure. The conclusions of this study are as follows:

1. An initial IRI value of 67.9 cm/km was used in this experiment, taking into account the PSI history data of pavement sections used.
2. Utilizing Level 1 input data in the prediction of asphalt concrete (AC) rutting gave accurate results, although in a case using Level 3 input data, SC rutting was overpredicted. Another

overprediction was observed when Level 2 input data were used for rutting of the base and subgrade.
3. Traffic input was another important factor in the roughness prediction of the MEPDG.
4. It was also found that in predicting PSI using the MEPDG, the software was not sensitive enough in reflecting variations in climate, traffic, and materials.
5. The authors recommend locally calibrating the MEPDG for Tennessee pavement systems to produce more accurate predictions.

Darter at al. (2014) locally calibrated DARWin-ME for Arizona conditions. Alligator cracking, fatigue, IRI, asphalt, and subgrade rutting models were locally calibrated using SAS statistical methods, and the accuracy of the models was significantly improved.

Rigid Pavements

While 11 US state highway agencies have approved the use of national calibration coefficients for their JPCP performance prediction models, 8 agencies have adopted locally calibrated coefficients, according to a recent American Concrete Pavement Association (ACPA) survey (Mu et al. 2015). Table A.18 shows which calibration coefficients have been adopted by state highway agencies for JPCP performance prediction models.

Table A.18. Local calibration summary for JPCP systems

State	Cracking Model	Faulting Model	IRI Model
1. Arizona	3 of 5 Coeff. Changed	8 of 9 Changed	4 of 5 Changed
2. Colorado	NNC	9 of 9 Changed	NNC
3. Florida	4 of 5 Changed	2 of 9 Changed	1 of 5 Changed
4. Utah	NNC	NNC	NNC
5. Wyoming	NNC	NNC	NNC
6. Delaware	ONC	ONC	ONC
7. Indiana	ONC	ONC	ONC
8. Iowa	4 of 5 Changed	5 of 9 Changed	4 of 5 Changed
9. Kansas	ONC	ONC	ONC
10. Louisiana	1 of 5 Changed	1 of 9 Changed	ONC
11. Missouri	ONC	ONC	3 of 4 Changed
12. New York	ONC	ONC	ONC
13. North Carolina	ONC	ONC	ONC
14. Ohio	ONC	ONC	3 of 4 Changed
15. Oklahoma	ONC	ONC	ONC
16. Pennsylvania	ONC	ONC	ONC
17. South Dakota	ONC	ONC	ONC
18. Virginia	ONC	ONC	ONC
19. Washington	2 of 5 Changed	ONC	ONC

Note: NNC: new national calibration; ONC: original national calibration

Source: Mu et al. 2015

WSDOT (Li et al. 2006) developed procedures to calibrate the MEPDG (Version 0.9) rigid pavement performance models using data obtained from the WSPMS. Some significant conclusions from this study are as follows:

- WSDOT rigid pavement performance prediction models require calibration factors significantly different from the default values.
- The MEPDG software does not model longitudinal cracking of rigid pavement, which is significant in WSDOT pavements.
- WSPMS does not separate longitudinal and transverse cracking in rigid pavements, a deficiency that makes calibration of the software's transverse cracking model difficult.
- The software does not model studded tire wear, which is significant in WSDOT pavements.

This study also reported that (a) the calibrated software can be used to predict future deterioration caused by faulting, but it cannot be used to predict cracking caused by the transverse or longitudinal cracking issues in rigid pavement, and (b) with a few improvements and after resolving software bugs, the MEPDG software can be used as an advanced tool to design rigid pavements and predict future pavement performance. The local calibration results of typical Washington State rigid pavement systems determined from this study are presented in Table A.19.

Table A.19. Calibration coefficients of the MEPDG (version 0.9) rigid pavement distress models in Washington State

Calibration Factor		Default for New Pavements	Undoweled	Undoweled – MP[a]	DBR[b,c]
Cracking	C_1	2	2.4	2.4	2.4
	C_2	1.22	1.45	1.45	1.45
	C_4	1	0.13855	0.13855	0.13855
	C_5	-1.68	-2.115	-2.115	-2.115
Faulting	C_1	1.29	0.4	0.4	0.934
	C_2	1.1	0.341	0.341	0.6
	C_3	0.001725	0.000535	0.000535	0.001725
	C_4	0.0008	0.000248	0.000248	0.0004
	C_5	250	77.5	77.5	250
	C_6	0.4	0.0064	0.064	0.4
	C_7	1.2	2.04	9.67	0.65
	C_8	400	400	400	400
Roughness[d]	C_1	0.8203	0.8203	0.8203	0.8203
	C_2	0.4417	0.4417	0.4417	0.4417
	C_3	1.4929	1.4929	1.4929	1.4929
	C_4	25.24	25.24	25.24	25.24

Notes:
a. Mountain pass climate
b. Dowel bar retrofitted
c. DBR calibration factors are the same as default "restoration" values in NCHRP 1-37A software
d. Roughness calibration factors are the same as the default values

Source: Li et al. 2006

Khazanovich et al. (2008) evaluated MEPDG rigid pavement performance prediction models for the design of low-volume concrete pavements in Minnesota. It was found that the faulting model in MEPDG versions 0.8 and 0.9 produced acceptable predictions, whereas the cracking model

had to be adjusted. The cracking model was recalibrated using the design and performance data for 65 pavement sections located in Minnesota, Iowa, Wisconsin, and Illinois. The recalibrated coefficients in this study of the cracking model predictions of MEPDG versions 0.8 and 0.9 are (1) $C_1 = 1.9875$ and (2) $C_2 = -2.145$. These values are recalibrated into $C_1 = 0.9$ and $C_2 = -2.64$ by using MEPDG version 1.0 (Velasquez et al. 2009). Because the MEPDG software evaluated in these studies was not a final product, the authors recommended that these values should be updated for the final version of the MEPDG software.

Darter et al. (2009) found that the nationally calibrated MEPDG model predicted faulting, transverse cracking, and IRI well under Utah conditions with an adequate goodness of fit and no significant bias. Bustos et al. (2009) attempted to adjust and calibrate the MEPDG rigid pavement distress models for Argentina conditions. A sensitivity analysis of the distress model transfer functions was conducted to identify the most important calibration coefficient. The C_6 of the joint faulting model transfer function and the C_1 or C_2 of the cracking model transfer function were the most sensitive coefficients. Delgadillo et al. (2011) also presented local calibration coefficients for the transverse cracking and faulting of JPCP in Chile.

The scope of Titus-Glover and Mallela (2009) was to determine whether the global calibration factors for the MEPDG adequately predict pavement performance in Ohio rigid pavements and to initiate the local calibration process if needed. A validation study was employed for pavement prediction models to determine which models give accurate pavement predictions. Based on the validation study, it was found that the smoothness model for new JPCP needed to be locally calibrated. The new local calibration for the locally calibrated model can be seen in Table A.20.

Table A.20. New local calibration coefficients of the MEPDG rigid pavement distress models in Ohio

Pavement Type	JPCP Model IRI Local Calibration Coefficients			
	CRK (C1)	SPALL (C2)	TFAULT (C3)	SF (C4)
New JPCP	0.82	3.7	1.711	5.703

Source: Titus-Glover and Mallela 2009

The scope of Mallela et al. (2009) was to determine whether the global calibration factors for the MEPDG adequately predict pavement performance in Missouri rigid pavements and to initiate the local calibration process if needed. A validation study was employed for pavement prediction models to determine which models give accurate pavement predictions. Based on the validation study, it was found that the smoothness model for JPCP needed to be locally calibrated. The new local calibration for the locally calibrated model can be seen in Table A.21.

Table A.21. New local calibration coefficients of the MEPDG rigid pavement distress models in Missouri

Pavement Type	JPCP Model IRI Local Calibration Coefficients			
	CRK (C1)	SPALL (C2)	TFAULT (C3)	SF (C4)
New JPCP	0.82	1.17	1.43	66.8

Source: Mallela et al. 2009

Li et al. (2010) recalibrated the MEPDG (version 1.0) for rigid pavement systems based on the local conditions of Washington State. The first local calibration was conducted for WSDOT using MEPDG version 0.6. Because the software has evolved since then, recalibration was a necessity. As a result of the recalibration process, the recalibrated local calibration coefficients shown in Table A.22 were found.

Table A.22. Recalibrated local calibration coefficients of the MEPDG for transverse cracking model models in Washington

Calibration Factor			Elasticity	Default	Recalibration Results
Rigid Pavement	Cracking	C1	-7.579	2	1.93
		C2	-7.079	1.22	1.177
		C3	0.658	1	1
		C4	-0.579	-1.98	-1.98

Source: Li et al. 2010

For the faulting and roughness models, the default calibration confidents gave good results. Therefore, the recalibration for these models was not conducted.

Mallela et al. (2013) employed the local calibration procedure of DARWin-ME for Colorado conditions. The local calibration methodology consists of three steps: verification, calibration, and validation. First, the researchers run the software using global calibration coefficients for all rigid pavement projects to determine the goodness of fit and bias between the predicted and actual performance results of the pavements. If the verification results give high goodness of fit and low bias, the global calibration coefficients are announced as local calibration coefficients. If not, the local calibration process is initiated to develop a better set of calibration coefficients giving the highest goodness of fit and lowest bias. The local calibration results also need to be verified with a validation process.

As a result of the verification process, all of the global performance models for new JPCPs (transverse cracking, transverse joint faulting, and smoothness [IRI]) performed well enough, and it was determined that local calibration of the models was not necessary for Colorado conditions. That is, the global models gave a good goodness of fit and bias and required no local calibration effort.

Darter at al. (2014) locally calibrated DARWin-ME for Arizona conditions. This methodology consists of three steps: verification, calibration, and validation. First, the researchers run the software using global calibration coefficients for all rigid pavement projects to determine the goodness of fit and the bias between the predicted and actual performance results of the pavements. If the verification results produce high goodness of fit and low bias, the global calibration coefficients are taken as local calibration coefficients. If not, a local calibration process is initiated to seek a set of calibration coefficients that gives the highest goodness of fit and lowest bias. The local calibration results also must be verified through a validation process.

For JPCP systems, the verification of transverse cracking gave poor goodness of fit and bias, so local calibration of the transverse cracking model was initiated. Possible causes for the poor goodness of fit were also investigated. JPCPs with asphalt-treated or aggregate bases gave accurate transverse cracking predictions compared to those constructed over lean concrete bases. In local calibration, SAS statistical software was used to determine local calibration coefficients that improved the model predictions, producing significantly better goodness of fit and lower bias. The goodness of fit of the faulting model was found to be fair, but it overpredicted faulting with high bias, so local calibration was necessary for the faulting model. Again, SAS statistical software was used to determine local coefficients that improved the model predictions with significantly better goodness of fit and lower bias. For the IRI model, as a result of verification the IRI values were overpredicted, so local calibration for this model was also necessary, with SAS statistical software used to determine local coefficients that improved the model predictions with significantly better goodness of fit and lower bias, as listed in Table A.23.

Table A.23. Comparison of accuracy between global and ADOT-calibrated MEPDG models for Arizona JPCP systems

Pavement Type	Distress/IRI Models	Global Models		ADOT-Calibrated Models	
		Global R^2 (%)	Global Model SEE*	Arizona R^2 (%)	Arizona SEE
New JPCP	Transverse cracking	20	9%	78	6%
	Transverse joint faulting	45	0.03 inch	52	0.03 inch
	IRI	35	25 inches/mi	81	10 inches/mi

Source: Darter et al. 2014

Mu et al. (2015) summarizes the local calibration efforts of state highway agencies. At the time of the paper's publication, the local calibration process for JPCP had been finalized by 19 states, with 11 states accepting the national calibration coefficients and the remaining 8 states adopting one or more new calibration coefficients. The paper first elaborates on the local calibration effort of each state adopting new calibration coefficients and the effectiveness of these efforts. The paper concludes that while the improvements with respect to bias reduction are significant, the precision (standard error of the estimate) was rarely improved. Second, the authors focus on distress prediction models; the transverse cracking, faulting, and IRI models were evaluated using the new calibration coefficients adopted by 8 states as well as the national calibration

coefficients. Third, the authors emphasize the path dependence of the transverse cracking model, i.e., how using different calibration coefficients would result in the same effects as those predicted. Finally, the paper uses two hypothetical JPCP sections (one with a low traffic volume, the other one with a high traffic volume) as case studies to determine why using new local calibration coefficients or national calibration coefficients predict different distress results. The paper's conclusions are as follows:

- The local calibration process for JPCP was finished by 19 states, and 11 states accepted using national calibration coefficients.
- The local calibration procedure is path dependent, meaning that using different calibration approaches would result in different coefficients.
- For those states adopting different calibration coefficients than the national ones, the estimates' biases are mostly reduced while the standard error rarely decreases.
- For those states adopting different calibration coefficients than the national ones, the local calibration procedure results in less cracking but higher IRI predictions compared to predictions using the national calibration coefficients.

Mallela et al. (2015) recalibrated the JPCP cracking and faulting models in the AASHTO mechanistic-empirical design procedure under NCHRP 20-07 using corrected coefficient of thermal expansion (CTE) values acquired through a new CTE test procedure (AASHTO T 336-09 2009). Lower CTE values were produced when the new test procedure was used (AASHTO T 336-09 2009) instead of the previous test procedure (AASHTO TP 60-00 2004). The difference between erroneous and corrected CTE values was found to be -0.8 in./in./°F on average, with a range of 0 to -1.2 in./in./°F. Table A.24 shows the erroneous and corrected CTE values.

Table A.24. Comparison of erroneous CTEs (NCHRP 1-40D) and corrected CTEs (NCHRP 20-07)

Primary Aggregate Origin	Primary Aggregate Class	NCHRP 1-40D			NCHRP 20-07 (LTPP Projects with Single Coarse Agg. Type)			NCHRP 20-07 (LTPP Projects with Two or More Coarse Agg. Type)		
		Avg. CTE 10^{-6}/°F	Std. Dev. 10^{-6}/°F	No.	Avg. CTE 10^{-6}/°F	Std. Dev. 10^{-6}/°F	No.	Avg. CTE 10^{-6}/°F	Std. Dev. 10^{-6}/°F	No.
Igneous (Extrusive)	Andesite	5.3	0.5	23	NA	NA	NA	4.4	0.5	33
Igneous (Extrusive)	Basalt	5.2	0.7	47	4.4	0.5	18	4.4	0.6	87
Igneous (Plutonic)	Diabase	5.2	0.5	17	5.2	0.5	21	4.6	0.6	66
Igneous (Plutonic)	Granite	5.8	0.6	83	4.8	0.6	69	4.9	0.6	167
Metamorphic	Schist	5.6	0.5	17	4.4	0.4	17	4.7	0.7	24
Sedimentary	Chert	6.6	0.8	28	6.1	0.6	25	5.9	0.7	62
Sedimentary	Dolomite	5.8	0.8	124	5.0	0.7	30	4.9	0.6	195
Sedimentary	Limestone	5.4	0.7	236	4.4	0.7	160	4.4	0.6	425
Sedimentary	Quartzite	6.2	0.7	69	5.2	0.5	9	5.3	0.5	73
Sedimentary	Sandstone	6.1	0.8	18	5.8	0.5	7	5.2	0.6	29
	BF slag	—	—	—	—	—	—	4.8	0.7	22

Source: Mallela et al. 2015

Using the corrected CTE values, JPCP cracking and faulting models were calibrated using the LTPP database. The revised calibrated joint faulting model coefficients based on this study are presented in Table A.25.

Table A.25. Revised calibrated joint faulting model coefficients

Model Coefficients	Value
C1	0.51040
C2	0.00838
C3	0.00147
C4	0.008345
C5	5999
C6	0.8404
C7	5.9293
C8	400

Source: Mallela et al. 2015

The researchers compared slab thickness predictions from the faulting and transverse cracking models using erroneous CTE values (NCHRP 1-40 D) and corrected CTE values (NCHRP 20-07) (Figure A.10).

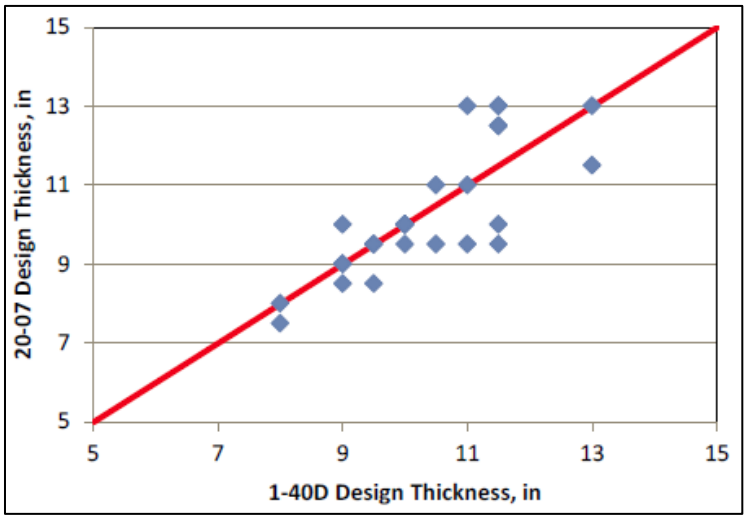

Source: Mallela et al. 2015

Figure A.10. 2007 and 2011 thickness designs for 13 projects at two levels of traffic each

APPENDIX B. DESIGN EXAMPLES OF NEW JPCP, NEW HMA, AND HMA OVER JPCP USING AASHTOWARE PAVEMENT ME DESIGN SOFTWARE

New Rigid Pavement

The design example of a new JPCP section in Des Moines, Iowa, was using AASHTOWare Pavement ME Design software. The following input categories are required for the design procedure:

- Traffic inputs
- Climate inputs
- JPCP design properties
- Pavement structure–related inputs
- Project-specific calibration factors

The following inputs are used in this specific design example.

Design Life

- Design life: 30 years
- Pavement construction month: September 2014
- Traffic opening month: October 2014
- Type of design: new pavement – JPCP

Construction Requirements

- A good quality of construction with an initial IRI between 50 and 75 in./mi (assume 63 in./mi for design purposes)

Traffic

- Two-way average annual daily truck traffic (AADTT) on this highway estimated to be 5,000 trucks during the first year of its service
- Two lanes in the design direction with 90% of the trucks in the design lane
- Truck traffic equally distributed in both directions
- Operational speed of 60 mph
- Traffic increases by 2.0% of the preceding year's traffic (compounded annually)
- Vehicle class distribution: TTC 4

Performance Criteria

- Initial IRI (in./mi): 63
- Terminal IRI (in./mi): 172
- JPCP transverse cracking (percent slabs): 15
- Mean joint faulting (in.): 0.12
- Reliability level for all criteria: 90%

Layer Properties

- PCC course: 10 in./MOR = 600 psi
- Nonstabilized base: 6 in./M_r = 35,000 psi
- Subgrade: semi–infinite thickness/M_r = 10,000 psi

where, MOR= Modulus of rupture and M_r = Resilient modulus

JPCP Design Properties

- PCC joint spacing: 20 ft
- Sealant type: no sealant, liquid or silicone
- Doweled joints: 1.5 in. of dowel diameter
- Widened slab: 14 ft
- Shoulders not tied

Figures B.1 through B.10 show screenshots of the design steps using AASHTOWare Pavement ME Design.

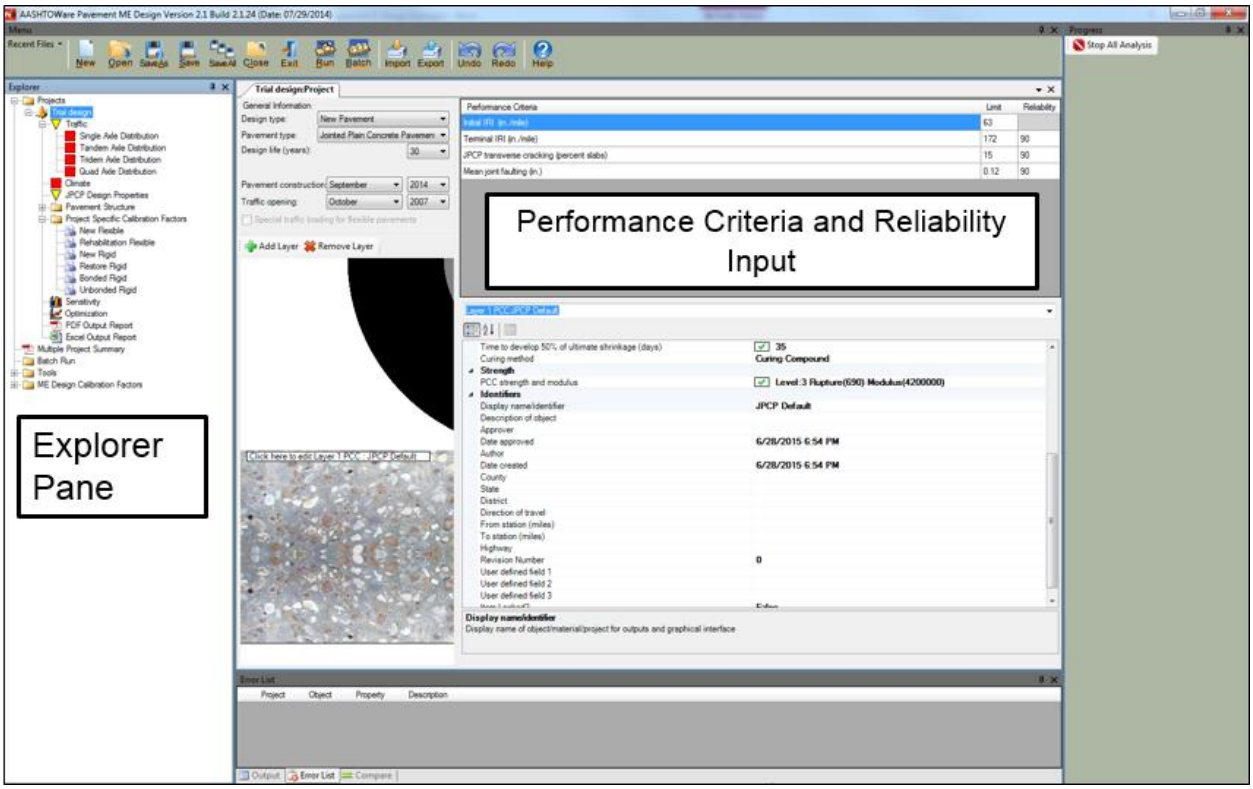

Figure B.1. General inputs, design criteria and reliability

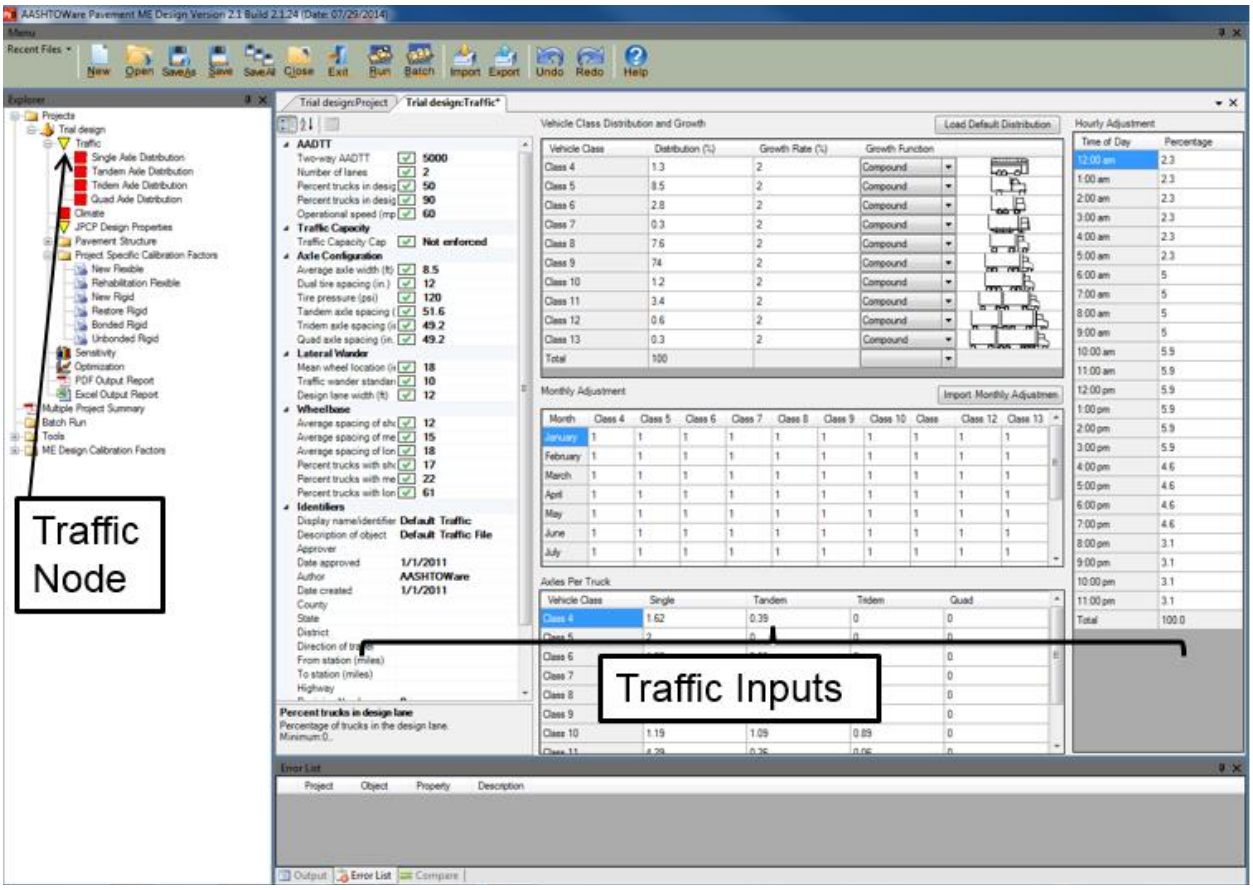

Figure B.2. Traffic inputs used in the design

Vehicle Class Distribution and Growth — Load Default Distribution

Vehicle Class	Distribution (%)	Growth Rate (%)	Growth Function
Class 4	1.3	2	Compound
Class 5	8.5	2	Compound
Class 6	2.8	2	Compound
Class 7	0.3	2	Compound
Class 8	7.6	2	Compound
Class 9	74	2	Compound
Class 10	1.2	2	Compound
Class 11	3.4	2	Compound
Class 12	0.6	2	Compound
Class 13	0.3	2	Compound
Total	100		

Figure B.3. Vehicle class distribution and growth used in the design

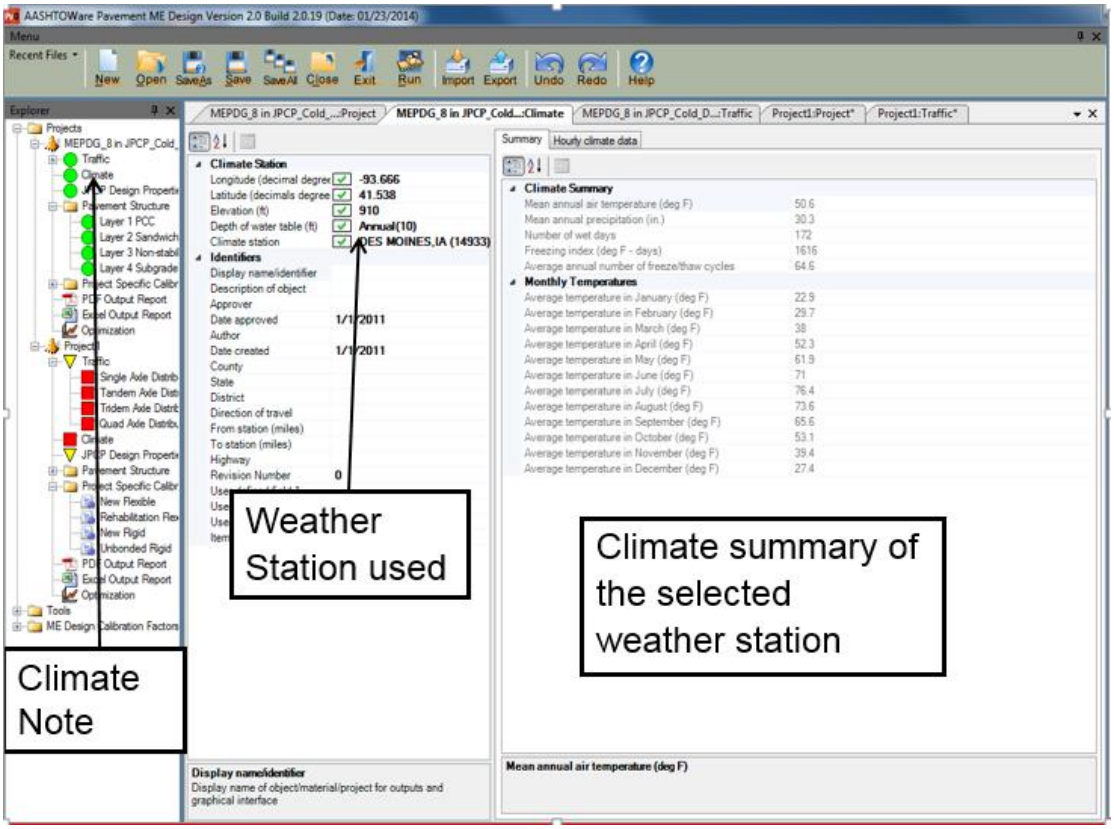

Figure B.4. Climate input used in the design

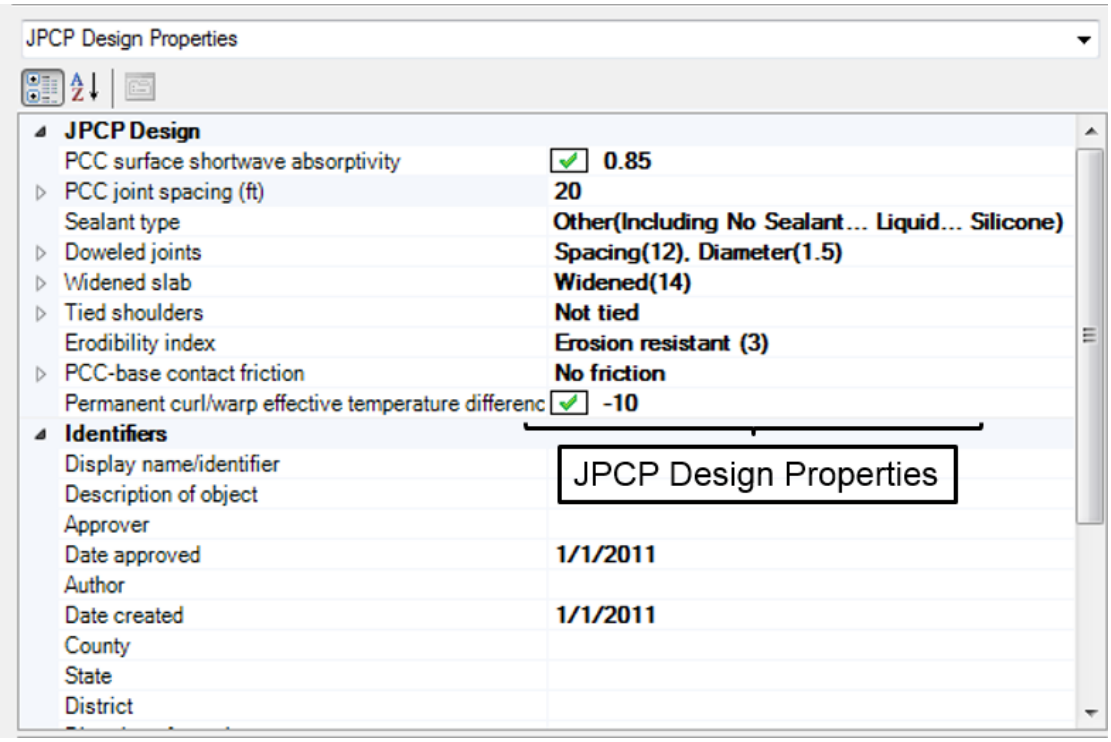

Figure B.5. JPCP design properties

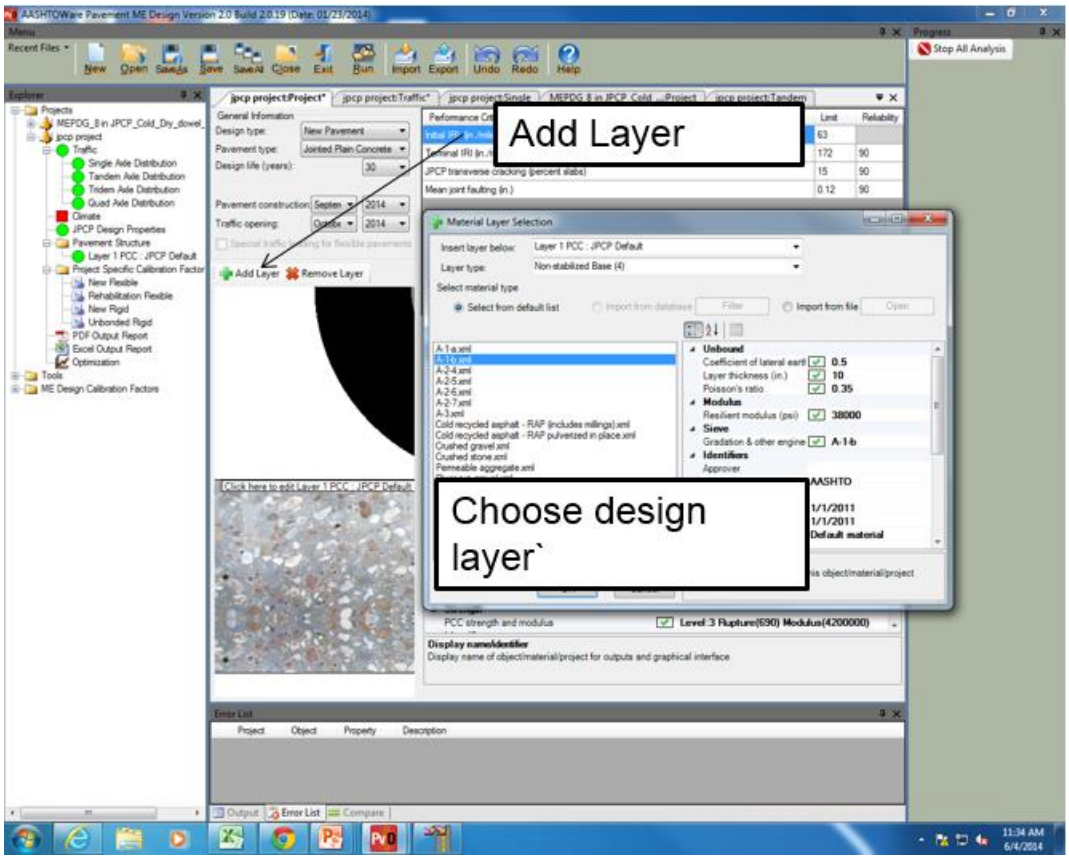

Figure B.6. Pavement structure input

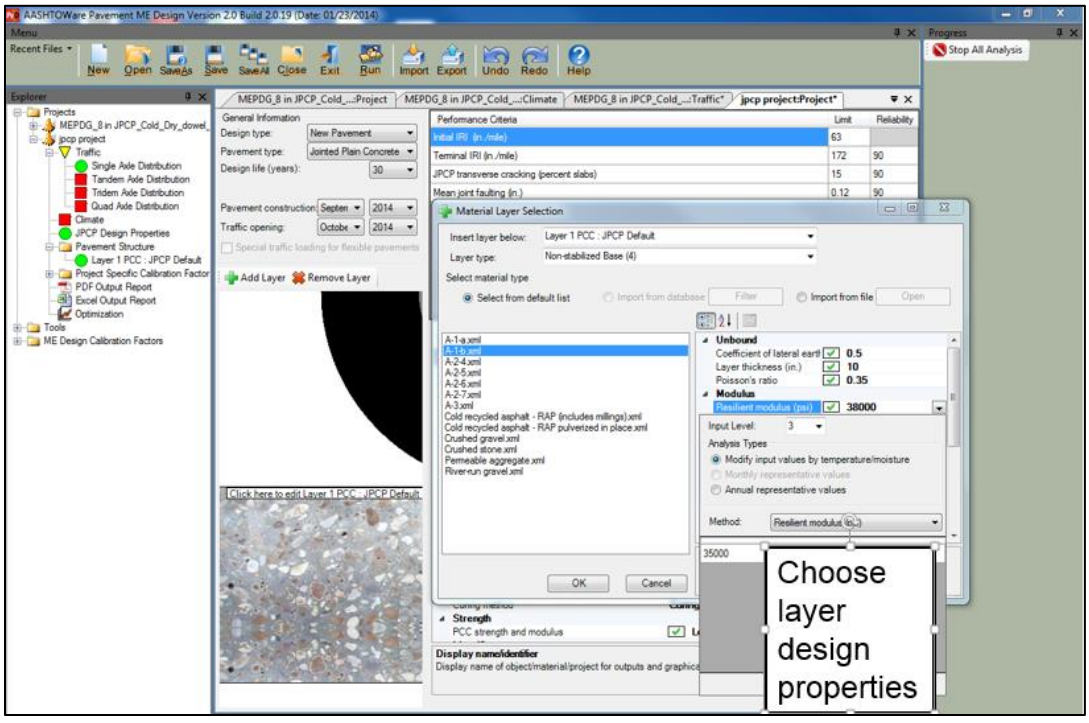

Figure B.7. Layer design properties

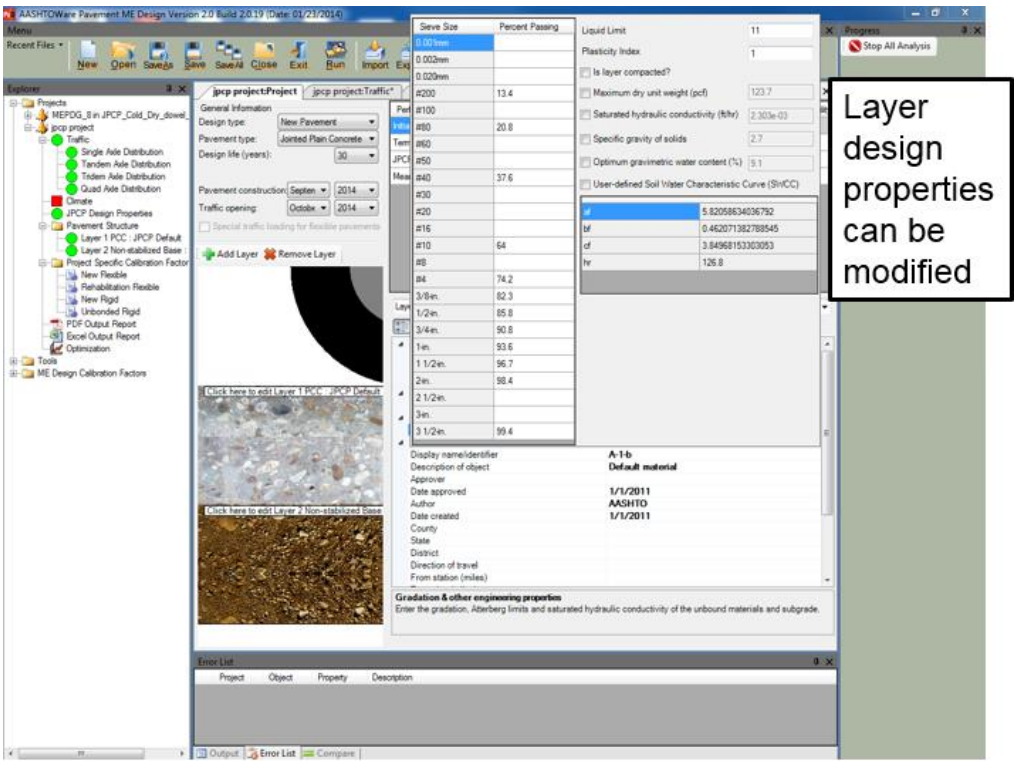

Figure B.8. Modification of layer design properties

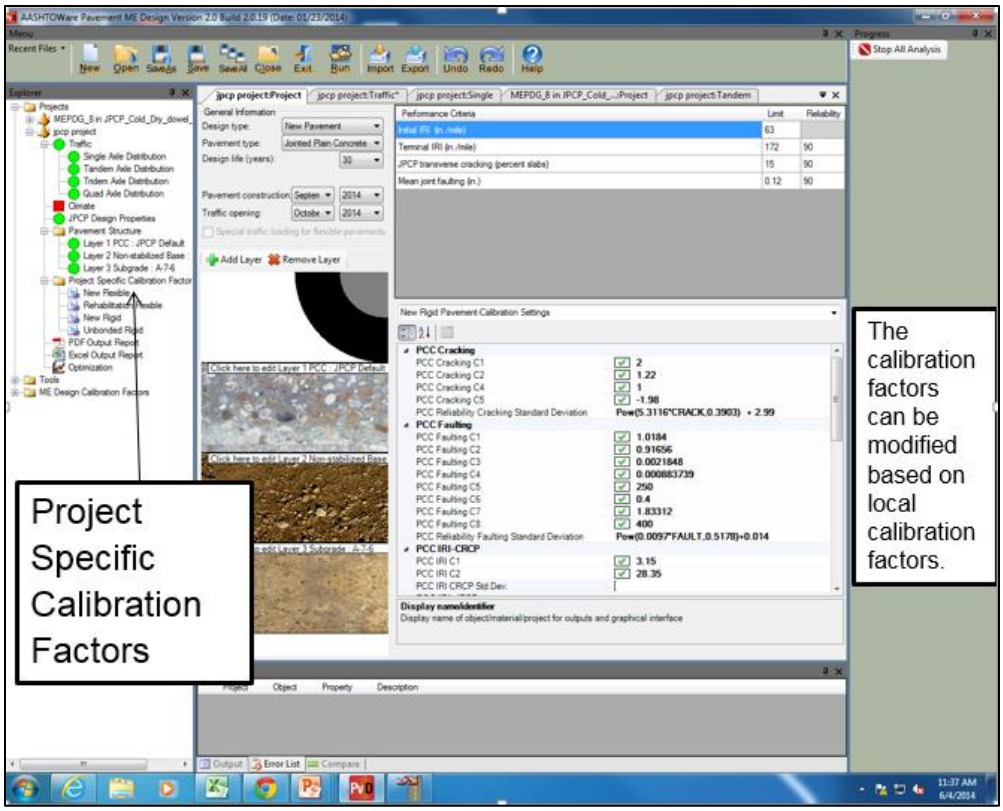

Figure B.9. Inputting local calibration coefficients

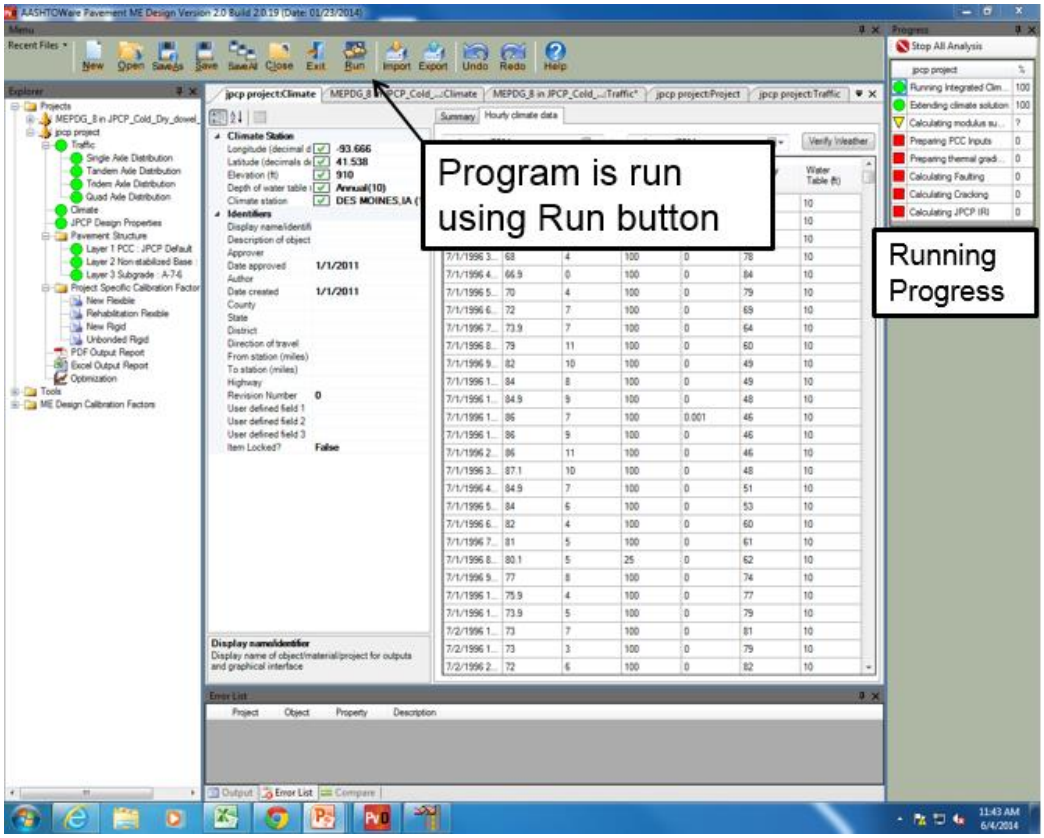

Figure B.10. Running the software

Once the run is completed, two kinds of output reports are generated (Figures B.11 and B.12):

- PDF output report
- Excel output report

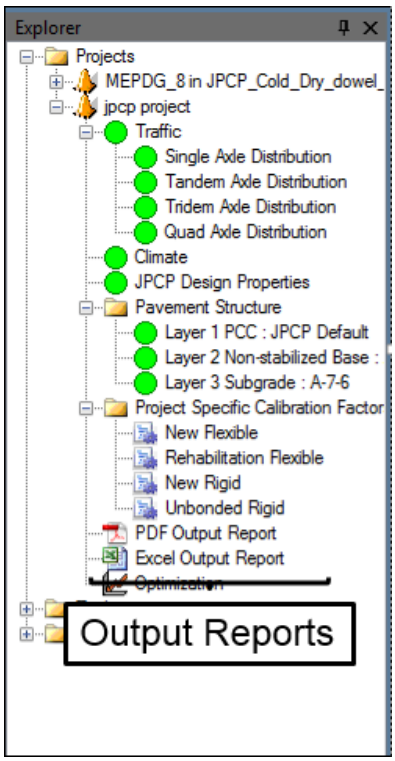

Figure B.11. Output reports

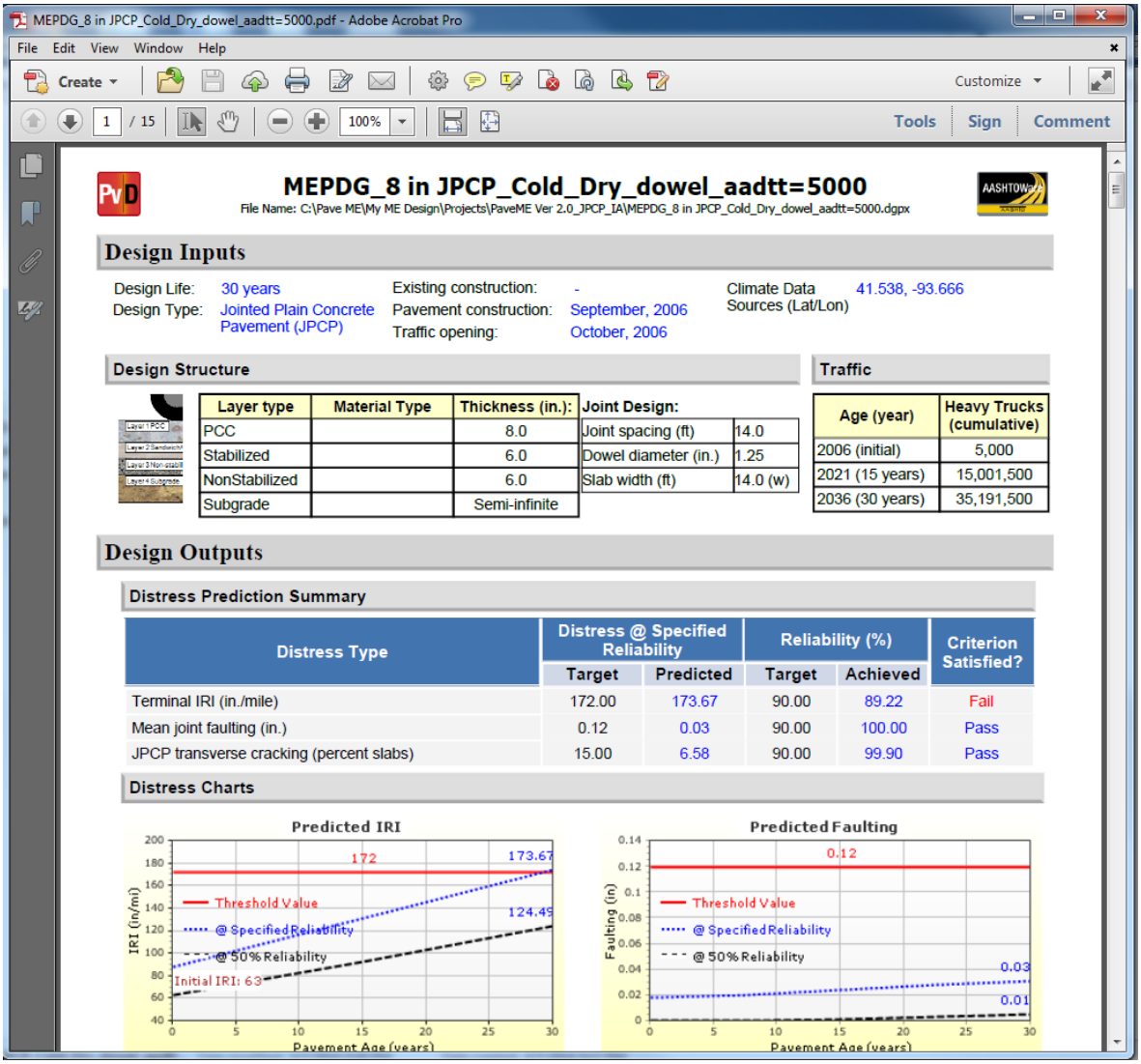

Figure B.12. PDF output report

If the trial fails, the designer can modify the design inputs based on the failed criteria by using the optimization node (Figure B.13).

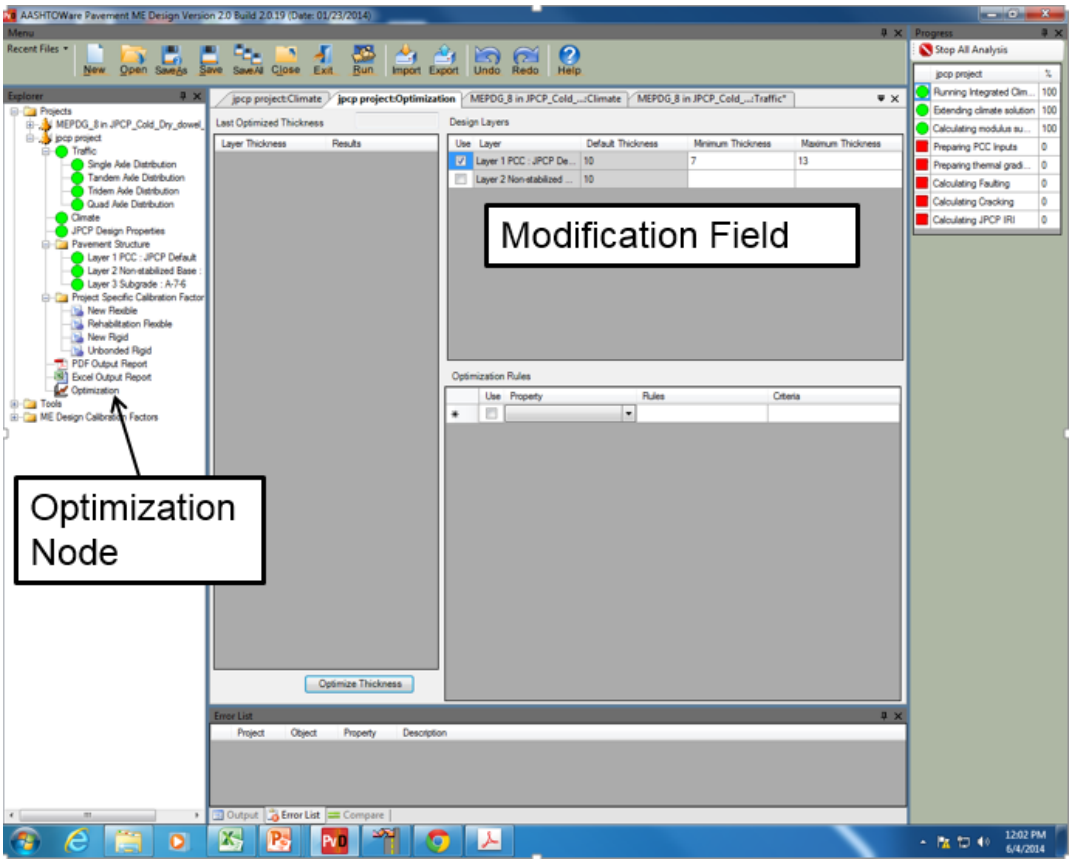

Figure B.13. Optimization tool

New HMA Pavement

The design of a new HMA pavement section in Des Moines, Iowa, was performed using AASHTOWare Pavement ME Design software. The following input categories are required for the design procedure:

- Traffic inputs
- Climate inputs
- Pavement structure related inputs
- Project specific calibration factors

The following inputs are used in this specific design example.

Design Life

- Design life: 20 years
- Base/Subgrade construction month: August 2014
- Pavement construction month: September 2014

- Traffic opening month: October 2014
- Type of design: New pavement – flexible pavement

Construction Requirements

- A good quality of construction with an initial IRI between 50 and 75 in./mi (assume 63 in./mi for design purposes)

Traffic

- Two-way average annual daily truck traffic (AADTT) on this highway estimated to be 5,000 trucks during the first year of its service
- Two lanes in the design direction with 90% of the trucks in the design lane
- Truck traffic equally distributed in both directions
- Operational speed of 60 mph
- Traffic increases by 2.0% of the preceding year's traffic (compounded annually)
- Vehicle class distribution: TTC 4

Performance Criteria

- Initial IRI (in./mi): 63
- Terminal IRI (in./mi): 172
- AC top-down fatigue cracking (ft/mi): 2000
- AC bottom-up fatigue cracking (percent): 25
- AC thermal cracking (ft/mi): 1000
- Permanent deformation – total pavement (in.): 0.75
- Permanent deformation – AC only (in.): 0.25
- Reliability level for all criteria: 90%

Layer Properties

- HMA layer: 12 in. with Superpave performance grading (PG) 58-28
- Subgrade (fill/borrow): 12 in. with M_r =10,000 psi
- Subgrade: semi-infinite thickness and M_r =10,000 psi

where, M_r = Resilient modulus

Figures B.14 through B.23 show screenshots of the design steps using AASHTOWare Pavement ME Design. The hourly climatic database for the US and Canada can be downloaded from the AASHTOWare Pavement ME Design website: www.me-design.com.

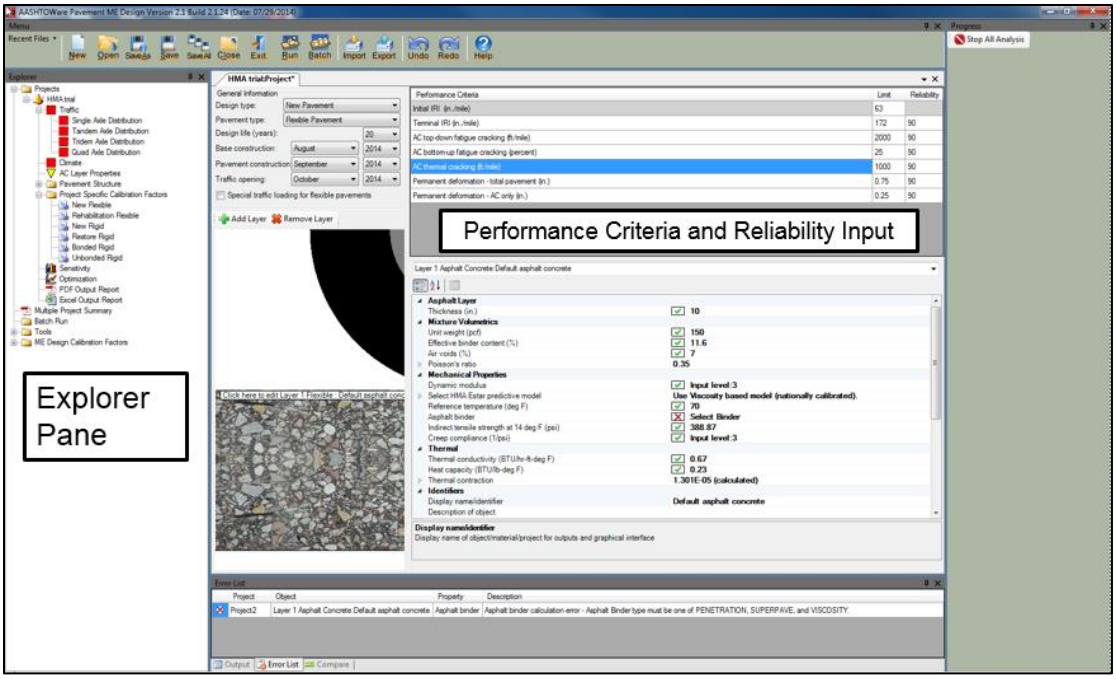

Figure B.14. General inputs, design criteria and reliability

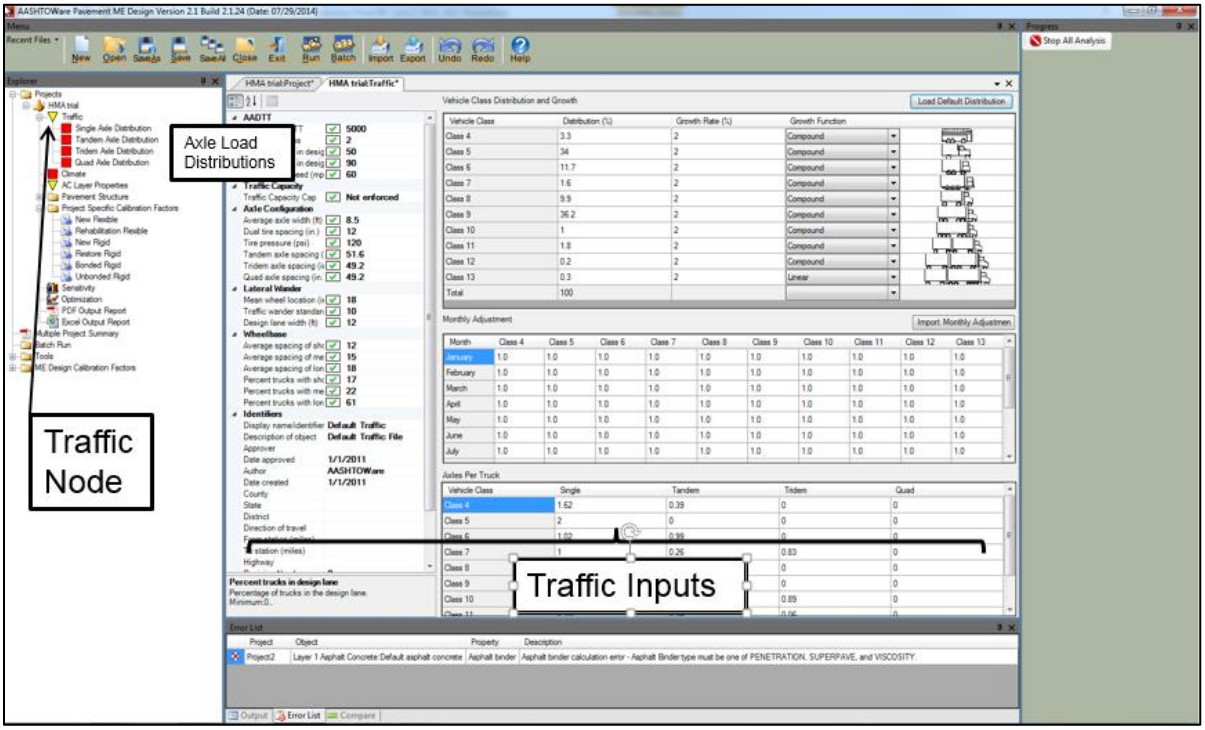

Figure B.15. Traffic inputs

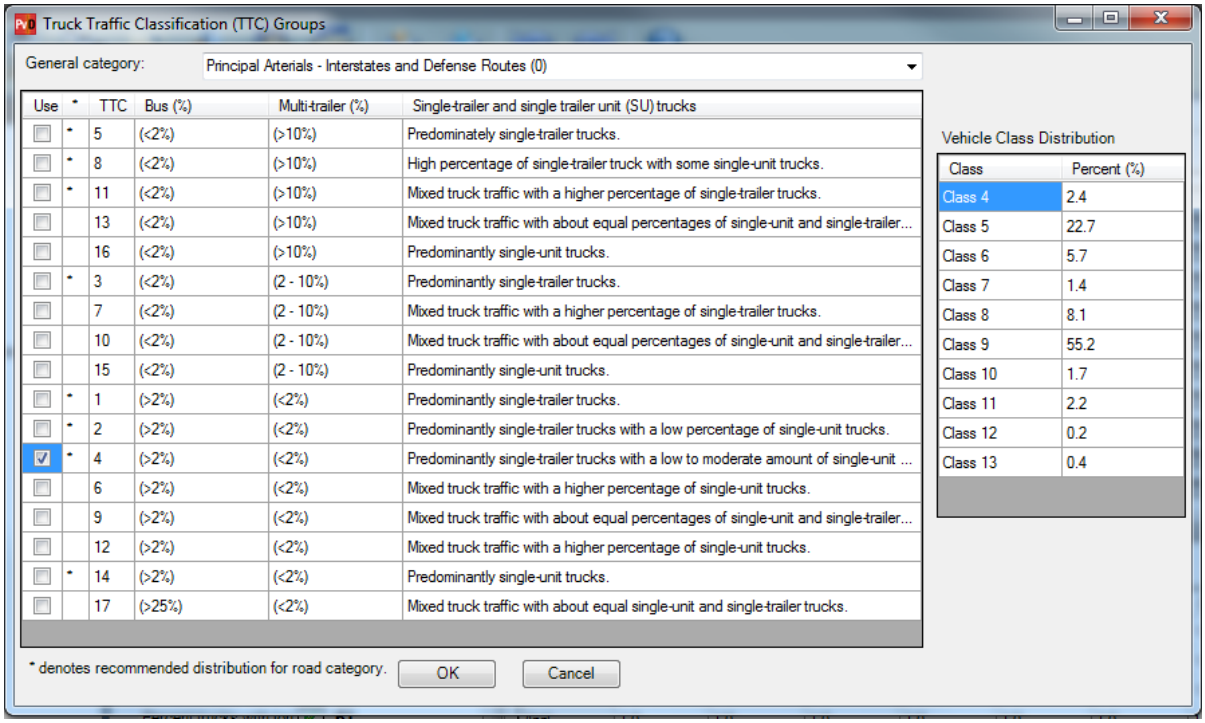

Figure B.16. Truck traffic classification

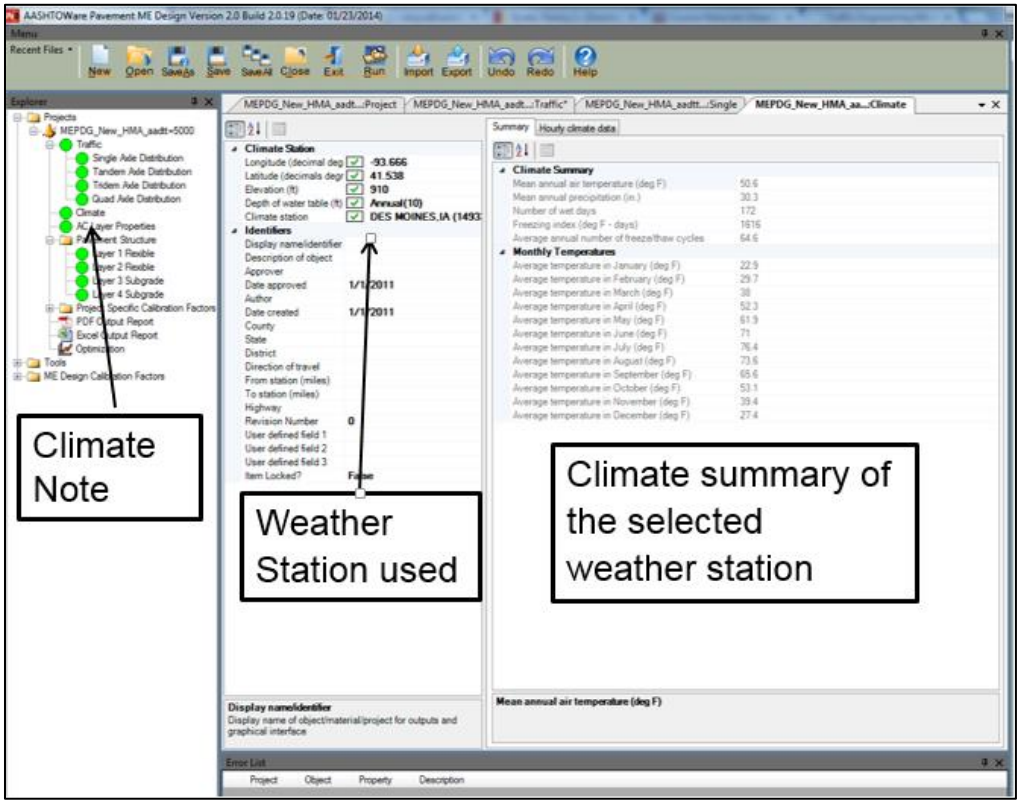

Figure B.17. Climate inputs

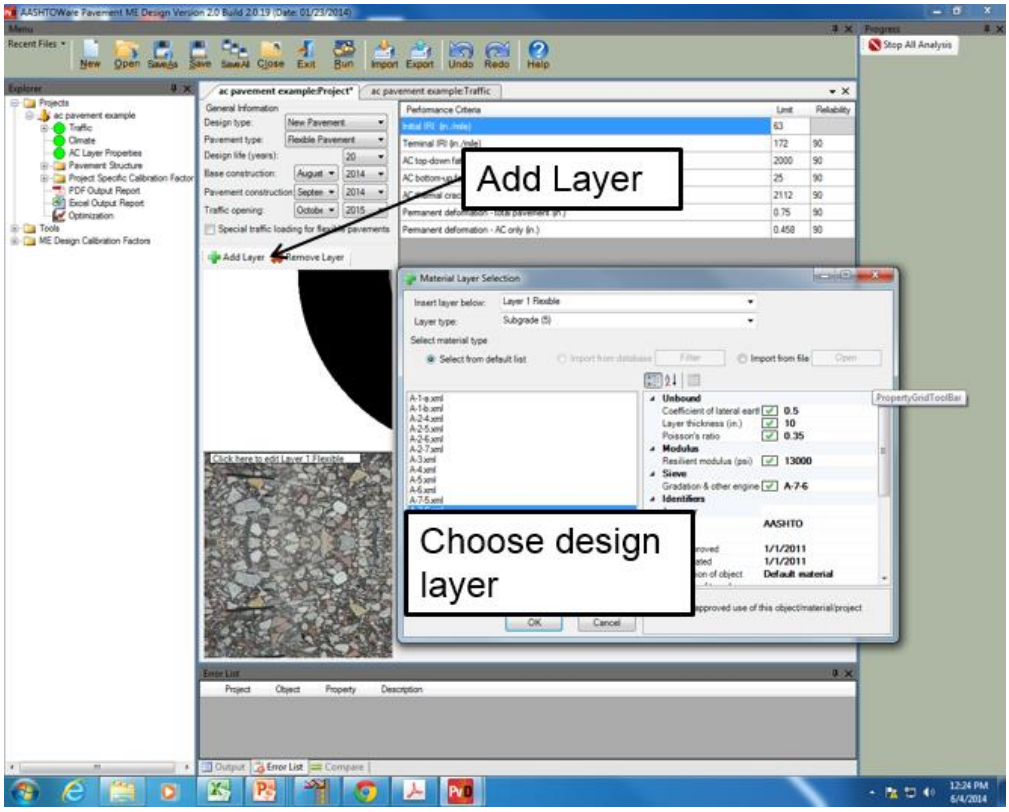

Figure B.18. Pavement structure input for new HMA

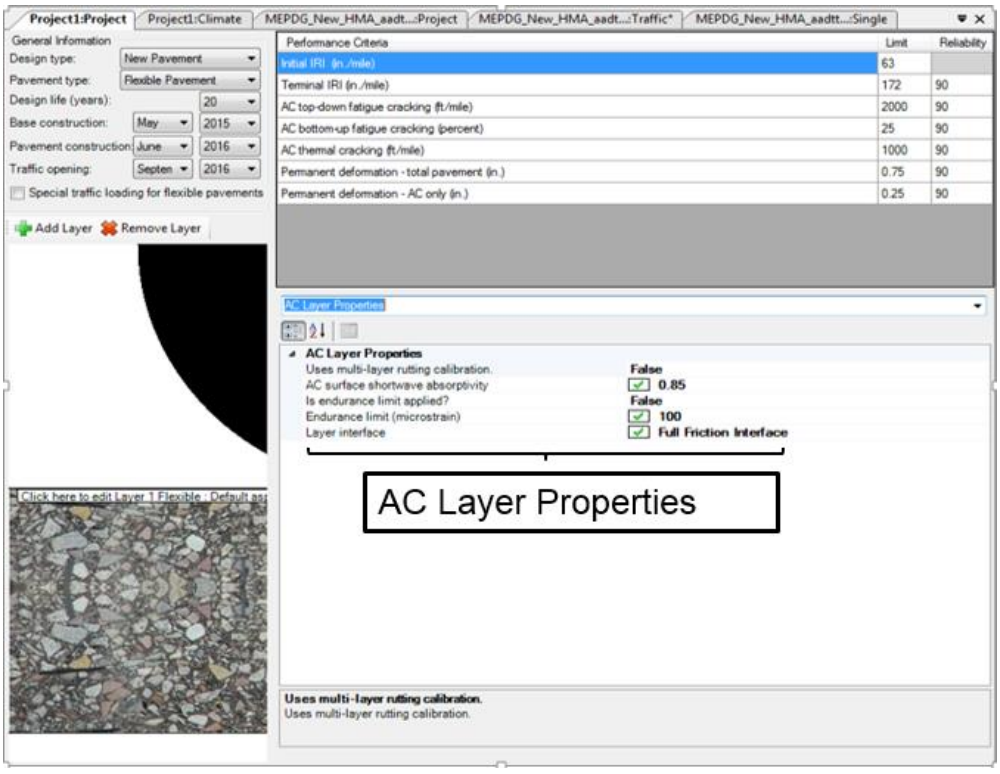

Figure B.19. AC layer properties

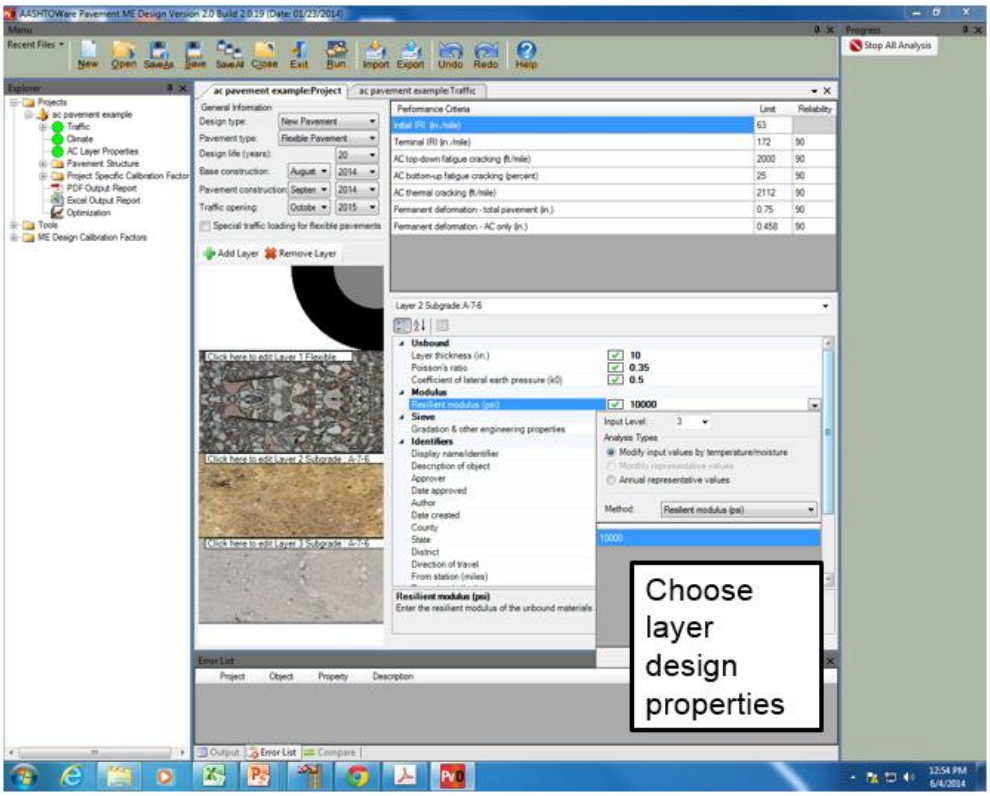

Figure B.20. Layer design properties

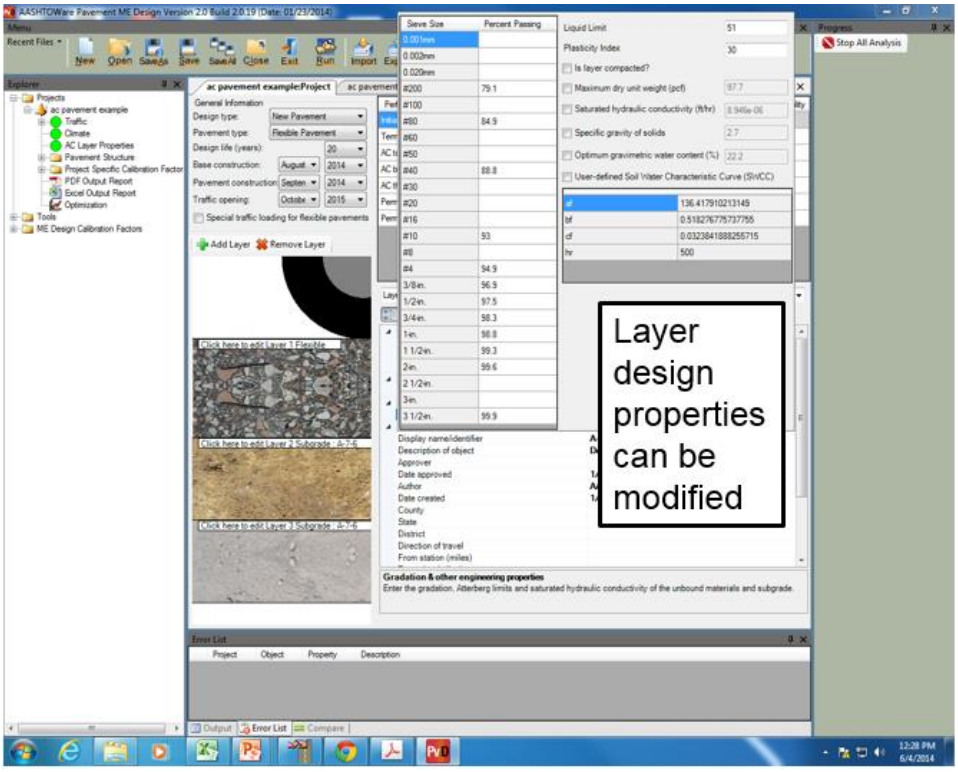

Figure B.21. Modification of layer design properties of new HMA pavement

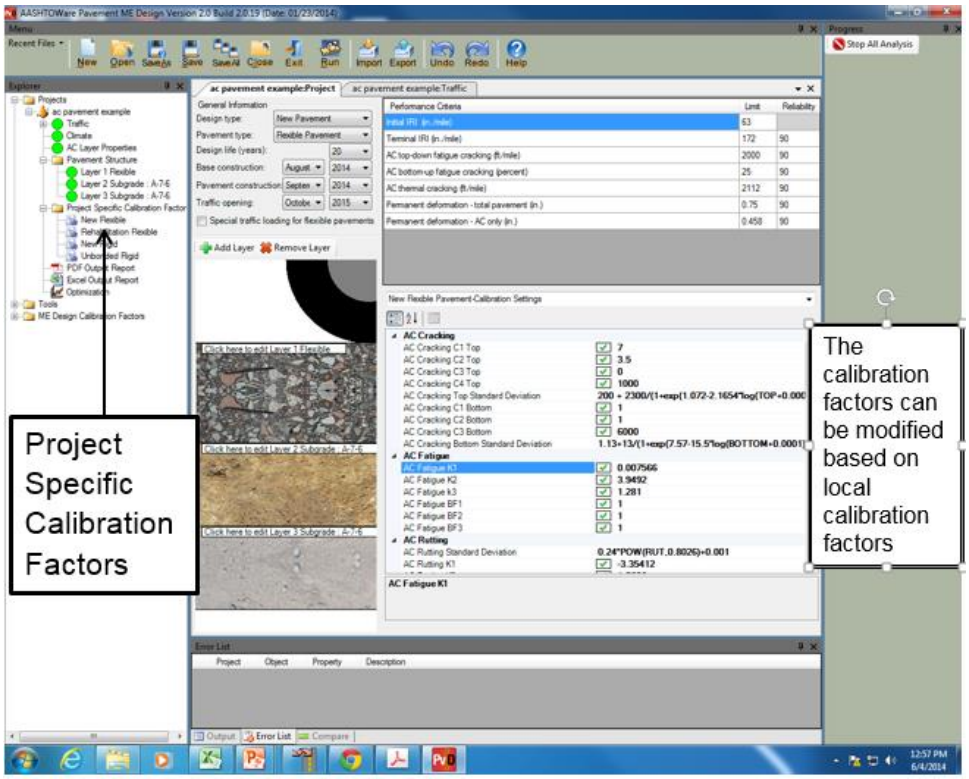

Figure B.22. Inputting HMA local calibration coefficients

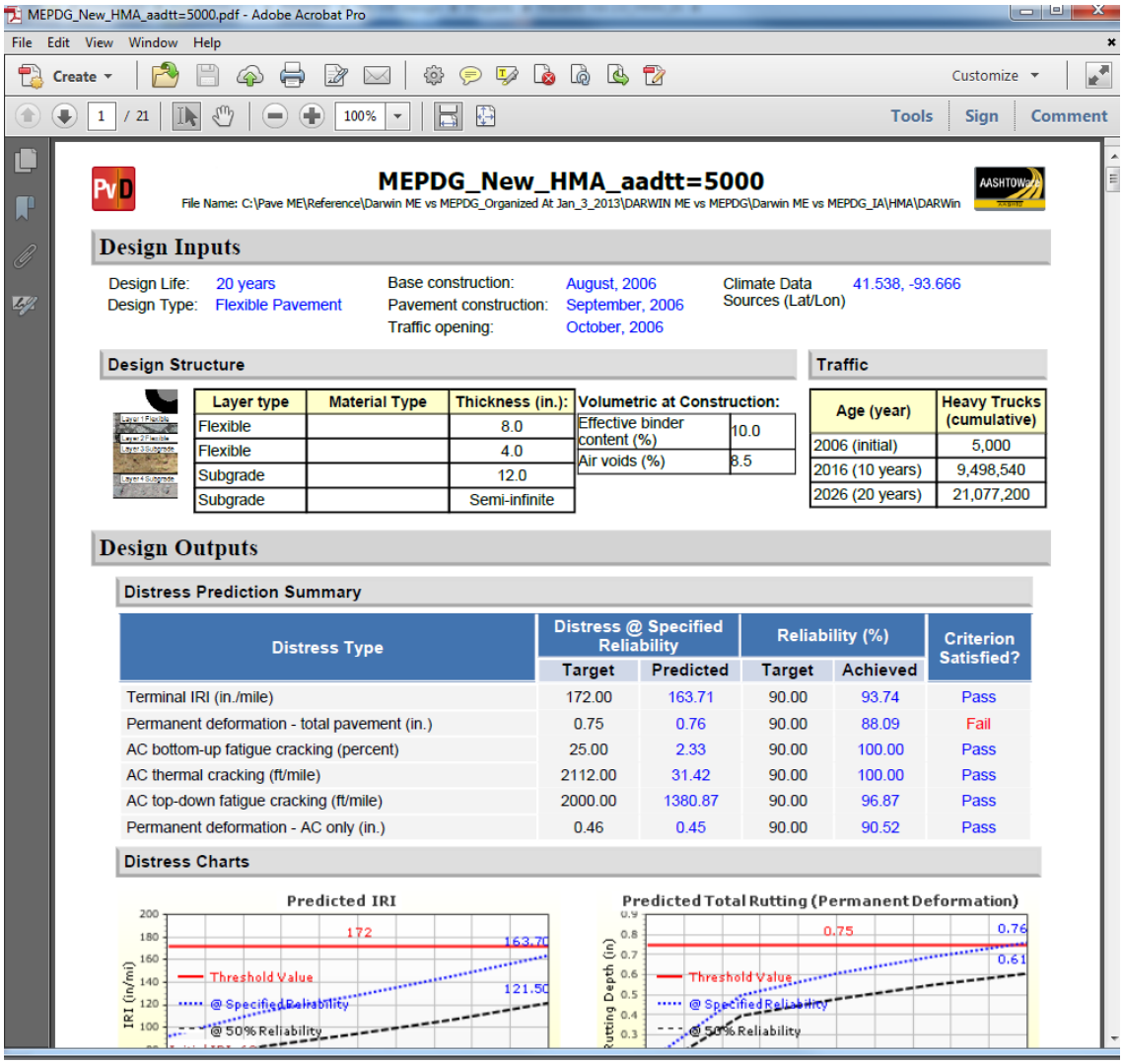

Figure B.23. PDF output report for new HMA pavement

HMA over JPCP

The design of an HMA over JPCP section in Des Moines, Iowa, was performed using AASHTOWare Pavement ME Design software. The following input categories are required for the design procedure:

- Traffic inputs
- Climate inputs
- Pavement structure related inputs
- Existing JPCP design properties
- Existing JPCP condition
- Project specific calibration factors

The following inputs are used in this specific design example:

Design Life

- Design life: 30 years
- Existing construction: August 2014
- Pavement construction: September 2014
- Traffic opening: October 2014
- Type of design: Overlay – AC over JPCP

Construction Requirements

- A good quality of construction with an initial IRI between 50 and 75 in./mi (assume 63 in./mi for design purposes)

Traffic

- Two-way AADTT on this highway estimated to be 5,000 trucks during the first year of its service
- Two lanes in the design direction with 95% of the trucks in the design lane
- Truck traffic equally distributed in both directions
- Operational speed of 60 mph
- Traffic increases by 2.0% of the preceding year's traffic (compounded annually)
- Vehicle class distribution: TTC 4

Performance Criteria

- Initial IRI (in./mi): 63
- Terminal IRI (in./mi): 172
- AC top-down fatigue cracking (ft/mi): 2000
- AC bottom-up fatigue cracking (percent): 25
- AC thermal cracking (ft/mi): 1000
- Permanent deformation – total pavement (in.): 0.75
- Permanent deformation – AC only (in.): 0.25
- AC total cracking – bottom up + reflective (percent): 10
- JPCP transverse cracking (percent slabs): 15
- Reliability level for all criteria: 90%

Layer Properties

- HMA layer: 5 in./PG 58-28
- Existing PCC layer: 10 in./MOR = 600 psi

- Nonstabilized base: 5 in./Mr. =35,000 psi
- Subgrade: semi–infinite thickness /Mr. = 10,000 psi

JPCP design properties:

- PCC joint spacing: 20 ft
- Sealant type: no sealant, liquid or silicone
- Doweled joints: 1.5 in. of dowel diameter
- Widened slab: 14 ft
- Shoulders not tied
- Existing JPCP condition
- Percent slabs replaced/distressed (transverse cracks) before restoration: 15%
- Percent slabs repaired/replaced after restoration: 0%

Figures B.24 through B.35 show screenshots of the design steps using AASHTOWare Pavement ME Design.

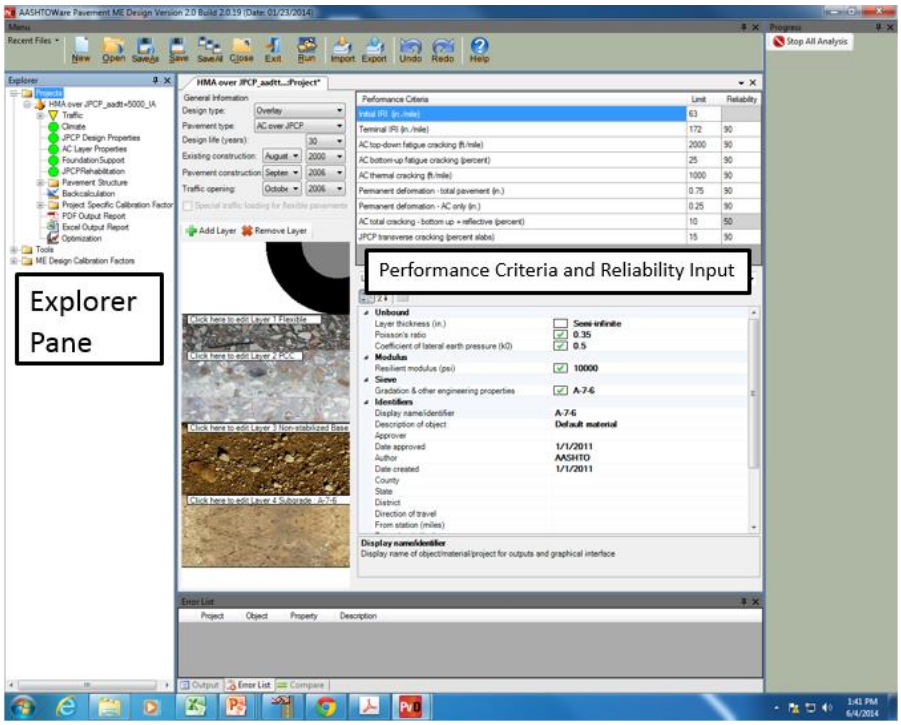

Figure B.24. General inputs, design criteria and reliability

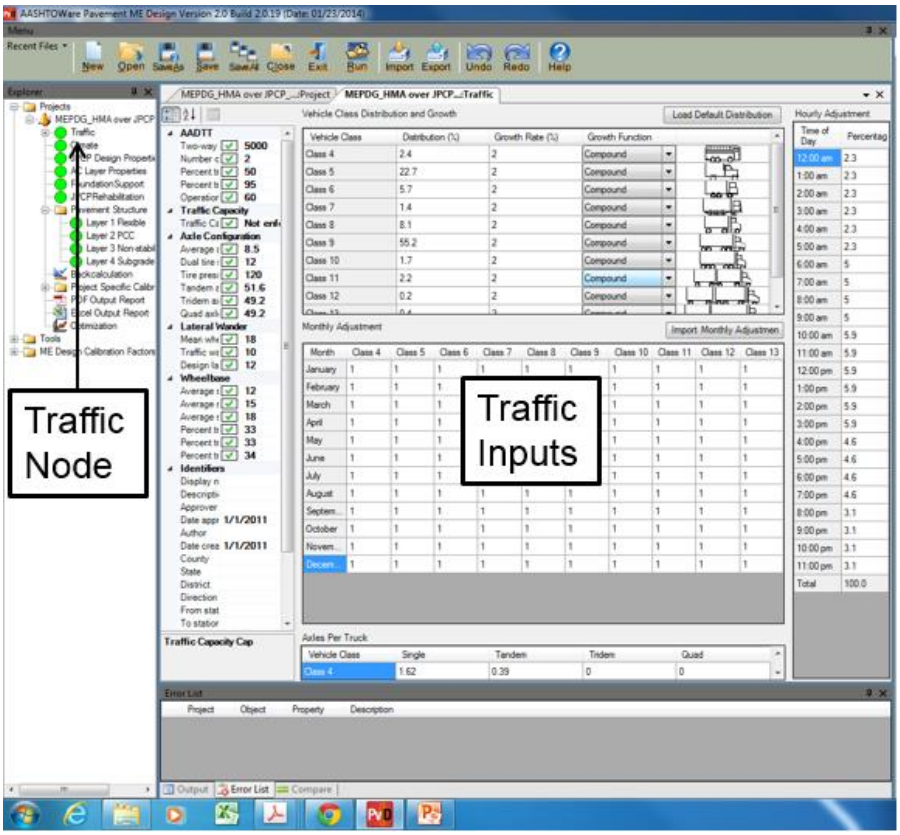

Figure B.25. Traffic inputs

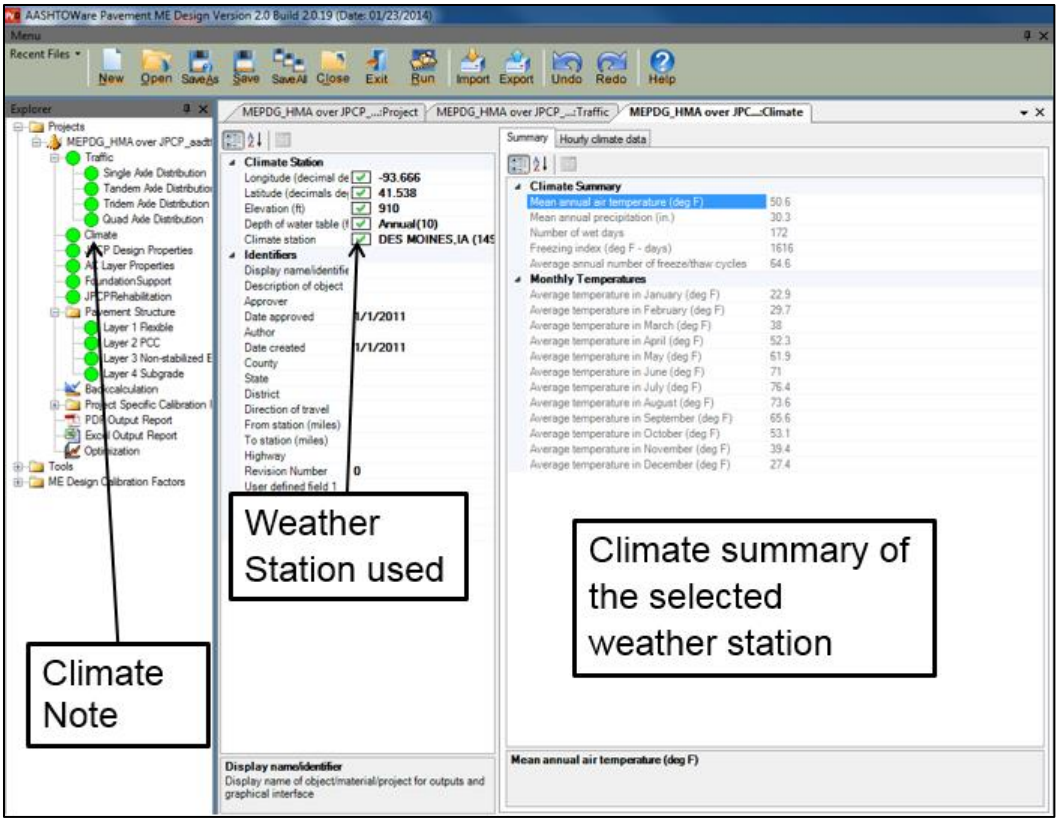

Figure B.26. Climate inputs

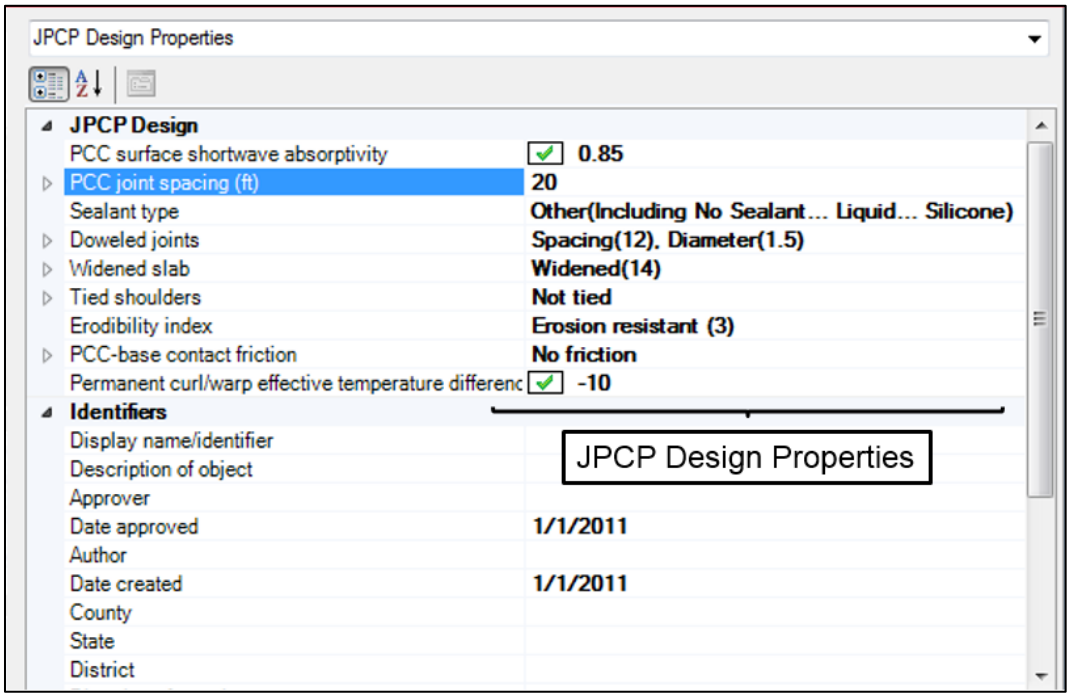

Figure B.27. JPCP design properties for the HMA over JPCP

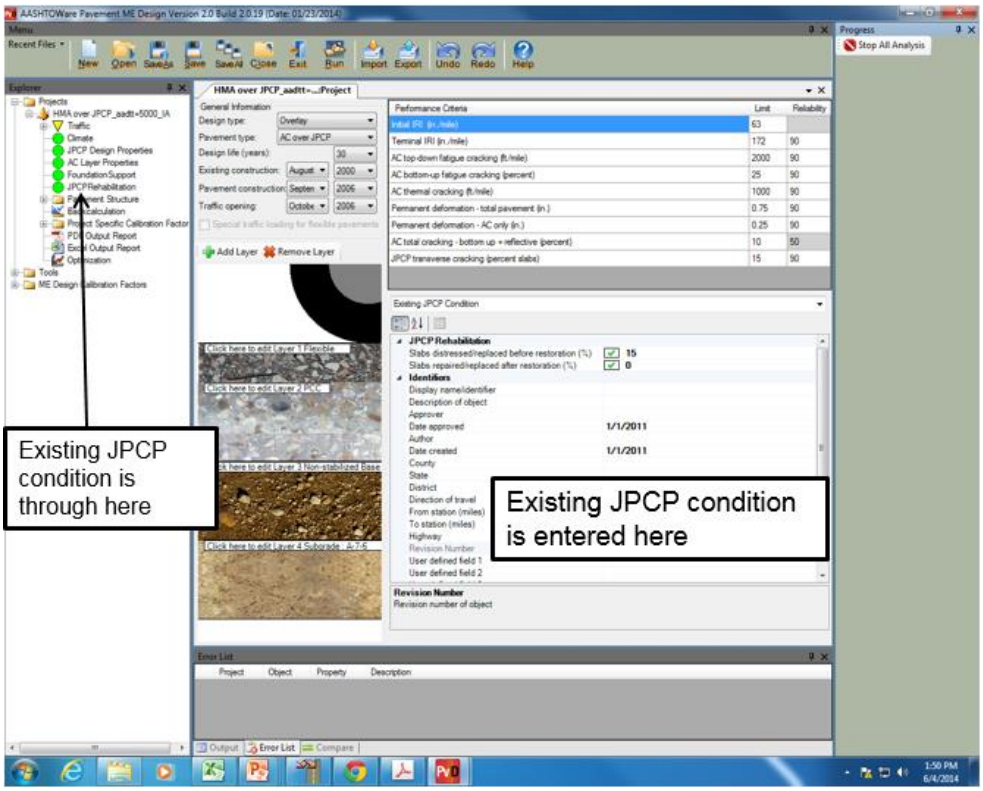

Figure B.28. Existing JPCP condition of the HMA over JPCP

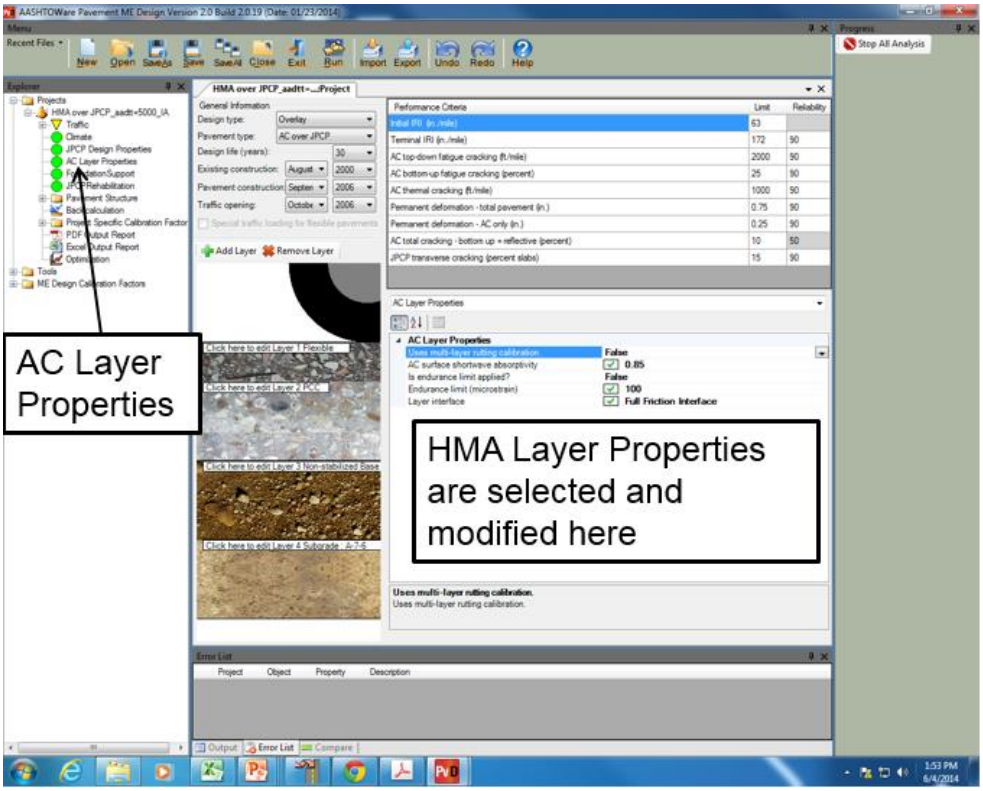

Figure B.29. AC layer design properties

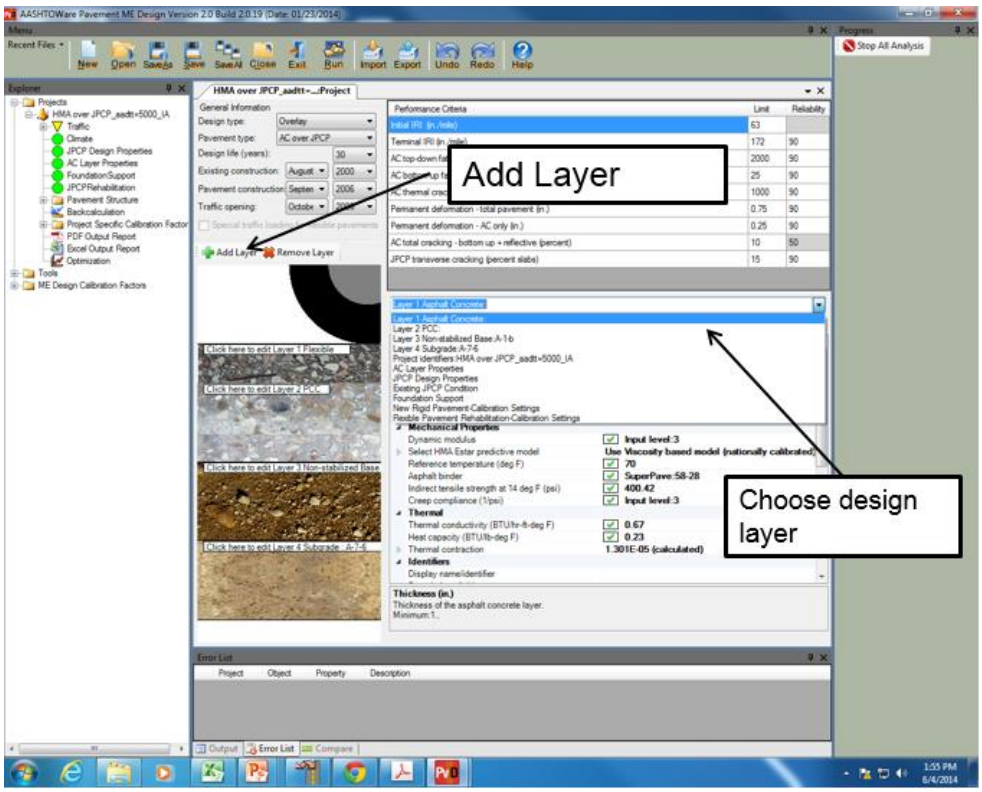

Figure B.30. Pavement structure input for the HMA over JPCP

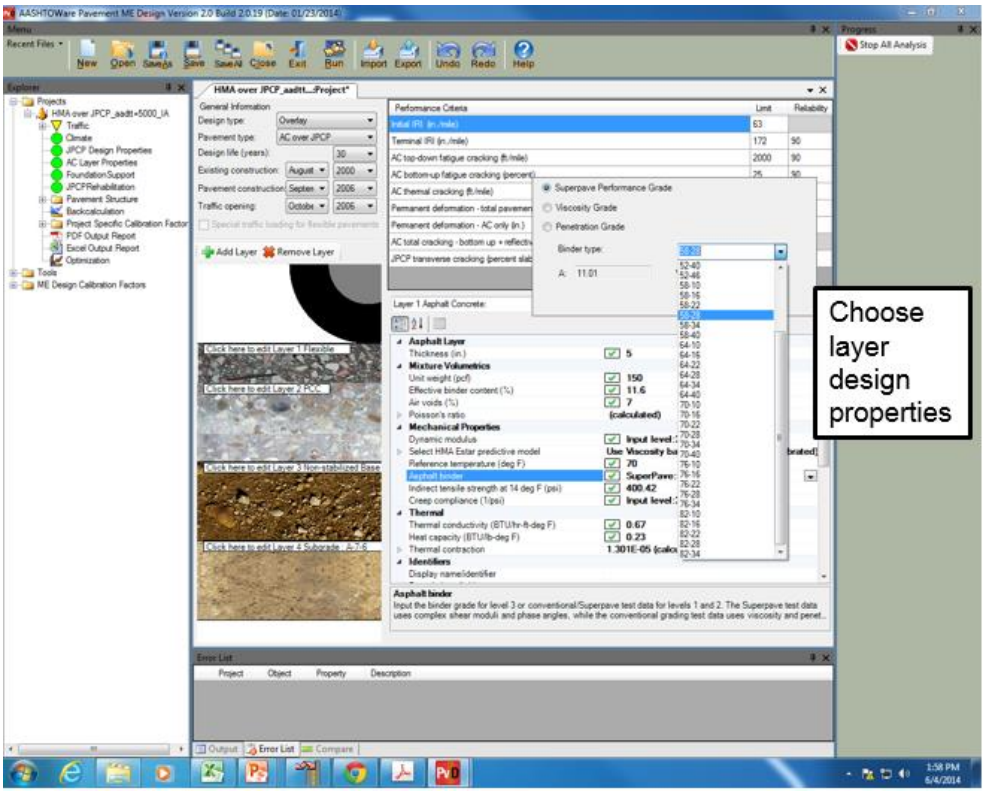

Figure B.31. Choosing layer design properties of the HMA over JPCP

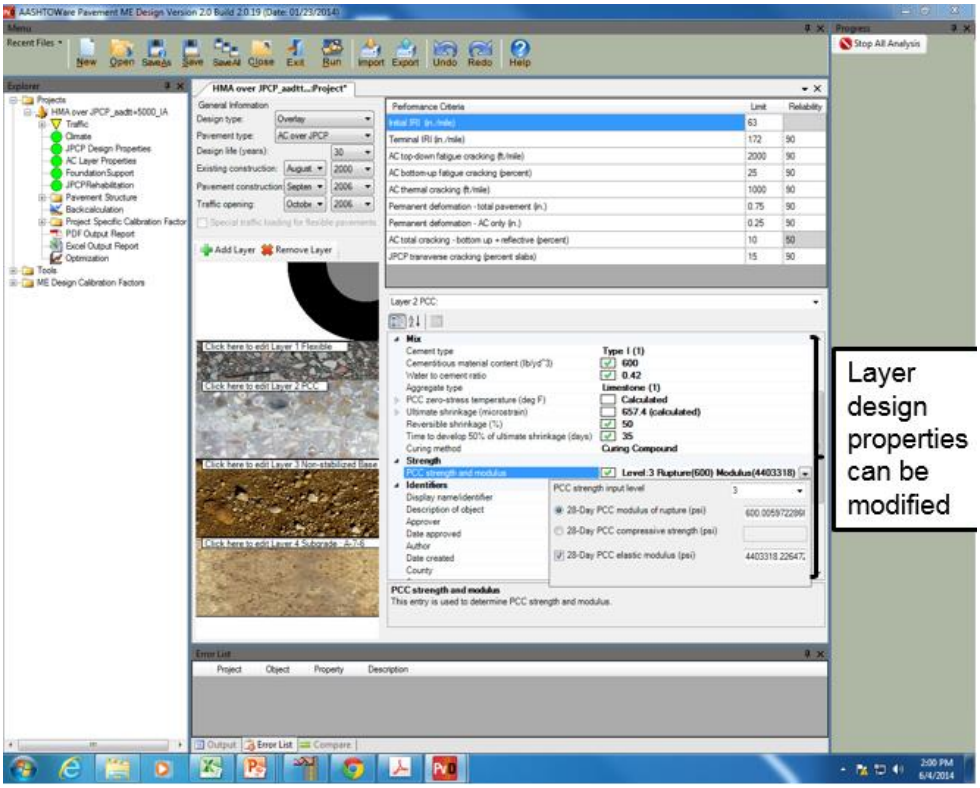

Figure B.32. Modification of layer design properties

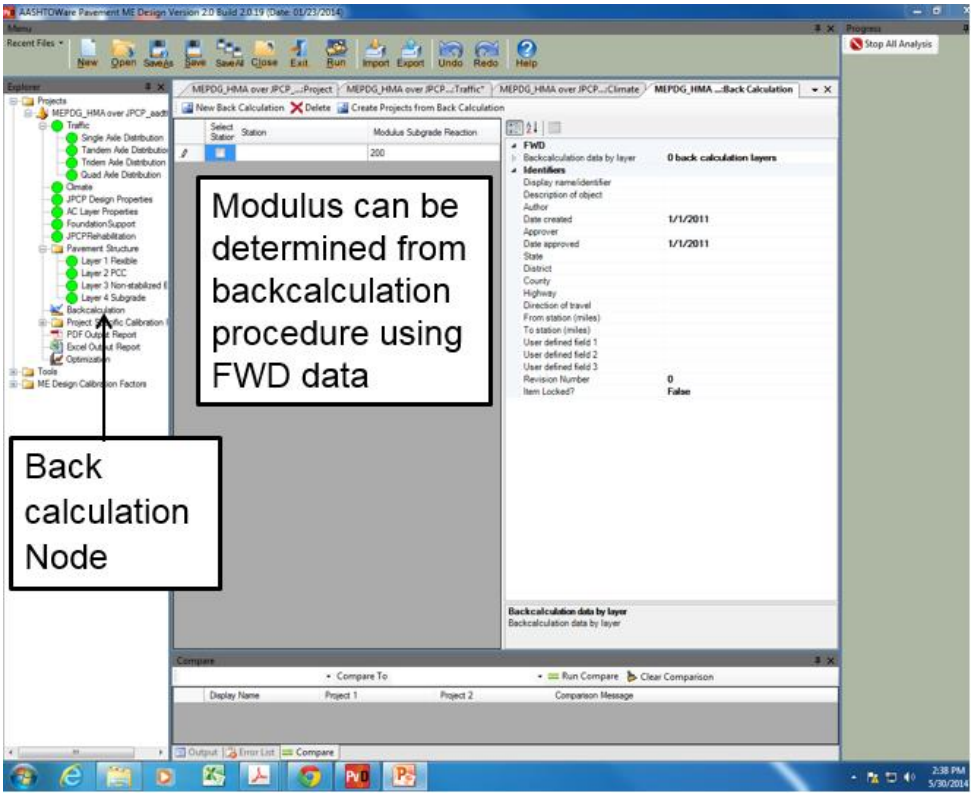

Figure B.33. Use of back-calculation node

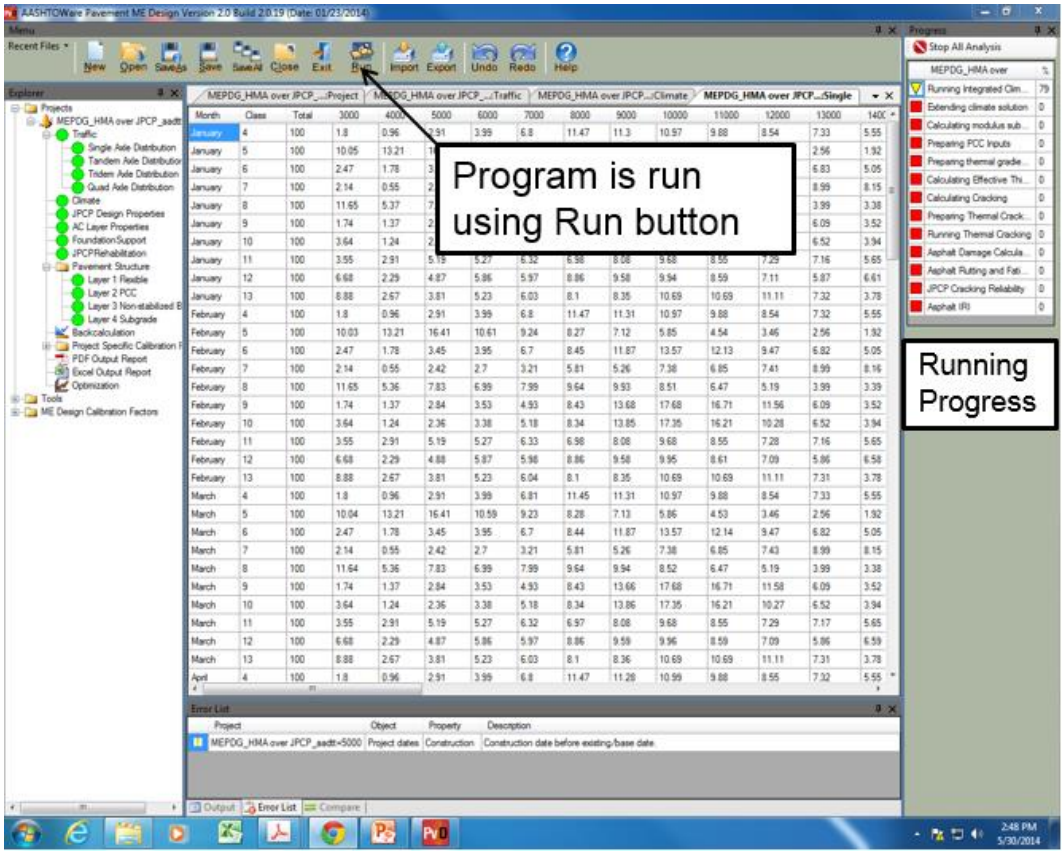

Figure B.34. Running the software

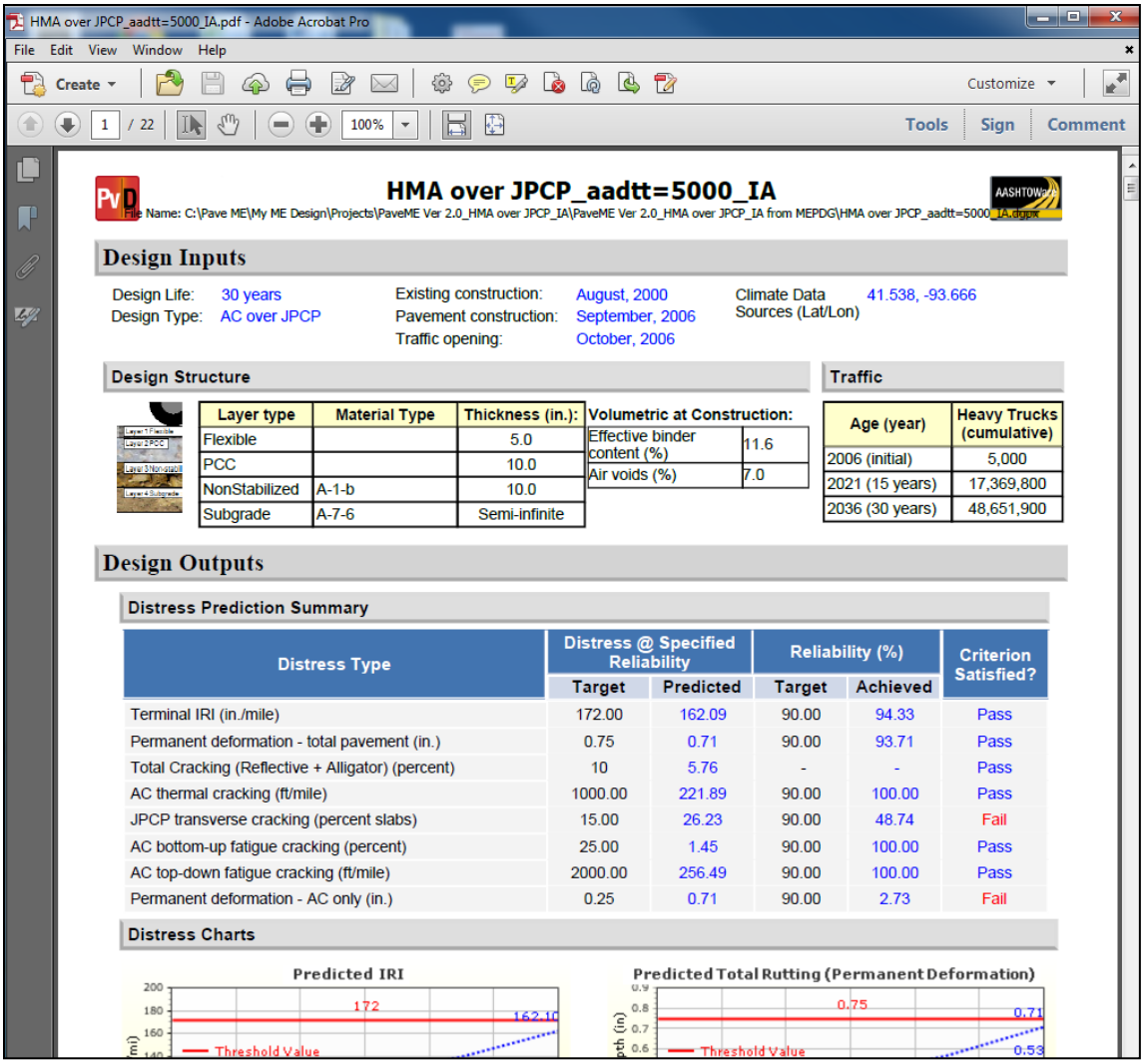

Figure B.35. PDF output report for the HMA over JPCP section

APPENDIX C: SENSITIVITY ANALYSIS OF LOCAL CALIBRATION COEFFICIENTS

Sensitivity analysis basically indicates the sensitivity (change) in an output (y) as a result of a change in the input (x). In this study, a sensitivity analysis of the calibration coefficients for each pavement performance model was performed to understand which calibration coefficients play a major role in a model.

One-at-a-time (OAT) sensitivity analysis was utilized to quantify the sensitivity of each equation calibration coefficient in this study. OAT sensitivity analysis determines the extent of change in the output as response to a change in only one input at a time (Schwartz et al. 2011). Two numerical parameters, a coefficient sensitivity index (S_{ijk}) and a coefficient-normalized sensitivity index (S^n_{ijk}), were calculated for each calibration coefficient to assess the sensitivity of each calibration coefficient quantitatively and compare the magnitudes of sensitivities amongst themselves.

The coefficient sensitivity index (S_{ijk}) can be calculated as follows (Schwartz et al. 2011):

$$S_{ijk} = \frac{\partial Y_j}{\partial X_k}\Big|_i \cong \frac{\Delta Y_j}{\Delta X_k}\Big|_i \quad \textbf{(C.1)}$$

$$\frac{\Delta Y_j}{\Delta X_k}\Big|_i = \frac{Y_{j,i+1} - Y_{j,i}}{X_{k,i+1} - X_{k,i}} \qquad \text{when } X_{j,i+1} > X_{j,i} \quad \textbf{(C.2)}$$

$$\frac{\Delta Y_j}{\Delta X_k}\Big|_i = \frac{Y_{j,i} - Y_{j,i-1}}{X_{k,i} - X_{k,i-1}} \qquad \text{when } X_{j,i-1} < X_{j,i} \quad \textbf{C.3)}$$

where, Y_{ji} and X_{ki} are the values of the performance prediction j and calibration coefficient k evaluated at national calibration coefficient condition i in a model. The partial derivative in the coefficient of sensitivity index can be approximated into a standard central difference approximation (Equation C.1). S_{ijk} implies the percentage change in performance prediction Y_j as a result of the percentage change in the calibration coefficient X_k at national calibration coefficient condition i in the model. To exemplify the interpretation of S_{ijk}, the value of 0.5 for S_{ijk} would imply that a 40% change in the calibration coefficient value of X_{ki} would cause a 20% change in performance prediction Y_{ji} (Schwartz et al. 2011)

For each calibration coefficient, X_k, two coefficient sensitivity indices (S_{ijk}) were calculated using the 20% increased and 20% decreased values of the calibration coefficients ($X_{j,1.2i} > X_{j,i}$ and $X_{j,0.8i} < X_{j,i}$). To compare the coefficient sensitivity indices among calibration coefficients, the indices should be normalized. Note that the normalization of S_{ijk} was performed using the associated national calibration coefficient. A "national coefficient" normalized sensitivity index (S^n_{ijk}) can be calculated as follows (Schwartz et al. 2011):

$$S_{ijk}^{n} = \frac{\partial Y_j}{\partial X_k}\Big|_i \left(\frac{X_{ki}}{Y_{ji}}\right) \cong \frac{\Delta Y_j}{\Delta X_k}\Big|_i \left(\frac{X_{ki}}{Y_{ji}}\right) \quad \textbf{(C.4)}$$

New Rigid Pavement

In the sensitivity analysis of jointed plain concrete pavement (JPCP) performance models, a JPCP section representing typical Iowa JPCPs was determined. This pavement section is on I-29 between mileposts 76.54 and 90.72 in Harrison County, Iowa. The pavement section is composed of a 12 in. portland cement concrete (PCC) layer with 4 in. granular subbase layer. It has two lanes with a projected annual average daily truck traffic (AADTT) of 3,104 in the construction year.

Table C.1 indicates the sensitivity analysis results of the JPCP faulting model calibration coefficients.

Table C.1. Summary of calibration coefficient sensitivity indices for the JPCP faulting model

Calibration factors	Coefficient sensitivity index (S_{ijk})		Coefficient Sensitivity Index	Rank
	$X_{j,i+1} > X_{j,i}$	$X_{j,i-1} < X_{j,i}$		
C6	0.00335	0.00223	2.22	1
C1	0.00065	0.00058	1.24	2
C2	0.00046	0.00042	0.80	3
C3	0.17882	0.17882	0.78	4
C4	0.12794	0.12794	0.22	6
C7	0.00006	0.00006	0.22	5
C5	0.00000	0.00000	0.07	7

A negative sign in the coefficient sensitivity index implies that as the equation calibration coefficient increases, the faulting prediction decreases, or vice versa. As can be seen in Table C.1, C6 is the most sensitive coefficient in this model. Table C.2 and Table C.3 present the sensitivity analysis results of the transverse cracking and International Roughness Index (IRI) model coefficients, respectively.

Table C.2. Summary of calibration coefficient sensitivity indices for the JPCP transverse cracking model

Calibration Factors	Coefficient sensitivity index (S_{ijk})		Coefficient Sensitivity Index	Rank
	$X_{j,i+1}>X_{j,i}$	$X_{j,i-1} < X_{j,i}$		
C1	-201.03	-27.93	-2.58	1
C2	-320.49	-45.29	-2.52	2
C5	-8.96	-12.32	0.24	3
C4	-9.80	-10.25	-0.11	4

Table C.3. Summary of calibration coefficient sensitivity indices for the JPCP IRI model

Calibration Factors	Coefficient sensitivity index (S_{ijk})		Coefficient Sensitivity Index	Rank
	$X_{j,i+1}>X_{j,i}$	$X_{j,i-1} < X_{j,i}$		
C4	1.66	1.66	0.20	1
C1	47.78	47.78	0.18	2
C2	0.95	0.95	0.0020	3
C3	0.04	0.04	0.0003	4

As can be seen from Tables C.2 and C.3, C1 and C4 are the most sensitive coefficients for the transverse cracking and IRI models, respectively.

New HMA and HMA over JPCP

The same rutting, fatigue cracking, thermal cracking, and IRI models are used in both hot mix asphalt (HMA) and HMA over JPCP systems. The only difference between the models in these pavement systems is that in the HMA over JPCP IRI model, reflective cracking predictions are also included in the IRI equations as a part of the total transverse cracking predictions. Therefore, only the sensitivity analysis of the HMA pavement performance model calibration coefficients is presented here.

In the sensitivity analysis, an HMA section representing typical Iowa HMA pavements was determined. This pavement section is on US 61 between mileposts 167.95 and 174.74 in Jackson County, Iowa. The pavement section is composed of an 11 in. HMA layer with a 12 in. subgrade layer. It has two lanes with a projected AADTT of 1,162 in the construction year.

Table C.4, Table C.5, Table C.6, Table C.7, Table C.8, Table C.9, and Table C.10 present the sensitivity analysis results of asphalt concrete (AC) rutting, subgrade rutting, HMA fatigue, alligator (bottom-up) cracking, longitudinal (top-down) cracking, thermal cracking and IRI models for the HMA and HMA over JPCP types, respectively.

Table C.4. Summary of calibration coefficient sensitivity indices for HMA rutting model

Calibration Factors	Coefficient sensitivity index (S_{ijk})		Coefficient Sensitivity Index	Rank
	$X_{j,i+1}>X_{j,i}$	$X_{j,i-1} < X_{j,i}$		
BR2	2.11	0.51	9.65	1
BR3	1.94	0.50	8.94	2
BR1	0.14	0.14	1.00	3

Table C.5. Summary of calibration coefficient sensitivity indices for HMA subgrade rutting model

Calibration Factors	Coefficient sensitivity index (S_{ijk})		Coefficient Sensitivity Index	Rank
	$X_{j,i+1}>X_{j,i}$	$X_{j,i-1} < X_{j,i}$		
BS1	0.24	0.24	1.00	1

Table C.6. Summary of calibration coefficient sensitivity indices for HMA fatigue model

Calibration Factors	Coefficient sensitivity index (S_{ijk})		Coefficient Sensitivity Index	Rank
	$X_{j,i+1}>X_{j,i}$	$X_{j,i-1} < X_{j,i}$		
BF2	-1.54	-3183.455	-5153.72	1
BF3	46.51	1.49	77.67	2
BF1	-0.26	-0.39	-1.04	3

Table C.7. Summary of calibration coefficient sensitivity indices for HMA alligator (bottom-up) cracking model

Calibration Factors	Coefficient sensitivity index (S_{ijk})		Coefficient Sensitivity Index	Rank
	$X_{j,i+1}>X_{j,i}$	$X_{j,i-1} < X_{j,i}$		
C1_Bottom	-0.69	-1.81	-5.65	1
C2_Bottom	-0.24	-0.31	-1.24	2
C4_Bottom	0.00	0.00	1.00	3

Table C.8. Summary of calibration coefficient sensitivity indices for HMA longitudinal (top-down) cracking model

Calibration Factors	Coefficient sensitivity index (S_{ijk})		Coefficient Sensitivity Index	Rank
	$X_{j,i+1}>X_{j,i}$	$X_{j,i-1} < X_{j,i}$		
C1_Top	-0.04	-0.17	-9.54	1
C2_Top	-0.07	-0.18	-5.64	2
C4_Top	0.00	0.00	1.00	3

Table C.9. Summary of calibration coefficient sensitivity indices for HMA thermal (transverse) cracking model

Calibration Factors	Coefficient sensitivity index (S_{ijk})		Coefficient Sensitivity Index	Rank
	$X_{j,i+1}>X_{j,i}$	$X_{j,i-1} < X_{j,i}$		
K_Level 3	1155.9	2120.0	3.17	1

Table C.10. Summary of calibration coefficient sensitivity indices for HMA IRI model

Calibration Factors	Coefficient sensitivity index (S_{ijk})		Coefficient Sensitivity Index	Rank
	$X_{j,i+1}>X_{j,i}$	$X_{j,i-1} < X_{j,i}$		
C4	2366.67	2333.33	0.35	1
C1	0.38	0.38	0.15	2
C3	812.50	750.00	0.06	3
C2	0.00	0.00	0.00	4